DOKUZ EYLÜL UNIVERSITY

GRADUATE SCHOOL OF NATURAL AND APPLIED SCIENCES

THEORETICAL AND EXPERIMENTAL STUDY OF TRANSIENT FLOWS IN PRESSURISED PIPELINES

by

Nuri Seçkin KAYIKÇI

September, 2007

İZMİR

THEORETICAL AND EXPERIMENTAL STUDY OF TRANSIENT FLOWS IN PRESSURISED PIPELINES

A Thesis Submitted to the
Graduate School of Natural and Applied Sciences of Dokuz Eylül University
In Partial Fulfillment of the Requirements for the Degree of Doctor of Philosophy in Civil Engineering, Hydraulics, Hydrology and Water Resources Engineering program

by
Nuri Seçkin KAYIKÇI

September, 2007
İZMİR

Ph.D. THESIS EXAMINATION RESULT FORM

We have read the thesis entitled **"THEORETICAL AND EXPERIMENTAL STUDY OF TRANSIENT FLOWS IN PRESSURISED PIPELINES"** completed by **NURİ SEÇKİN KAYIKÇI** under supervision of **PROF. DR. M. ŞÜKRÜ GÜNEY** and we certify that in our opinion it is fully adequate, in scope and in quality, as a thesis for the degree of Doctor of Philosophy.

.....

Supervisor

.....	.....
Thesis Committee Member	Thesis Committee Member
.....	.....
Examining Committee Member	Examining Committee Member

Prof.Dr. Cahit HELVACI
Director
Graduate School of Natural and Applied Sciences

ACKNOWLEDGMENTS

Author thank to Prof. Dr. M. Şükrü GÜNEY for his helps and directions during the setting up of the pipelines in the laboratory and due to financial supports of project department of Dokuz Eylül University.

Nuri Seçkin KAYIKÇI

THEORETICAL AND EXPERIMENTAL STUDY OF TRANSIENT FLOWS IN PRESSURISED PIPELINES

ABSTRACT

The aim of the study is the investigation of unsteady flows due to pump rundown in pressurised steel pipeline systems. The numerical results are found by means of a computer program using characteristics method. Theoretical computations realised by Fortran computer programs and experimental results obtained from pressure transient data logger were compared to each other and all results were evaluated. Centrifugal pump was shut down manually and developed pressure heads were drawn on the same graphics. Experiments are carried out for different steady state discharges. Results are observed and examined about the response behaviour of the computer programs against to more realistic results provided by the pressure transient data logger. It is observed that the theoretical and experimental results are in an acceptable accord in the first system. This accordance is better for lower and moderate discharges. The accord between theoretical and experimental results may be improved by translating the behaviour of the check valve more realistically in second system.

Keywords : Unsteady Flows, Centrifugal Pump, Pump rundown, Method of Characteristics, Steel Pipeline, Reduced Bore Ball Valve, Disc Type Check Valve

BASINÇLI BORULARDA KARARSIZ AKIMLARIN TEORİK VE DENEYSEL OLARAK ÇALIŞILMASI

ÖZ

Çalışmanın amacı basınçlı çelik boru sistemlerinde pompanın anlık olarak durmasından dolayı oluşan kararsız akımların araştırılmasıdır. Karakteristikler metodunu kullanarak bilgisayar programı yardımıyla sayısal sonuçlar bulunmuştur. Fortran bilgisayar programı ile gerçekleştirilmiş teorik hesaplamalar ve kararsız akım basınç ölçer cihazından elde edilmiş deneysel sonuçlar birbirleriyle karşılaştırılmış ve değerlendirilmiştir. Santrifüj pompası elle kapatılmış ve ölçülen basınç yükseklikleri hesaplanan teorik değerlerle beraber aynı şekil üzerinde gösterilmiştir. Deneyler farklı kararlı akım debi değerlerinde gerçekleştirilmiştir. Birinci sistemde teorik ve deneysel neticelerin kabul edilebilir mertebede uyumlu oldukları gözlenmiştir. Bu uyum düşük ve orta kararlı akım debileri için daha iyi olmuştur. İkinci sistemde ise çek-valfin davranışı çok iyi yansıtılamadığından dolayı teorik ve deneysel neticeler arasında uyumsuzluklar gözlenmiştir. Kabul edilebilir bir uyum çek-valfin davranışının daha kapsamlı bir şekilde araştırılıp belirlenmesi ile mümkün olabilecektir.

Anahtar kelimeler : Kararsız akımlar, Santrifüj pompası, Pompanın durması, Karaktaristikler Metodu, Çelik boru hattı, Dar geçişli küresel vana, Disk tipi çekvalf

CONTENTS

Page

THESIS EXAMINATION RESULT FORM ii
ACKNOWLEDGEMENTS iii
ABSTRACT iv
ÖZ……v

CHAPTER ONE – INTRODUCTION 1

1.1 Definitions 1
1.2 History of water hammer analysis……1
1.3 The scope of the study 9

CHAPTER TWO – BASIC EQUATIONS OF UNSTEADY FLOW 10

2.1 Equation of Motion 10
2.2 Continuity Equation 13
2.3 Celerity in pipelines……17

CHAPTER THREE –NUMERICAL SOLUTION WITH THE USE OF METHOD OF CHARACTERISTICS 19

3.1 Characteristic Equations 19
3.2 Equations in Finite Difference Form……22
3.3 Boundary Conditions……...25
3.4 Courant Criterion……27
3.5 Losses at regulating valve and relevant equations……...28
3.5.1 Positive Flow 28
3.5.2 Negative (Reverse) Flow……..30
3.6 Calculation of Darcy Weisbach Friction Coefficient…….……31

CHAPTER FOUR – TRANSIENTS CAUSED BY CENTRIFUGAL PUMPS. 32

4.1 Introduction 32
4.2 Similarity laws and pump characteristics…….33
4.3 Head balance and torque angular reducing equations for the 1st system…….48
4.3.1 Head balance equation for the 1st system 48
4.3.2 Speed change equation for the first system……..51
4.3.3 Newton Raphson numerical method for first system……..53
4.4 Head balance and torque angular reducing equations for the 2nd system…....56
4.4.1 Head balance equation for the 2nd system……56
4.4.2 Torque angular deceleration equation (calculation of speed change equation) for the second system……...58
4.4.3 Newton Raphson method for the second system…….58
4.5 Use of the Newton Raphson numerical method for determination of steady state parameters……..…59
4.6 Presence of disc type check valve in second system……..61

CHAPTER FIVE – EXPERIMENTAL SET UP 62

5.1 The first experimental set up 62
5.2 The second experimental set up……...66
5.3 Pump characteristic curves……...70
5.4 Pressure transient data logger……...81
5.5 Computation of valve and elbow loss coefficients……..82
5.5.1 The use of the differential manometer..... 82
5.5.2 The loss coefficients of reduced bore ball valve……..83
5.5.3 The loss coefficients of elbows……....85
5.6 The loss coefficients of disc type check valve and valves for the second system……..86
5.7 Calibration of triangular weir……...88

CHAPTER SIX – DESCRIPTION OF COMPUTER PROGRAMS 90

6.1 The flow chart of the computer program..... 90
6.2 Description of parameters used in the computer programs……..91
6.2.1 Fortran computer program used for the first system 91
6.2.2 Fortran computer program used for the second system……....94

CHAPTER SEVEN – EXPERIMENTAL RESULTS 95

7.1 Results of experiments performed in the first system 95
7.1.1 Results of experiments performed for lower steady state discharge 95
7.1.2 Results of experiments performed for moderate steady state discharge..98
7.1.3 Results of experiments performed for upper steady state discharge…..100
7.2 Results of experiments performed in the second system 100
7.2.1 Results of experiment performed for lower steady state discharges 101
7.2.2 Results of experiment performed for moderate steady state discharge..106
7.2.3 Results of experiment performed for upper steady state discharge……109

CHAPTER EIGHT – THEORETICAL RESULTS 112

8.1 Results of computations performed for the first system..... 112
8.1.1 Results of computation performed for lower steady state discharge..... 112
8.1.2 Results of computation performed for moderate steady state discharge116
8.1.3 Results of computation performed for upper steady state discharge…..121
8.2 Results of computations performed for the second system..... 124
8.2.1 Results of computation performed for lower steady state discharges ... 124
8.2.2 Results of computation performed for moderate steady state discharge129
8.2.3 Results of computation performed for upper steady state discharges…135

CHAPTER NINE – COMPARISON OF EXPERIMENTAL AND THEORETICAL RESULTS..... 140

9.1 Comparison of experimental results with those obtained from computations performed for the first system 140

9.1.1 Comparison of experimental results with theoretical results performed for lower steady state discharges 140

9.1.2 Comparison of experimental results with theoretical results performed for moderate steady state discharges…….....141

9.1.3 Comparison of experimental results with theoretical results performed for upper steady state discharge……143

9.2 Comparison of experimental results with those obtained from computations performed for the second system 143

9.2.1 Comparison of experimental results with theoretical results performed for lower steady state discharge..... 144

9.2.2 Comparison of experimental results with theoretical results performed for moderate steady state discharges…….146

9.2.3 Comparison of experimental results with theoretical results performed for upper steady state discharges……...…150

CHAPTER TEN – CONCLUSIONS..... 152

REFERENCES..... 154

APPENDIX A 159

APPENDIX B……..172

APPENDIX C…….....178

CHAPTER ONE
INTRODUCTION

1.1 Definitions

The flow processes are governed by equation of motion (or momentum, dynamic) and equation of continuity (conservation of mass). In steady flow, there is no change in conditions at a point with time. In unsteady flow, conditions at a point may change with time. Steady flow is a special case of unsteady flow in which the steady flow equations must satisfy. The terms water hammer and transient flow are used synonymously to describe unsteady flow of fluids in pipelines, although use of the former is customarily restricted to water. The term surge refers to those unsteady flow situations that can be analysed by considering the fluid to be incompressible and the conduit wall rigid. Liquid column separation refers to the situation in a pipeline in which gas and (or) vapour is collected at some section (Wylie & Streeter, 1993).

1.2 History of the water hammer analysis

The study of transient flows has been started with the study of sound waves in the air. Separately, studies related to wave propagation inside the shallow water and blood flow in the artery have been also performed.

Newton has been studied the propagation of the sound waves in the air and water waves into the channels. Lagrange has been examined sound velocity in the air theoretically as well. Euler derived partial differential equation for propagated wave. Lagrange analysed flows of compressible and incompressible fluids. For this objective, he developed concept of velocity potential (Chaudhry, 1987).

In 1789, Monge developed a graphical method integrating partial differential equations. Method of characteristics was described. Young studied the propagation of pressure wave inside the pipes. Helmholtz has attracted attention to pressure wave velocity in the water inside the pipes, which was less than in unconfined water. He

interpreted this difference to elasticity of pipe wall accurately. In 1850's Weber studied the incompressible fluid flow in the elastic pipes. He conducted the experiments and specified the velocity of pressure waves. He developed dynamic and continuity equations. Resal has developed second order wave equation together with continuity and dynamic equations. In 1878 Korteweg firstly determined wave velocity considering both elasticity of pipe wall and fluid. Michaud has studied water hammer problem. In 1883 Gromeka included friction losses in the analysis of water hammer for first stage. He has assumed that liquid is incompressible and friction losses are directly proportional to flow velocity (Koç, 2001). Weston and Carpenter have realised certain experiments to develop empirical relation between pressure rise against to reduced flow velocity inside the pipes. These experiments were unsuccessful because of the inadequate pipe length. Frizell has developed expressions for rising pressure value due to sudden pause of flow and velocity of water hammer pressures. He also studied branching pipes (Chaudhry, 1987).

In 1897, Joukowski has conducted extensive experiments using the pipes in Moscow, Russia. He published his classical report upon water hammer basic theory. He developed a formula for wave velocity considering elasticity for both water and pipe wall, and relation between pressure rising resulting from reduction of flow velocity. Developed methods were based on conservation of energy and continuity equation. He discussed propagation and reflection of pressure wave throughout the pipe. He also studied the effects of air chambers, surge tanks, security valves damping water hammer pressures. He has founded that if valve is closed before 2L/a second, maximum pressure will be occurred where L is the pipe length and a is the wave celerity (Chaudhry, 1987).

Allievi published general water hammer theory in 1902. His produced dynamic equation was more accurate than that of Korteweg. He constituted and presented graphics for pressure drop as a result of systematic opening or closing valves. Allievi became creative person of basic water hammer theory (Chaudhry, 1987).

Between 1940 and 1960, Gray realised water hammer analysis using computer application and method of characteristics. Lai used Gray's studies in his doctorate study and together with Streeter, they presented their publications using computers and method of characteristics.

Since 1960 to 1970, method of characteristics was developed by Streeter and he studied column separation and boundary conditions for pumps and air chambers. Graphical methods were presented by John Parmakian (1963). Velocity of water hammer wave in an elastic pipe was studied by Halliwell in 1963. In 1965, M. Marchal, G. Flesch, P. Suter examined the calculation of water hammer problems by means of a digital computers. In 1968, the paper about water hammer control into the pipeline systems has been presented by Kinno (Koç, 2001). H. Kinno in 1968 realised his study upon water hammer control in centrifugal pump systems. Wood realised the research on calculation of water hammer pressure due to valve closure in 1968.

A lot of studies about water hammer and transient flows in pressurised pipelines, have been realised since 1970. Some of them investigated the effects of valve closing upon transient flows, the high and low pressures as a result of sudden pause or sudden starting of operation of pump, power failures of turbines, the water hammer using different methods, transient flows in branching pipes, the prevention of water hammer pressures. After 1970, water hammer calculations are performed by both computers and graphical methods. In 1973, Wood and Jhones clarified water hammer pressures for various types of valves. In July 1973, computer analysis of water hammer in pipeline systems was performed by Sheer, Baasch and Gibbs. In 1975, Streeter and Wylie realised their study as 'Transient analysis of offshore loading systems'. In 1977, Benjamin Donsky presented upsurge and speed rise charts due to pump shut down (Donsky, 1961). Vardy studied the method of characteristics for the solution of unsteady flow networks in 1977. In 1980, Provoost realised the study upon the dynamic behaviour of non return valves. One dimensional model for transient gas-liquid flows in ducts was examined in 1980 by Hancox, Ferch, Liu and Nieman. Wave propagation in plastically deforming ducts was studied in 1980 by

Twyman, Thorley and Hewavitarne. In 1987, Wiggert, Hatfield and Stuckenbruch realised water hammer analysis in pipes using characteristic methods (Koç, 2001). In 1989, Thorley presented his study as 'Check valve behaviour under transient flow conditions'. Stittgen and Zielke performed a study in 1990 as fluid structure interaction in the flexible curved pipes. Besides these studies, various scientific books and reports upon water hammer and unsteady flows are prepared and published by Watters, 1979, Chaudhry, 1987, Tullis, 1989, Thorley, 1991, International Association of Hydraulic Research, IAHR, 1994, Larock and Jeppson, 2000, Streeter and Wylie, 1993.

Zaruba also published his studies upon water hammer in 1993. Popescu, Arsenie and Vlase presented their book in 2003 which contains water hammer, unsteady flow computations and experimental results conducted in Romania and they explained the applications and practices upon the water structures placed on Danube River and some pipelines. Some computer programs are developed by hydraulic departments of several universities and engineering firms related to water hammer, transient flows and unsteady flow calculations in pipelines such as, Washington State University prepared by Chaudhry, some other universities in USA and Europe, for instance, engineering company, Haestad Inc in USA, Denmark, Delft Hydraulics etc.

Werner Burmann (1975) investigated the behaviour of water hammer phenomena in pipe systems of several different flow sections. In this report, the solution of the differential equations covering non-stationary fluid flow in pipe systems of several different flow sections by means of the method of characteristics is sketched.

Karney Bryan W. and Duncan McInnis (1990) studied transient flow in water distribution systems. They emphasize that the details of how a hydraulic system is modelled or represented can have a critical impact on the predicted transient conditions.

William Rahmeyer (1996) published a paper titled as 'Dynamic Flow Testing of Check Valves'. The two objectives of this paper are to present a test method by

which check valves can be dynamically tested for sudden closure due to reverse flow, and to discuss the valve and pipe characteristics which affect the reverse velocities and pressure surges at the check valves.

Ezzeddine Hadj-Taieb and Taieb Lili (1998) presented their study about the transient flow in homogeneous gas-liquid mixtures in rigid and quasi-rigid pipes. Two mathematical models based on the gas-fluid mass ratio are presented. The fluid pressure and velocity are considered as two principal dependent variables and the gas-fluid mass ratio is assumed to be constant. By application of the conservation of mass and momentum laws, non-linear hyperbolic systems of two differential equations are obtained and integrated numerically by a finite difference conservative scheme. Numerical solutions are compared with numerical results available in literature and experiment developed in the laboratory. The results show that the pressure wave propagation is significantly influenced by the gas-fluid mass ratio and the elasticity of pipe wall. They indicate that the pipe elasticity and liquid compressibility may be neglected for great values of gas-liquid mass ratio but not for the smaller ones.

Colin Kirkland (1998) presented a paper related to the controlled release and intake of air into the pipelines to maximize their performance. This paper describe some of the roles that the air release valve plays in various pipelines, and how it can be safely and effectively used in order to achieve greater results.

Yukio Kono, Masaji Watanabe and Tomonoki Ito (1998) introduced a method in which the upstream finite different approximation is applied to the systems governing a liquid and a two phase flow of the mixture of the liquid and the vapour. They also introduced some results of analysis using this method and compare those with experimental results and concluded that this method is capable for solving the non-linear hyperbolic type partial differential equation and parabolic equation simultaneously.

Kameswara Rao C.V. and Eswaran K. (1999) performed their study titled as ‘Pressure Transients in Incompressible Fluid Pipeline Networks’. They explained that pressure surges in pipeline are caused due to different events either planned or accidental. It is essential to determine the magnitude and frequency of pressures and forces triggered due to these transients to estimate the stresses and vibration levels in the pipeline networks. In their paper, an effort is made to study these transients in incompressible fluid flow systems and the development of a computer program HYTRAN is described. This computer program comprehensively incorporates the method of characteristics for the calculation of the time dependent head and velocity of the fluid at any point in a complex fluid/water pipeline network upon the beginning of any event such as pump failure, load reduction on a turbine, etc. The time history of the machine parameters in the case of pumps and turbines during such events can also be obtained as output. Two case studies have been taken up and the results are discussed.

Computer program named ‘Pipenet-Transient Module’ was produced in 1999 by Sunrise Systems Ltd. The PIPENET Transient Module provides a speedy and cost effective means of in-house rigorous transient analysis. The transient module can be used for predicting pressure surges, calculating hydraulic transient forces or even modelling control systems in flow networks.

A German technical/scientific institute has developed a new passive security system in 2003 for pipelines to avoid pressure surges in both down- and upstream sections of the pipe system that contains fast closing valves. Innovative aspects are system operates without additional energy support, water hammer is strongly reduced, cavitation hammer due to vapour bubble collapse is totally avoided, valve closing process performed is always the fastest without risk of pipe damage, optimal adaptation of closing process to operation parameter and switching state of the respective plant.

George E. Alves (2004) presented his study titled ‘Hydraulic Analysis of Sudden Flow Changes in a Complex Piping Circuit’. He explained that a problem arose if

there were sudden failures of power to one or more pumps of a larger scale complex piping circuit composed of several individual pumping systems. His study describes the application of several published methods of hydraulic transient analysis to the problem. The performance of the system computed under several assumptions is discussed, and a comparison is made with experimentally determined values.

Daniel Ward (2004) realised the study titled 'Automatic and Remotely Controlled Shutoff for Direct Flow Liquid Manure Application Systems'.

G.A. Clark, A.G. Smajstrla and D.Z. Haman (2004) studied water hammer in Irrigation Systems' in University of Florida, Gainesville. This publication discusses the causes of water hammer and the importance of proper system design and management to ensure a cost effective, long-lasting irrigation system.

A. Bergant, A.R. Simpson and A.S. Tijsseling (2005) realised a study titled 'Water Hammer with Column Separation: A Historical Review'. This study reviews water hammer with column separation from the discovery of the phenomenon in the late 19th century, the recognition of its danger in the 1930s, the development of numerical methods in the 1960s and 1970s, to the standard models used in commercial software packages in the late 20th century.

Tilman Diesselhorst and Ulrich Neumann (2005) performed the study of 'Optimization of Loads in Piping Systems by the Realistic Calculation Method: Applying Fluid-Structure Interaction (FSI) and Dynamic Friction'. They demonstrated that to reduce costs and to extend the life time of piping systems their design loads due to valve action have to be optimized. To get the best effect, the results of the fluid dynamic and structural calculations should be realistic as far as possible. Therefore the calculation programs were coupled to consider the fluid structure interaction and the effect of dynamic fluid friction was introduced to get realistic results of oscillations due to pressure surges. Detailed modelling of check valve behaviour allows minimizing the pressure surge loading by improving the valve function and adapting it to the system behaviour. The method was validated at

measurements of load cases in power plant piping systems. Results with different load cases show the effectiveness of reducing the fluid forces on piping. Examples are presented to prove the reduction of supports.

Algirdas Kaliatka, Eugenijus Uspuras and Mindaugas Vaisnoras (2005) presented water hammer phenomenon simulations employing the RELAP5 code, a comparison of RELAP5 calculated and measured at CWHTF and AEKI test facilities pressure transient values after a fast opening of the valve and at the appearance of condensation – induced water hammer. An analysis of rarefaction wave travels inside the pipe and the condensation of vapour bubbles in the liquid column for CWHTF experiment is presented. The dependence of the pressure peaks on the evacuation height and the length of the pipeline were investigated. A comparison of RELAP5 code CWHTF experiment simulation by using similar equilibrium options (HEM) and without these options is also presented. The capability of RELAP5 computer code to simulate condensation induced water hammer was investigated.

Kala K. Fleming, Joseph P. Dugandzic, Mark W. LeChevallier and Rich W. Gullick (2006) prepared the research project titled as 'Susceptibility of Potable Water Distribution Systems to Negative Pressure Transients'. They stated that investigating pressure transients improves understanding of how a system will behave in response to a variety of events such as power cut, routine pump shut downs, valve operations, flushing, fire fighting, main breaks and other events that can create significant, rapid, temporary drops in system pressure. This project built upon the work done in previous projects. The purpose of investigating pressure transients is to improve the operator's understanding of how the system will behave in response to a variety of events such as power cut, pump shut downs, valve operations, flushing, fire fighting, main breaks and other events that can create significant rapid drops in system pressure and/or low pressure waves. A review of system conditions and utility procedures are recommended to effectively minimize a system's effects to pressure transients.

Robert A. Leishear (2007) performed his study named ‘Dynamic Pipe Stresses During Water Hammer: A Finite Element Approach’. According to his study, in the wake of the pressure wave, dynamic stresses are created in the pipe wall, which contribute to pipe failures. A finite element analysis computer program was used to determine the three dimensional dynamic stresses that result from pipe wall vibration at a distance from the end of a pipe, during a water hammer event. The analysis was used to model a moving shock wave in a pipe, using a step pressure wave. Both aluminum and steel were modelled for an 8 NPS pipe, using ABAQUS. For either material, the maximum stress was seen to be equal when damping was neglected. At the time the maximum stress occured, the hoop stress was equivalent to twice the stress that would be expected if an equivalent static stress was applied to the inner wall of the pipe. Also the radial stress doubled the magnitude of the applied pressure.

1.3 The scope of the study

The objective of this study is to investigate transient flow due to pump failure. It is aimed to investigate the agreement between results obtained from measurements and those obtained from numerical calculations. The appeared upper and lower pressures in the system as a result of sudden pump failure or shutdown at steady state in the reservoir-pump-pressurised steel pipeline systems are examined.

This study is performed in Şahabettin Demirağ Hydraulic Research Laboratory in Dokuz Eylül University of Civil Engineering Department in İzmir, Turkey. Two different experimental set up are constructed. The first system includes a pipe of 28 meters without a check valve. In the other system, the pipe has a length of 108 meters and a check valve is placed after the pump. In the former system, unsteady flow pressures are measured at downstream of the pump. The unsteady flow pressures are recorded by means of measuring data logger in the latter system at downstream end of the pump and nearly at mid-point of the pipe. Pressures and discharges are calculated at nodal points by using Fortran computer programs.

CHAPTER TWO
BASIC EQUATIONS OF UNSTEADY FLOW

One dimensional differential equations of transient flow may be obtained by Newton's second law of motion and conservation of mass. In these expressions, the dependent variables are H, hydraulic grade line (HGL, piezometric head) and V, average velocity (or Q, discharge). Independent variables, the distance along measured pipe length from upstream end and the time are denoted by x and t.

2.1 Equation of motion

By referring to Figure 2.1, the Newton's second law of motion is applied ($\Sigma F=m.a$). The subscript x denotes the space derivative.

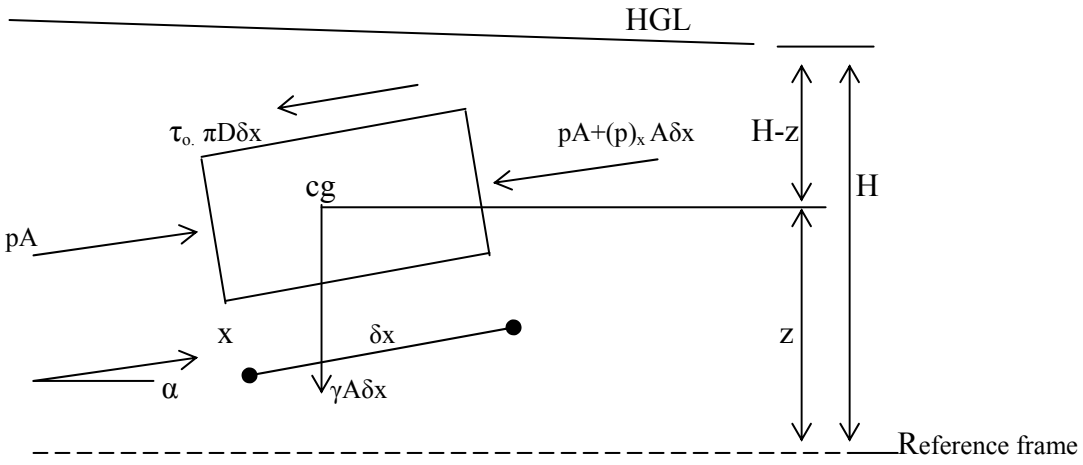

Figure 2.1: Free body diagram of cylindrical tube for application of equation of motion.

The forces on the free body in the x direction are the pressure forces, shear force and gravity force.

$$pA-\left[pA+\frac{\partial(p)}{\partial x}A\delta x\right]-\tau_0\pi D\delta x-\gamma A\delta x\sin\alpha=\rho A\delta x\frac{dV}{dt} \qquad (2\text{-}1)$$

where p is the centreline pressure, A is the cross sectional area of the pipe, δx is the length of cylinder tube, α is the pipe inclination angle with the horizontal, τ_o is the wall shear stress, D is the pipe diameter, γ is the specific weight of fluid, ρ is the mass density of fluid, V is the average velocity and g is the acceleration due to gravity.

After some algebra, we obtain the Equation (2-2),

$$\frac{\partial p}{\partial x} A + \tau_0 \pi D + \rho g A \sin\alpha + \rho A \frac{dV}{dt} = 0 \tag{2-2}$$

Wall shear stress τ_o is assumed to be the same as steady turbulent flow.

$$\tau_0 = \frac{\rho f V|V|}{8} \tag{2-3}$$

where f is Darcy Weisbach friction coefficient. If J_e denotes energy grade line slope,

$$J_e = \frac{f.V.|V|}{D.2g} \tag{2-4}$$

In order to take into consideration the negative flow, absolute value of velocity term in Equation (2-3) is taken. Because shear stress must be surely reverse to the velocity direction. dV/dt is total derivative and from the chain rule,

$$\frac{dV}{dt} = V\frac{\partial V}{\partial x} + \frac{\partial V}{\partial t} \tag{2-5}$$

Velocity V of fluid slice changes both with distance and time. Substituting Equations (2-3) and (2-5) into Equation (2-2) and dividing all terms by ρA, one obtains

$$\frac{1}{\rho}\frac{\partial p}{\partial x}+\frac{fV|V|}{2D}+g\sin\alpha+V\frac{\partial V}{\partial x}+\frac{\partial V}{\partial t}=0 \tag{2-6}$$

Piezometric head H (or HGL elevation above reference frame) may be introduced by using the common relationship,

$$p=\rho g(H-z) \tag{2-7}$$

For fluid slice,

$$\sin\alpha=\frac{\partial z}{\partial x} \tag{2-8}$$

The following Equation is obtained,

$$\frac{\partial p}{\partial x}=\rho g\left(\frac{\partial H}{\partial x}-\sin\alpha\right) \tag{2-9}$$

In this expression, the density, ρ is assumed to be constant. Equation (2-6) is valid for both liquids and gases, but Equation (2-9) is restricted with liquids. Substituting Equation (2-9) into Equation (2-6),

$$g\frac{\partial H}{\partial x}+V\frac{\partial V}{\partial x}+\frac{\partial V}{\partial t}+\frac{fV|V|}{2D}=0 \tag{2-10}$$

Equation (2-10) is for unsteady flows and called equation of motion. For the special case of steady flows in pipes with constant diameter, ∂V/∂x and ∂V/∂t are zero. In this case,

$$g\frac{\partial H}{\partial x}=\frac{-fV|V|}{2D} \tag{2-11}$$

$$\Delta H = \frac{-f\Delta x V|V|}{2gD} \tag{2-12}$$

The common Darcy-Weisbach equation is obtained.

2.2 Continuity Equation

Elastic deformations are allowed. The conservation of mass law expresses that rate of mass inflow into the control volume equals time rate of mass increase within the control volume shown in Figure 2.2.

$$\frac{-\partial(\rho A(V))}{\partial x}\delta x = \frac{\partial}{\partial t}(\rho A \delta x) \tag{2-13}$$

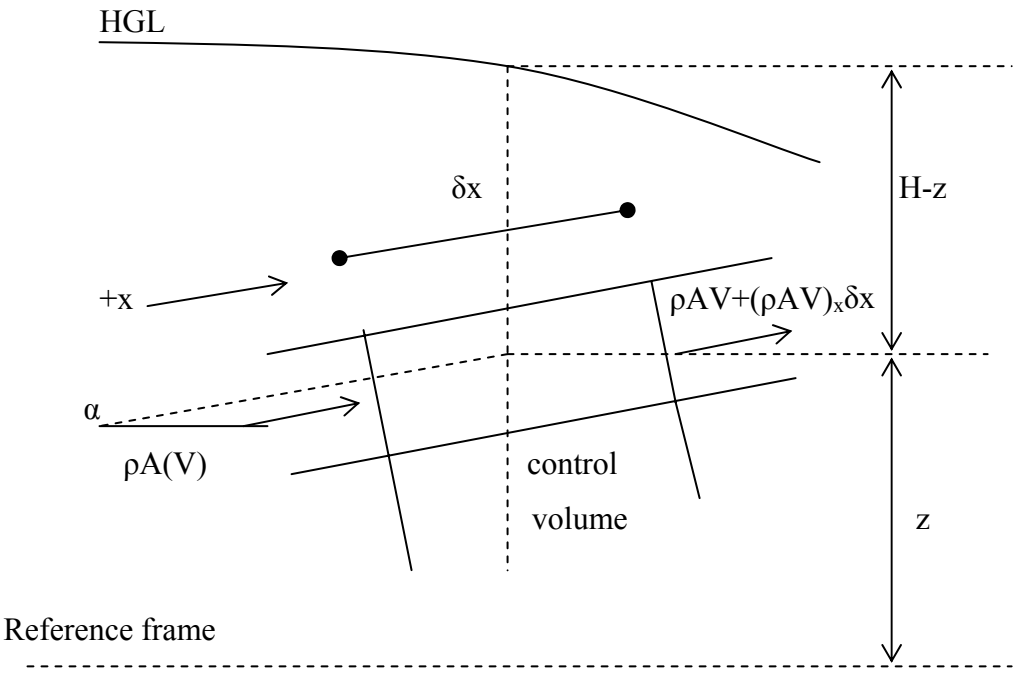

Figure 2.2: Control volume for continuity equation.

$$\frac{\partial(\rho A V)}{\partial x}+\frac{\partial(\rho A)}{\partial t}=0 \tag{2-14}$$

By expanding the first term in the left side of Equation (2-14),

$$\rho A\frac{\partial V}{\partial x}+V\frac{\partial(\rho A)}{\partial x}+\frac{\partial(\rho A)}{\partial t}=0 \tag{2-15}$$

In Equation (2-15), last two terms indicate the total derivative of ρA. From Chain rule,

$$\frac{d(\rho A)}{dt}=V\frac{\partial(\rho A)}{\partial x}+\frac{\partial(\rho A)}{\partial t} \tag{2-16}$$

If we divide the all terms by (ρA) in Equation (2-15) and place the Equation (2-16) into Equation (2-15),

$$\frac{1}{\rho A}\left[\frac{d(\rho A)}{dt}\right]+\frac{\partial V}{\partial x}=0 \tag{2-17}$$

We can write the Equation (2-17) such that,

$$\frac{1}{\rho A}\left(\rho\frac{dA}{dt}+\frac{d\rho}{dt}A\right)+\frac{\partial V}{\partial x}=0 \tag{2-18}$$

Or ,

$$\frac{1}{A}\frac{dA}{dt}+\frac{1}{\rho}\frac{d\rho}{dt}+\frac{\partial V}{\partial x}=0 \tag{2-19}$$

Equation (2-19) may be used in both cylindrical pipes and tubes having variable diameter. This is also valid for very flexible tubes and gaseous flows (Wylie & Streeter, 1993).

The first term of Equation (2-19) relates to elasticity of pipe wall and deformation rate (strain) due to pressure change. Second term takes into account the compressibility of the liquid. From the expression of the bulk modulus,

$$\frac{d\rho}{dt}\frac{1}{\rho} = \frac{1}{K}\frac{dp}{dt} \tag{2-20}$$

Where, K is the bulk modulus of elasticity of fluid, e is the thickness of the pipe wall, E is the Young modulus of elasticity of pipe material. The variation of axial tensile stress σ_1 with time may be designated for three conditions as follow:

a) pipeline is anchored only at upstream end,

$$\frac{d\sigma_1}{dt} = \frac{A}{\pi De}\frac{dp}{dt} = \frac{D}{4e}\frac{dp}{dt} \tag{2-21}$$

b) Pipeline is anchored against longitudinal motions.

$$\frac{d\sigma_1}{dt} = \mu\frac{d\sigma_2}{dt} \tag{2-22}$$

c) Pipeline has expansion joints along its length.

$$\frac{d\sigma_1}{dt} = 0 \tag{2-23}$$

After some algebra Equation (2-19) becomes

$$\frac{1}{\rho}\frac{dp}{dt} + a^2\frac{\partial V}{\partial x} = 0 \tag{2-24}$$

Where a is the wave velocity (celerity).

$$a^2 = \frac{\frac{K}{\rho}}{1+\left[\left(\frac{K}{E}\right)\left(\frac{D}{e}\right)C_1\right]} \tag{2-25}$$

The coefficient, C_1 is described for each condition separately,

a) pipeline is anchored only at upstream end,

$$c_1 = 1 - \frac{\mu}{2} \tag{2-26}$$

b) Pipeline is anchored against longitudinal motions.

$$c_1 = 1 - \mu^2 \tag{2-27}$$

c) Pipeline has expansion joints along its length.

$$c_1 = 1 \tag{2-28}$$

Where, μ is the Poisson's ratio. From the definition of piezometric head,

$$\frac{dp}{dt} = \rho g\left(\frac{dH}{dt} - \frac{dz}{dt}\right) \tag{2-29}$$

$$\frac{dp}{dt} = \rho g\left(V\frac{\partial H}{\partial x} + \frac{\partial H}{\partial t} - V\frac{\partial z}{\partial x} - \frac{\partial z}{\partial t}\right) \tag{2-30}$$

If the pipeline has not transverse motion, $\partial z/\partial t=0$ and $\partial z/\partial x\text{-}Sin\alpha=0$. Equation (2-24) becomes :

$$V\frac{\partial H}{\partial x} + \frac{\partial H}{\partial t} - VSin\alpha + \frac{a^2}{g}\frac{\partial V}{\partial x} = 0 \tag{2-31}$$

This equation is called one dimensional continuity equation (Wylie & Streeter, 1993).

2.3 Celerity in pipelines

In the wave propagation speed formula, Equation (2-25), K is the bulk modulus of elasticity of water and E is the Young modulus of elasticity of steel pipe in Pa. The value of K for water is $2.24.10^9$ Pa and that of E for steel pipes is $2.07.10^{11}$ Pa.

If the D/e ratio is less than 40, thick walled pipe formulas are used. If this ratio is greater than 40, one uses thin walled pipe formulas (Watters, 1979). In pipeline system used in this research, this ratio D/e is equal to 0.125/0.005=25. This value is less than 40. Consequently, we will use proposed formulas for thick walled pipes in the analysis. Conditions are such that

a) pipeline is anchored only at upstream end,

$$C_1 = \frac{2e}{D}(1+\mu) + \frac{D}{D+e}\left(1-\frac{\mu}{2}\right) \tag{2-32}$$

b) Pipeline is anchored against longitudinal motions.

$$C_1 = \frac{2e}{D}(1+\mu) + \frac{D(1-\mu^2)}{D+e} \tag{2-33}$$

c) Pipeline has expansion joints along its length.

$$C_1 = \frac{2e}{D}(1+\mu) + \frac{D}{D+e} \tag{2-34}$$

In our experimental set up, pipeline is anchored against longitudinal motions. Therefore, we will use condition (b), Equation (2-33) and Equation (2-25) in the calculation of celerity. In these formulas, μ is the Poisson's ratio and taken as 0.3 for

steel pipes. Further ρ, mass density is taken as 1000 kg/m^3 for water. C1 is calculated as 0.979. However according to realised computation using Equation (2-25), we will take the celerity value in our transient flow calculations as 1331 m/s.

For the case a, C1 is 0.921 and the celerity is 1339 m/s. For the case c, C1 is 1.065 and celerity is 1318 m/s. C1 and celerity value for our system according to case b, were realised between the case a and case c.

CHAPTER THREE
NUMERICAL SOLUTION WITH THE USE OF METHOD OF CHARACTERISTICS

Equation of motion (dynamic or momentum equation) and continuity equation were developed in Chapter Two, are first order hyperbolic partial differential equations. Analytical solution of these equations is not possible. As a first step, partial differential equations are transformed to ordinary differential equations by using the characteristic method, and then, they are solved numerically by explicit finite difference scheme (Wylie & Streeter, 1978, 1993).

3.1 Characteristic equations

Equation of motion and Equation of continuity are transformed to two ordinary differential equations by the method of characteristics. Less important terms, V.∂V/∂x in Equation (2-10), V.∂H/∂x and V.sinα in Equation (2-31) are neglected for the sake of simplicity (Wylie & Streeter, 1978, 1993).

By neglecting the above mentioned terms, Equation (2-10) and (2-31) become

$$L_1 = g\frac{\partial H}{\partial x} + \frac{\partial V}{\partial t} + \frac{fV|V|}{2D} = 0 \tag{3-1}$$

$$L_2 = \frac{\partial H}{\partial t} + \frac{a^2}{g}\frac{\partial V}{\partial x} = 0 \tag{3-2}$$

These equations are combined linearly by using unknown multiplier λ.

$$L = L_1 + \lambda L_2 = \lambda\left[\frac{\partial H}{\partial x}\frac{g}{\lambda} + \frac{\partial H}{\partial t}\right] + \left[\frac{\partial V}{\partial x}\lambda\frac{a^2}{g} + \frac{\partial V}{\partial t}\right] + \frac{fV|V|}{2D} = 0 \tag{3-3}$$

Considering the chain rule,

$$\frac{dH}{dt} = \frac{\partial H}{\partial x}\frac{dx}{dt} + \frac{\partial H}{\partial t} \quad ; \quad \frac{dV}{dt} = V\frac{\partial V}{\partial x} + \frac{\partial V}{\partial t} \tag{3-4.a}$$

$$\frac{dV}{dt} = \frac{\partial V}{\partial x}\frac{dx}{dt} + \frac{\partial V}{\partial t} \quad ; \quad \frac{dH}{dt} = V\frac{\partial H}{\partial x} + \frac{\partial H}{\partial t} \tag{3-4.b}$$

From examination of Equation (3-3), it is seen that, if

$$\frac{dx}{dt} = \frac{g}{\lambda} = \frac{\lambda a^2}{g} \tag{3-5}$$

The Equation (3-3) becomes ordinary differential equation. If we substitute Equations (3-4) and (3-5) into Equation (3-3),

$$\lambda\frac{dH}{dt} + \frac{dV}{dt} + \frac{fV|V|}{2D} = 0 \tag{3-6}$$

If we solve Equation (3-5) for λ, we obtain particular values of λ,

$$\lambda = \mp\frac{g}{a} \tag{3-7}$$

If we substitute these λ values into Equation (3-5),

$$\frac{dx}{dt} = \mp a \tag{3-8}$$

The substitution of positive and negative values of λ in Equation (3-7) into Equation (3-6) yields two pairs of equations. These equations are named as C^+ and C^- characteristics equations. If the slope is positive then C^+, if the slope is negative then C^- equations are formed.

Equation (3-9) is valid along the C^+ characteristics defined by Equation (3-10).

$$\frac{g}{a}\frac{dH}{dt}+\frac{dV}{dt}+\frac{fV|V|}{2D}=0 \tag{3-9}$$

$$\frac{dx}{dt}=a \tag{3-10}$$

Equation (3-11) is valid along the C^- characteristics defined by Equation (3-12).

$$\frac{-g}{a}\frac{dH}{dt}+\frac{dV}{dt}+\frac{fV|V|}{2D}=0 \tag{3-11}$$

$$\frac{dx}{dt}=-a \tag{3-12}$$

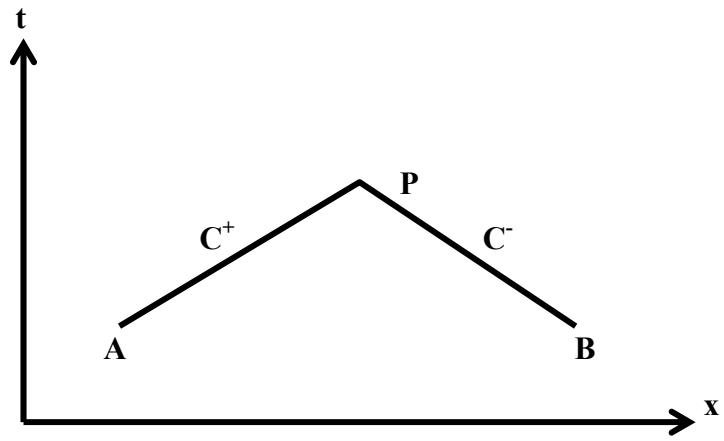

Figure 3.1 : Characteristic lines in the x-t plane.

The wave celerity, a is considered as a constant in the pipeline. Hence, Equations (3-10) and (3-12) correspond to straight lines on the x-t plane. These lines are called

characteristics. Equations (3-9) and (3-11) are called compatibility equations. Each of these equations is valid only along suitable characteristic line. (Wylie & Streeter, 1978, 1993).

3.2 Equations in finite difference form

Length of the pipeline, L is divided into N equal reaches. Each of these reaches is $\Delta x=L/N$ long. Time increment is $\Delta t=\Delta x/a$. If dependent variables V and H in Equation (3-10) are known at point A, this equation can be integrated between points A and P, and the obtained equation contains the unknowns at point P, namely V_P and H_P.

Equation (3-12) is valid along the negative sloped characteristic as shown by BP in Figure 3.2. Integration of the C^- compatibility equation along the line BP, with conditions known at B and unknown at P, leads to a second equation in terms of the same two unknown variables at P, namely V_P and H_P. The simultaneous solution yields conditions at the particular time and position in the xt plane designated by point P.

By multiplying Equation (3-10) with (a/g)dt=dx/g, writing discharge term in place of velocity and introducing the pipeline area, Equation becomes,

$$\int_{H_A}^{H_P} dH + \frac{a}{gA}\int_{Q_A}^{Q_P} dQ + \frac{f}{2gDA^2}\int_{x_A}^{x_P} Q|Q|dx = 0 \qquad \text{(3-13.a)}$$

$$\int_{H_B}^{H_P} dH + \frac{a}{gA}\int_{Q_B}^{Q_P} dQ + \frac{f}{2gDA^2}\int_{x_B}^{x_P} Q|Q|dx = 0 \qquad \text{(3-13.b)}$$

Expressions below are obtained after the integration of Equations (3-13) along the two characteristics.

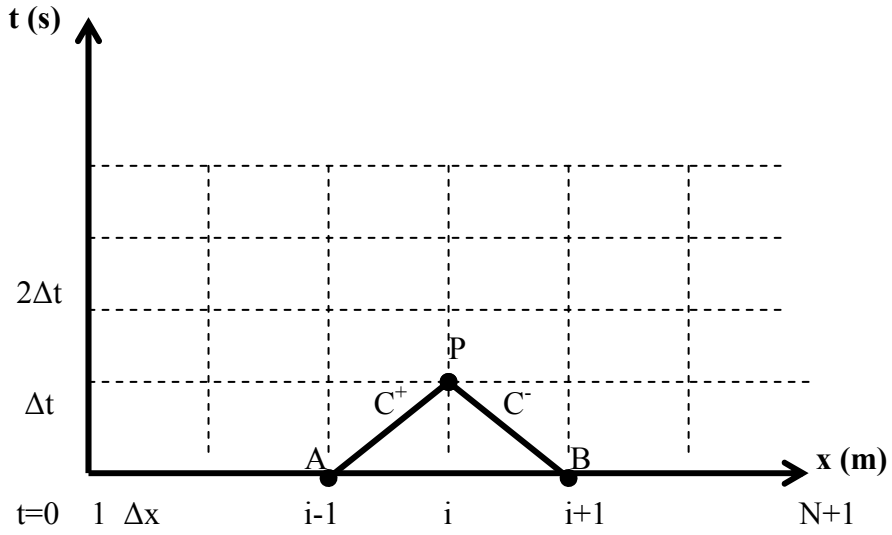

Figure 3.2: x-t grid for solving single pipe problems.

$$H_P - H_A + \frac{a}{gA}(Q_P - Q_A) + \frac{f\Delta x}{2gDA^2} Q_A|Q_A| = 0 \tag{3-14}$$

$$H_P - H_B - \frac{a}{gA}(Q_P - Q_B) - \frac{f\Delta x}{2gDA^2} Q_B|Q_B| = 0 \tag{3-15}$$

These two compatibility equations introduce the piezometric head along pipeline and discharge during transient flow. Solving these equations for H_P,

$$C^+ : H_P = H_A - B(Q_P - Q_A) - RQ_A|Q_A| \tag{3-16}$$

$$C^- : H_P = H_B + B(Q_P - Q_B) + RQ_B|Q_B| \tag{3-17}$$

Where B=a/(gA) which is pipe impedance and R=(fΔx)/(2gDA^2) which is pipeline resistance coefficient.

In steady state conditions, $Q_A=Q_B=Q_P$ and (RQ_AQ_A) is the steady state friction loss along the reach Δx.

The solution of liquid transient problem is generally started with steady state conditions at time zero. For t=0, H and Q are known as initial values at each calculating section. H and Q are calculated for each grid point over t=Δt. Then procedure is repeated for t=2Δt. Procedure is continued until the total number of time step is covered.

Equations (3-16) and (3-17) can be written in simplified form and compatible to computer applications.

$$C^{+}: H_{Pi} = C_P - BQ_{Pi} \tag{3-18}$$

$$C^{-}: H_{Pi} = C_M + BQ_{Pi} \tag{3-19}$$

Where C_P and C_M are known constants.

$$C_P = H_{i-1} + BQ_{i-1} - RQ_{i-1}|Q_{i-1}| \tag{3-20}$$

$$C_M = H_{i+1} - BQ_{i+1} + RQ_{i+1}|Q_{i+1}| \tag{3-21}$$

Eliminating of Q_{Pi} in Equations (3-18) and (3-19),

$$H_{Pi} = \frac{C_P + C_M}{2} \tag{3-22}$$

After the calculation of H_{Pi}, Q_{Pi} can be calculated either from Equation (3-18) or Equation (3-19).

H and Q values having subscripts such as (i-1) and (i+1) at each section are always available from previous time step. They are given either initial conditions or appear as a consequence of previous stage calculations.

3.3 Boundary conditions

At end points, there exists only one compatibility equation but two unknowns. Because of that a second equation corresponding to boundary condition is required. The equation along negative characteristic for upstream end and the equation along positive characteristic for downstream end are combined with the relevant boundary condition.

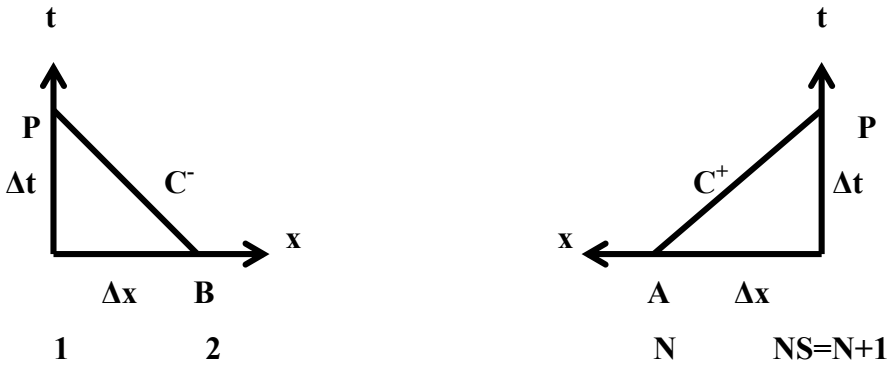

a : Upstream end b: Downstream end

Figure 3.3: Characteristic at boundaries

If we consider a reservoir at upstream end, water surface elevation of upstream reservoir can be assumed as a constant. Water surface elevation defines upstream boundary condition. $H_{P,1}=H_R$. H_R is the water surface elevation of upstream reservoir upon reference level. If the reservoir level is changed as a known pattern (for example, as a sinus wave), boundary condition will be such a manner that,

$$H_{P1} = H_R + \Delta H Sin\omega t \tag{3-23}$$

Where ω is the angular velocity in rad/s and ΔH is the wave amplitude in m. H_{P1} is known at each time step and Q_{p1} is determined from Equation (3-24) directly.

$$Q_{P1} = \frac{H_{P1} - C_M}{B} \tag{3-24}$$

If the centrifugal pump exists at upstream end, the head discharge characteristic curve of centrifugal pump operating at constant speed may be included in the analysis. If the pump provides the flow from suction reservoir, equation below may be used.

$$H_{P1} = H_S + Q_{P1}(a_1 + a_2 Q_{P1}) \tag{3-25}$$

Where H_S is the shutoff head, a_1 and a_2 are the constants describing characteristic curve. If we solve Equation (3-19) and Equation (3-25) simultaneously,

$$Q_{P1} = \frac{1}{2a_2}\left[B - a_1 - \sqrt{\left(B - a_1^{\,2}\right) + 4a_2\left(C_M - H_S\right)}\right] \tag{3-26}$$

is obtained. With known Q_1, H_1 from either Equation (3-19) or Equation (3-25) is determined.

If there is a valve at downstream end of the pipe whose index is NS=N+1, the valve closure law may be written as,

$$Q_{PNS} = \frac{Q_0}{\sqrt{H_0}}\tau\sqrt{H_{PNS}} \tag{3-27}$$

Where Q_0 is the steady state discharge, $\Delta H = H_{PNS}$ is the sudden drop of HGL (of piezometric head) at valve, H_0 is the steady state head loss throughout the valve. For steady flow, $\tau=1$. τ is called the dimensionless valve opening. When there is no flow, $\tau=0$. Solving Equations (3-24) and (3-36) simultaneously,

$$Q_{PNS} = -B.C_V + \sqrt{\left(B.C_V\right)^2 + 2C_V C_P} \tag{3-28}$$

Where $C_V=(Q_0\tau)^2/(2H_0)$. Values corresponding to H_{PNS} can be determined from Equation (3-18) or Equation (3-27).

In our first system, there is a pump at the beginning of the pipeline and a triangular weir at the downstream end. Discharge adjustment valve is placed at an interior point of the pipe. During the measurements, valves openings are kept constant and therefore in the calculations, $\tau = 1$.

In the second system, there is a pump with valve and check valve at the upstream end, a reservoir at the downstream end.

3.4 Courant Criterion

According to Courant criterion,

$$\Delta t \leq \frac{\Delta x}{V \pm a} \tag{3-29}$$

In which Δt is time step or time increment in seconds, Δx is the length of one reach in meters, V is the flow velocity in m/s and a is the pressure wave propagation celerity in m/s. If the flow velocity V is neglected before the celerity, then the common form $\Delta t = \Delta x / a$ is obtained.

Wylie & Streeter, 1993 provided the following criterion to obtain stable results and to prevent discrepancy in the results of numerical solution.

$$\Delta t \leq \frac{\left(I.\pi.N_R\right)}{100.T_R} \tag{3-30}$$

In which I is the moment of inertia of the rotating parts which is equal to WR_g^2/g.

Δt value must be lower or equal to the right side of the Equations (3-29) and (3-30). This is the provision to obtain stable results in the Fortran computer program calculations. If we select the Δt value greater than the value calculated from the right sides of the Equations (3-29) and (3-30), the results will be unstable.

3.5 Losses at regulating valve and relevant equations

3.5.1 Positive Flow

Let us denote by HPU the piezometric head before the valve (point U) and HPD the piezometric head after the valve (point D).

There are four unknowns which are HPU, HPD, Q_{PU} and Q_{PD}. We need four equations. These equations are C^+, C^-, continuity and energy equations. The continuity equation is,

$$Q_{PU} = Q_{PD} = Q_{Pi} \tag{3-31}$$

If CK denotes the valve head loss coefficient, the energy equation will be as :

$$HPU = HPD + \frac{CK.Q_{Pi}^{\ 2}}{2g.A^2} \tag{3-32}$$

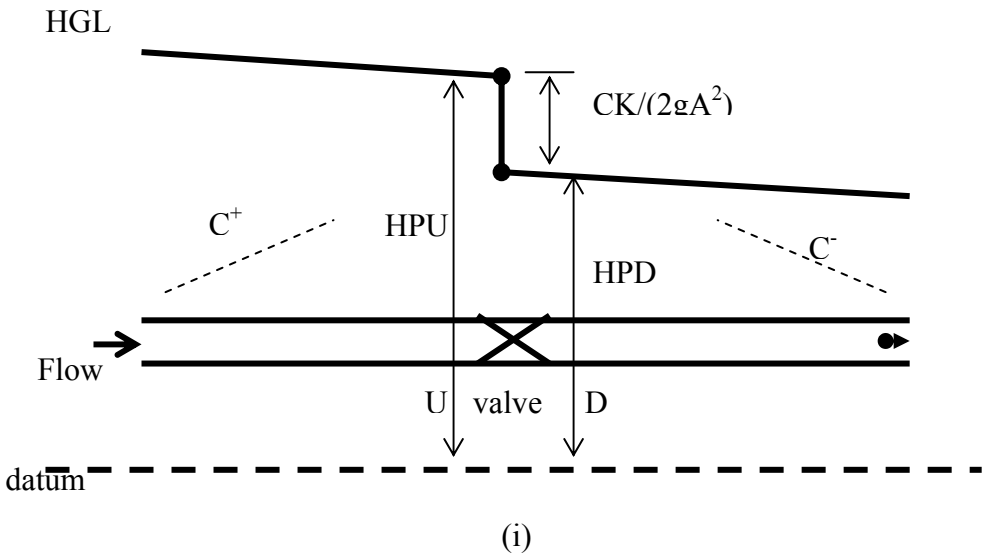

Figure 3.4: Head loss through the reduced bore ball valve.

The characteristic equations :

$$C^+ : HPU = CP - B.Q_{Pi} \tag{3-33}$$

$$C^{-}: HPD = CM + B.Q_{Pi} \tag{3-34}$$

Where

$$CP = H_{i-1} + BQ_i - RQ_{i-1}|Q_{i-1}| \tag{3-35}$$

$$CM = H_{i+1} - BQ_{i+1} + RQ_{i+1}|Q_{i+1}| \tag{3-36}$$

After the simultaneous solution, one obtains

$$Q_{Pi} = 0.5(-C4 + \sqrt{C4^2 - 4C5}) \tag{3-37}$$

Where ,

$$C4 = \frac{2B}{C3} \tag{3-38}$$

$$C5 = \frac{CM - CP}{C3} \tag{3-39}$$

$$C3 = \frac{CK}{2gA^2} \tag{3-40}$$

HPU and HPD are determined by using Equations (3-33) and (3-34), after the calculation of Q_{Pi} value from Equation (3-37).

C4 and C5 are the constants.

3.5.2 Negative (Reverse) Flow

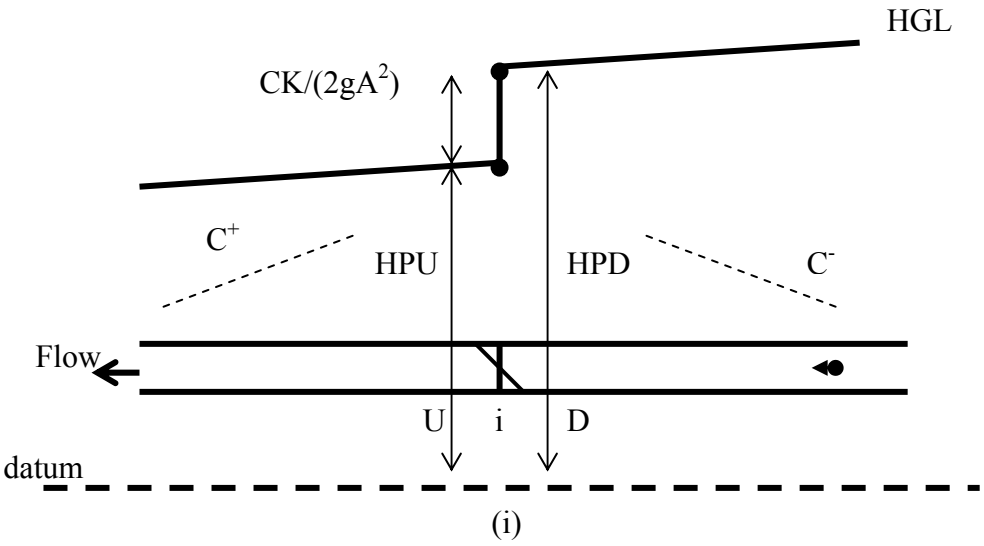

Figure 3.5: Head loss through the reduced bore ball valve for reverse flow.

The continuity equation requires

$$Q_{PU} = Q_{PD} = Q_{Pi} \tag{3-41}$$

The energy equation is

$$HPD = HPU + \frac{CK.Q_{Pi}^{\ 2}}{2g.A^2} \tag{3-42}$$

The characteristic equations may be written as

$$C^+ : HPU = CP - B.Q_{Pi} \tag{3-43}$$

$$C^- : HPD = CM + B.Q_{Pi} \tag{3-44}$$

Where

$$CP = H_{i-1} + BQ_i - RQ_{i-1}|Q_{i-1}| \tag{3-45}$$

$$CM = H_{i+1} - BQ_{i+1} + RQ_{i+1}|Q_{i+1}| \tag{3-46}$$

After the simultaneous solution, one obtains

$$Q_{Pi} = 0.5(C4 - \sqrt{C4^2 + 4C5}) = X_2 \tag{3-47}$$

Similarly HPU and HPD are obtained from the relevant characteristic equations.

3.6 Calculation of Darcy-Weisbach friction coefficient

Darcy Weisbach friction coefficient is assumed to be equal to that corresponding to the steady state given by Equation (3-48) (Yanmaz, 2001).

$$\frac{1}{\sqrt{f}} = 1.14 - 2\log(\frac{k_s}{D} + \frac{21.25}{R_e^{0,9}}) \quad ; \quad \text{for } R_e > 3000 \tag{3-48}$$

Where f is the Darcy-Weisbach friction coefficient, R_e=VD/ν is Reynold's number, k_s/D is relative roughness. Roughness height, k_s is read from the table as 0.00015 m for steel pipes.

In the Fortran computer programs, Darcy Weisbach friction coefficient is calculated by using Equation (3-48) for steady state discharges.

CHAPTER FOUR
TRANSIENTS CAUSED BY CENTRIFUGAL PUMPS

4.1 Introduction

Many transient situations caused by pumps are due to sudden starting up of pump, sudden pause or sudden power failure of pump, associated with opening or closing of valve. In this research, we examine the sudden power failure of pump excluding valve opening or closing.

Changes in operating condition of turbo machine result to develope transient flow in hydraulic system. Method of characteristics discussed in chapter three is used for analysing this transient. Special boundary conditions at the upstream and downstream ends of the pipeline are developed.

Transients caused by pump operation are generally violent and pipeline should be designed to withstand the negative and positive pressures which will be developed in the pipeline. After the electricity connection is cut off, pump speed reduces. Flow inside the discharge line reduces to zero rapidly and then returns to the pump. While the impeller of pump is rotated in respective normal direction, in the situation of deceleration to the zero velocity, to zero rotational speed, pump is said to operate in 'zone of energy dissipation'. When the pump returns reverse, pump is said to operate in 'turbine zone'. Because of the reverse flow, pump velocity decrease to zero rapidly and then pump starts to operate in reverse direction. Pump velocity increases in reverse direction until the pump velocity reaches normal run away speed (Chaudhry, 1987). In the second pipeline system, a disc type check valve is used in order to prevent reverse flow after the power failure.

If HGL (piezometric head line) drops to below of pipeline elevation at any point, pressure will be negative and if the decrease in pressure is severe, cavitation may occur and water column in the pipeline may be separated in this point. Excessive pressure will be produced when the two columns are joined again.

4.2 Similarity laws and pump characteristics

There are four quantities describing the pump characteristics. Total dynamic head H, discharge Q, shaft torque T and rotational speed N. Two of these four quantities are considered independently, i.e. for specific Q and N, H and T are designated from characteristics. Two basic assumptions are made. 1) Steady state characteristics are hold for unsteady state conditions. 2) Similarity relations are valid (Wylie & Streeter, 1978, 1993). Similarity equations are designated as below.

$$\frac{Q_1}{\left(N_1 D_1^{\,3}\right)} = \frac{Q_2}{(N_2 D_2^{\,3})} \tag{4-1.a}$$

$$\frac{H_1}{(N_1 D_1)^2} = \frac{H_2}{(N_2 D_2)^2} \tag{4-1.b}$$

Where, 1 and 2 subscripts are referred to two different dimensional units of similarity series. For a given unit, Equations (4-1) takes a form such that,

$$\frac{H_1}{N_1^{\,2}} = \frac{H_2}{N_2^{\,2}} \tag{4-2.a}$$

$$\frac{Q_1}{N_1} = \frac{Q_2}{N_2} \tag{4-2.b}$$

Similarity theory assumes that the efficiency does not change with pump's dimension. Hence

$$\frac{T_1 N_1}{Q_1 H_1} = \frac{T_2 N_2}{Q_2 H_2} \tag{4-3}$$

Other combinations of Equations (4-2) and (4-3) produce the expressions below.

$$\frac{T_1}{N_1^2}=\frac{T_2}{N_2^2} \qquad \frac{H_1}{Q_1^2}=\frac{H_2}{Q_2^2} \qquad \frac{T_1}{Q_1^2}=\frac{T_2}{Q_2^2} \tag{4-4}$$

If we study with dimensionless characteristics,

$$h=\frac{H}{H_R} \qquad \beta=\frac{T}{T_R} \qquad v=\frac{Q}{Q_R} \qquad \alpha=\frac{N}{N_R} \tag{4-5}$$

Where, the subscript R denotes the rated quantities which correspond to values of H, T, Q and N at the best efficiency point on the pump characteristic curve. Dimensionless similarity relations can be expressed as follows,

$$\frac{h}{\alpha^2} vs. \frac{v}{\alpha} \qquad \frac{\beta}{\alpha^2} vs. \frac{v}{\alpha} \qquad \frac{h}{v^2} vs. \frac{\alpha}{v} \qquad \frac{\beta}{v^2} vs. \frac{\alpha}{v} \tag{4-6}$$

From the computational aspect, these relations are not convenient. Because the signs of h, β, v and α might be change due to different operating zones and during the transients, the values of all may go to zero. Marchal, Flesch, Suter have been coped with this difficulty using the expressions below (Wylie & Streeter, 1978, 1993).

$$\frac{h}{\alpha^2+v^2} vs. \tan^{-1}\left(\frac{v}{\alpha}\right) \tag{4-7.a}$$

$$\frac{\beta}{\alpha^2+v^2} vs. \tan^{-1}\left(\frac{v}{\alpha}\right) \tag{4-7.b}$$

The angle $\theta=x=\pi+\tan^{-1}(v/\alpha)$ may be drawn as absisca against WH(x) or WB(x) as shown in Figure 4.1. Where

$$WH(x)=\frac{h}{\alpha^2+v^2} \tag{4-8.a}$$

$$WB(x) = \frac{\beta}{\alpha^2 + v^2} \tag{4-8.b}$$

$$x = \pi + \tan^{-1}\left(\frac{v}{\alpha}\right) \tag{4-8.c}$$

H, Q, efficiency (η), and power (P) values have been provided from the pump manufacturer for a given N value as pump characteristic curve. Torque values are calculated using these data. These four values produce h, v, β and α at the time in which rated values are given.

Angle, x, WH, WB may be determined for each operation point by the use of Equation (4-8). Producing 89 values of WH and WB with $\Delta x=\pi/44$ radians are demonstrated as reasonable number (Wylie & Streeter, 1978). With specified N_S (specific speed), WH is called the dimensionless head data and WB is called the dimensionless torque data (Wylie & Streeter, 1978, 1993).

In many design conditions, complete pump characteristics (WH and WB) are not available in the manufacturer. From other available test data, WH and WB values can be generated. Curves tend to similar shapes for same specific speeds.

$$N_S = \frac{N_R \sqrt{Q_R}}{H_R^{\frac{3}{4}}} \tag{4-9}$$

Where N_S is the dimensionless specific speed, N_R is the rated rotational velocity in rpm, Q_R is the rated discharge in m^3/s, H_R is the rated head in meters. If such data are not available, data can be selected by comparison with other curves which are valid for various specific speeds available in literature. These data are dimensionless, therefore they can be used in both English Gravitational System of Units (EGSU) and International System of Units (SI) (Wylie & Streeter, 1978, 1993).

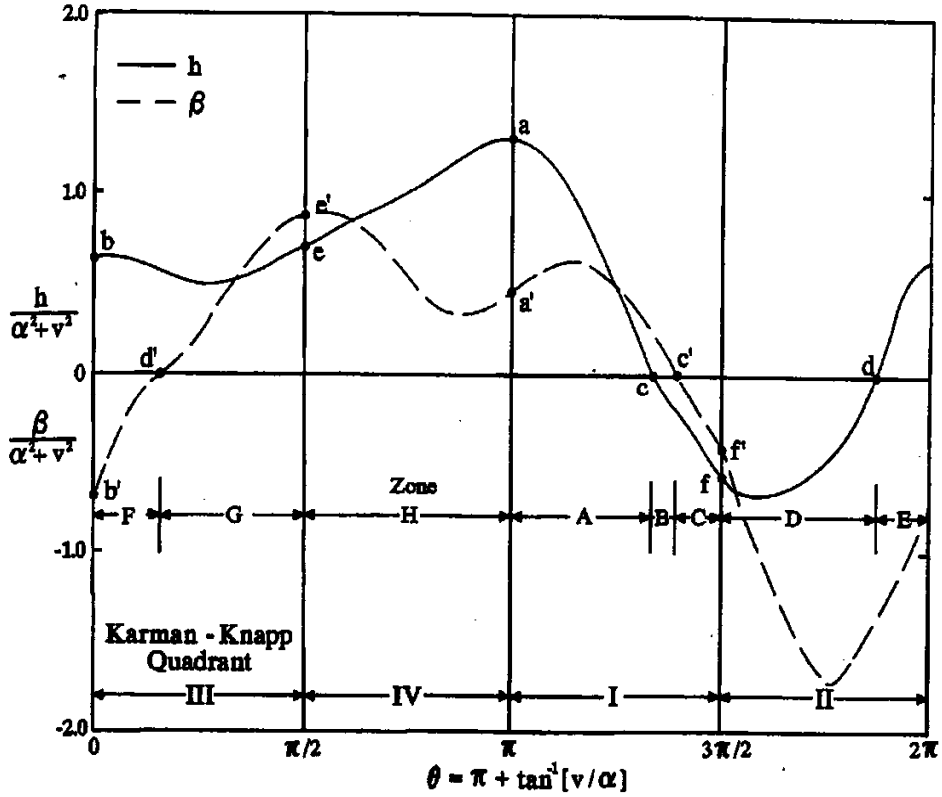

Figure 4.1: Complete pump characteristics (89 values of WH and 89 values of WB vs. θ, theta angles) for Ns=25 (SI) (Mays, 1999).

Our pump is operated in normal zone in steady state in the first quadrant, zone A excluding zones B and C.

After the pump is run down, v will be decreased to zero, dissipation zone (Quadrant 4, Zone H) will be dominant. In this zone, α is already greater than zero but there are deceleration in both v and α. Then pump will operate in turbine zone in the third quadrant. In turbine zone, pump impeller rotates with reverse speed due to backward flow, i.e. $v \leq 0$ and $\alpha < 0$ (Zone G). Quadrant 2 corresponds to reverse speed dissipation zone.

To obtain graphs of WH and WB related to our pump shown the steps given in Table 4-1 are followed.

Table 4.1: Calculation of WH and WB values of our pump for normal pump operation zone.

Theta	α	V	Q,m^3/h	H, m	P, kw	h	Beta,β	WH	WB
184.09	1	0.01	2.15	14.00	3.10	1.27	0.63	1.27	0.63
188.18	1	0.08	11.43	14.00	3.17	1.27	0.64	1.26	0.64
192.27	1	0.16	20.83	14.00	3.50	1.27	0.71	1.24	0.69
196.36	1	0.23	30.44	14.00	3.60	1.27	0.73	1.20	0.69
200.45	1	0.31	40.40	14.00	3.70	1.27	0.75	1.15	0.68
204.54	1	0.39	50.80	13.90	3.80	1.26	0.77	1.09	0.67
208.63	1	0.47	61.80	13.75	4.00	1.25	0.81	1.01	0.66
212.72	1	0.56	73.56	13.70	4.10	1.24	0.83	0.94	0.63
216.81	1	0.66	86.33	13.40	4.20	1.21	0.85	0.84	0.59
220.90	1	0.77	100.38	12.80	4.50	1.16	0.91	0.72	0.57
224.99	1	0.89	116.08	11.90	4.70	1.08	0.95	0.60	0.53
229.09	1	1.03	133.96	10.50	4.80	0.95	0.97	0.46	0.47
233.18	1	1.19	154.67	9.00	5.00	0.81	1.02	0.33	0.42

Graphs given in Figure 4.2 and 4.3 are drawn with respect to WH and WB values obtained and specified and calculated in Table 4.1 for normal pump operation zone.

For instance, if we calculate the first row of Table 4.1, we first determine the column 1 about π / 44 radians. To find angle Theta, θ, (180/44)*45=184.09. We calculate the v from Equation (4-8.c), that is, α.tan(theta-π)=v . The value of α is known as 1 for steady state normal pump operation zone. The value of Q is determined from that $Q=v.Q_R$ read from the pump characteristic curve of values of H, and P against to discharge, Q given in Figure 5.7. Once h, β are determined from Equation (4-5), $h=H/H_R$ and $\beta=P/P_R$ in which H_R, Q_R and P_R correspond to 11 m, 130 m^3/h and 4.9 kw respectively for rated conditions. From Equations (4-8.a) and (4-8.b), we find the values of WH and WB for normal pump operation zone and we drawn the graphs in Figure 4.2 and 4.3 representing the WH and WB values for normal pump operation zone with dark blue lines in the figures as also specified in Table 4.1.

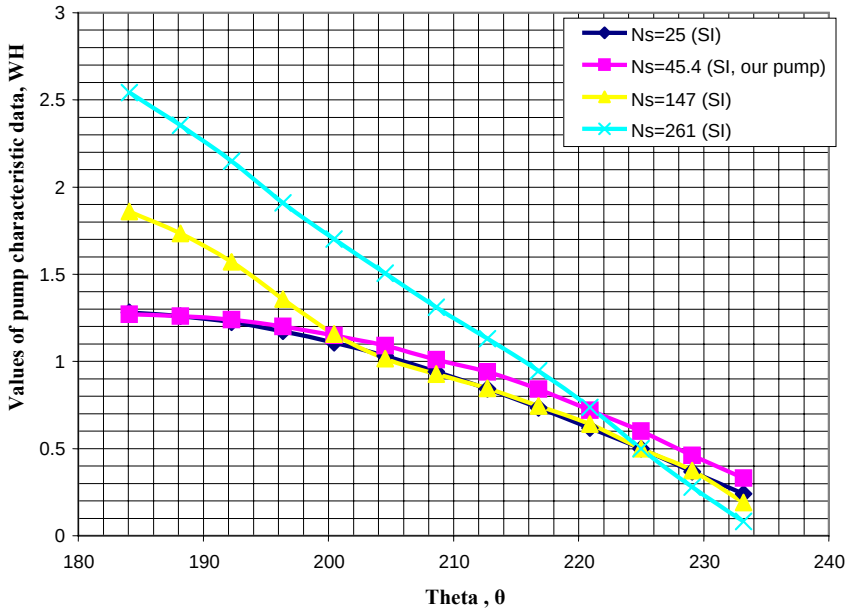

Figure 4.2: Dimensionless head data, WH, drawn for normal pump operation zone. X axis corresponds to theta (θ) and y axis corresponds to WH values (Wylie & Streeter, 1993) (between 184.09 degrees Theta angle with 233.18 degrees Theta angle).

As seen form the graph, lines for N_S=25 and 45.54 are in good agreement with each other. Because of this agreement, we can consider the dimensionless head data in our computations in system one and system two corresponding to specific speed 25 (SI). But we also realised interpolations between N_S=25 (SI) and N_S=147 (SI) to find values of WH and WB, and in the computer program we used the interpolated values corresponding to N_S=45.55 (SI) (for our pump).

In Figures 4.2 and 4.3, values of WH and WB against to three different specific speeds have no dimensions. Therefore WH and WB values presented by Wylie & Streeter, 1993 are valid both in English Gravitational System of Units (EGSU) and International System of Units, SI. WH and WB values against to three different specific speeds, Ns presented in Wylie & Streeter (1978, 1993) were developed from

Hollander's experiments. 89 values of WH and WB have proved to be a reasonable number (Wylie & Streeter, 1978, 1993).

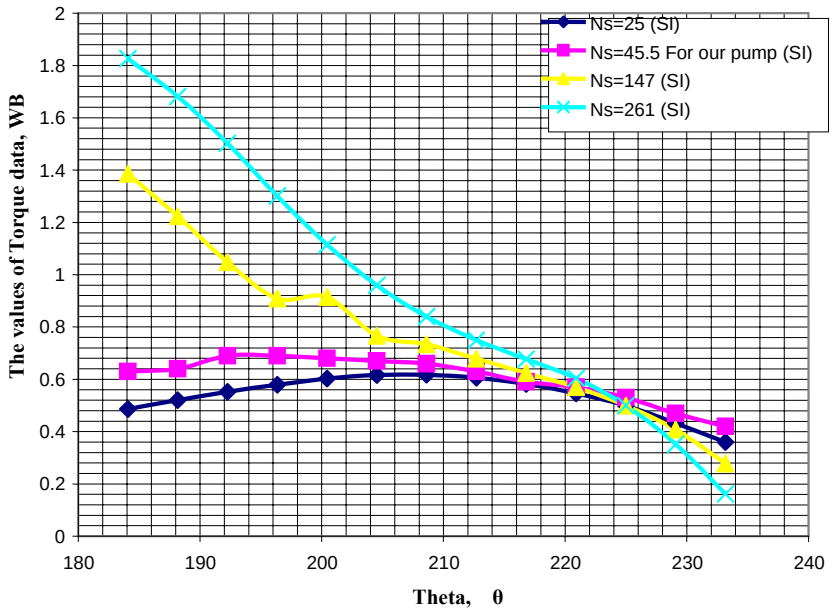

Figure 4.3: Dimensionless torque data, WB, drawn for normal pump operation zone. X axis represents the theta (θ) and y axis represents the WB values (Wylie & Streeter, 1993). (Note that between 184.09 degrees with 233.18 degrees Theta angle).

WH and WB values corresponding to three different values of Ns (25, 147 and 261) are presented in Table 4.2. Table 4.3 contains the WH and WB values corresponding to our pump (Ns=45.5) obtained from interpolation between Ns=25 and Ns=147.

Table 4.2: Dimensionless pump characteristics for various specific speeds against to π/44 radians equal angles.

	N_S=25 (SI)		N_S=147 (SI)		N_S=261 (SI)	
Theta	$h/(\alpha^2+v^2)$	$\beta/(\alpha^2+v^2)$	$h/(\alpha^2+v^2)$	$\beta/(\alpha^2+v^2)$	$h/(\alpha^2+v^2)$	$\beta/(\alpha^2+v^2)$
0.000	0.634	-0.684	-0.690	-1.420	-2.230	-2.260
4.090	0.643	-0.547	-0.599	-1.328	-2.000	-2.061

Table 4.2: (Continued)

8.181	0.646	-0.414	-0.512	-1.211	-1.662	-1.772
12.272	0.640	-0.292	-0.418	-1.056	-1.314	-1.465
16.363	0.629	-0.167	-0.304	-0.870	-1.089	-1.253
20.454	0.613	-0.105	-0.181	-0.677	-0.914	-1.088
24.545	0.595	-0.053	-0.078	-0.573	-0.750	-0.921
28.636	0.575	-0.012	-0.011	-0.518	-0.601	-0.789
32.727	0.552	0.042	0.032	-0.380	-0.440	-0.632
36.818	0.533	0.097	0.074	-0.232	-0.284	-0.457
40.909	0.516	0.156	0.130	-0.160	-0.130	-0.300
44.999	0.505	0.227	0.190	0.000	0.055	-0.075
49.090	0.504	0.300	0.265	0.118	0.222	0.052
53.181	0.510	0.371	0.363	0.308	0.357	0.234
57.272	0.512	0.444	0.461	0.442	0.493	0.425
61.363	0.522	0.522	0.553	0.574	0.616	0.558
65.454	0.539	0.596	0.674	0.739	0.675	0.630
69.545	0.559	0.672	0.848	0.929	0.580	0.621
73.636	0.580	0.738	1.075	1.147	0.691	0.546
77.727	0.601	0.763	1.337	1.370	0.752	0.525
81.818	0.630	0.797	1.629	1.599	0.825	0.488
85.909	0.662	0.837	1.929	1.839	0.930	0.512
89.999	0.692	0.865	2.180	2.080	1.080	0.660
94.090	0.722	0.883	2.334	2.300	1.236	0.850
98.181	0.753	0.886	2.518	2.480	1.389	1.014
102.272	0.782	0.877	2.726	2.630	1.548	1.162
106.363	0.808	0.859	2.863	2.724	1.727	1.334
110.425	0.832	0.838	2.948	2.687	1.919	1.512
114.545	0.857	0.804	3.026	2.715	2.066	1.683
118.636	0.879	0.756	3.015	2.688	2.252	1.886
122.727	0.904	0.703	2.927	2.555	2.490	2.105
126.818	0.930	0.645	2.873	2.434	2.727	2.325
130.909	0.959	0.583	2.771	2.288	3.002	2.580

Table 4.2 : (Continued)

134.999	0.996	0.520	2.640	2.110	3.225	2.770
139.090	1.027	0.454	2.497	1.948	3.355	2.886
143.181	1.060	0.408	2.441	1.825	3.475	2.959
147.272	1.090	0.370	2.378	1.732	3.562	2.979
151.363	1.124	0.343	2.336	1.644	3.604	2.962
155.454	1.165	0.331	2.288	1.576	3.582	2.877
159.545	1.204	0.329	2.209	1.533	3.540	2.713
163.636	1.238	0.338	2.162	1.522	3.477	2.556
167.727	1.258	0.354	2.140	1.519	3.321	2.403
171.818	1.271	0.372	2.109	1.523	3.148	2.237
175.909	1.282	0.405	2.054	1.523	2.962	2.080
179.999	1.288	0.450	1.970	1.490	2.750	1.950
184.090	1.281	0.486	1.860	1.386	2.542	1.826
188.181	1.260	0.520	1.735	1.223	2.354	1.681
192.272	1.225	0.552	1.571	1.048	2.149	1.503
196.363	1.172	0.579	1.357	0.909	1.909	1.301
200.454	1.107	0.603	1.157	0.914	1.702	1.115
204.545	1.031	0.616	1.016	0.766	1.506	0.960
208.636	0.942	0.617	0.927	0.734	1.310	0.840
212.727	0.842	0.606	0.846	0.678	1.131	0.750
216.818	0.733	0.582	0.744	0.624	0.947	0.677
220.909	0.617	0.546	0.640	0.570	0.737	0.604
224.999	0.500	0.500	0.500	0.500	0.500	0.500
229.090	0.368	0.432	0.374	0.407	0.279	0.352
233.181	0.240	0.360	0.191	0.278	0.082	0.161
237.272	0.125	0.288	0.001	0.146	-0.112	-0.040
241.363	0.011	0.214	-0.190	0.023	-0.300	-0.225
245.454	-0.102	0.123	-0.384	-0.175	-0.505	-0.403
249.545	-0.168	0.037	-0.585	-0.379	-0.672	-0.545
253.636	-0.255	-0.053	-0.786	-0.585	-0.797	-0.610
257.727	-0.342	-0.161	-0.972	-0.778	-0.872	-0.662

Table 4.2 : (Continued)

261.818	-0.423	-0.248	-1.185	-1.008	-0.920	-0.699
265.909	-0.494	-0.314	-1.372	-1.277	-0.949	-0.719
269.999	-0.556	-0.372	-1.500	-1.560	-0.960	-0.730
274.090	-0.620	-0.580	-1.940	-2.070	-1.080	-0.810
278.181	-0.655	-0.740	-2.160	-2.480	-1.300	-1.070
282.272	-0.670	-0.880	-2.290	-2.700	-1.500	-1.360
286.363	-0.670	-1.000	-2.350	-2.770	-1.700	-1.640
290.454	-0.660	-1.120	-2.350	-2.800	-1.890	-1.880
294.545	-0.655	-1.250	-2.230	-2.800	-2.080	-2.080
298.636	-0,640	-1.370	-2.200	-2.760	-2.270	-2.270
302.727	-0.600	-1.490	-2.130	-2.710	-2.470	-2.470
306.818	-0.570	-1.590	-2.050	-2.640	-2.650	-2.650
310.909	-0.520	-1.660	-1.970	-2.540	-2.810	-2.810
314.999	-0.470	-1.690	-1.895	-2.440	-2.950	-2.950
319.090	-0.430	-1.770	-1.810	-2.340	-3.040	-3.040
323.181	-0.360	-1.650	-1.730	-2.240	-3.100	-3.100
327.272	-0.275	-1.590	-1.600	-2.120	-3.150	-3.150
331.363	-0.160	-1.520	-1.420	-2.000	-3.170	-3.170
335.454	-0.040	-1.420	-1.130	-1.940	-3.170	-3.200
339.545	0.130	-1.320	-0.950	-1.900	-3.130	-3.160
343.636	0.295	-1.230	-0.930	-1.900	-3.070	-3.090
347.727	0.430	-1.100	-0.950	-1.850	-2.960	-2.990
351.818	0.550	-0.980	-1.000	-1.750	-2.820	-2.860
355.909	0.620	-0.820	-0.920	-1.630	-2.590	-2.660
360.000	0.634	-0.684	-0.690	-1.420	-2.230	-2.260

Table 4.3: Dimensionless pump characteristics for N_s=45.5 (SI) (for our pump) interpolated between N_s=25 (SI) and N_s=147 (SI) against to $\pi/44$ radians equal angles.

	N_S=25 (SI)		N_S=45.5 (SI)		N_S=147 (SI)	
Theta	$h/(\alpha^2+v^2)$	$\beta/(\alpha^2+v^2)$	$h/(\alpha^2+v^2)$	$\beta/(\alpha^2+v^2)$	$h/(\alpha^2+v^2)$	$\beta/(\alpha^2+v^2)$

Table 4.3 : (Continued)

0.000	0.634	-0.684	0.411	-0.808	-0.690	-1.420
4.090	0.643	-0.547	0.4338	-0.6785	-0.599	-1.328
8.181	0.646	-0.414	0.451	-0.5482	-0.512	-1.211
12.272	0.640	-0.292	0.4618	-0.4207	-0.418	-1.056
16.363	0.629	-0.167	0.4719	-0.302	-0.304	-0.870
20.454	0.613	-0.105	0.4793	-0.2013	-0.181	-0.677
24.545	0.595	-0.053	0.4816	-0.1406	-0.078	-0.573
28.636	0.575	-0.012	0.4763	-0.0972	-0.011	-0.518
32.727	0.552	0.042	0.4644	-0.0291	0.032	-0.380
36.818	0.533	0.097	0.4557	0.0416	0.074	-0.232
40.909	0.516	0.156	0.451	0.1028	0.130	-0.160
44.999	0.505	0.227	0.4519	0.1888	0.190	0.000
49.090	0.504	0.300	0.4637	0.2693	0.265	0.118
53.181	0.510	0.371	0.4852	0.3604	0.363	0.308
57.272	0.512	0.444	0.5034	0.4437	0.461	0.442
61.363	0.522	0.522	0.5272	0.5308	0.553	0.574
65.454	0.539	0.596	0.5617	0.6201	0.674	0.739
69.545	0.559	0.672	0.6077	0.7153	0.848	0.929
73.636	0.580	0.738	0.6634	0.8096	1.075	1.147
77.727	0.601	0.763	0.725	0.8652	1.337	1.370
81.818	0.630	0.797	0.7983	0.9321	1.629	1.599
85.909	0.662	0.837	0.8754	1.0058	1.929	1.839
89.999	0.692	0.865	0.9426	1.0696	2.180	2.080
94.090	0.722	0.883	0.9935	1.1217	2.334	2.300
98.181	0.753	0.886	1.0503	1.1545	2.518	2.480
102.272	0.782	0.877	1.1094	1.1723	2.726	2.630
106.363	0.808	0.859	1.1541	1.1731	2.863	2.724
110.425	0.832	0.838	1.1884	1.1494	2.948	2.687
114.545	0.857	0.804	1.2223	1.1259	3.026	2.715
118.636	0.879	0.756	1.2388	1.0831	3.015	2.688
122.727	0.904	0.703	1.2447	1.0149	2.927	2.555

Table 4.3 : (Continued)

126.818	0.930	0.645	1.2573	0.9463	2.873	2.434
130.909	0.959	0.583	1.2642	0.8702	2.771	2.288
134.999	0.996	0.520	1.2729	0.7878	2.640	2.110
139.090	1.027	0.454	1.2746	0.7056	2.497	1.948
143.181	1.060	0.408	1.2926	0.6467	2.441	1.825
147.272	1.090	0.370	1.3069	0.5994	2.378	1.732
151.363	1.124	0.343	1.3281	0.5621	2.336	1.644
155.454	1.165	0.331	1.3541	0.5407	2.288	1.576
159.545	1.204	0.329	1.3733	0.5318	2.209	1.533
163.636	1.238	0.338	1.3936	0.5374	2.162	1.522
167.727	1.258	0.354	1.4066	0.5502	2.140	1.519
171.818	1.271	0.372	1.4121	0.5659	2.109	1.523
175.909	1.282	0.405	1.4120	0.5933	2.054	1.523
179.999	1.288	0.450	1.4029	0.6252	1.970	1.490
184.090	1.281	0.486	1.3785	0.6376	1.860	1.386
188.181	1.260	0.520	1.3400	0.6384	1.735	1.223
192.272	1.225	0.552	1.2833	0.6355	1.571	1.048
196.363	1.172	0.579	1.2032	0.6346	1.357	0.909
200.454	1.107	0.603	1.1154	0.6385	1.157	0.914
204.545	1.031	0.616	1.0436	0.6413	1.016	0.766
208.636	0.942	0.617	0.9395	0.6367	0.927	0.734
212.727	0.842	0.606	0.8427	0.6181	0.846	0.678
216.818	0.733	0.582	0.7349	0.5891	0.744	0.624
220.909	0.617	0.546	0.6209	0.5500	0.640	0.570
224.999	0.500	0.500	0.5000	0.5000	0.500	0.500
229.090	0.368	0.432	0.3690	0.4278	0.374	0.407
233.181	0.240	0.360	0.2317	0.3462	0.191	0.278
237.272	0.125	0.288	0.1041	0.2641	0.001	0.146
241.363	0.011	0.214	-0.0229	0.1818	-0.190	0.023
245.454	-0.102	0.123	-0.1495	0.0728	-0.384	-0.175
249.545	-0.168	0.037	-0.2382	-0.0331	-0.585	-0.379

Table 4.3 : (Continued)

253.636	-0.255	-0.053	-0.3444	-0.1426	-0.786	-0.585
257.727	-0.342	-0.161	-0.4481	-0.2649	-0.972	-0.778
261.818	-0.423	-0.248	-0.5513	-0.3760	-1.185	-1.008
265.909	-0.494	-0.314	-0.6419	-0.4762	-1.372	-1.277
269.999	-0.556	-0.372	-0.7150	-0.5721	-1.500	-1.560
274.090	-0.620	-0.580	-0.8423	-0.8310	-1.940	-2.070
278.181	-0.655	-0.740	-0.9085	-1.0331	-2.160	-2.480
282.272	-0.670	-0.880	-0.9429	-1.1865	-2.290	-2.700
286.363	-0.670	-1.000	-0.9530	-1.2981	-2.350	-2.770
290.454	-0.660	-1.120	-0.9446	-1.4030	-2.350	-2.800
294.545	-0.655	-1.250	-0.9203	-1.5110	-2.230	-2.800
298.636	-0.640	-1.370	-0.9027	-1.6041	-2.200	-2.760
302.727	-0.600	-1.490	-0.8577	-1.6955	-2.130	-2.710
306.818	-0.570	-1.590	-0.8193	-1.7668	-2.050	-2.640
310.909	-0.520	-1.660	-0.7642	-1.8082	-1.970	-2.540
314.999	-0.470	-1.690	-0.7100	-1.8163	-1.895	-2.440
319.090	-0.430	-1.770	-0.6624	-1.8660	-1.810	-2.340
323.181	-0.360	-1.650	-0.5907	-1.7494	-1.730	-2.240
327.272	-0.275	-1.590	-0.4982	-1.6793	-1.600	-2.120
331.363	-0.160	-1.520	-0.3722	-1.6008	-1.420	-2.000
335.454	-0.040	-1.420	-0.2236	-1.5076	-1.130	-1.940
339.545	0.130	-1.320	-0.0519	-1.4177	-0.950	-1.900
343.636	0.295	-1.230	0.0887	-1.3428	-0.930	-1.900
347.727	0.430	-1.100	0.1976	-1.2263	-0.950	-1.850
351.818	0.550	-0.980	0.2889	-1.1097	-1.000	-1.750
355.909	0.620	-0.820	0.3606	-0.9564	-0.920	-1.630
360.000	0.634	-0.684	0.4110	-0.8080	-0.690	-1.420

Interpolated dimensionless head and torque values for the whole range of θ are given in Figures 4.4 and 4.5 respectively with those corresponding to Ns=25 and Ns=147.

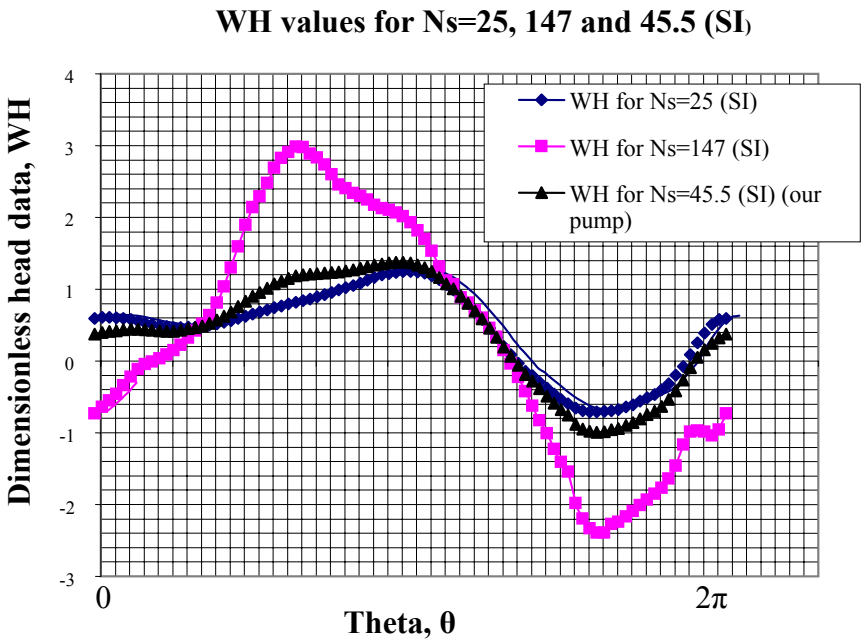

Figure 4.4: Dimensionless head data, WH corresponding to Theta, θ

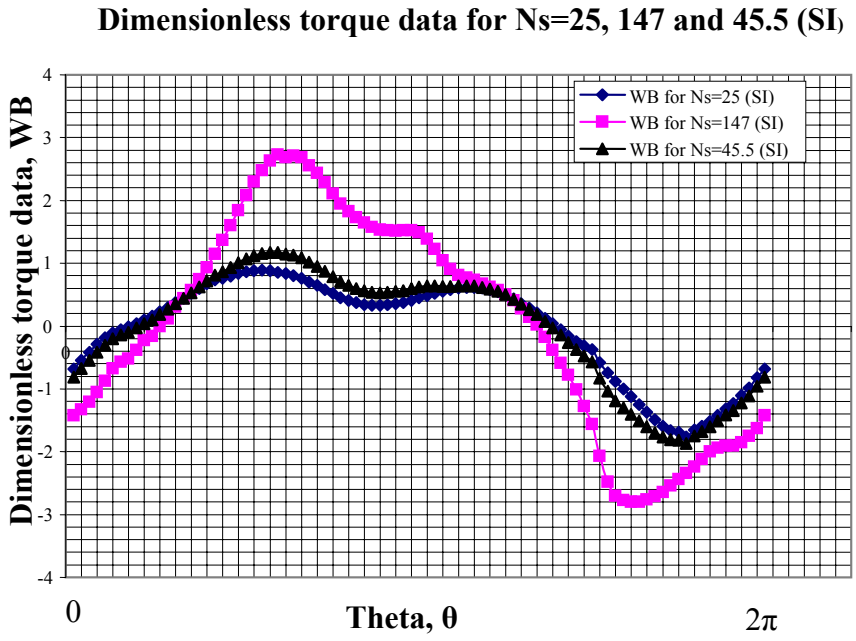

Figure 4.5: Dimensionless torque data, WB corresponding to Theta, θ

The moment of inertia (WRR) of the rotating parts is also needed. This information will be reliable if it is provided from the manufacturer. If not available, some

empirical relations given in literature should be used. Donsky presents a graphic of WRR (the weight of motor rotor times square of radius of gyration) for most of motors. Estimated equation is

$$WRR = 3550\left(\frac{HP}{N}\right)^{1.435} \tag{4-10}$$

Where HP is the power in horse power unit (1 KW=1.338 HP), N is the steady state rotational speed in rpm. The unit of WRR is $lb.ft^2$. We must convert the unit of WRR to $Nt.m^2$ for the convenience to International System of Units (SI).

The value of WRR can be calculated from Equation (4-10). But this formula may produce acceptable results for pumps manufactured before 1960. Calculated WRR value may be upper for pumps manufactured after 1960 (Wylie & Streeter, 1978). Other types of formulas have been presented by Thorley (1991) as an alternative to Equation (4-10) presented by Donsky. According to Thorley (1991),

$$I = I_P + I_M \tag{4-11}$$

Where I is the total rotational inertia in $kg.m^2$, I_P is the inertia of the pump impellers including the entrained water and shaft in $kg.m^2$ and I_M is the rotational inertia of motor in $kg.m^2$.

$$I_P = 1.5.10^7\left(\frac{P_R}{N_R{}^3}\right)^{0.9556} \tag{4-12}$$

$$I_M = 118\left(\frac{P_R}{N_R}\right)^{1.48} \tag{4-13}$$

Where P_R is the rated shaft power in kW and N_R is the rated rotational (radial) speed in rpm. Considered WRR value in our computations is summation of the results from

Equations (4-11), WRR is 0.83 Nt.m^2 which corresponds to latter specified value above suitable for SI. We considered in our computations the formula proposed by Thorley (1991), Equation (4-11). Thorley argue that for preliminary studies this value has sufficient accuracy but for final computations Thorley advice that WRR value should be taken as doubled.

Rated torque value, T_R is needed for our computations as an input value to the computer programs, which can be determined from the formula below.

$$T_R = \frac{30P_R}{\pi N_R} \tag{4-14}$$

Where P_R is the rated power in Watts and N_R is the rotational speed in rpm. According to Equation (4-14), T_R value in the computations is considered as 32.18 Nt.m. α, β, v and h are all positive over the normal pump operation. They can be negative individually or as a group during the transient flows.

4.3 Head balance and Torque angular reducing equations for the 1st system

During computations at the upstream end, the required equations are torque-angular reducing equations describing velocity change against torque as differential equation for pump and head balance equation along pump.

4.3.1 Head balance equation for the 1st system

At the upstream end there exists a pump which delivers water to the system without any valve.

Since suction flange is not long, it is not considered during transient analysis. Therefore the pump is assumed to be located at the upstream end of the system. H_s represent the piezometric head at suction sump.

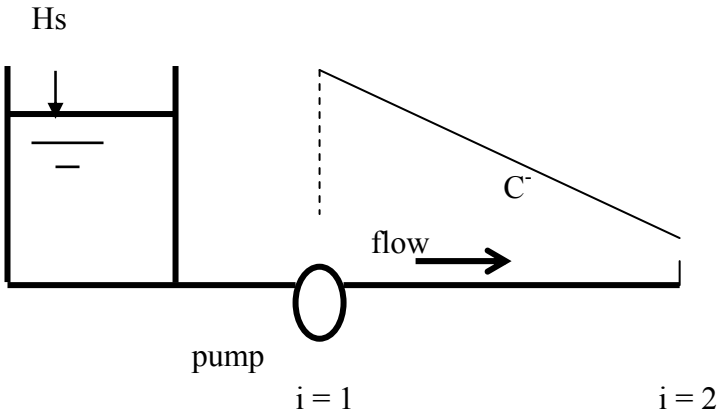

Figure 4.6: Sketch of pump in our first pipeline system

If H_s represent the piezometric head at suction sump, the head balance relationship will be

$$H_S + H = H_{P1} \tag{4-15}$$

In which, H is the total dynamic head added by pump. Total dynamic head, H is translated by assuming that WH varies linearly,

$$tdh = H = H_R h = H_R\left(\alpha^2 + v^2\right)\left(A_0 + A1(\pi + \tan^{-1}\frac{v}{\alpha})\right) \tag{4-16}$$

A linear relationship is assumed to be valid for the segment of WH corresponding to considered time interval. The total dynamic head, tdh is given from the dimensionless similarity relationships in Equation (4-16).

The curve of WH as a function of $x=\pi+\tan^{-1}(v/\alpha)$ is replaced by a straight line representing the characteristic pump head for the proper vicinity of x. In Figure 4.7, the approximate location of $\pi+\tan^{-1}(v/\alpha)$ obtained by interpolating v and α from the previous calculations, a straight line is defined through the two adjoining data points, as follows,

$$I = {}^{x}\!/_{\Delta x} + 1 \tag{4-17}$$

In Figure 4.7, $(I-1)\Delta x, WH(I)$ and $I\Delta x, WH(I+1)$ are the Cartesian coordinates.

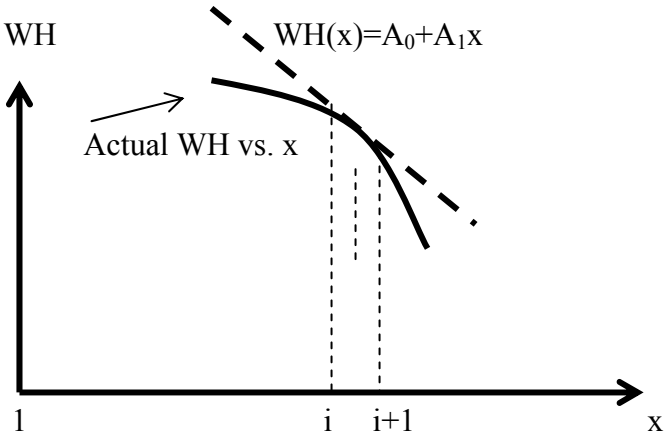

Figure 4.7: Replacement of pump curve with a straight line.

The Cartesian coordinates of two data points are substituted into $WH=A_0+A_1x$,

$$A_1 = \left[WH(I+1) - WH(I)\right]/\Delta x$$
$$A_0 = WH(I+1) - IA_1\Delta x \tag{4-18}$$

$$C^- : HP_1 = CM + BM.Q_{P1} \;\; ; \;\; CM = H_2 - BQ_2 \;\; ; \;\; BM = B + R|Q_2| \tag{4-19}$$

From Equation (4-15),

During the computations, suction pipe has not been considered. If the suction reservoir is taken as datum,

$$H = H_{P1} \tag{4-20}$$

$$H_R(\alpha^2 + v^2)(A_0 + A1.(\pi + \tan^{-1}(\frac{v}{\alpha}))) - CM - BM.Q_1 = 0 \quad (4\text{-}21)$$

By substituting Equation (4-5),

$$Q_1 = v.Q_R$$

Resultant head balance equation for system one will be such that,

$$F_H = H_R(\alpha^2 + v^2)(A_0 + A1.(\pi + \tan^{-1}(\frac{v}{\alpha}))) - CM - BM.v.Q_R = 0 \quad (4\text{-}22)$$

4.3.2 Speed change equation for first system

The change in rotational speed of the pump depends upon the unbalanced torque applied.

$$T = -\frac{WR_g^{\ 2}}{g}\frac{dw}{dt} \quad (4\text{-}23)$$

In which W is the weight of rotating parts plus entrained liquid and R_g is the radius of gyration of the rotating mass, w is the angular velocity in radians per second and dw/dt is the angular acceleration in rad/s^2. The unbalanced torque is represented as the average of T_0, the known torque at beginning of Δt and T_P the unknown torque at the end of Δt. Since

$$w = N_R\frac{2\pi}{60}\alpha \qquad \beta_0 = \frac{T_0}{T_R} \qquad \beta = \frac{T_P}{T_R} \quad (4\text{-}24)$$

Equation (4-25) takes the form that for two Δt,

$$\beta = \frac{WR_g^{\ 2}}{g}\frac{N_R}{T_R}\frac{\pi}{30}\frac{(\alpha_0 - \alpha)}{\Delta t} - \beta_0 \quad (4\text{-}25)$$

α_0 is the dimensionless speed at beginning of Δt. By defining

$$CTORQ = \frac{WR_g^{\,2}}{g}\frac{N_R}{T_R}\frac{\pi}{30.\Delta t} \tag{4-26}$$

Equation (4-27) becomes

$$\beta + \beta_0 - CTORQ(\alpha_0 - \alpha) = 0 \tag{4-27}$$

By assuming linear variation of WB through time interval Δt

$$\frac{\beta}{\alpha^2 + v^2} = WB(x) = B_0 + B_1(\pi + \tan^{-1}\frac{v}{\alpha}) \tag{4-28}$$

In which B_0 and B_1 are found in the same manner as A_0 and A_1. By combining Equations (4-27) and (4-28),

$$F_T = (\alpha^2 + v^2)\left[B_0 + B_1\left(\pi + \tan^{-1}\frac{v}{\alpha}\right)\right] + \beta_0 - CTORQ(\alpha_0 - \alpha) = 0 \tag{4-29}$$

which is the speed change equation in v and α.

The zero subscripts on the dimensionless speed and torque refer to the values two time steps earlier. We calculate the heads at each 2Δt.

Equations (4-22) and (4-29) are solved simultaneously for α and v using the Newton Raphson numerical procedure.

By using founded values of v and α after the simultaneous solution, we correct the v and α values and hence we found the new values of v and α. With the new values of v and α, we find the transient discharge and transient piezometric head values.

4.3.3 Newton Raphson numerical method for first system

If we refer to single pump boundary condition for system one calculations, the solutions of Equations (4-22) and (4-29) is carried out numerically by the Newton-Raphson method. In here, there are two independent variables as α and v in the expressions of Equations (4-22) and (4-29).

In the case of function with one variable, x_{n+1} may be found by using the following Newton Raphson formula.

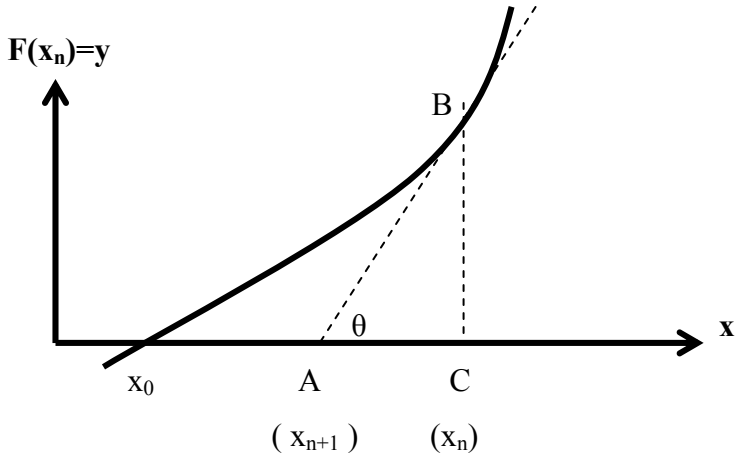

Figure 4.8: Derivation of Newton Raphson formula for one variable.

From Figure 4.8, we define the tan(θ) at point A.

$$\tan\theta = slope = \frac{|BC|}{|AC|} = \frac{F(x_n)}{x_n - x_{n+1}} = \frac{dF(x_n)}{dx}$$

$$x_{n+1} = x_n - \frac{F(x_n)}{\frac{dF(x_n)}{dx}} \tag{4-30}$$

For functions with two variables, say P(x,y) and Q(x,y), from truncated approximation of Taylor series,

$$P(x_n, y_n) = P_n + (x_{n+1} - x_n)P_{nx} + (y_{n+1} - y_n)P_{ny} = 0$$

$$Q(x_n, y_n) = Q_n + (x_{n+1} - x_n)Q_{nx} + (y_{n+1} - y_n)Q_{ny} = 0 \tag{4-31}$$

may be written, where subscripts denote partial derivatives. If we substitute $P(x,y)=F_H(v,\alpha)$ and $Q(x,y)=F_T(v,\alpha)$

$$F_H + F_{Hv}\Delta v + F_{H\alpha}\Delta\alpha = 0$$

$$F_T + F_{Tv}\Delta v + F_{T\alpha}\Delta\alpha = 0 \tag{4-32}$$

v and α are unknown to be determined. As a first step in the solution v and α may be approximated at the end of Δt by an extrapolation of the two next earlier values.

If v_{00} denotes one time step early from v_0,

$$v = 2v_0 - v_{00}$$

$$\alpha = 2\alpha_0 - \alpha_{00} \tag{4-33}$$

F_H, F_{Hv}, $F_{H\alpha}$, F_T, F_{Tv}, $F_{T\alpha}$ are evaluated for this v and α. The derivatives are

$$F_{Hv} = -Q_R(BP + BM) + H_R\left\{2v\left[A_0 + A_1\left(\pi + \tan^{-1}\frac{v}{\alpha}\right)\right] + A_1\alpha\right\} \tag{4-34}$$

$$F_{H\alpha} = H_R\left\{2\alpha\left[A_0 + A_1\left(\alpha + \tan^{-1}\frac{v}{\alpha}\right)\right] - vA_1\right\} \tag{4-35}$$

$$F_{Tv} = 2v\left[B_0 + B_1\left(\pi + \tan^{-1}\frac{v}{\alpha}\right)\right] + \alpha B_1 \tag{4-36}$$

$$F_{T\alpha} = 2\alpha\left[B_0 + B_1\left(\pi + \tan^{-1}\frac{v}{\alpha}\right)\right] - vB_1 + C_{TORQ} \tag{4-37}$$

Equation (4-32) may be solved for Δv, Δα.

$$\Delta\alpha = \frac{\frac{F_T}{F_{Tv}} - \frac{F_H}{F_{Hv}}}{\frac{F_{H\alpha}}{F_{Hv}} - \frac{F_{T\alpha}}{F_{Tv}}} \tag{4-38}$$

$$\Delta v = -\frac{F_H}{F_{Hv}} - \Delta\alpha\frac{F_{H\alpha}}{F_{Hv}} \tag{4-39}$$

Then the new α and v values are evaluated. These new values are the improved values and this procedure is repeated either a fixed number of times or until the tolerance TOL is met. The tolerance represents difference between estimated and calculated values and may be around 0.0002.

$$\alpha = \alpha + \Delta\alpha$$

$$v = v + \Delta v \tag{4-40}$$

$$|\Delta v| + |\Delta\alpha| \langle TOL \tag{4-41}$$

After these equations are solved, the values A_0, A_1, B_0, B_1 must be verified. First we calculate the integer

$$II = \left(\pi + \tan^{-1}\frac{v}{\alpha}\right)/(\Delta x + 1) \tag{4-42}$$

If this equals I in the Equation (4-17) then the solution is represented by the proper straight line segments of WH and WB. If II does not equal I, then the procedure should be repeated by replacing I by II. This may be tried 3 or 4 times, if the equality is not obtained then the program should be stopped with a comment that the boundary condition is in trouble.

4.4 Head balance and Torque angular reducing equations for the 2nd system

4.4.1 Head balance equation for the 2nd system

As shown in Figure 4.9, there exist a check valve and a regulating valve placed nearby the pump at the upstream end. If H and h_L denote the total dynamic head of the pump and local losses respectively

$$H = H_{P1} + h_L \tag{4-43}$$

may be written. The local losses, h_L are due to presence of check valve and valve. The C^- equation between points (1) and (2),

$$HP_1 = CM + BM.Q_{P1} \tag{4-44}$$

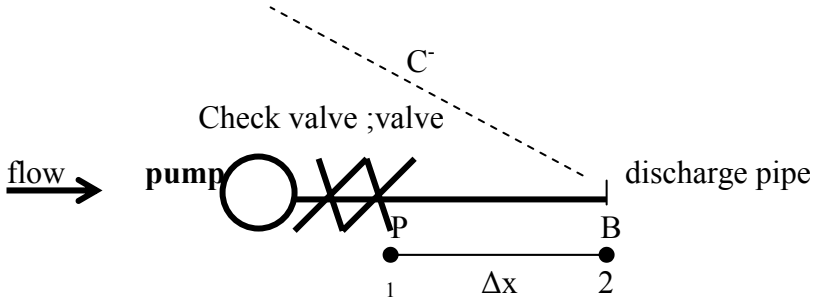

Figure 4.9: Sketch of the pump in a pipeline for system two including check valve and valve.

If one writes the C^- equation for the first reach of the discharge pipe,

$$H_{P1} = H_2 + B[Q_{P1} - Q_2] + R.Q_2.|Q_2| \tag{4-45}$$

Since there is no change in liquid storage between A and B, according to continuity equation, $Q_1=Q_2$. In Equation (4-43), H is obtained from Equation (4-16).

Head losses terms in Equation (4-43) may be written as

$$\text{Valve head losses} = h_L = \frac{DH01.v.|v|}{\tau_1^{\,2}} + \frac{CV.v.|v|}{\tau_2^{\,2}} \quad ; \qquad \text{where} \tag{4-46}$$

$$DH01 = \frac{AKV1.Q_{P1}^{\,2}}{2g.A^2} \; ; \; CV = \frac{CK.Q_{P1}^{\,2}}{2g.A^2} \tag{4-47}$$

In Equation (4-47), AKV1 and CK correspond to local minor loss coefficients of valve and check valve respectively. τ_1 and τ_2 are the opening of valve and that of check valve.

If one writes

$$Q_{P1} = vQ_R \tag{4-48}$$

and by substitution of Equations (4-44), (4-45), (4-46), (4-47) and (4-48) into Equation (4-43),

$$F_H = -CM - BM.Q_R.v + H_R\left(\alpha^2 + v^2\right)\left[A_0 + A_1\left(\pi + \tan^{-1}\frac{v}{\alpha}\right)\right] - \frac{DH01.v.|v| - CV.v.|v|}{\tau^2} = 0 \tag{4-49}$$

There are two unknowns α and v only. This equation is to be solved together with the speed change equation (Wylie & Streeter, 1978).

4.4.2 Torque angular deceleration equation (calculation of speed change equation) for the second system

Our equations specified in Section 4.3.1 for first system which are Equations (4-23), (4-24), (4-25), (4-26), (4-27), (4-28) and (4-29) are exactly valid for this section, i.e. for second system.

4.4.3 Newton Raphson Method for the second system

F_H, F_{Hv}, $F_{H\alpha}$, F_T, F_{Tv}, $F_{T\alpha}$ are evaluated for instantaneous v and α. The derivatives are

$$F_{Hv} = TA^2(H_R\left\{2v\left[A_0 + A_1\left(\pi + \tan^{-1}\frac{v}{\alpha}\right)\right] + A_1\alpha\right\} - BM.Q_R) - 2DH01.|v| - 2CV.|v| \tag{4-50}$$

$$F_{H\alpha} = TA^2(H_R\left\{2\alpha\left[A_0 + A_1\left(\alpha + \tan^{-1}\frac{v}{\alpha}\right)\right] - vA_1\right\}) \tag{4-51}$$

$$F_{Tv} = 2v\left[B_0 + B_1\left(\pi + \tan^{-1}\frac{v}{\alpha}\right)\right] + \alpha B_1 \tag{4-52}$$

$$F_{T\alpha} = 2\alpha\left[B_0 + B_1\left(\pi + \tan^{-1}\frac{v}{\alpha}\right)\right] - vB_1 + C_{TORQ} \tag{4-53}$$

In Equations (4-50) and (4-51), TA is the value of TAU at current Δt. TAU corresponds to valve opening. Equation (4-32) may be solved for Δv, Δα.

$$\Delta\alpha = \frac{\frac{F_T}{F_{Tv}} - \frac{F_H}{F_{Hv}}}{\frac{F_{H\alpha}}{F_{Hv}} - \frac{F_{T\alpha}}{F_{Tv}}} \tag{4-54}$$

$$\Delta v = -\frac{F_H}{F_{Hv}} - \Delta\alpha \frac{F_{H\alpha}}{F_{Hv}}$$

Then the new α and v values are evaluated.

4.5 Use of the Newton Raphson numerical method for determination of steady state parameters

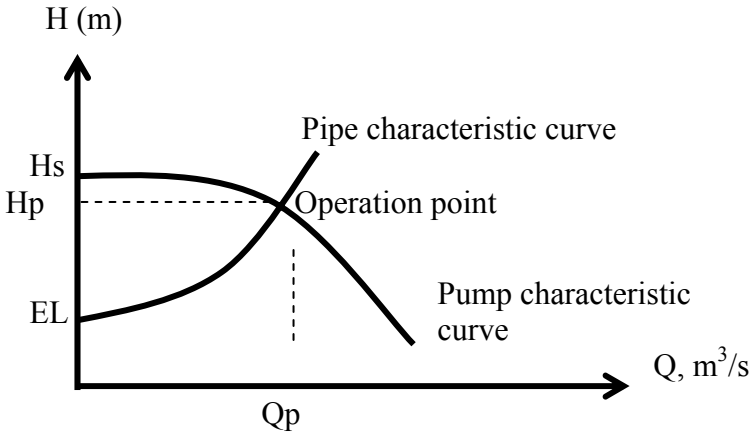

Figure 4.10: Determination of operation point.

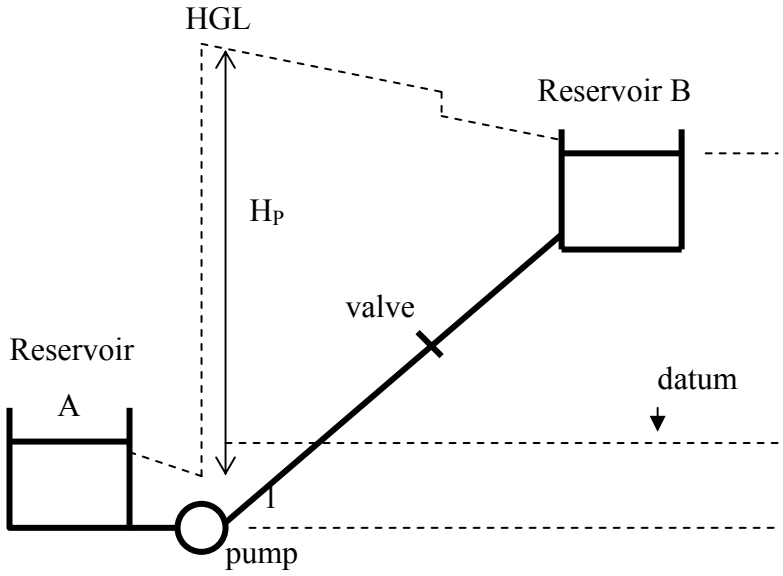

Figure 4-11: Reservoir-pump-pipeline system

Referring to Figure 4.10 and 4.11, one may write the energy equation between suction reservoir A and downstream reservoir B.

$$z_A + \frac{P_A}{\gamma} + \frac{V_A^{\ 2}}{2g} + H_P = z_B + \frac{P_B}{\gamma} + \frac{V_B^{\ 2}}{2g} + h_F + h_L \tag{4-55}$$

In which, z_A and z_B are the elevations at point A (upstream reservoir water surface) and point B (downstream reservoir water surface), respectively. P_A/γ and P_B/γ terms are the pressure heads at point A and point B, and equal to zero. $V_A^2/2g$ and $V_B^2/2g$ are the velocity heads and may be assumed to be equal to zero. H_P is the head in meters added by pump. h_F and h_L represent the major head loss due to friction (Darcy-Weisbach formula) and minor head loss due to local elements, respectively. These losses may be written as follows,

$$h_f + h_l = (\sum \frac{f.L}{D} + \sum K)\frac{V^2}{2g} = (\sum \frac{f.L}{2gDA^2} + \sum \frac{K}{2gA^2})Q^2 = C.Q^2 \tag{4-56}$$

In which f is Darcy Weisbach friction factor, L is length of pipe (m) and K is the local head loss coefficient.

If $z_B - z_A = EL$

The pipe characteristic may be expressed as

$$H_P = EL + C.Q^2 \tag{4-57}$$

One can write also

$$H_P = h.H_R = H_R(\alpha^2 + v^2)(A_0 + A_1 x) \tag{4-58}$$

The operation point is found by intersecting the pump characteristic curve and the pipe characteristic curve as shown in Figure 4.10. For steady state α=1, after combination of the relevant equations, one obtains

$$F_H = -EL - CQ^2 + H_R(1+v^2)(A_0 + A_1.x) \tag{4-59}$$

which is the equation for solving v corresponding to steady state conditions by means of Newton Raphson method.

4.6 Presence of disc type check valve in second system

The second system includes disc type check valve at node 1. If a check valve is used at the pump discharge, the crude assumption may be made that the head loss is constant for all forward flow. For a more accurate treatment, the valve head loss may be expressed as a function of discharge found from valve tests.

To find the criteria for backward flow through the pump and check valve, we set v=0 in Equation (4-49). There is no backward flow due to disc type check valve, after v has been decelerated from steady state value to zero.

CHAPTER FIVE
EXPERIMENTAL SET-UP

Experiments are carried out on two different systems.

5.1 The first experimental set up

In the first system, the pipeline length is 28 meters. Pipe diameter is constant along the pipeline and it is 0.125 meter. Roughness height, k_s is taken as 0.00015 meter obtained from the table for steel pipe. The experimental set up is sketched in Figure 5.1.

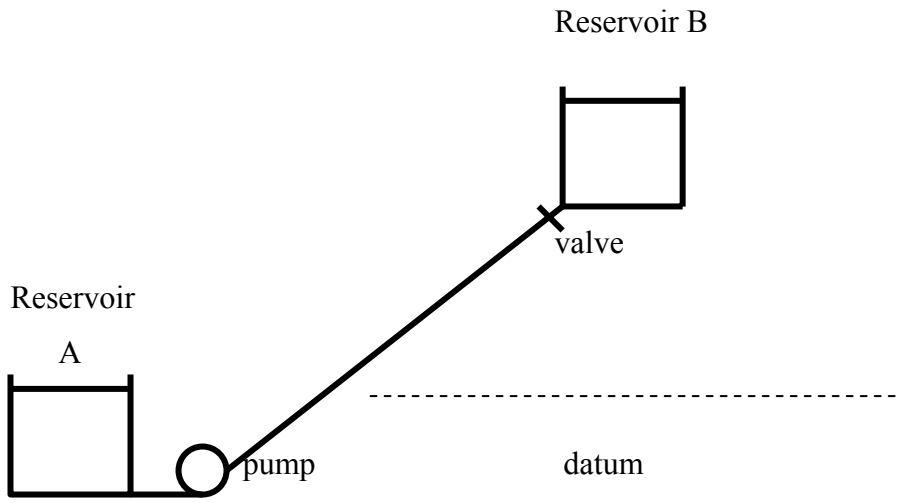

Figure 5.1: Sketch of the first system.

There exist 9 elbows, 1 reduced bore ball valve and 1 tee in the first system.

There is main water tank (reservoir A) immediately at upstream of the pump. Main water tank is placed at upstream of the pump both in first and second systems, and constitutes a source to both systems and constructed in reinforced concrete.

V notched triangular weir is placed at the downstream end point of the systems. The discharge is measured by this V notched triangular weir of 90 degrees.

Triangular weir is calibrated before starting to experiments. It also serves as downstream reservoir B.

The sketch of the V notched triangular weir is given in Figure 5.2

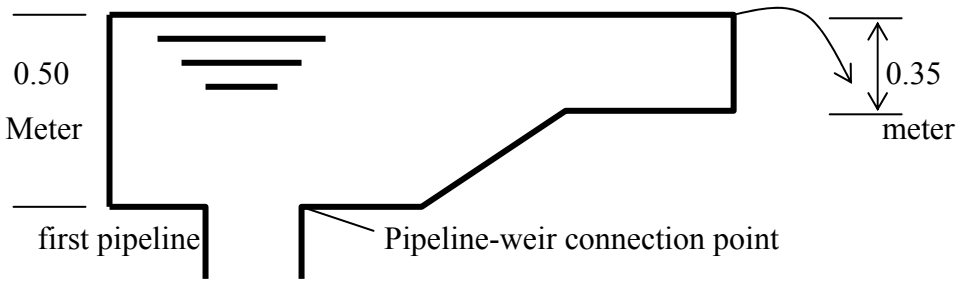

Figure 5.2: The profile of V notched triangular weir of 90 degrees.

In the first pipeline system, pressure measuring point is placed immediately at 0.50 meter after the pump. The end of the measuring device (transducer) is assembled by screwing to this measuring point. The suction pipe is 0.60 meter long.

In Figure 5.3, the location of measuring point in the first system is shown.

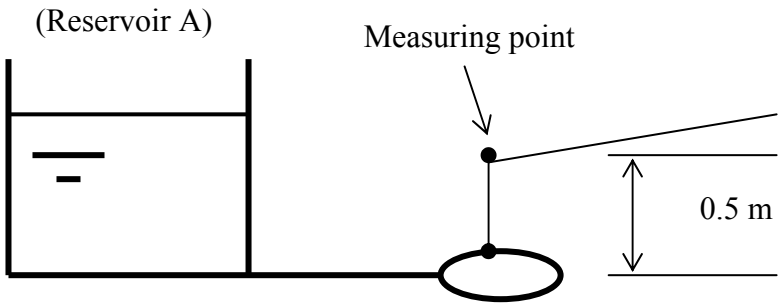

Figure 5.3: The location of measuring point in first system.

After spilling to triangular weir placed at downstream end, water is carried again to main upstream water tank by means of a pipe from downstream tank. Water circulates in the close circuit.

The distances of the pipeline segments from the pump and their elevations are given in Table 5.1. The plan view of the first system is given in Figure 5.4.

The plan view of main upstream water tank (reservoir A) and pump room have also been sketched in Figure 5.4. The dimensions of the main water tank and those of the pump room are 4.50 m*4.50 m and 2.5 m*2.5 m respectively. Water level inside the tank may be seen by the opening of the lid. The reinforced concrete walls of the pump room and the main water tank are 0.30 m thick. In Figure 5.4, ‘e’ letter represents the elbow. The direction of flowing water is shown on the Figure.

Table 5.1: Distances and elevations from the pump in the first system.

Points	Distance from the pump as origin (meters)	Elevation according to datum (pump axis), m
A	1.25	1.25
B	2.50	1.25
C	7.00	1.44
D	8.90	1.46
E	18.90	1.77
F	19.53	2.43
G	20.23	2.45
H	20.73	2.99
I	26.94	2.99
J	28.04	4.20

The characteristics of the pump used in each system are identical. Measuring point is placed immediately after the pump.

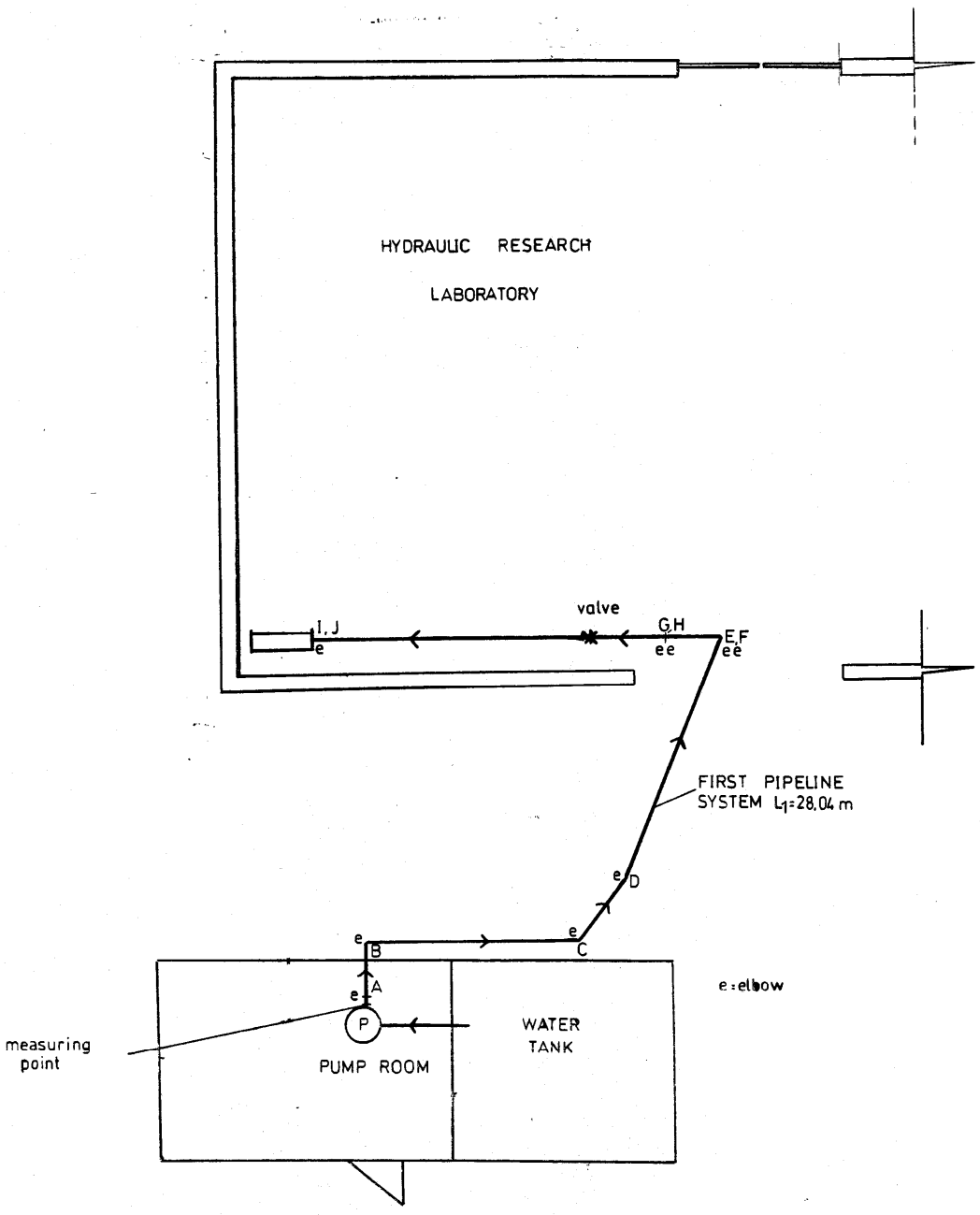

Figure 5.4: Plan view of the first system and the pump room

5.2 Second experimental set-up

In the second system, the length of the pipeline is 108 meters. The elevation difference between pump and downstream end point of the pipeline is 5.3 meters (Figure 5.5). Pipe diameter is 0.125 meter and remains constant along the pipeline reach. There are disc type check valve and reduced bore ball valve immediately at upstream of pump. Roughness height, k_s is taken as 0.00015 m for steel pipe same as in first system. The characteristics of the pump used in each system are identical. The second system contains 14 90^0 elbows, 1 disc type check valve, 2 reduced bore ball valves and 19 junction points.

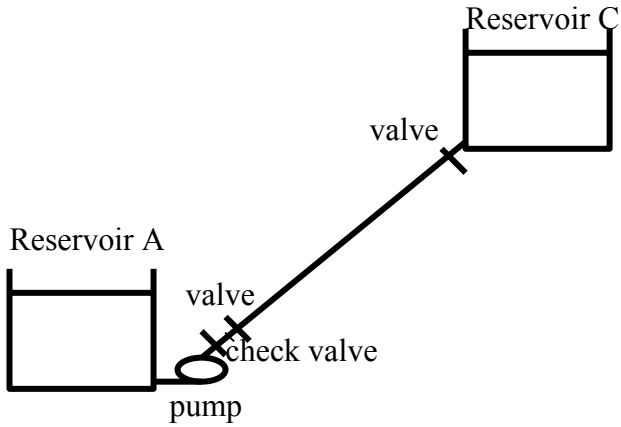

Figure 5.5: Sketch of the second pipeline system.

The location of first measuring point in second system is shown in Figure 5.6. The distances of the pipeline segment from the pump and their elevations are given in Table 5.2. The plan view of the second system is given in Figure 5.7.

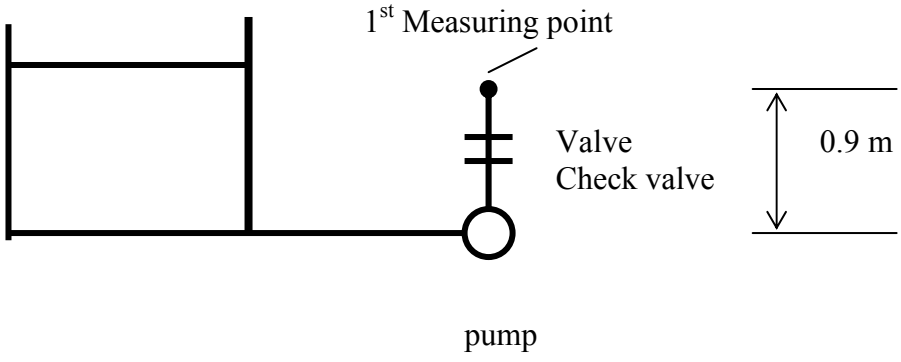

Figure 5.6: The location of first measuring point in second system.

Table 5.2: Distances and elevations from the pump for the second system.

Points	Distance from the pump as origin (meters)	Elevation according to datum (pump axis), m
A^{I}	1.250	1.250
A	2.750	1.250
B	7.700	1.410
C	9.600	1.240
D	18.800	1.510
E	19.800	2.590
F	20.950	2.620
G	27.950	2.540
H	34.150	2.560
I	40.250	2.550
J	46.350	2.520
K	52.350	2.540
L	58.350	2.480
M	58.750	2.480
N	64.550	2.610
O	64.725	2.770
N^{I}	64.900	2.930
N^{II}	66.420	2.900
P	70.800	2.800
R	71.600	2.800
S	77.550	2.800
S^{I}	83.450	2.780
T	89.400	2.810
U	95.300	2.800
U^{I}	101.300	2.810
V	104.800	2.810
Y	105.200	2.810
Z	107.300	5.310

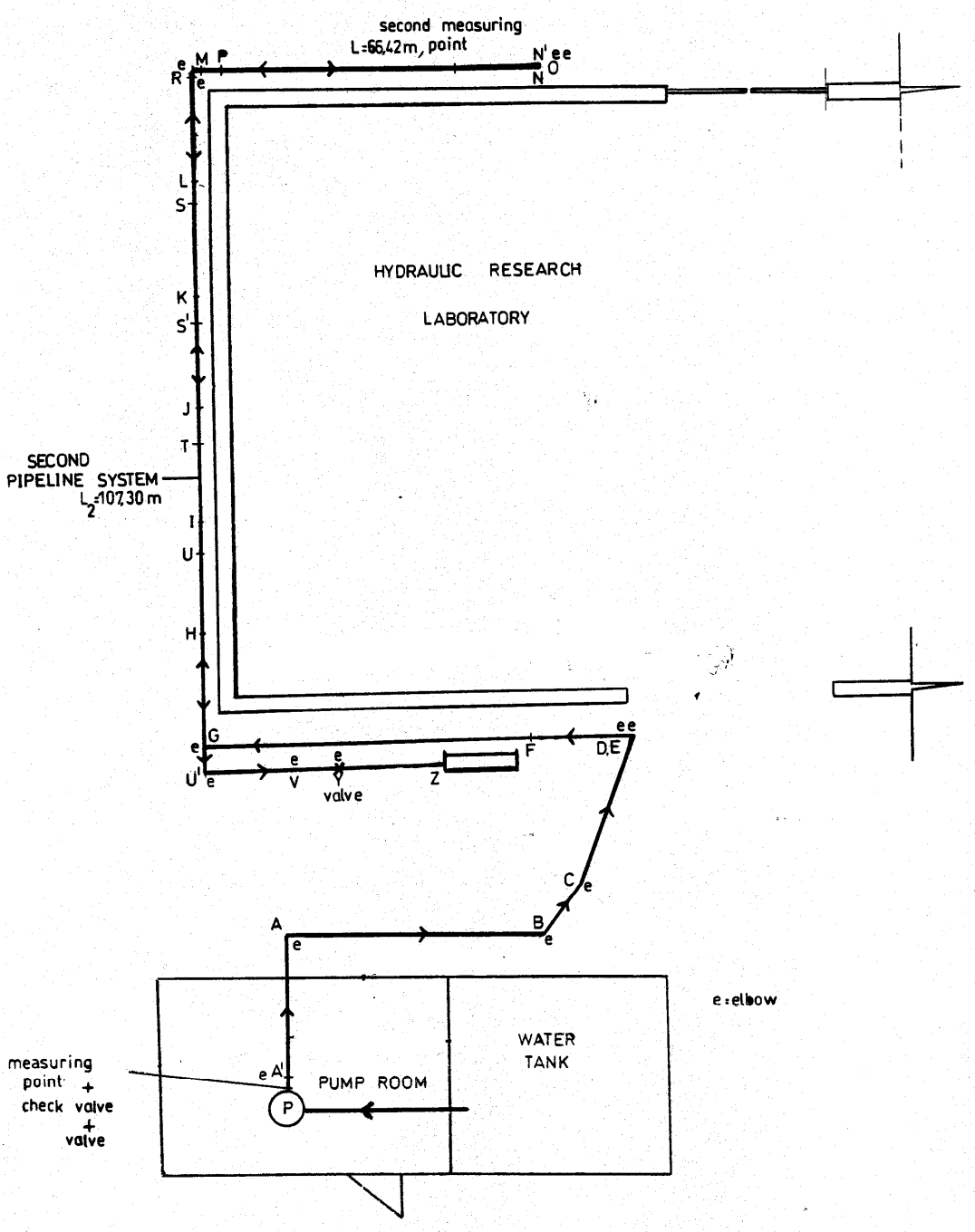

Figure 5.7: Plan view of the second system and the pump room.

Losses due to junction points are not considered in the transient flow calculations. Loss coefficients for elbows and reduced bore ball valve are included according to measurements carried out in the laboratory.

Disc type check valve is placed immediately at upstream of the pump. During the run down period of the pump, due to flow, check valve is closed. Due to closed check valve, backward flows through the pump cannot occur.

The tank at the downstream end of the second pipeline is manufactured from sheet iron. Two pipes are connected to the elevated tank at downstream end to establish the inflow and outflow as shown in Figure 5.8.

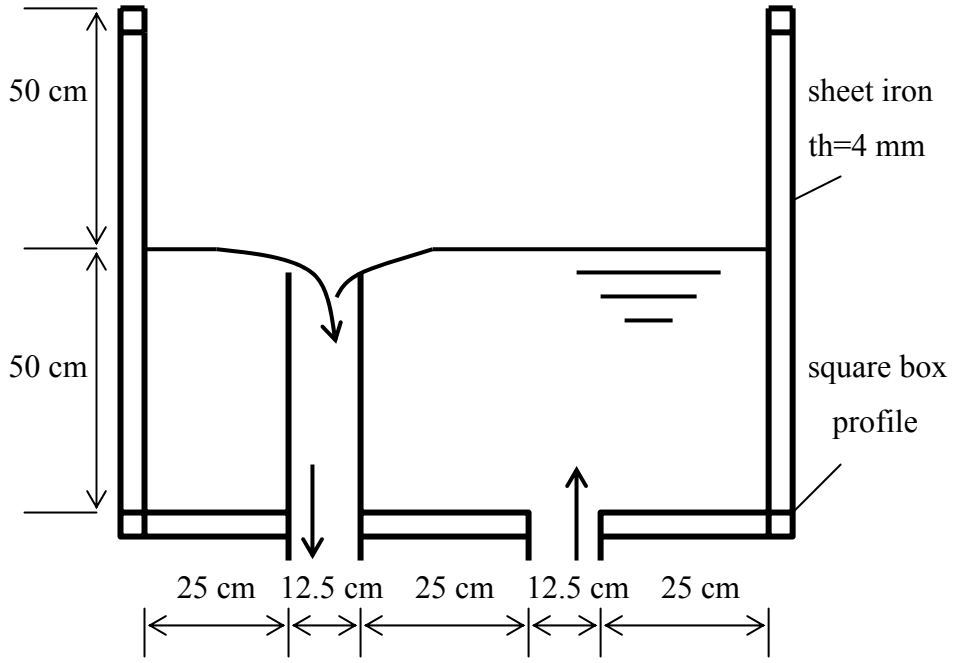

Figure 5.8: The profile of downstream water tank for second system (drawing is not scaled).

Water is collected in the tank and spills to outlet pipe. The tank is square with dimensions 1 m*1 m width and length each. Sheet iron has a thickness of 4 mm. 30 mm*30 mm square box profiles surround the sheet iron all around. In the second system, pressure is measured at two points. The first measurement point is located at

0.90 meter downstream of the pump as in the first system and second measurement point is an interior point located at 66.4 meters apart from the pump.

5.3 Pump Characteristic Curves

The geometric characteristics of the centrifugal pump are given in Figure 5.9.

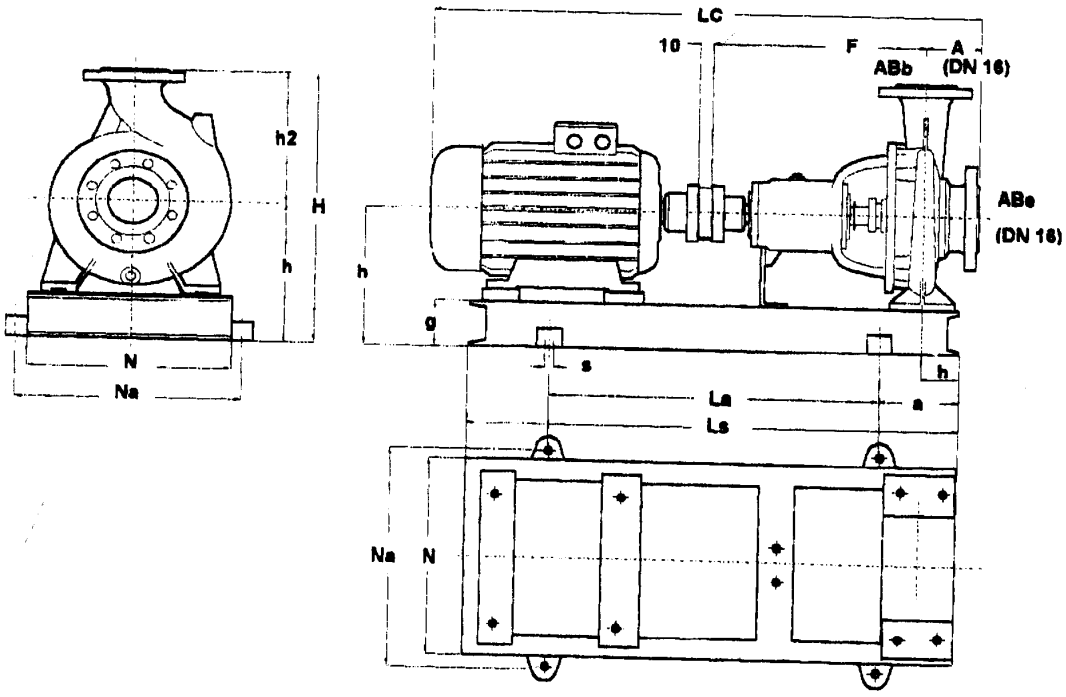

Figure 5.9: The geometries of the pump used in the systems (ABe=125 mm, ABb=125 mm, A=125 mm, F=470 mm, LC=1052 mm, N=385 mm, Ls=930 mm, Na=415 mm, La=650 mm, s=20 mm, a=100 mm, b=90 mm, g=100 mm, h=300 mm, H=580 mm, h2=280 mm, weight=184 kg).

In Table 5.3, the numerical values read from the pump characteristic curves are presented. At the best efficiency point (η = 79.3 %) the rated head and discharge values are 11 m and 36 lt/s respectively. In Figure 5.10, pump characteristic curves are given. In Table 5.4, torque and power values generated from pump characteristic curve values are presented.

The characteristics of the pump :

Trademark of the pumps: Standard (Made in Turkey), Type of pumps: SNK 100-200,

Rotational speed of the pump: 1450 rpm,

Suction orifice diameter: 125 mm,

Discharge orifice diameter: 125 mm,

Diameter of the impeller: 210 mm,

Power of motor: 5.5 KW:7.5 HP

Weight of the pump: 80 kg,

Discharge, Q (at best efficiency point): 130 m^3/h,

Head, H (at best efficiency point): 11 m,

Efficiency of the pump: 79.30 %,

Effective power: 4.91 KW,

Maximum effective power: 5.43 KW,

Table 5.3: Pump characteristic values (1KW=1.338 HP).

Head, H (meters)	Discharge, (m^3/h)	Discharge, (m^3/s)	Efficiency, (%)	Power, (KW)	Power, (HP)
14.00	0.00	0.00	0.00	3.100	4.140
13.50	80.00	0.022	68.50	4.253	5.690
13.10	90.00	0.025	72.50	4.431	5.928
12.70	100.00	0.027	76.00	4.550	6.087
12.20	110.00	0.030	77.00	4.740	6.342
11.70	120.00	0.033	79.00	4.794	6.414
11.00	130.00	0.036	79.30	4.886	6.537
10.30	140.00	0.038	78.00	4.922	6.585
9.50	150.00	0.041	74.50	5.128	6.861
8.60	160.00	0.044	70.00	5.303	7.095

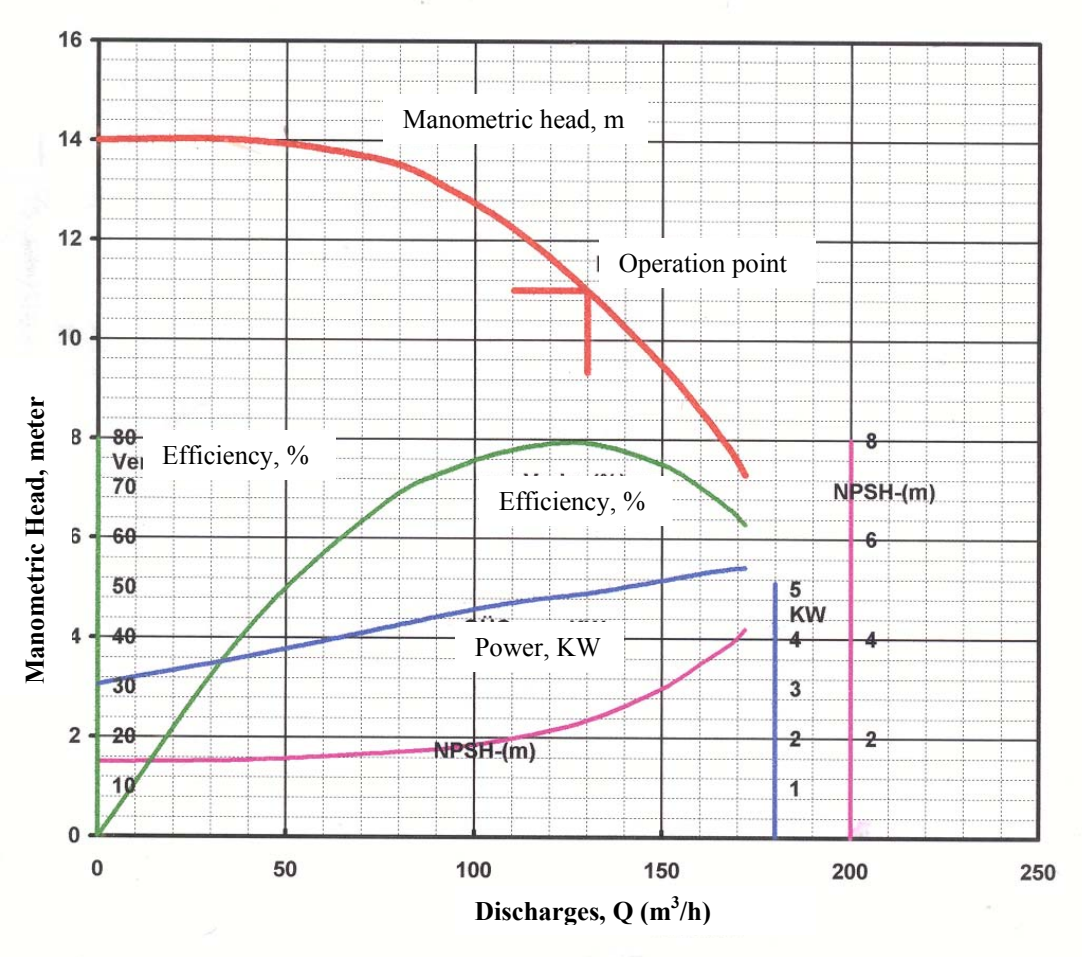

Figure 5.10: Pump characteristic curves.

Table 5.4: Torque, T values corresponding to H and Q values in pump characteristic curve.

P , (watt)	Head (meters)	Disc., Q (m^3/s)	Torque, (Nt.m)
3100.000	14.000	0.000	20.415
4253.000	13.500	0.022	28.009
4431.000	13.100	0.025	29.181
4550.000	12.700	0.027	29.965
4740.000	12.200	0.030	31.216
4794.000	11.700	0.033	31.571
4886.000	11.000	0.036	32.177
4922.000	10.300	0.038	32.414
5128.000	9.500	0.041	33.771
5303.000	8.600	0.044	34.924

Some photographs corresponding to pump room are given from Figure 5.11 to Figure 5.15.

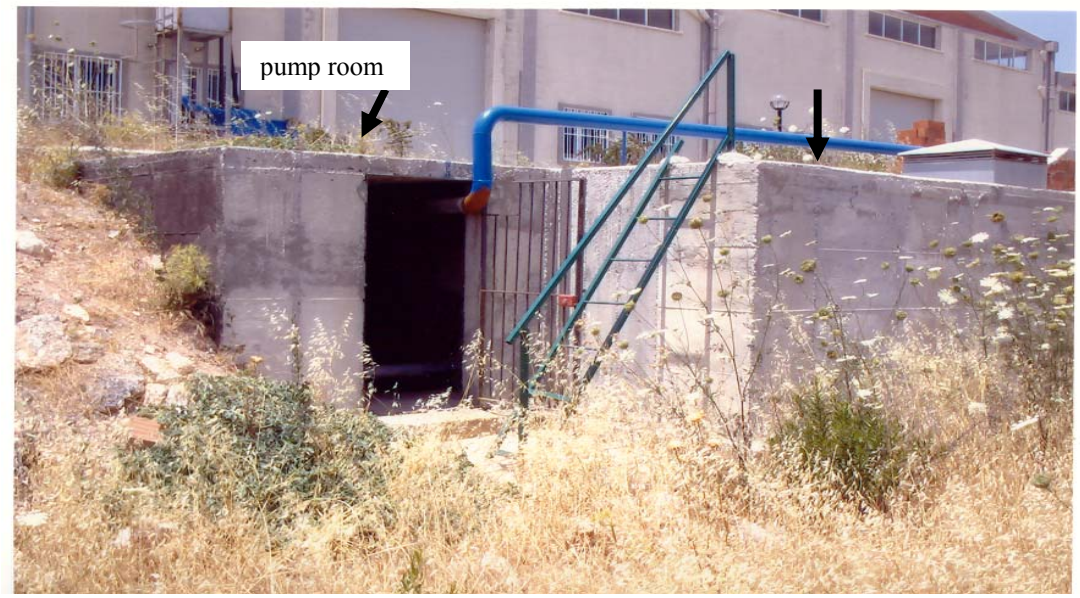

Figure 5.11: Pump room at the left and water tank at the right.

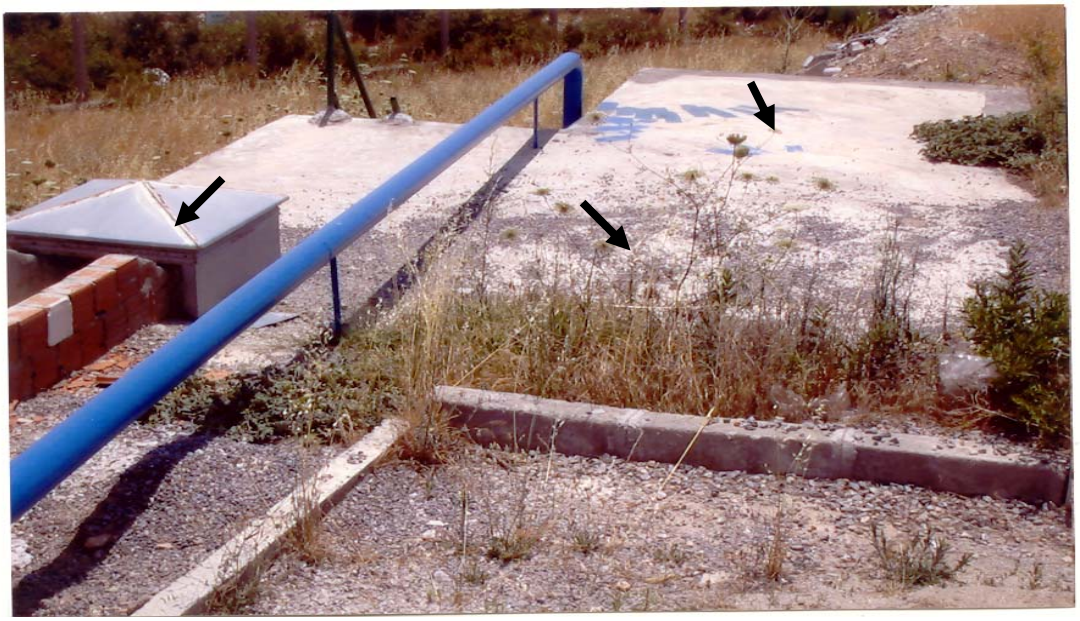

Figure 5.12: pump room at the forward, water tank at the backward and man hole of the tank.

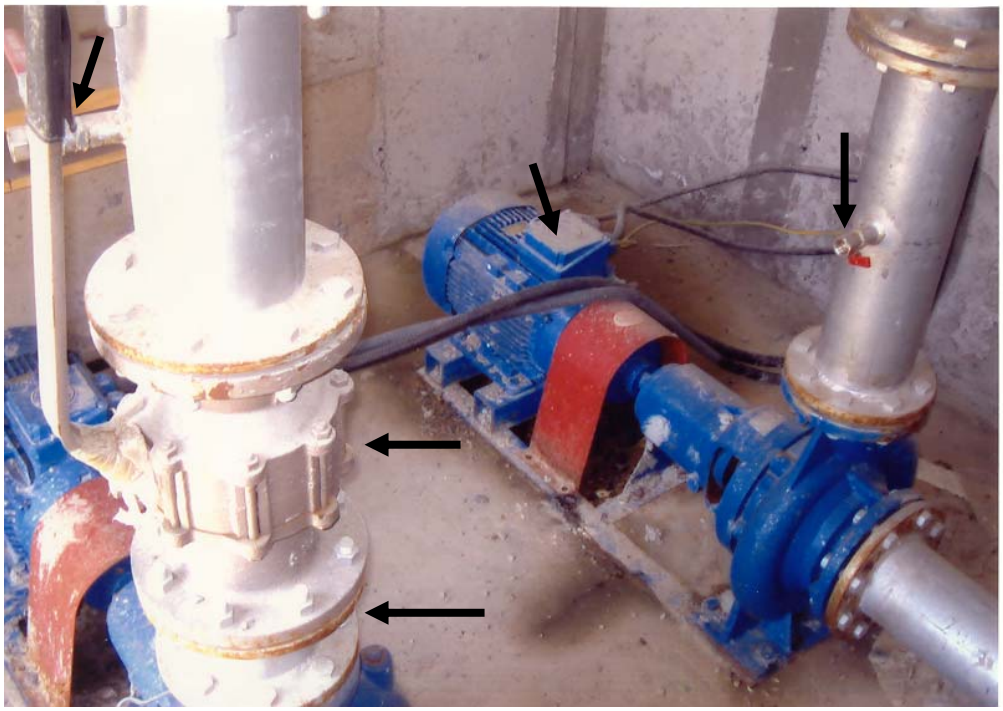

Figure 5.13: Inside of the pump room. Used pump for system 1 at the right and used pump for system 2 at the left. These pump are same. The view of first measuring points, valve and check valve.

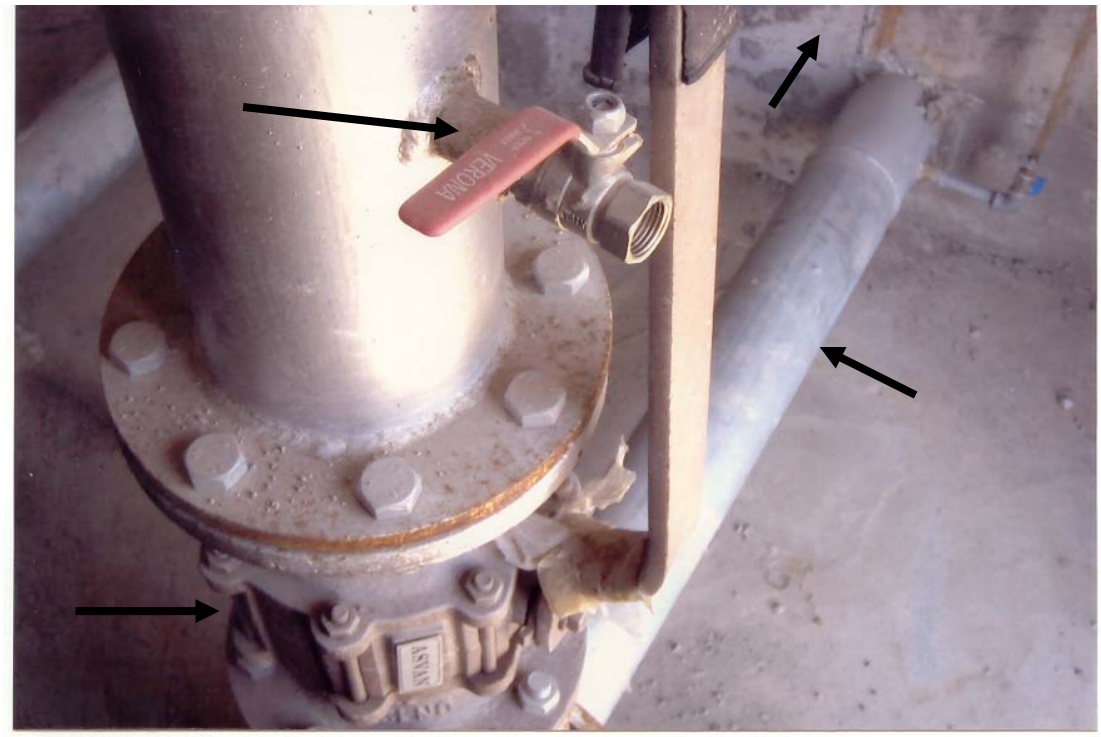

Figure 5.14: Discharge adjustment valve, measuring node 1 for system 2, suction flange and water tank.

Figure 5.15: To observe the water surface in the tank, the piezometric tube connected to suction flange and datum.

Figure 5.16 is about the triangular weir.

Figure 5.16: 90 degrees triangular V notched triangular weir to measure the steady state discharge for the first system.

Some views taken for first experimental setup are given from Figure 5.17 to 5.19.

Figure 5.17: The downstream part of the pipe for system 1, tee, discharge adjustment valve and triangular weir.

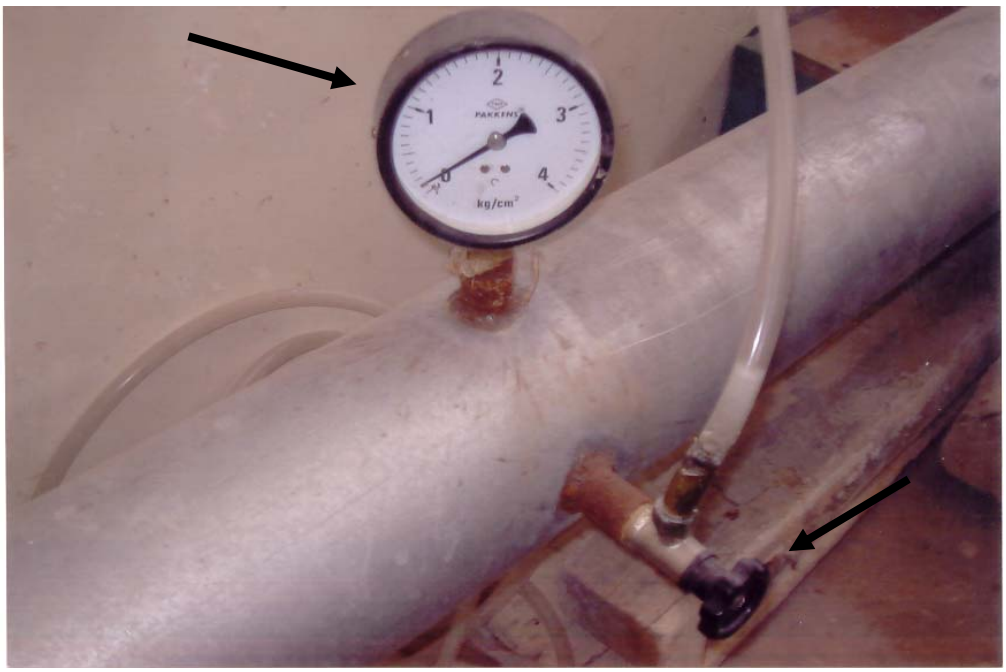

Figure 5.18: Gauge manometer to measure the pressure heads after valve and upstream connection point to differential glass manometer to find loss coefficient of discharge valve.

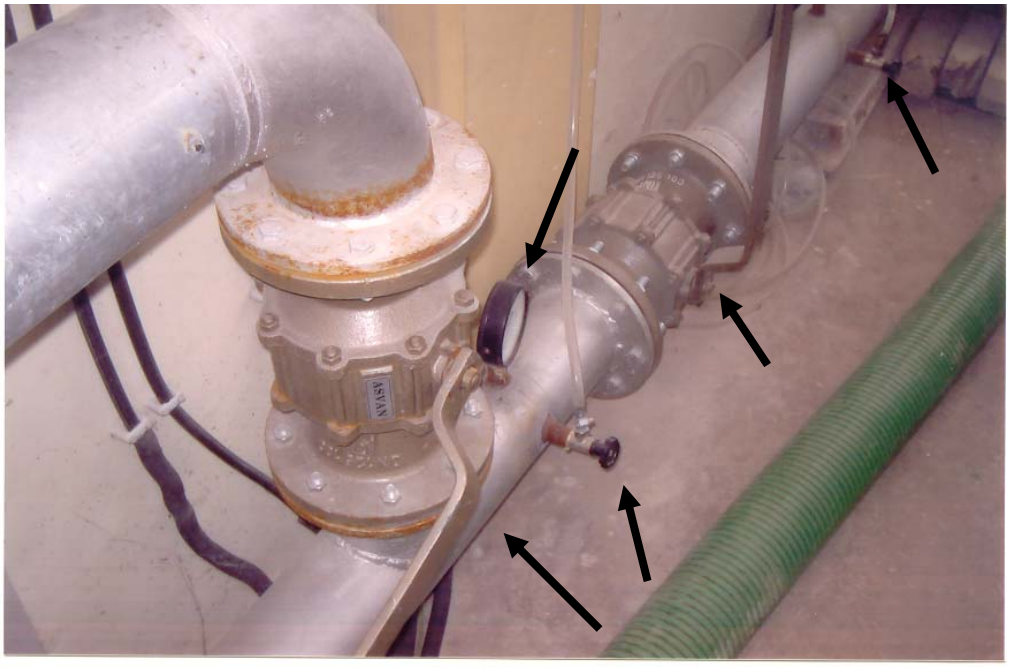

Figure 5.19: The view of tee, discharge regulation valve, upstream and downstream points to find local head loss coefficient of valve and gauge manometer for system 1.

The photographs of differential manometer are given in Figures 5.20 and 5.21.

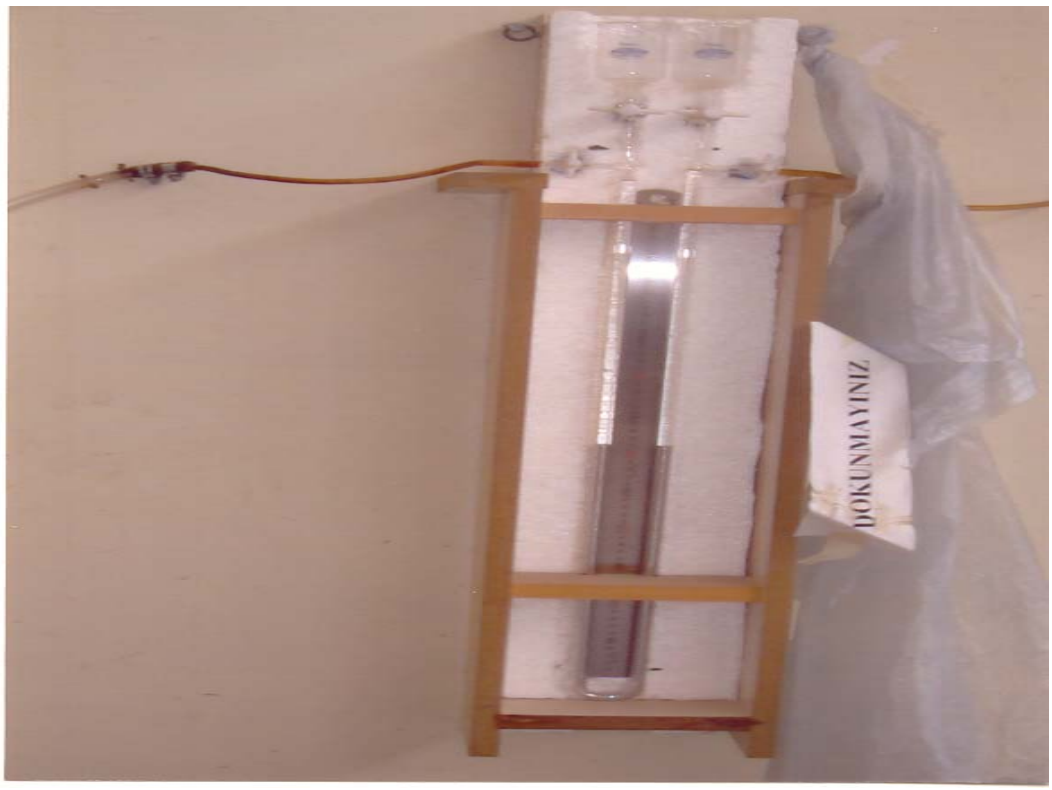

Figure 5.20: Manufactured glass differential manometer using mercury as fluid.

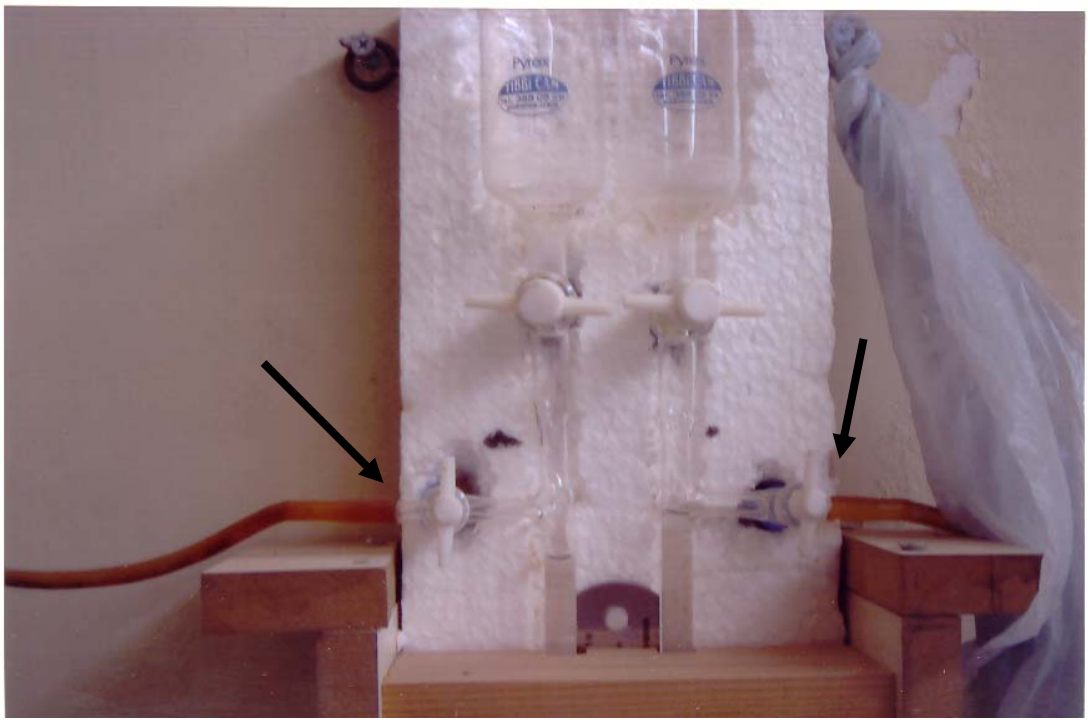

Figure 5.21: Two connection points of glass differential manometer to the upstream and downstream points of the discharge adjustment valve to find local had loss coefficient of the valve.

The photographs of second system are presented from Figure 5.22 to 5.26.

Figure 5.22: The view from the middle part of second pipeline and measuring point.

Figure 5.23: The view of second pipeline system.

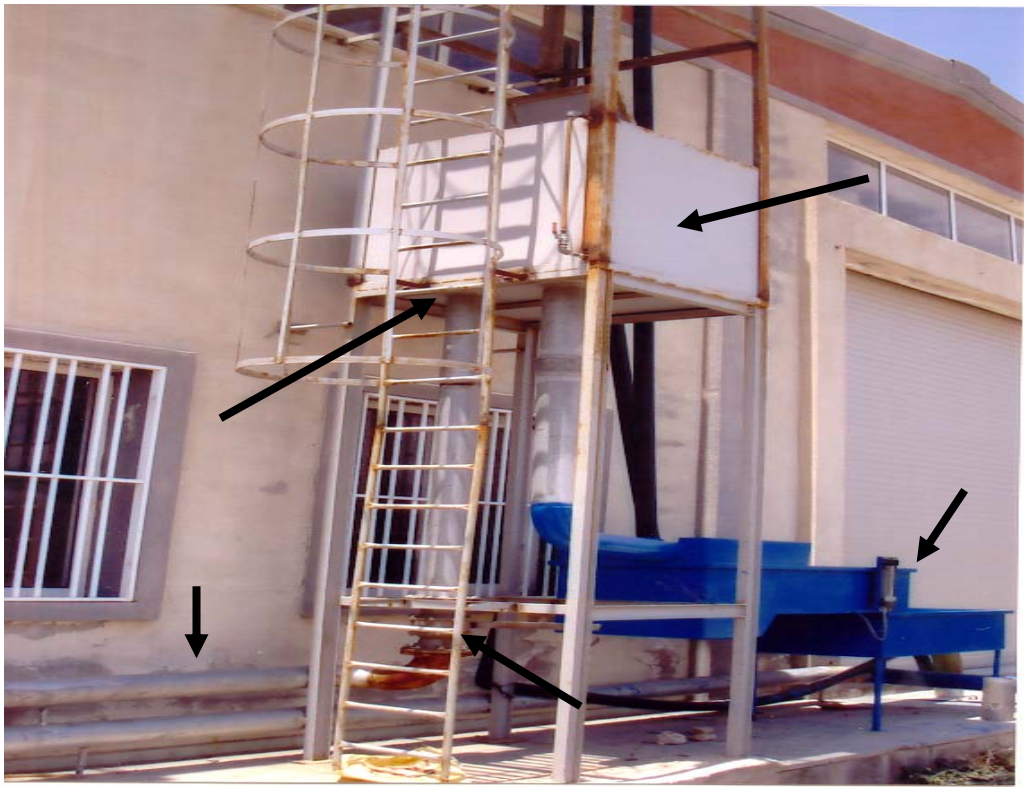

Figure 5.24: The discharge adjustment valve, the end point of the pipe, the downstream water tank and 90 degrees triangular V notched weir for system 2.

Figure 5.25: The view of junctions in second system (welded and screwed).

Figure 5.26: 90 degrees triangular V notched weir to measure the steady state discharge in system 2, same as used in the system 1.

5.4 Pressure transient data logger

There are certain numbers of technological equipments to measure transient pressures in the pipelines. Pressure transient data logger equipment has been provided from Radcom Ltd, USA, is used in this study (Figure 5.27).

Figure 5.27: Pressure transient data logger, Radcom Ltd.

Pressures have been measured in meters (pressure heads) with the aid of this equipment which is connected upon the pipeline directly. Its clock is adjusted to local time to measure transient pressures at known specific time. After the clock of the equipment has been reached to known specific time, equipment is started to operate automatically and recorded the transient pressures. On the other hand equipment can start to measure using one button click. Equipment records the transient pressures data into the logger inside the cover. After the measurements have been completed, equipment is connected to computer and data recorded inside the logger are transmitted to computer as tabulated data and graphics family. Hence, recorded data can be seen upon the computer screen. This equipment should be calibrated before starting the measuring process. Calibration process has been realised before to start the measurements. Logger presents the results in meters vs. time (seconds). Measurements can be performed up to maximum 0.20 meter

sensitivity. Logger equipment is operated with Lithium batteries of 5 years service life. Data values stored into the logger up to 2 million readings.

Experiment begins by starting up the pumps. Discharges are adjusted with the help of valves in order to obtain desired discharges. After the adjustment of system discharge and the establishment of steady state, pressure transient kit begins to record. Pump electricity is shut off manually. After measurements, the equipment is taken out from the pipeline, and then, it is connected to computer and recorded data are stored in the computer, thus new experimental values and new graph are saved.

5.5 Computation of valve and elbow loss coefficients

5.5.1 The use of the differential manometer

Valve and elbow loss coefficients are measured in the hydraulic laboratory. Reduced bore ball valve loss coefficients for various discharge values are measured using differential manometer and gauge manometer. Differential manometer was manufactured according to needed dimensions. The dimensions and simple sketch of the differential manometer is shown in Figure 5.28.

If differential manometer is connected to points A and B on the pipe

$$P_1 = P_2 \tag{5-1}$$

$$P_A + \gamma_w.z_1 = P_B + \gamma_w.z_2 + \gamma_M.\Delta z \tag{5-2}$$

$$P_A - P_B = (\gamma_M - \gamma_W)(z_1 - z_2) = (\gamma_M - \gamma_w).\Delta z \tag{5-3}$$

In Equation (5-3), P_A-P_B is the pressure head difference, γ_M is the unit weight of mercury inside the manometer, γ_w is the unit weight of water and z_1-z_2 is the difference between the mercury columns.

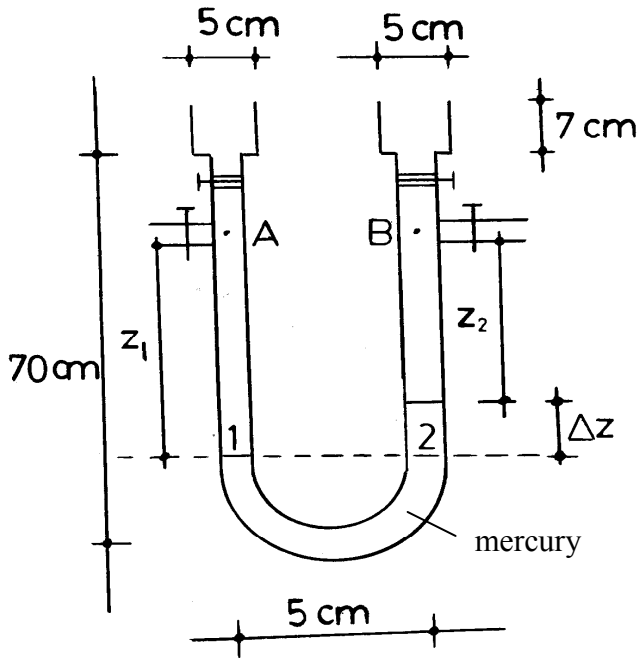

Figure 5.28: Sketch of the manufactured glass differential manometer.

Mercury is placed inside the manometer. Then manometer columns are connected to points on the pipeline, these points are placed at upstream and downstream of the valve. During the measurement, valve opening position does not change. Deviation of mercury columns is read. Then pressure difference is calculated. If the pipe is horizontal the local loss is expressed as :

$$h_L = \frac{(P_A - P_B)}{\gamma_W} = \frac{(\gamma_M - \gamma_W).\Delta z}{\gamma_W} \qquad (5\text{-}4)$$

5.5.2 The loss coefficients of reduced bore ball valve

During the pump shutdown, the discharge (and consequently the velocity) decreases continuously. As the head loss coefficients vary in terms of flow velocity, these coefficients should be determined as the function of the velocity. On the other hand, the steady state discharge is adjusted by changing the opening of the regulating

valve. The measurements are performed for different valves used in two different experimental systems.

Several measurements are performed with different valve openings in the first system. Head loss coefficients calculated from the measurements are given in Table 5.5 realised on the first system. The graphs and analytical expressions obtained from the curve fitting analysis are given in Figure 5.29

Table 5.5: Discharges, Q, velocities, V and valve loss coefficients, K (variable valve opening for the first system).

Discharge, Q (m^3/s)	Velocity, V (m/s)	Valve loss coefficient, K (dimensionless)
0.041	3.36	5.26
0.040	3.28	5.91
0.030	2.46	21.82
0.022	1.80	54.04
0.008	0.65	428.53

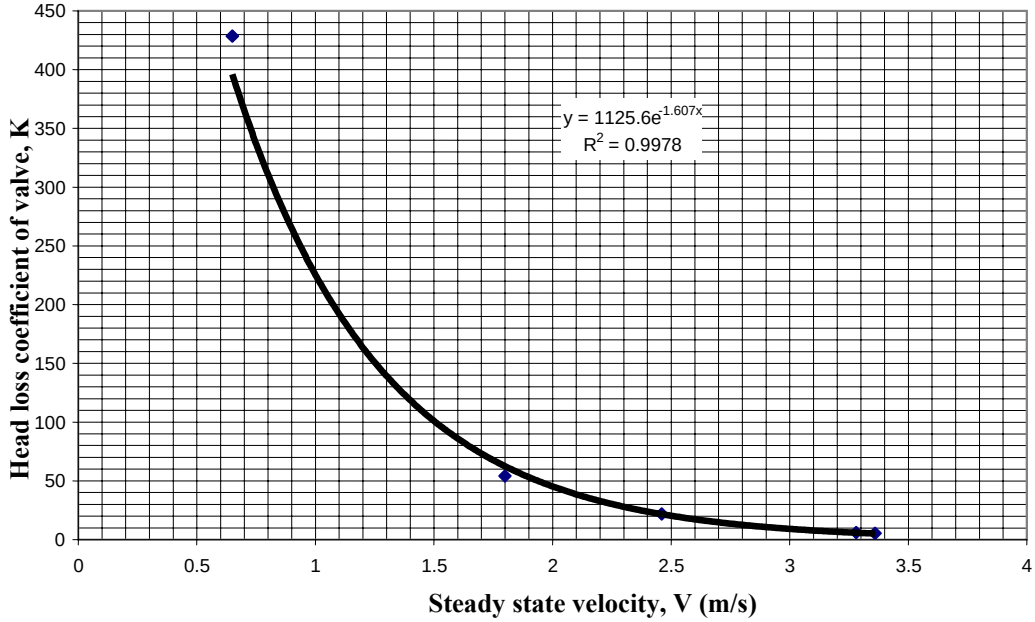

Figure 5.29: The valve loss coefficients, K versus flow velocity, V (variable valve opening).

The obtained analytical expression is : $K=1125.6.e^{(-1.607.V)}$.

5.5.3 The loss coefficients of elbows

The results of experiments to determine the 90^0 elbow loss coefficients are given in Table 5.6 and the graphs and analytical expressions obtained from the curve fitting analysis are given in Figure 5.30.

Table 5.6: Discharges, Q, velocities, V and elbow loss coefficients, K

Discharge, Q (m^3/s)	Velocity, V (m/s)	Valve loss coefficient, K (dimensionless)
0.024	1.97	1.76
0.019	1.61	1.90
0.012	1.02	4.67
0.007	0.56	15.38

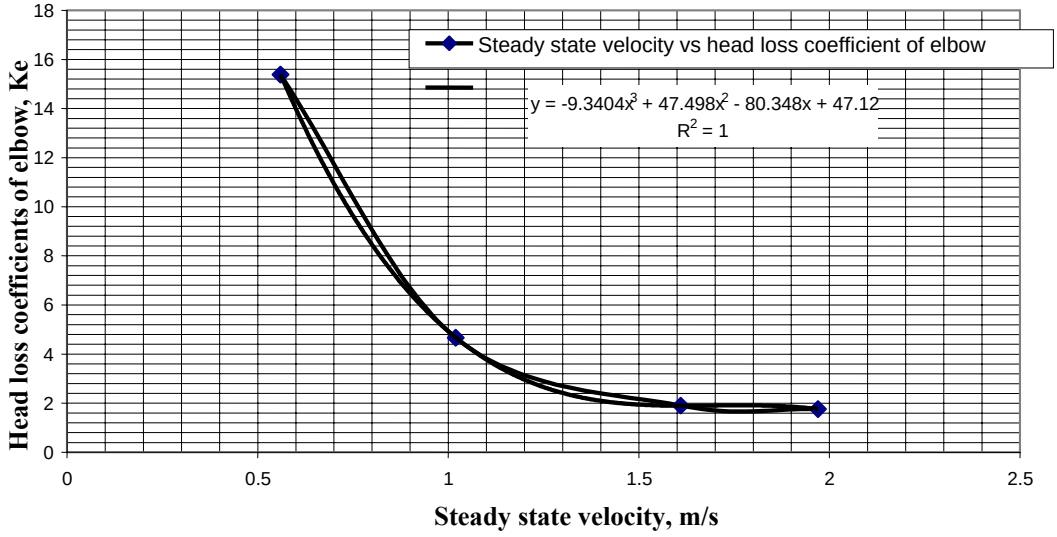

Figure 5.30: The elbow loss coefficients, K versus flow velocity, V.

The obtained analytical expression is : $Ke=-9.3404.V^3+47.498.V^2-80.348.V+47.12$.

5.6 The loss coefficients of the disc type check valve and valves for the second system.

The check valve loss coefficient is determined with the use of the pump characteristic curve. As there is reading after the valve and since the valve loss coefficient is known, the check valve loss coefficient may be deduced by subtraction from the relevant manometric head read from the pump characteristic curve.

During these measurements the full open valve loss coefficient (AKV1) and partially open valve loss coefficient (AKV2) are determined as well.

The results are collected in the Table 5.7. The graphs and analytical expressions obtained from the curve fitting analysis are given in Figure 5.31, Figure 5.32, Figure 5.33.

Table 5.7: Experimental values of local head loss coefficients.

Steady state discharge, Q (lt/s)	Velocity, V, (m/s)	CK, loss coefficient of Check valve	AKV1, loss coefficient of valve, node 1	AKV2, loss coefficient of valve, node 42
6.60	0.54	10.87	17.29	585.92
9.01	0.74	9.35	11.32	303.40
16.50	1.35	6.62	4.98	74.00
19.14	1.57	6.23	4.06	44.02
20.55	1.70	6.12	3.69	29.31
24.52	2.01	2.00	2.90	15.62
25.16	2.06	1.00	2.80	14.23

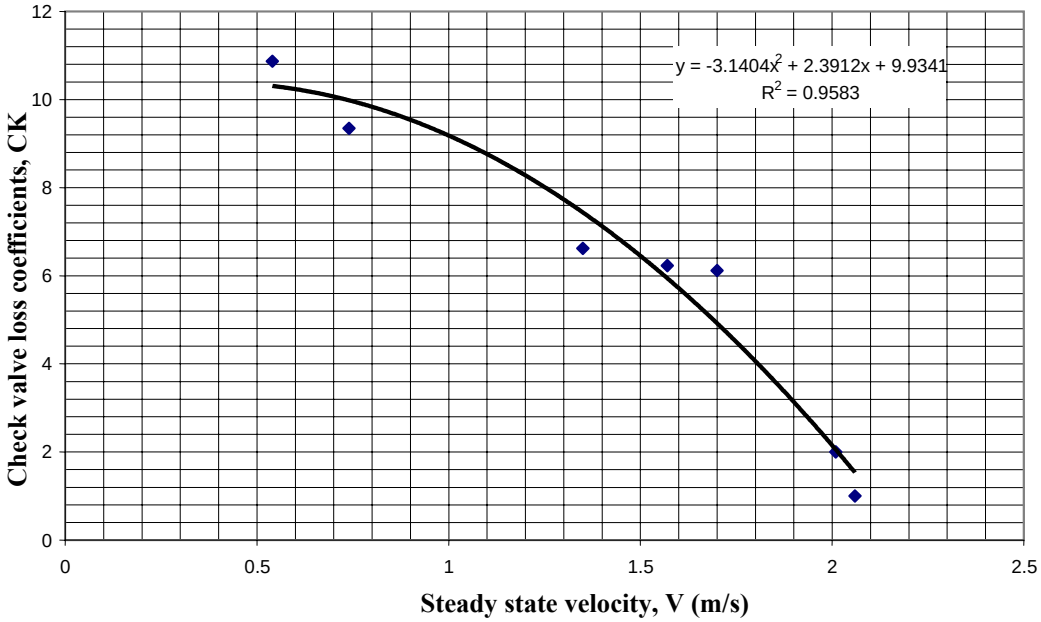

Figure 5.31: The check valve loss coefficients, K versus flow velocity, V.

The obtained analytical expression is : $CK=-3.1404.V^2+2.3912.V+9.9341$.

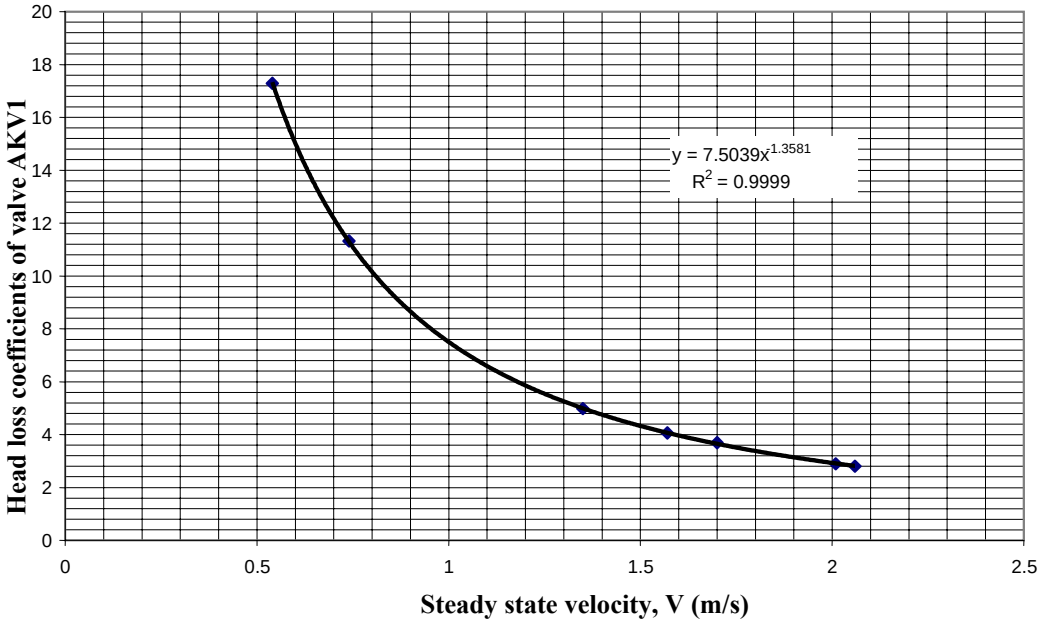

Figure 5.32: The full open valve loss coefficients, AKV1 versus flow velocity, V.

The obtained analytical expression is : $AKV1=7.5039.V^{-1.3581}$.

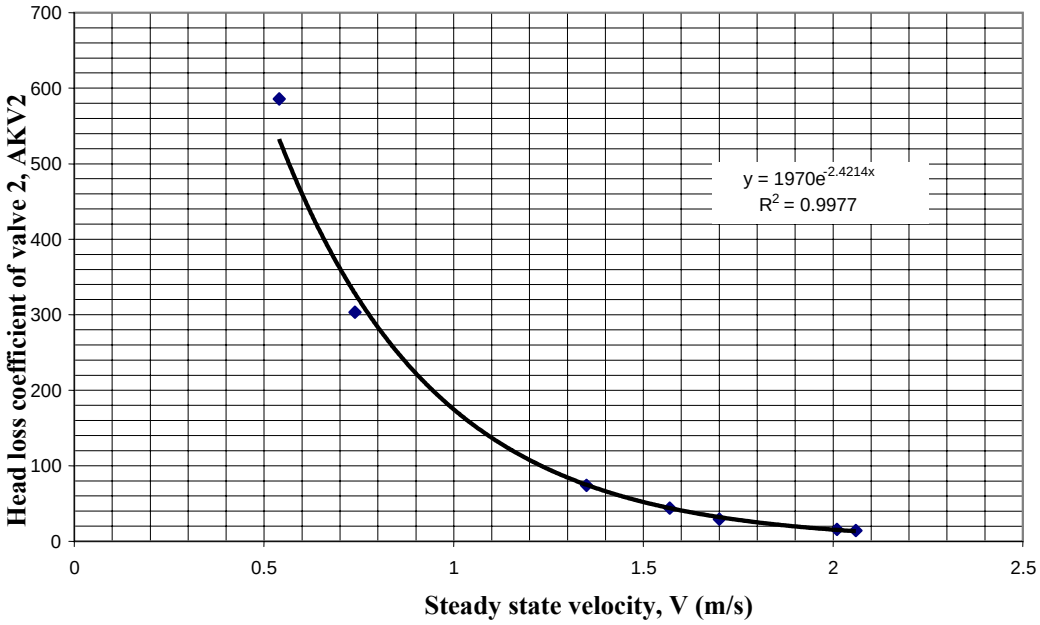

Figure 5.33: The partially open valve loss coefficients, AKV2 versus flow velocity, V.

The obtained analytical expression is : $AKV2=1970.e^{-2.4214.V}$.

5.7 Calibration of triangular weir

V notched triangular weirs of 90 degrees are manufactured in hydraulic laboratory. Various discharge conditions are obtained adjusting the reduced bore ball valve. Scaled water tank is used in order to measure the volume of water passing through the triangular weir in the specified time interval. Thus discharges through the weir are determined. During calibration, weir head on the V notched is measured, therefore, different discharge values corresponding to weir heads on the V notch are drawn and curve fitting is performed.

In Figure 5.34, the calibration curves of our V notched weir of 90 degrees are sketched. The expression of the calibration curve is $Q=1.53.(H)^{5/2}$. In this equation, Q is the discharge in m^3/s, H is the measured head on V notched in meters.

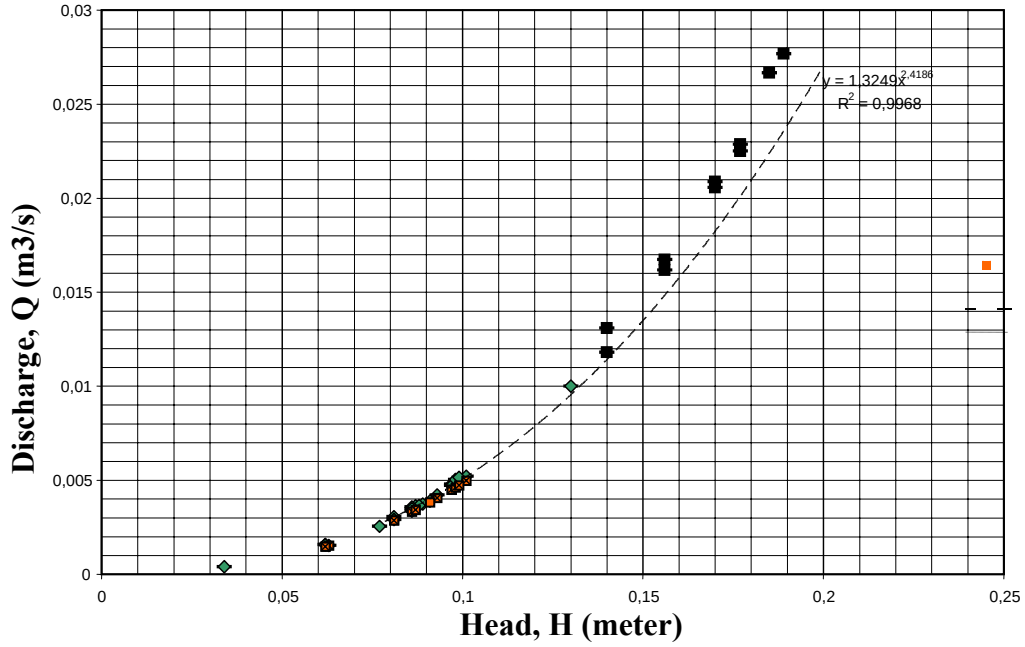

Figure 5.34: Calibration curves of V notched triangular weir of 90 degrees used in our systems. x axis represents the head in meters and y axis represents discharges in m^3/s.

The geometric characteristics of reduced bore ball valve and those of the disc type check valve, together with head loss coefficients provided from the literature are given in Appendix A.

CHAPTER SIX
DESCRIPTION OF COMPUTER PROGRAMS

Fortran computer programs proposed by Wylie and Streeter are used after some modifications and adaptation. Using these modified versions of Fortran computer programs, several computations are realised and results are interpreted.

6.1 The flow chart of the computer program

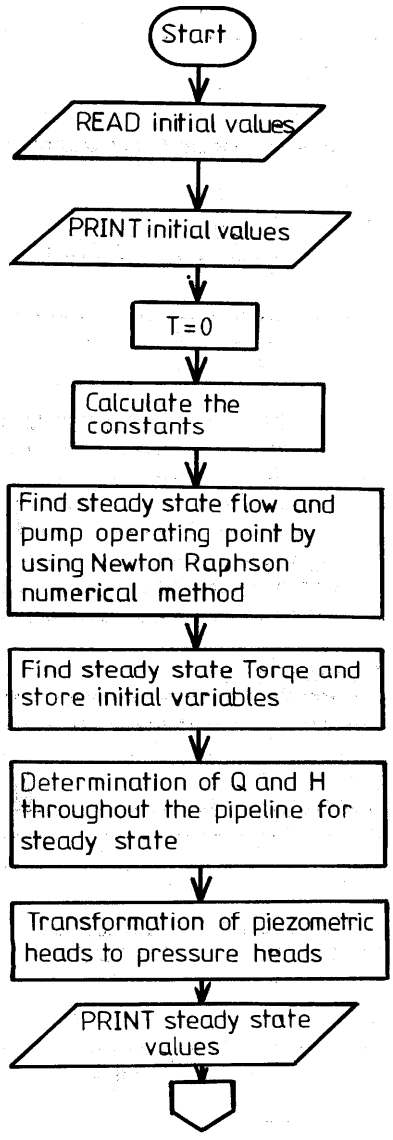

Figure 6.1 : Flow Diagram of Fortran computer program.

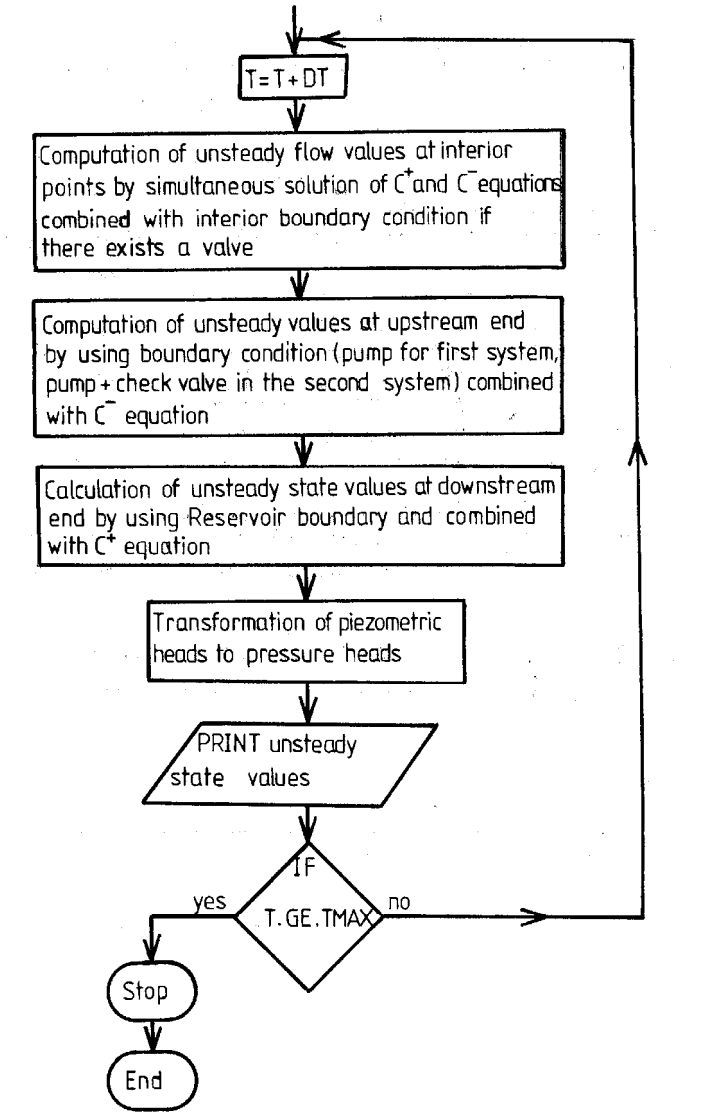

Figure 6.1 : Flow diagram of Fortran computer program (continued).

6.2 Description of parameters used in the computer programs

6.2.1 Fortran computer program used for the first system

The parameters used in the computer program adopted for the first system are described below :

EL: The elevation difference between the upstream water surface elevation and downstream water surface elevation (= Δz in the equations).

A : Wave celerity in m/s (= a in Equation).

XL: Pipeline length in m. (= L)

CK: The dimensionless valve head loss coefficient.

TM: The maximum time (seconds) in which the Fortran calculations perform.

RN : Rotational speed at rated condition in rpm (= N_R)

TR : Rated torque in Nt.m (= T_R)

HR : Rated head in meter (= H_R)

QR : Rated discharge in m^3/s (= Q_R)

WRR : Rotational moment of inertia in $Nt.m^2$ (= $W.R_g^2$)

TOL : Tolerance into Newton Raphson method to provide equality

N : Number of the equal reaches in the pipeline which is divided into N equal reaches.

F : Darcy Weisbach friction coefficient (= f)

D : Diameter of the pipe, m

G : Acceleration due to gravity (= g)

V : The ratio of the steady state discharge to discharge at rated condition.

VI : The ratio of the steady state discharge to discharge at rated condition.

V, V0, V00 : Dimensionless the ratio of steady state discharge to discharge at rated condition. Q/Q_R . V0 corresponds to Δt time step earlier. V00 corresponds to $2\Delta t$ time step earlier.

PI : Number of π (= 3.1416)

JPR : Integer number of time step iterations between each print

KIT : Maximum iteration number in Newton Raphson numerical procedure

DX : Dimensionless pump data space (Radians)

AL : Dimensionless pump rotational speed ratio.

AL0 : Dimensionless pump rotational speed ratio for Δt time step before

AL00 : Dimensionless pump rotational speed ratio for $2\Delta t$ time step before

DT : Time increment in the successive time step (s)

K : Counter designates maximum calculation time period number

WH (I) : Dimensionless pump (head) data

WB(I) : Dimensionless pump (torque) data

ZH(I) : Elevations of nodes throughout the pipe according to datum (upstream reservoir level) in m

AKS : Roughness height of steel pipe wall in m

QQA : Steady state discharges in m^3/s

H(I) : Piezometric heads in m

HPH(I) : Pressure heads in m

NSS : Number of node in which there is a discharge adjustment valve

VN : Kinematic viscosity of water in m^2/s

HMIN : Minimum pressure head in m

Q(I) : Discharge in transient condition, m^3/s

H(I) : Piezometric head in transient condition, m

HP11 : Pressure head in meters at node of valve immediately upstream of valve, m

HP1 : Piezometric head in meters at node of valve immediately upstream of valve, m

CP : The constant in C^+ equation given in Equation (3-20)

CM : The constant in C^- equation given in Equation (3-21)

C3 : Local head loss equation constant for valve given in Equation (3-40)

C4 : Constant in discharge equation in transient condition given in Equation (3-38)

C5 : Constant in discharge equation in transient condition given in Equation (3-39)

BP : The constant in C^+ equation

BM : The constant in C^- equation

B : Pipeline impedance, $s/m^2 = a / (g.AR)$

R : Resistance coefficient for one reach = $(f.\Delta x / (2g.D.AR^2))$

H3 : Local head loss at valve for steady state

X : Angle theta

A1 : The constant in linear similarity head equation given in Equation (4-18).

A0 : The constant in linear similarity head equation given in Equation (4-18)

B1 : The constant in linear similarity torque equation given in Equation (4-28)

B0 : The constant in linear similarity torque equation given in Equation (4-28)

DAL : Changing of α value given in Equation (4-38)

DV : Changing of v value given in Equation (4-39)

F1 : Head Balance equation given in Equation (4-22)

F1V : Partial derivative of head balance equation with respect to V given in Equation (4-34).
F1A : Partial derivative of head balance equation with respect to α given in Equation (4-35)
F2 : Speed change equation given in Equation (4-29).
F2V : Partial derivative of speed change equation with respect to V given in Equation (4-36)
F2A : Partial derivative of speed change equation with respect to α given in Equation (4-37)

6.2.2 Fortran computer program used for the second system

The terms described in section 6.2.1 are generally valid for the first system. In this section, we will mention only the additional or modified terms.

CK : Disc type check valve head loss coefficient
AKV1 : Head loss coefficient of valve immediately after pump
AKV2 : Head loss coefficient of valve at the end of the pipe
TAU : Check valve opening
DTAU : Time increment between Tau values (s)
NTAU : Number of Tau values.
NSV : Node number of valve at the end of the pipe
CCT : Check valve closing time (s)
M2 : Node number of second measuring point

CHAPTER SEVEN
EXPERIMENTAL RESULTS

7.1 Results of experiments performed in the first system

Several experiments are realised to study unsteady flows due to the pump failure in first system. But three of these experiments are presented in the following pages corresponding to lower steady state discharge, moderate steady state discharge and upper steady state discharge.

7.1.1 Results of experiment performed for lower steady state discharge

The results correspond to a steady state discharge of 6.2 lt/s (0.5 m/s) are given in Figure 7.1, Table 7.1 and Figure 7.2. The experimental curve obtained for a steady flow discharge of 8.16 lt/s (0.67 m/s) is presented in Figure 7.3.

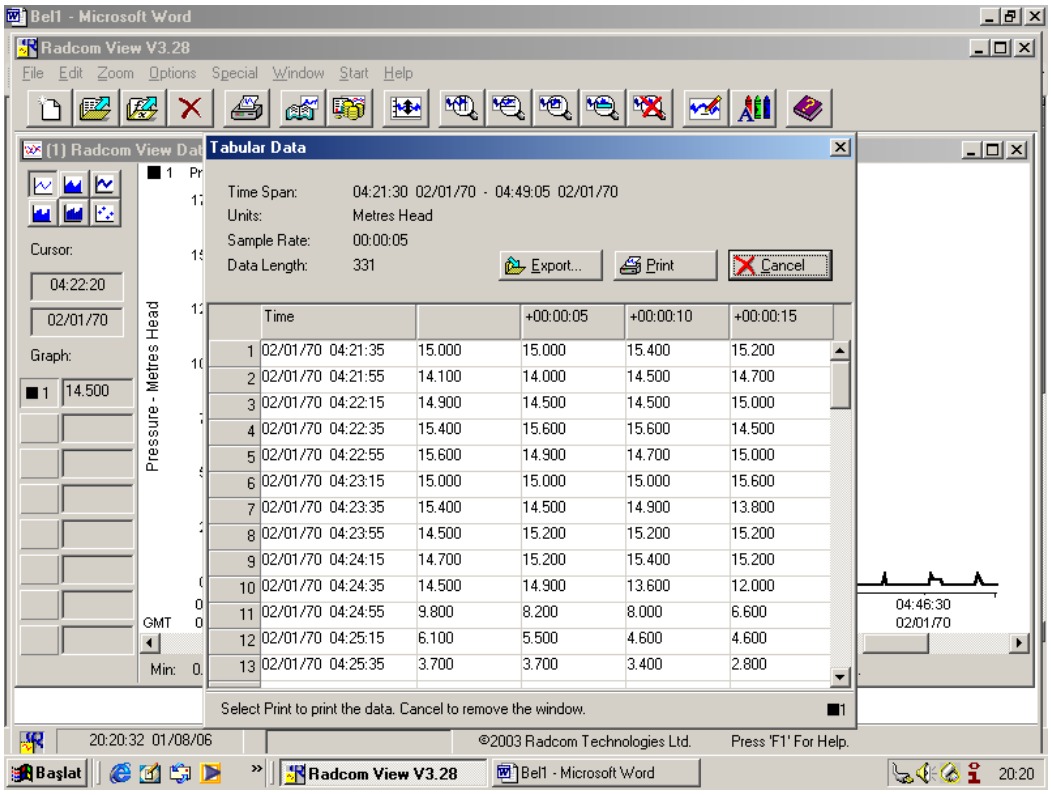

Figure 7.1: Pressure heads correspond to 6.2 lt/s lower steady state discharge.

Table 7.1: Measured pressure heads corresponding to 6.2 lt/s lower steady state discharge.

Time (minute-second-milli second)	Measured pressure heads (m)
04:23:50	13.80
04:23:55	14.50
04:24:00	15.20
04:24:05	15.20
04:24:10	15.20
04:24:15	14.70
04:24:20	15.20
04:24:25	15.40
04:24:30	15.20
04:24:35	14.50
04:24:40	14.90
04:24:45	13.60
04:24:50	12.00
04:24:55	9.80
04:25:00	8.20
04:25:05	8.00
04:25:10	6.60
04:25:15	6.10
04:25:20	5.50
04:25:25	4.60
04:25:30	4.60
04:25:35	3.70
04:25:40	3.70
04:25:45	3.40
04:25:50	2.80
04:25:55	2.80
04:26:00	2.30
04:26:05	2.30
04:26:10	2.30
04:26:15	2.50
04:26:20	2.10
04:26:25	2.10
04:26:30	1.70
04:26:35	1.70
04:26:40	1.70
04:26:45	2.30
04:26:50	1.70
04:26:55	1.70
04:27:00	1.60
04:27:05	1.60
04:27:10	1.40
04:27:15	1.20
04:27:20	1.20

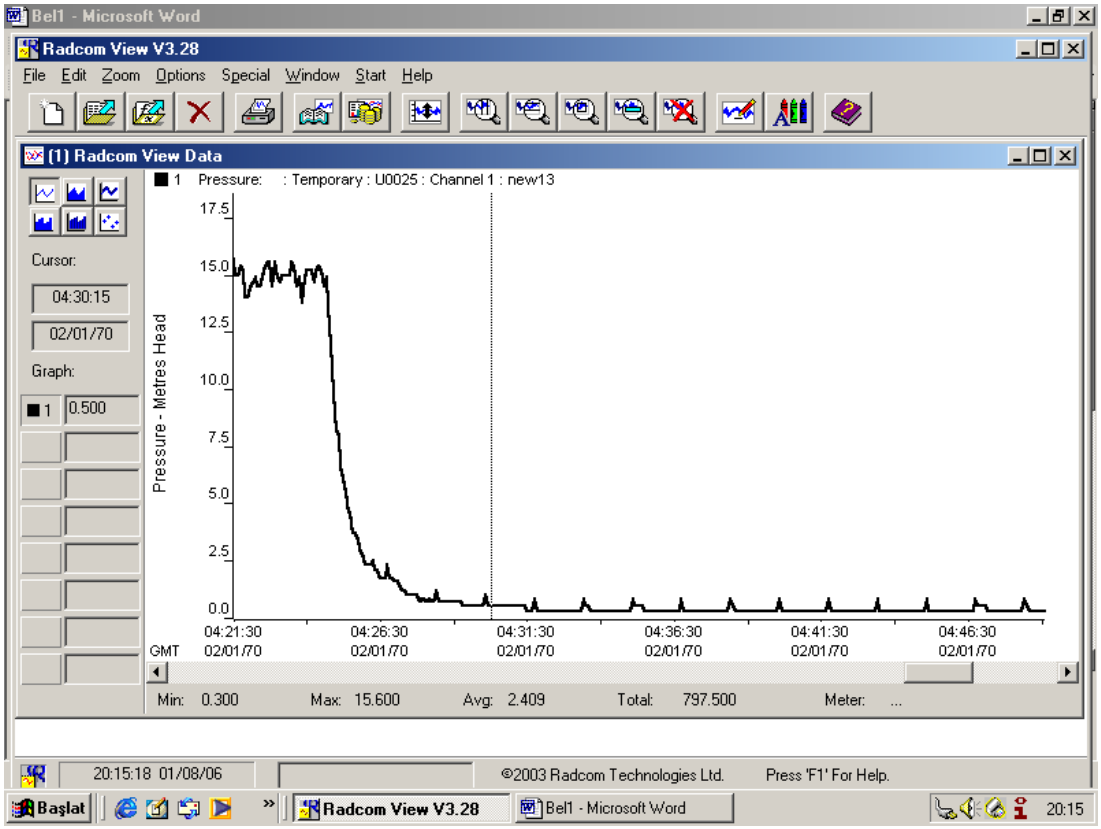

Figure 7.2: Pressure heads correspond to 6.2 lt/s lower steady state discharge.

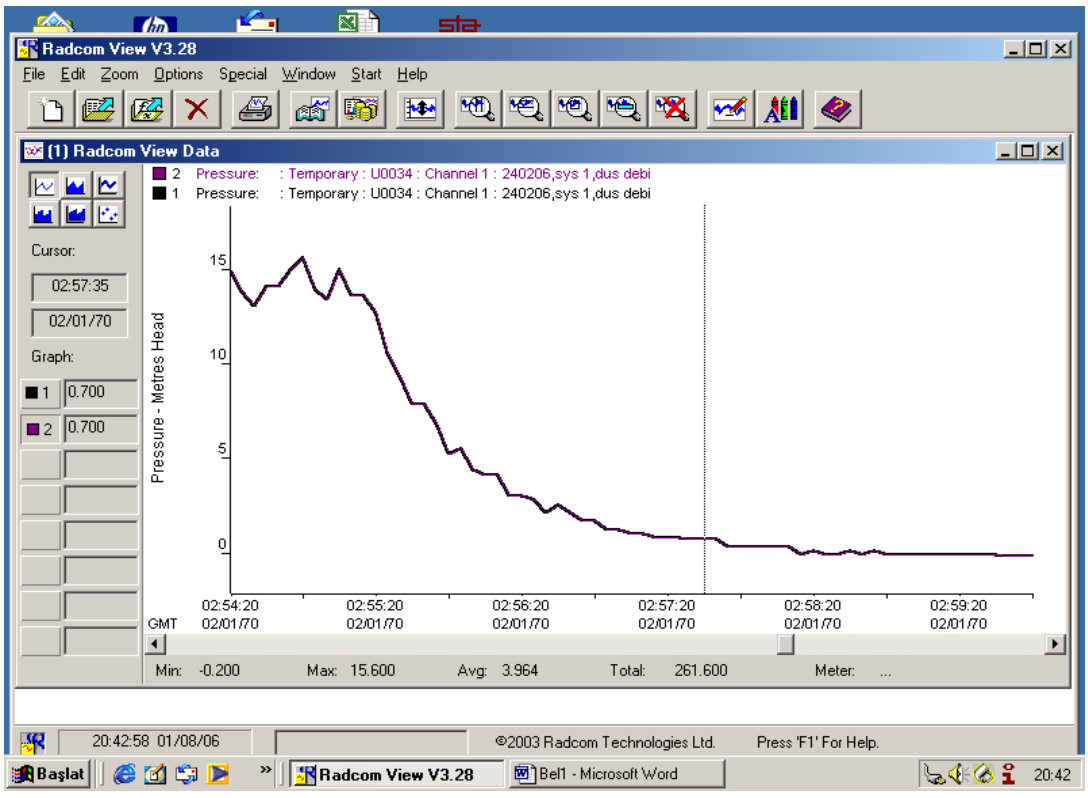

Figure 7.3: Pressure heads correspond to 8.16 lt/s lower steady state discharge.

7.1.2 Results of experiment performed for moderate steady state discharge

In these experiments, moderate steady state discharges were measured as 12.31 lt/s (1 m/s), 18.32 lt/s (1.5 m/s) and 22.635 lt/s (1.85 m/s). The graphs are shown in Figures 7.4, 7.5 and 7.6, respectively.

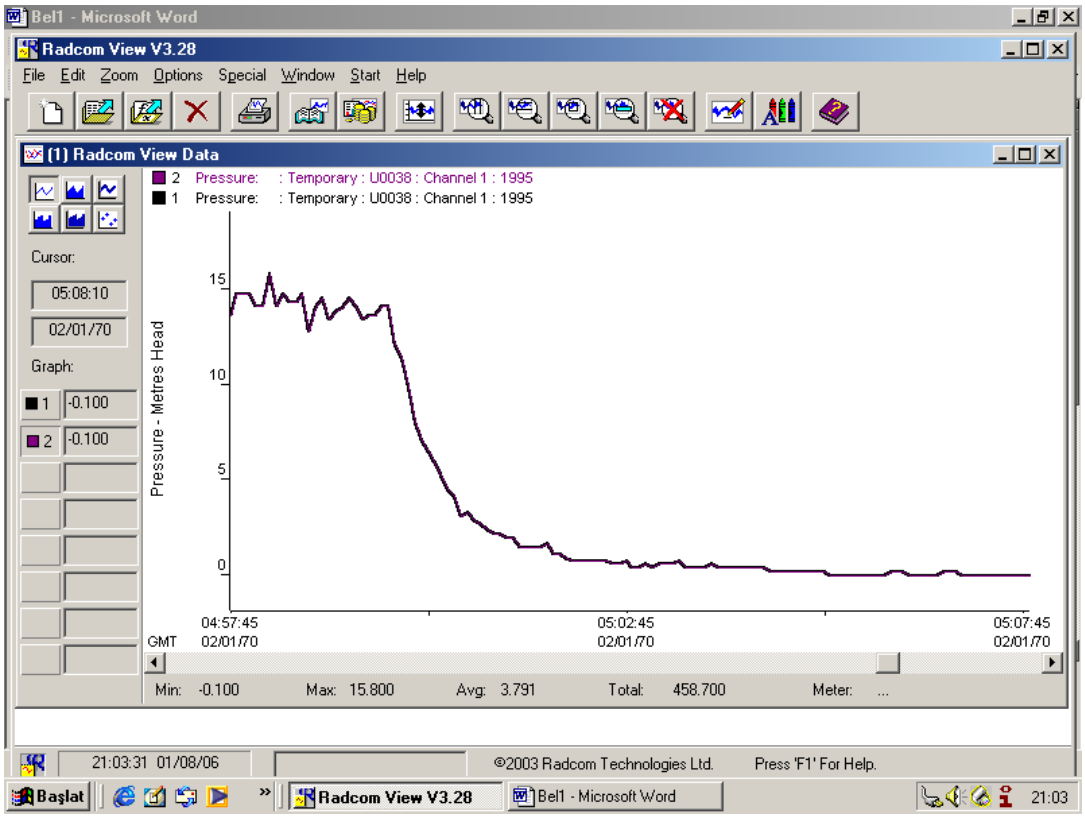

Figure 7.4: Pressure heads correspond to 12.31 lt/s moderate steady state discharge.

In Figure 7.5, in steady state flow conditions pressure heads are approximately 13.5 meters. Then the pump is shut down manually and transient flow starts. In the graph, x axis represents the time in minutes and y axis represents the pressure heads in meters.

In Figure 7.6, the steady state pressure head is about 12.5 meters which corresponds to steady state discharge of 22.63 lt/s. The tendency of the curves are similar in Figures 7.5 and 7.6.

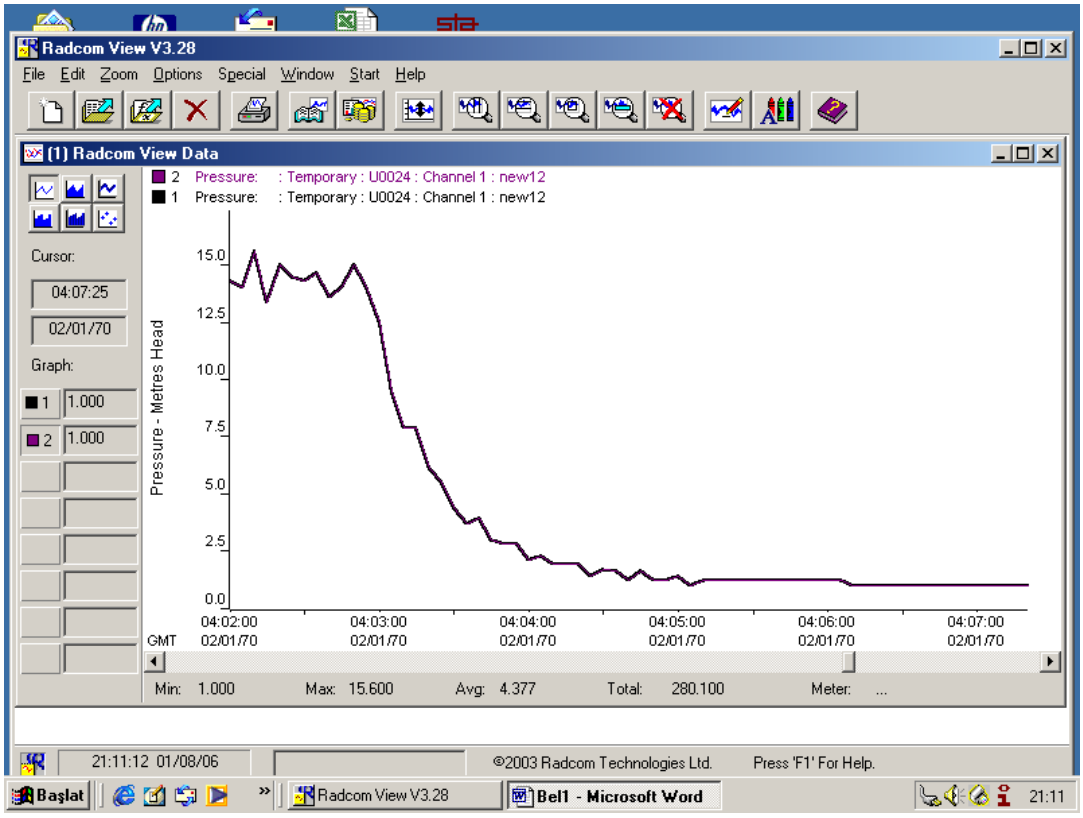

Figure 7.5: Pressure heads versus time corresponding to 18.32 lt/s moderate steady state discharge.

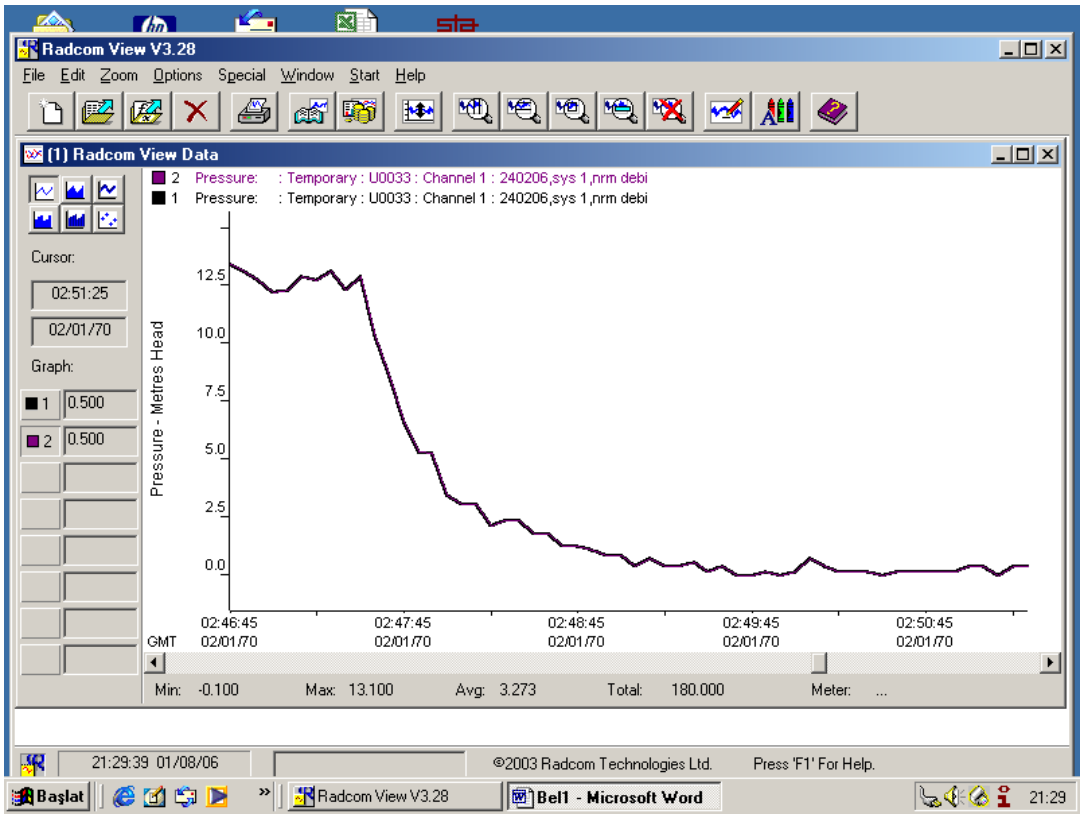

Figure 7.6: Run down period correspond to 22.63 lt/s moderate steady state discharge.

7.1.3 Results of experiment performed for upper steady state discharge

In this experiment, upper steady state discharge is measured as 39.00 lt/s and the related curve is presented in Figure 7.7.

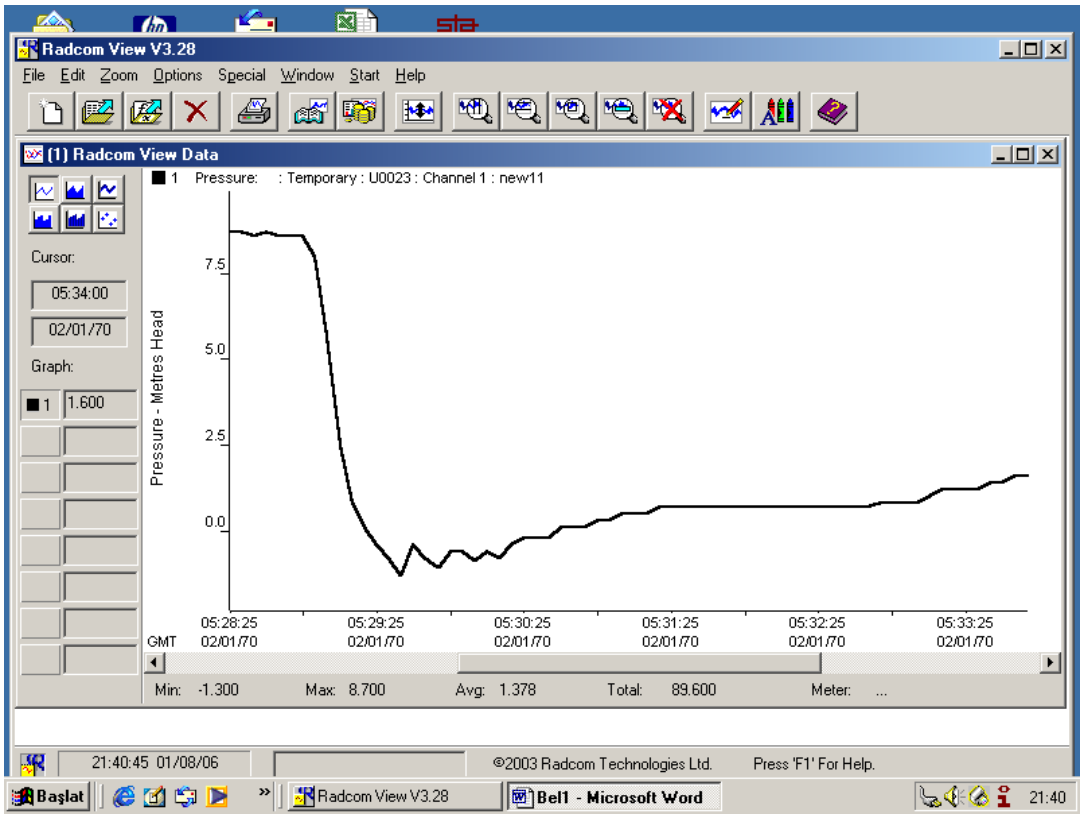

Figure 7.7: Run down period corresponding to 39 lt/s upper steady state discharge.

7.2 Results of experiments performed in the second system

In the similar manner as in Section 7.1, experiments were performed using lower, moderate and upper steady state discharges in the second system.

Although several experiments are realised to study unsteady flows due to the pump failure in second system, only some of them are presented.

7.2.1 Results of experiment performed for lower steady state discharge

In these experiments, lower steady state discharges were measured as 6.60 and 9.01 lt/s. The output measurement results and the graphics are shown below. In Table 7.2, pressure heads measured at the first and second measuring points in second system corresponds to 6.60 lt/s lower steady state discharge.

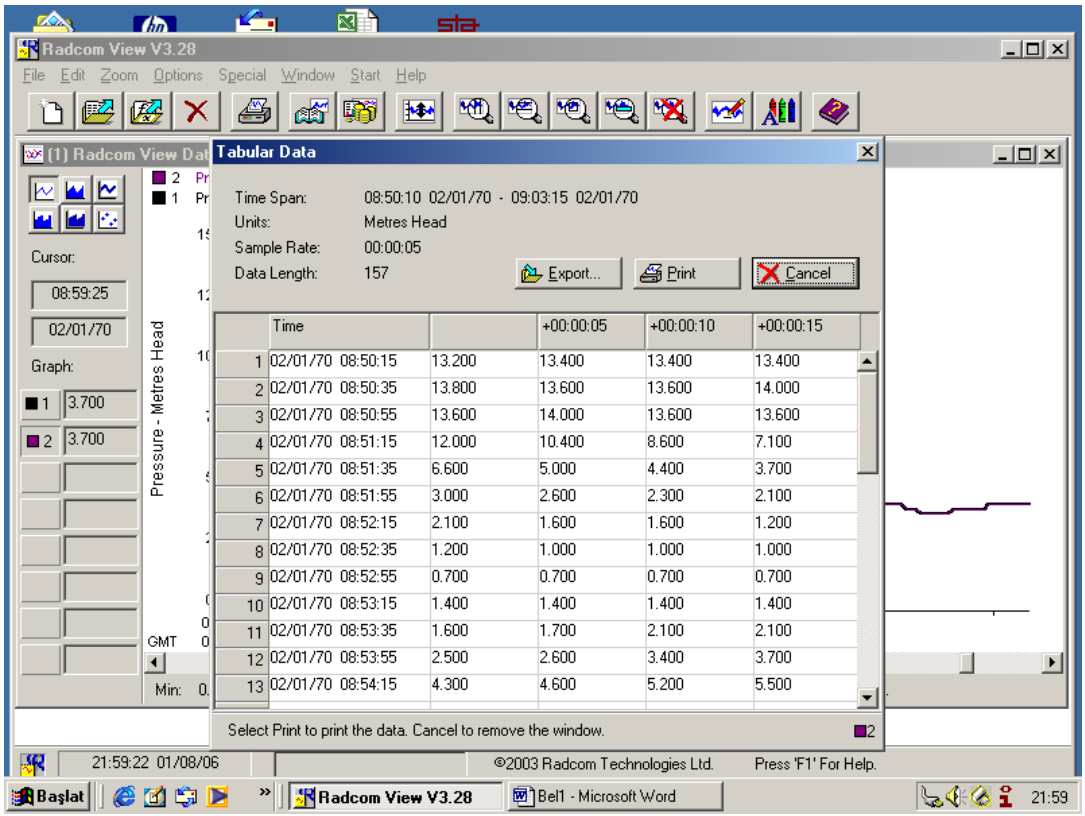

Figure 7.8: Pressure heads corresponding to 6.6 lt/s lower steady state discharge at point 1.

Table 7.2: Measured pressure heads corresponding to 6.6 lt/s lower steady state discharge for first and second measuring points.

Time (Minute-Second-Milli second)	Measured Pressure Heads, (meters), point 1	Time (Minute-Second-Milli second)	Measured Pressure Heads, (meters), point 2
08:50:15	13.20	07:54:35	11.10
08:50:20	13.40	07:54:40	10.90
08:50:25	13.40	07:54:45	10.70
08:50:30	13.40	07:54:50	10.70
08:50:35	13.80	07:54:55	11.30

Table 7.2 : (Continued)

08:50:40	13.60	07:55:00	11.10
08:50:45	13.60	07:55:05	11.30
08:50:50	14.00	07:55:10	11.10
08:50:55	13.60	07:55:15	11.10
08:51:00	14.00	07:55:20	10.70
08:51:05	13.60	07:55:25	10.90
08:51:10	13.60	07:55:30	11.30
08:51:15	12.00	07:55:35	10.70
08:51:20	10.40	07:55:40	10.00
08:51:25	8.60	07:55:45	8.90
08:51:30	7.10	07:55:50	7.90
08:51:35	6.60	07:55:55	6.80
08:51:40	5.00	07:56:00	5.70
08:51:45	4.40	07:56:05	5.20
08:51:50	3.70	07:56:10	4.30
08:51:55	3.00	07:56:15	3.70
08:52:00	2.60	07:56:20	3.20
08:52:05	2.30	07:56:25	2.80
08:52:10	2.10	07:56:30	2.30
08:52:15	2.10	07:56:35	1.90
08:52:20	1.60	07:56:40	1.70
08:52:25	1.60	07:56:45	1.40
08:52:30	1.20	07:56:50	1.40
08:52:35	1.20	07:56:55	1.20
08:52:40	1.00	07:57:00	1.00
08:52:45	1.00	07:57:05	0.70
08:52:50	1.00	07:57:10	0.70
08:52:55	0.70	07:57:15	0.50
08:53:00	0.70	07:57:20	0.50
08:53:05	0.70	07:57:25	0.50
08:53:10	0.70	07:57:30	0.30
08:53:15	1.40	07:57:35	0.50
08:53:20	1.40	07:57:40	0.50
08:53:25	1.40	07:57:45	0.80
08:53:30	1.40	07:57:50	0.80
08:53:35	1.60	07:57:55	0.80
08:53:40	1.70	07:58:00	0.70
08:53:45	2.10	07:58:05	0.70
08:53:50	2.10	07:58:10	0.70
08:53:55	2.50	07:58:15	0.80
08:54:00	2.60	07:58:20	1.00
08:54:05	3.40	07:58:25	1.20
08:54:10	3.70	07:58:30	1.60
08:54:15	4.30	07:58:35	1.70
08:54:20	4.60	07:58:40	1.90
08:54:25	5.20	07:58:45	1.90

Table 7.2 : (Continued)

08:54:30	5.50	07:58:50	2.10

08:54:35	6.10	07:58:55	2.30
08:54:40	6.20	07:59:00	2.60
08:54:45	6.40	07:59:05	2.80
08:54:50	6.40	07:59:10	3.00
08:54:55	6.40	07:59:15	2.80
08:55:00	6.40	07:59:20	2.80
08:55:05	5.90	07:59:25	2.60
08:55:10	5.30	07:59:30	2.30
08:55:15	5.20	07:59:35	2.10
08:55:20	4.60	07:59:40	2.10
08:55:25	4.30	07:59:45	1.90
08:55:30	4.10	07:59:50	1.70
08:55:35	3.90	07:59:55	1.70
08:55:40	3.50		
08:55:45	3.40		
08:55:50	3.00		
08:55:55	3.00		
08:56:00	2.80		
08:56:05	2.80		
08:56:10	2.80		
08:56:15	2.80		
08:56:20	3.00		
08:56:25	3.00		
08:56:30	3.40		
08:56:35	3.40		
08:56:40	3.50		
08:56:45	3.70		
08:56:50	3.90		
08:56:55	4.10		
08:57:00	4.30		
08:57:05	4.40		
08:57:10	4.60		
08:57:15	4.80		
08:57:20	5.00		
08:57:25	5.00		

In the Figures 7.9 and 7.10, the unsteady state flow pressure signals can be seen for first and second measuring points.

The results concerning the steady state discharge of 9.01 lt/s are presented in Figure 7.11 and Figure 7.12.

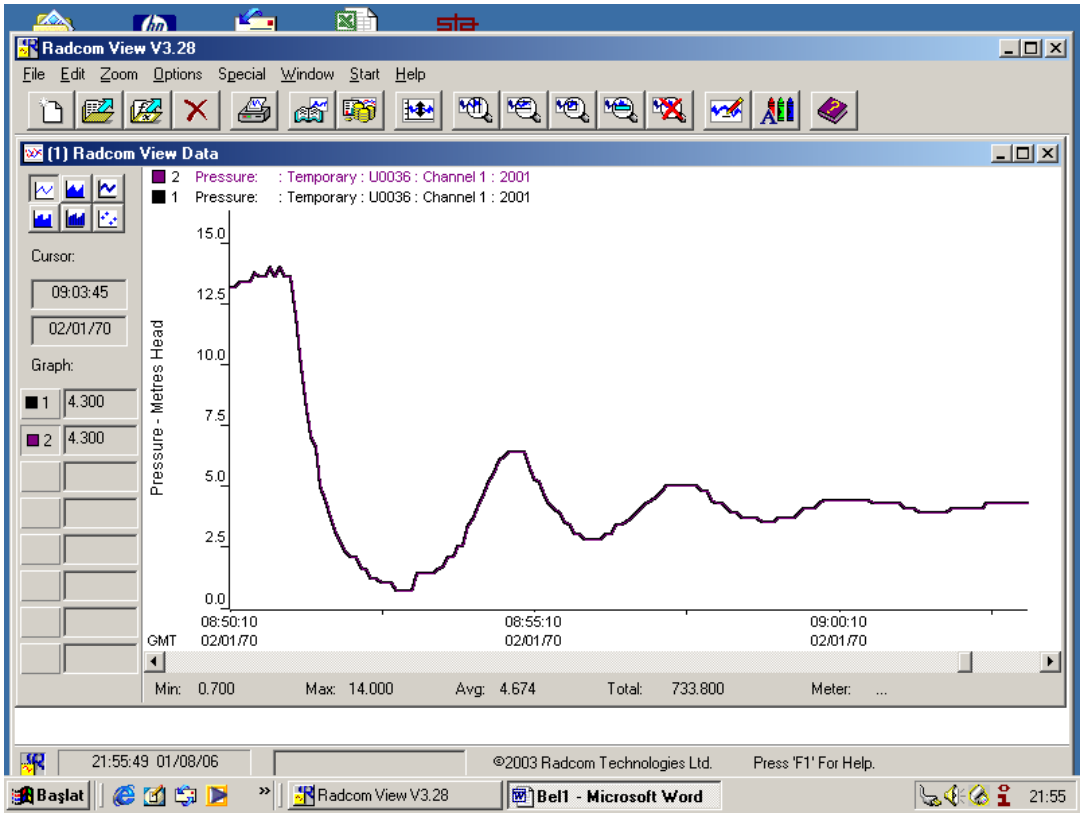

Figure 7.9: Run down period for 6.6 lt/s steady state discharge for first measuring point.

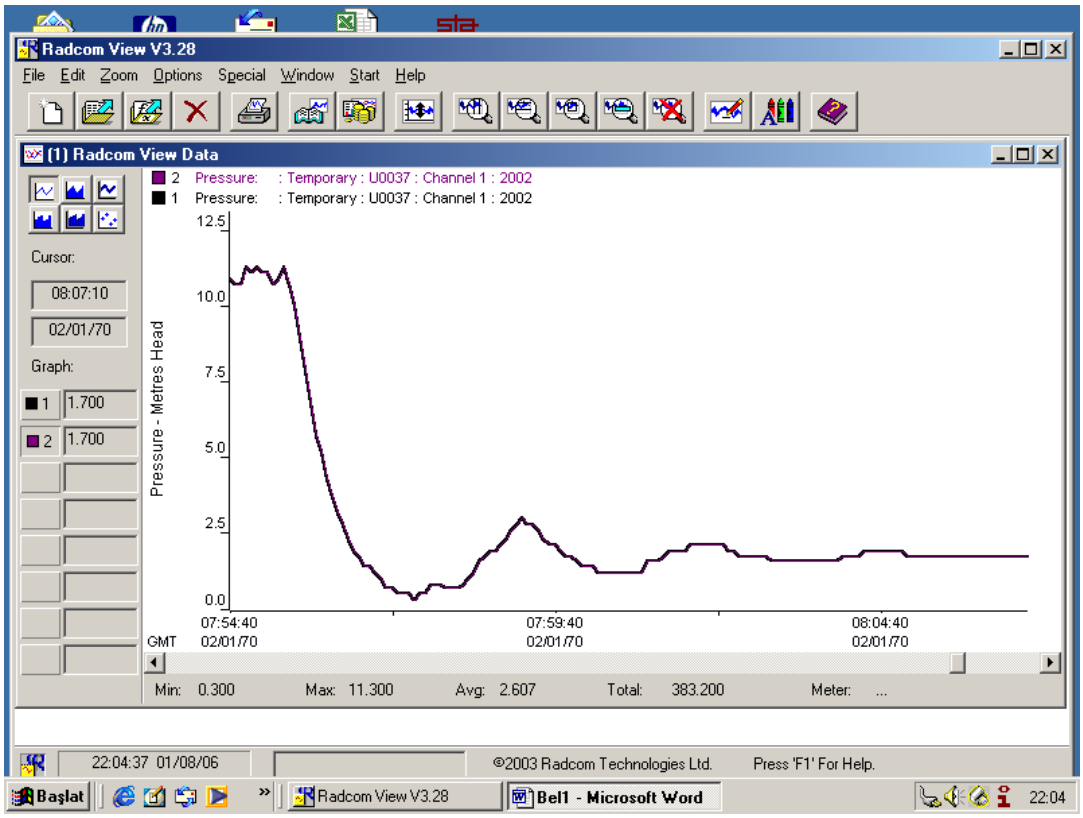

Figure 7.10: Run down period for 6.6 lt/s steady state discharge for second measuring point.

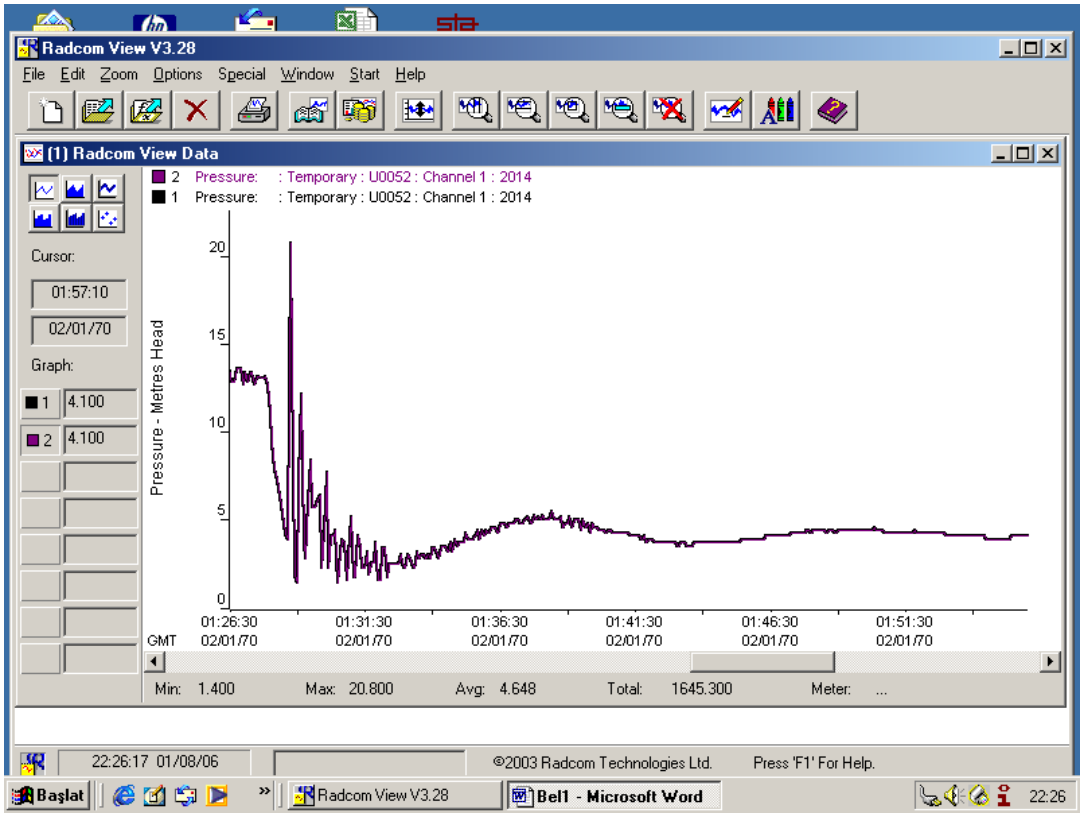

Figure 7.11: Run down period for 9.01 lt/s steady state discharge for first measuring point.

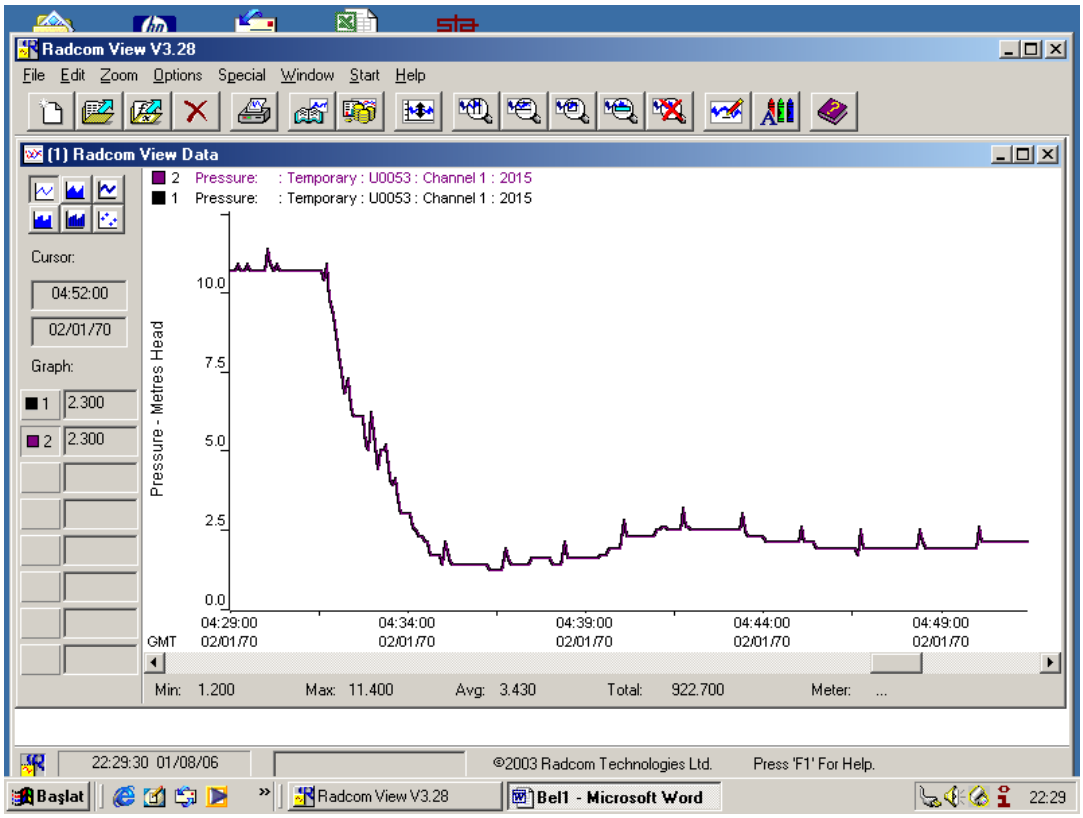

Figure 7.12: Run down period for 9.01 lt/s steady state discharge for second measuring point.

7.2.2 Results of experiment performed for moderate steady state discharge

In these experiments, moderate steady state discharges were measured as 16.5, 19.14 and 20.55 lt/s. The output measurement graphics are shown below. In Figures 7.13 and 7.14, pressure heads were measured at the first and second measuring points corresponding to 16.5 lt/s normal steady state discharge.

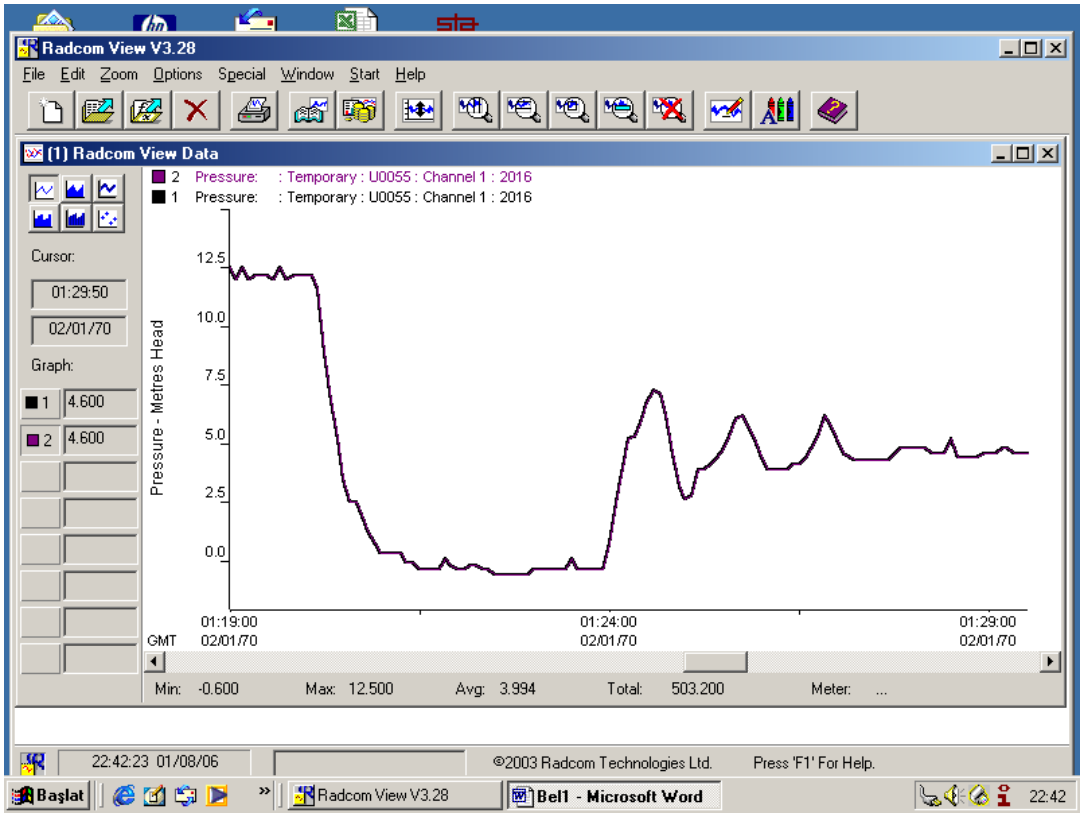

Figure 7.13: Run down period for 16.5 lt/s steady state discharge for first measuring point.

The results relative to a steady state discharge of 19.14 lt/s are given in Figure 7.15 and Figure 7.16.

Figure 7.17 and Figure 7.18 show the results corresponding to a steady state discharge of 20.55 lt/s.

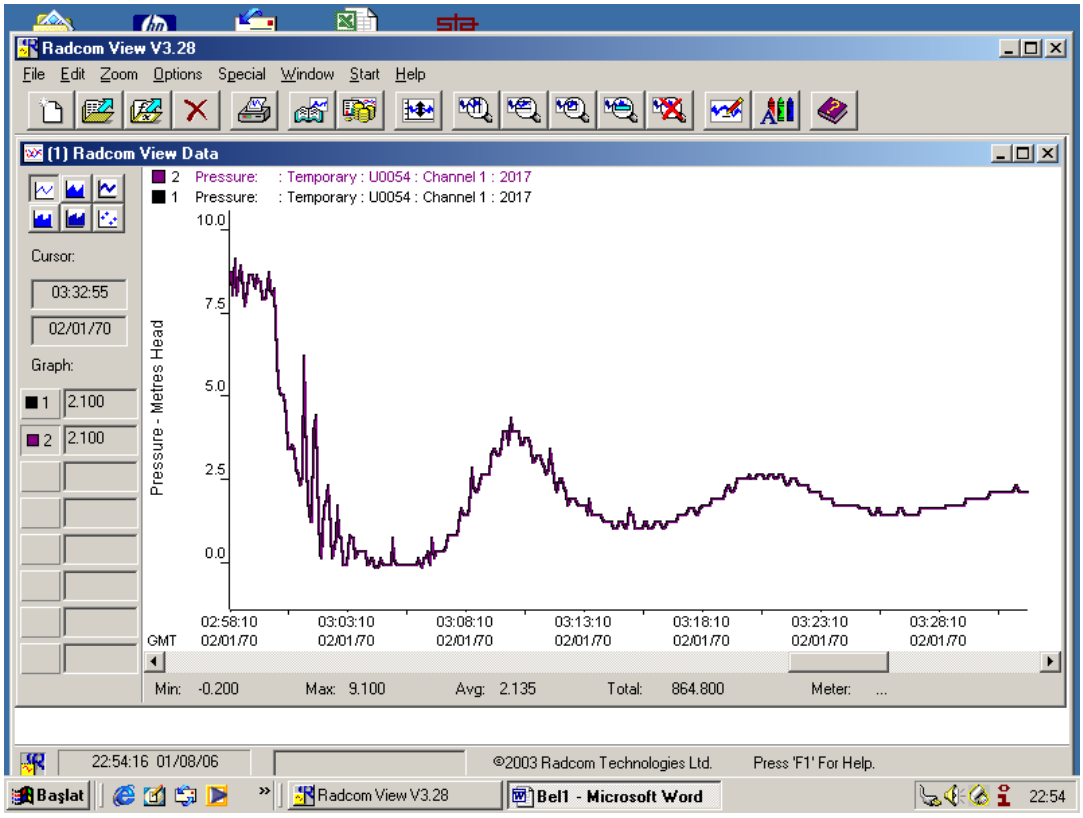

Figure 7.14: Run down period for 16.5 lt/s steady state discharge for second measuring point.

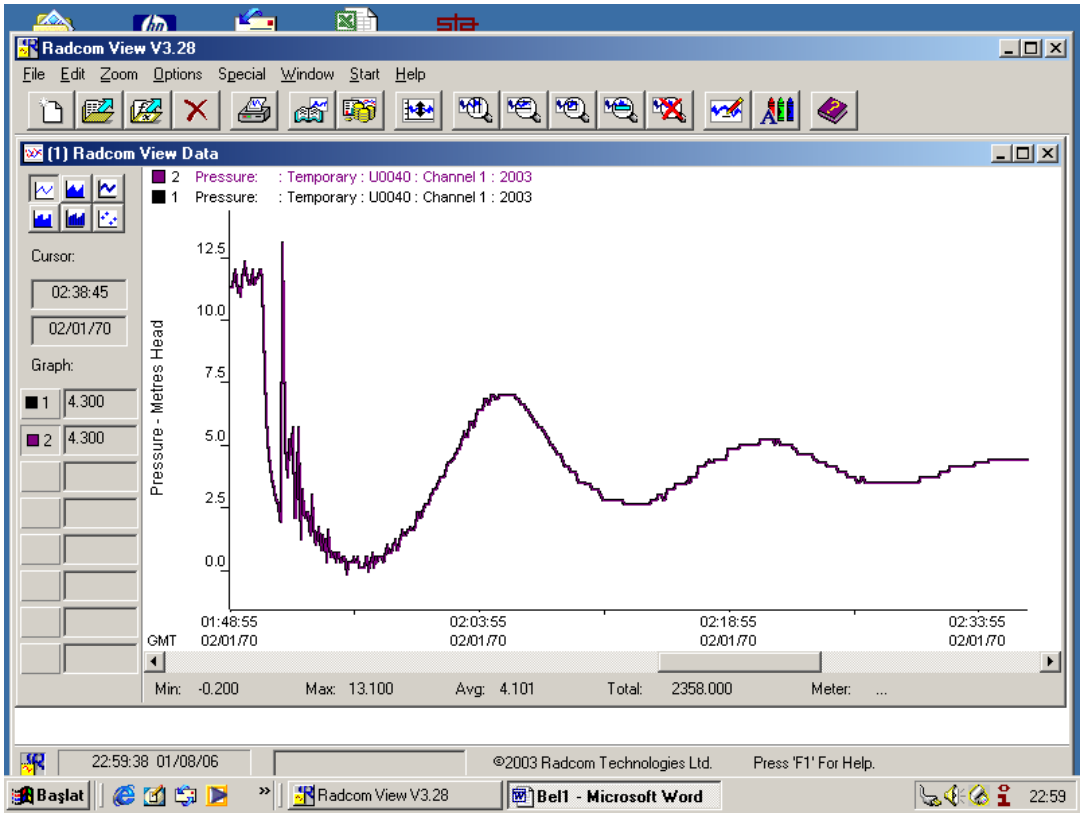

Figure 7.15: Run down period for 19.14 lt/s steady state discharge for first measuring point

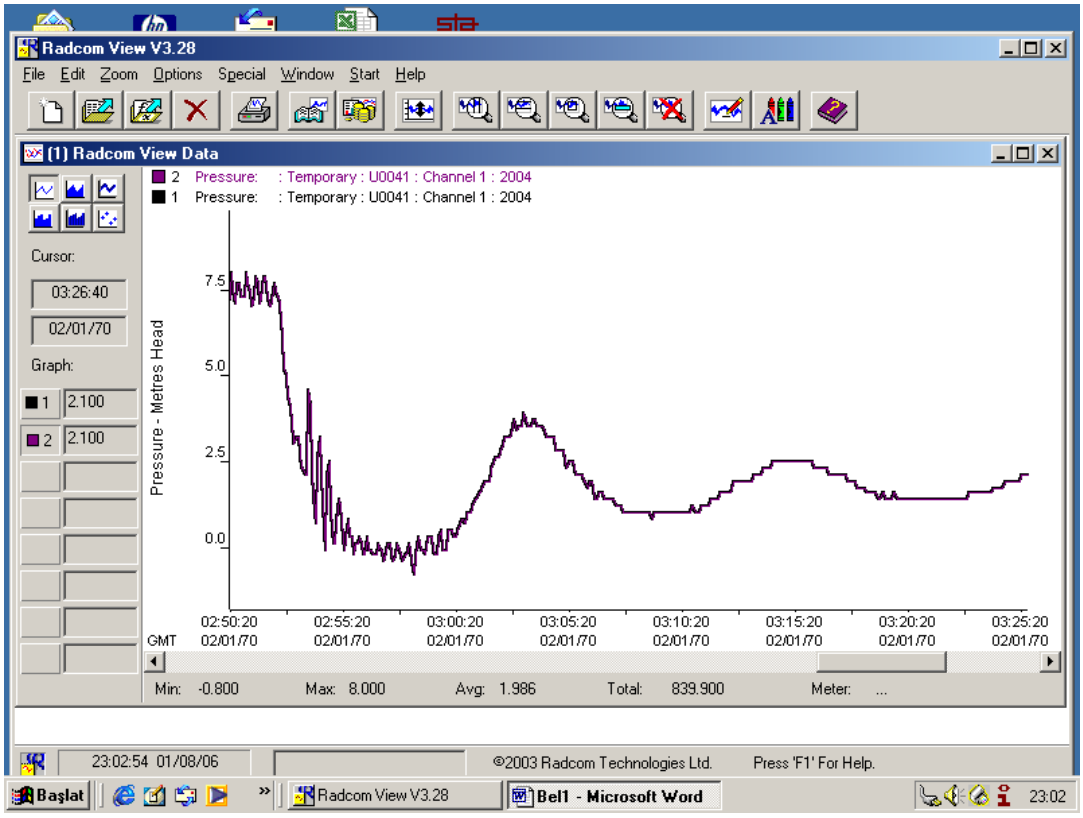

Figure 7.16: Run down period for 19.14 lt/s steady state discharge for second measuring point.

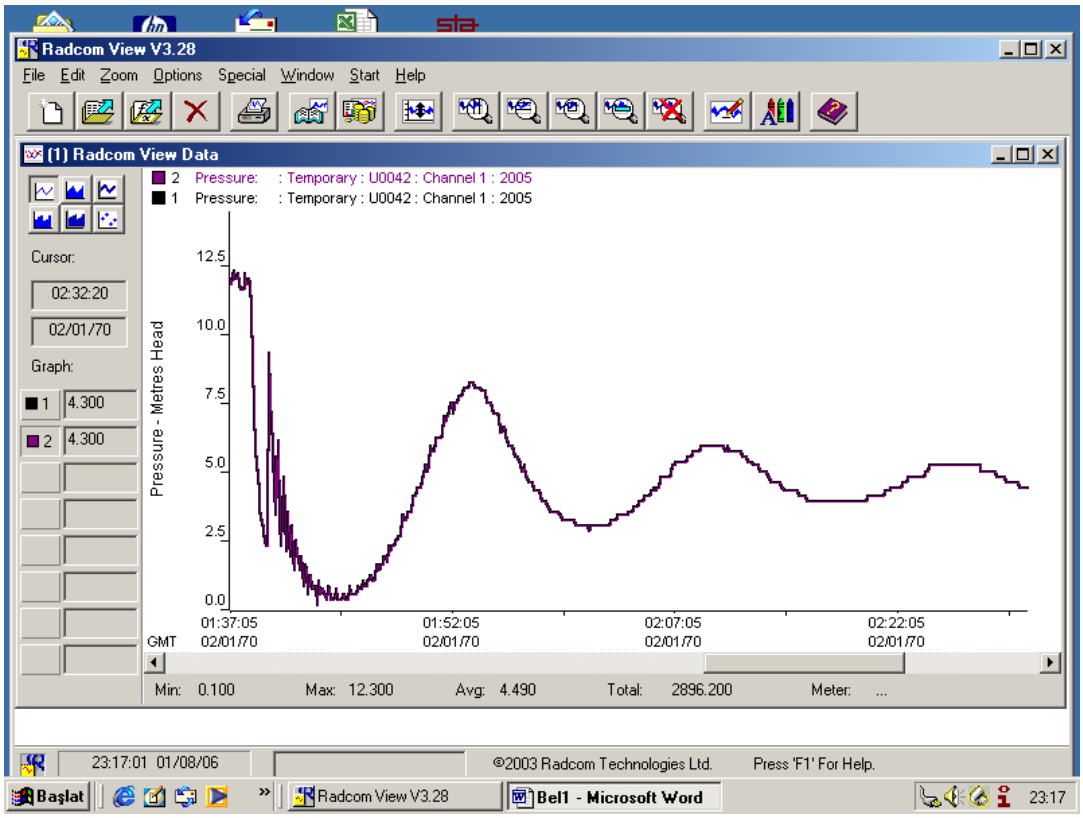

Figure 7.17: Run down period for 20.55 lt/s steady state discharge for first measuring point.

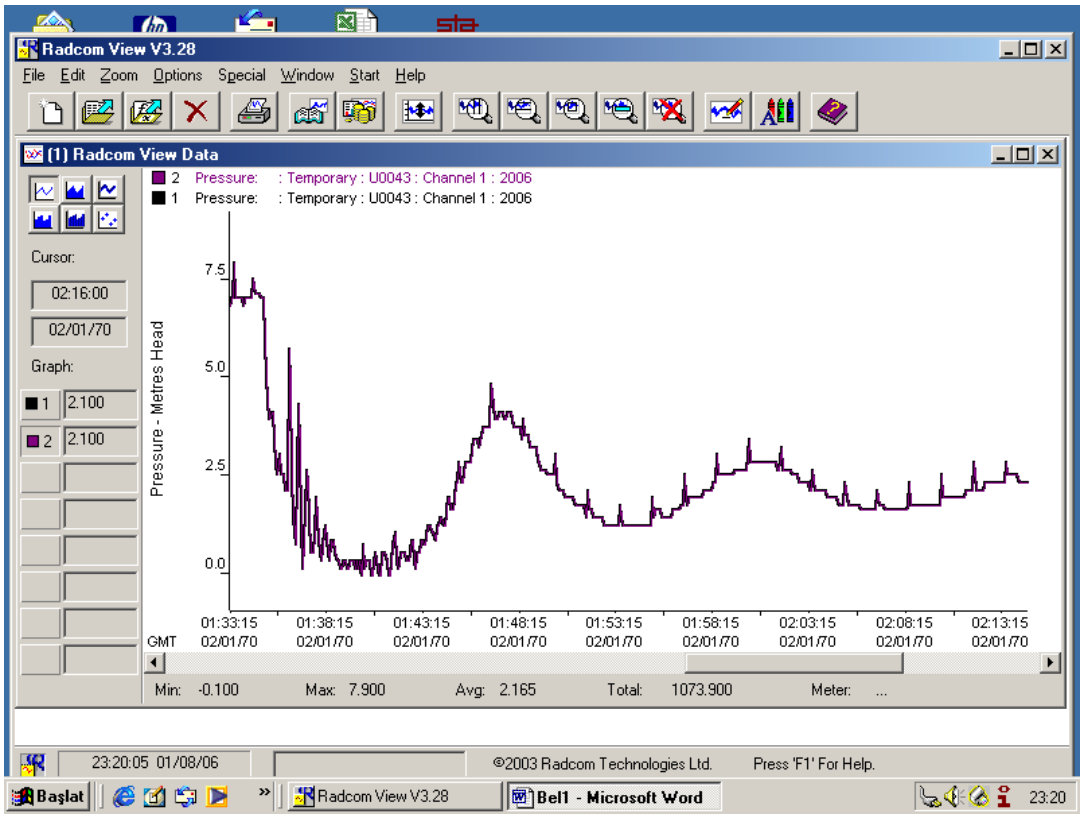

Figure 7.18: Run down period for 20.55 lt/s steady state discharge for second measuring point.

7.2.3 Results of experiment performed for upper steady state discharge

In these experiments, upper steady state discharges were measured as 24.51 and 25.16 lt/s. The output measurement graphics are shown in Figures 7.19, 7.20 and 7.21, 7.22, respectively.

According to the experimental curves, one can say that the check valve is not closed immediately after the shut down of the pump.

The water hammer pressure waves are registered after the closure of the check valve. The water hammer phenomenon starts with a negative pressure wave followed by positive pressure wave and the subsequence of negative / positive pressure waves. This phenomenon is damped and finished after certain time.

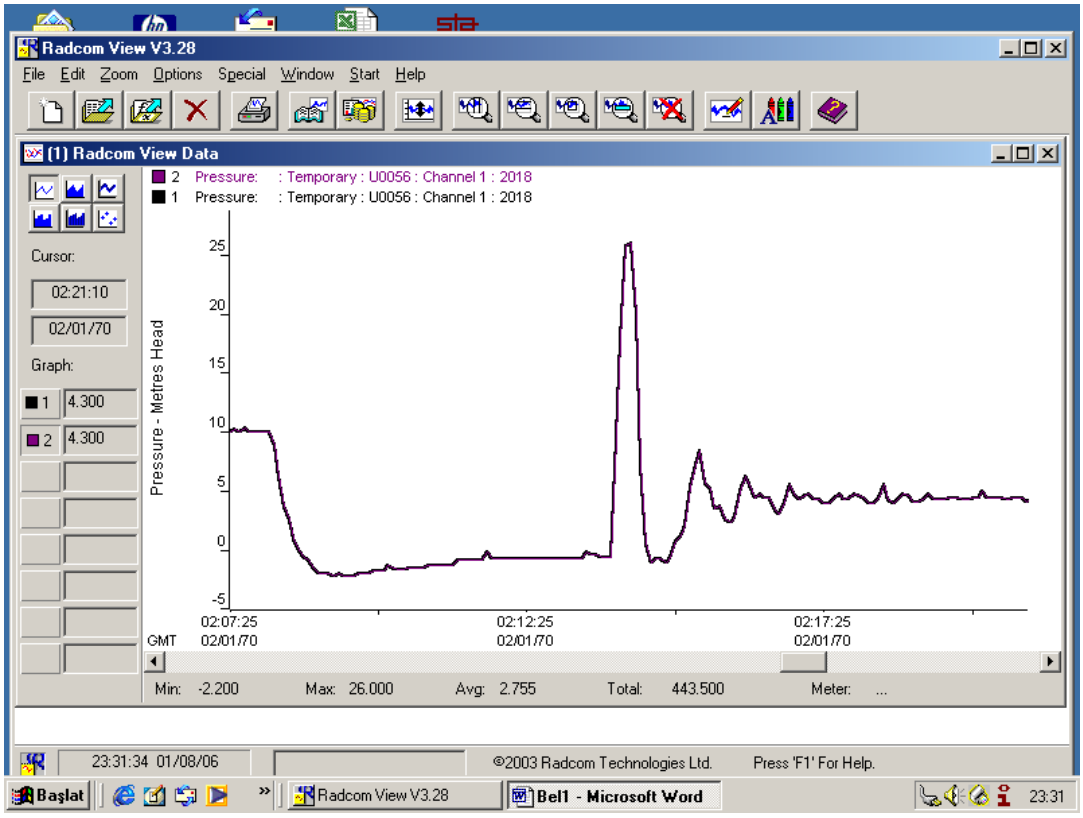

Figure 7.19: Run down period for 24.51 lt/s steady state discharge for first measuring point.

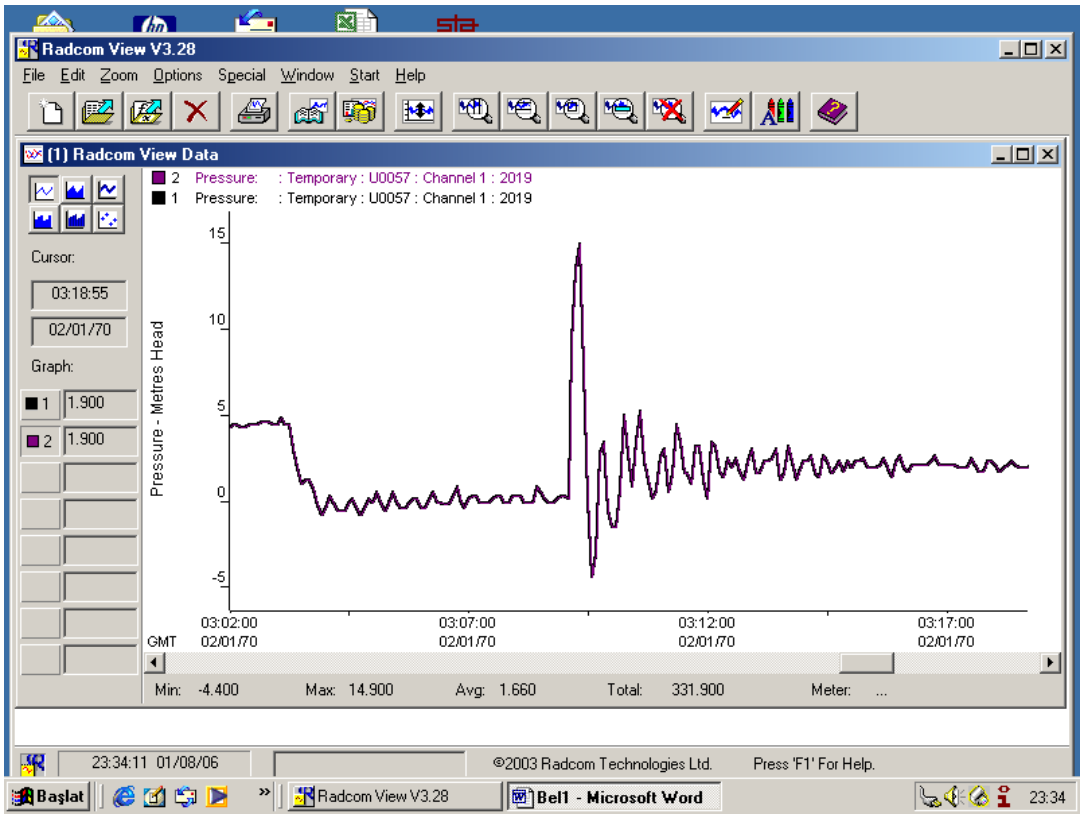

Figure 7.20: Run down period for 24.51 lt/s steady state discharge for second measuring point.

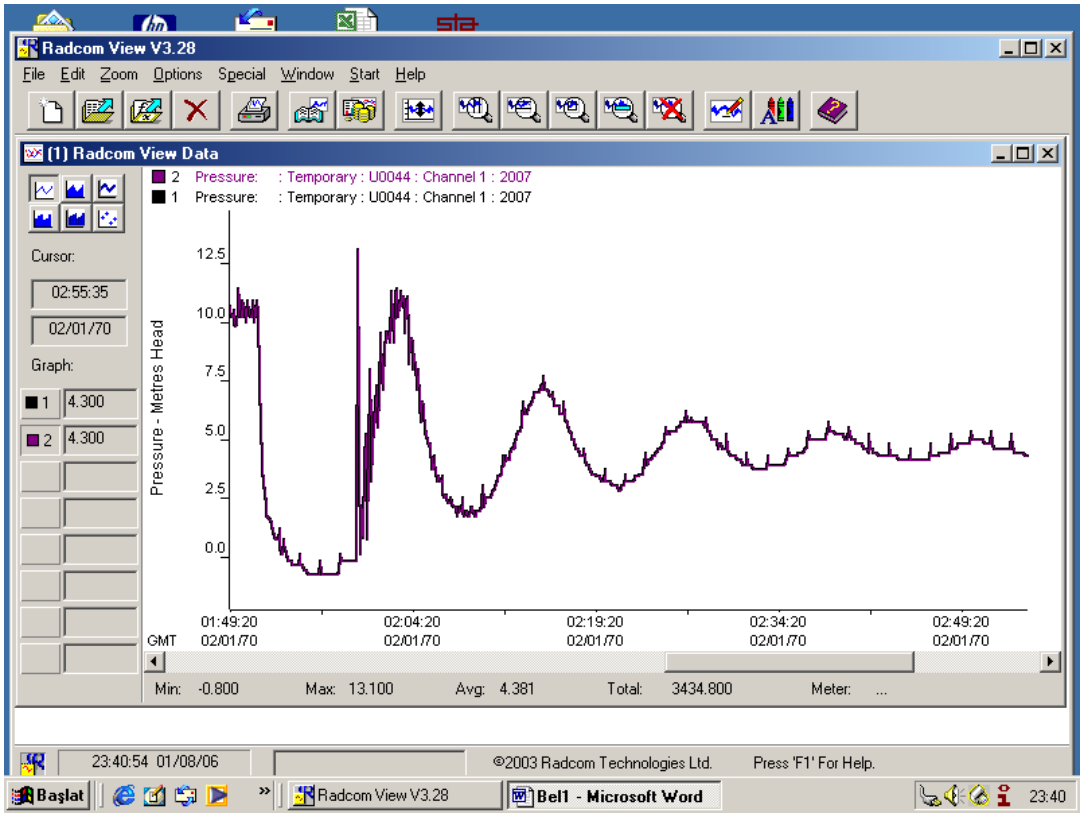

Figure 7.21: Run down period for 25.16 lt/s steady state discharge for first measuring point.

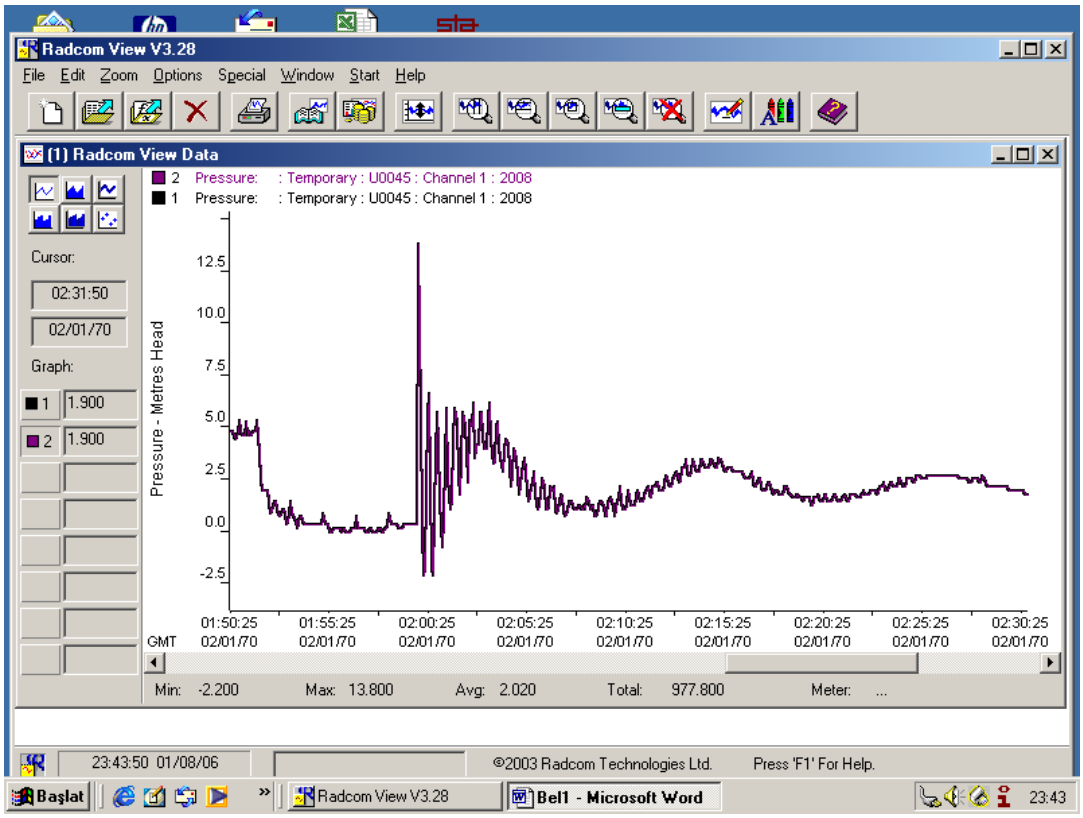

Figure 7.22: Run down period for 25.16 lt/s steady state discharge for second measuring point.

CHAPTER EIGHT
THEORETICAL RESULTS

Several computations are realised for the first system. These computations correspond to experimental conditions, namely those performed for lower steady state discharge, moderate steady state discharge and upper steady state discharge.

8.1 Results of computations performed for the first system

8.1.1 Results of computation performed for lower steady state discharge

The first page of output relative to a discharge of 6.2 lt/s is given in Figure 8.1. The relevant flow average velocity is 0.50 m/s. The graph of pressure heads and discharge values at measurement point drawn according to the results of numerical solution are given in Figures 8.2, 8.3, 8.4 and 8.5, respectively.

```
                          ******************
                          * INITIAL VALUES *
                          ******************


EL (M)=    3.7000        A (M3/SEC)= 1331.0000       XL (M)=   28.0000
F=      .0241            D (M)=     .1250            G (M/S2)=    9.8060
TM (S)=    8.0000        RN (RPM)= 1450.0000         TR (NT.M)=   32.1800
HR (M)=   11.0000        QR (M3/S)=     .0360        WRR (NT.M2)=     .8300
TOL=     .0002           V=     .1714                N= 28
DX (RAD)=     .0714      CK=  860.0000               PI=    3.1416
AL=    1.0000            AL0=    1.0000             AL00=    1.0000
AKS(M)=     .0002        DT (S)=     .0008          VN (M2/S)=   .000001
HMIN=     .0000          T=     .0000               JPR= 56
K=  0                    QQA (M3/S)=     .0062      KIT=  5
NSS= 23


                          ****************
                          * RESULT VALUES *
                          ****************


HP1=PIEZOMETRIC HEAD IN METERS BEFORE VALVE
HP2=PIEZOMETRIC HEAD IN METERS AFTER VALVE
HP=HEADLOSS IN METERS AT VALVE (NODE NSS)

HP1 HP2 HP   14.8736    3.7120   11.1616

NUMBER OF NODES AND PIEZOMETRIC HEADS AT NODES AS METERS :
```

Figure 8.1: Theoretical pressure head results obtained for 6.2 lt/s.

```
 1:    14.93    2:    14.93    3:    14.92    4:    14.92    5:    14.92
 6:    14.92    7:    14.91    8:    14.91    9:    14.91   10:    14.91
11:    14.90   12:    14.90   13:    14.90   14:    14.90   15:    14.89
16:    14.89   17:    14.89   18:    14.89   19:    14.88   20:    14.88
21:    14.88   22:    14.88   23:     3.71   24:     3.71   25:     3.71
26:     3.70   27:     3.70   28:     3.70   29:     3.70

ZH(I) VALUES AS METERS :

 1:     -.36    2:      .14    3:      .39    4:      .44    5:      .44
 6:      .49    7:      .54    8:      .59    9:      .59   10:      .62
11:      .64   12:      .69   13:      .71   14:      .74   15:      .76
16:      .79   17:      .84   18:      .85   19:      .89   20:      .93
21:     1.59   22:     2.14   23:     2.14   24:     2.14   25:     2.14
26:     2.14   27:     2.14   28:     2.14   29:     3.35


 TIME  ALPHA   BETA     V    Q(1)   Q(NS) HPH(1) HPH(NS) HP11  HPH(NSS)
 .000  1.000   .656   .172   .006   .006 15.289   .350 12.734  1.572
 .002   .998   .653   .172   .006   .006 15.214   .350 12.734  1.572
 .084   .878   .507   .159   .006   .006 11.853   .350 10.770  1.158
 .168   .783   .403   .139   .005   .005  9.502   .350  8.501  1.137
 .252   .707   .327   .120   .004   .004  7.816   .350  6.680  1.177
 .337   .644   .271   .103   .004   .004  6.565   .350  5.287  1.219
 .421   .591   .228   .088   .003   .003  5.612   .350  4.219  1.252
 .505   .547   .195   .075   .003   .003  4.865   .350  3.390  1.275
 .589   .509   .168   .062   .002   .002  4.268   .350  2.740  1.290
 .673   .476   .146   .050   .002   .002  3.788   .350  2.230  1.299
 .757   .447   .128   .038   .001   .001  3.397   .350  1.834  1.301
 .842   .422   .113   .025   .001   .001  3.073   .350  1.538  1.293
 .926   .399   .101   .013   .000   .000  2.802   .350  1.335  1.275
1.010   .379   .090  -.001   .000   .000  2.579   .350  1.240  1.240
1.094   .361   .079  -.017  -.001  -.001  2.388   .350  1.117  1.222
1.178   .346   .071  -.032  -.001  -.001  2.231   .350   .863  1.248
1.262   .332   .064  -.045  -.002  -.002  2.099   .350   .532  1.302
1.347   .319   .059  -.056  -.002  -.002  1.983   .350   .195  1.362
1.431   .307   .054  -.063  -.002  -.002  1.879   .350  -.101  1.415
1.515   .296   .051  -.069  -.002  -.002  1.784   .350  -.340  1.454
1.599   .285   .047  -.073  -.003  -.003  1.697   .350  -.527  1.481
1.683   .276   .044  -.076  -.003  -.003  1.618   .350  -.674  1.500
1.767   .267   .042  -.078  -.003  -.003  1.545   .350  -.791  1.512
1.852   .258   .039  -.080  -.003  -.003  1.477   .350  -.887  1.520
1.936   .250   .037  -.081  -.003  -.003  1.415   .350  -.969  1.525
2.020   .243   .035  -.082  -.003  -.003  1.359   .350 -1.040  1.529
2.104   .235   .033  -.084  -.003  -.003  1.306   .350 -1.103  1.532
2.188   .229   .032  -.084  -.003  -.003  1.258   .350 -1.160  1.534
2.272   .222   .030  -.085  -.003  -.003  1.214   .350 -1.211  1.536
2.356   .216   .029  -.086  -.003  -.003  1.173   .350 -1.258  1.538
2.441   .210   .028  -.087  -.003  -.003  1.134   .350 -1.301  1.539
2.525   .204   .027  -.087  -.003  -.003  1.099   .350 -1.340  1.540
2.609   .199   .025  -.088  -.003  -.003  1.065   .350 -1.377  1.541
2.693   .194   .024  -.088  -.003  -.003  1.034   .350 -1.411  1.542
2.777   .188   .024  -.089  -.003  -.003  1.005   .350 -1.443  1.543
2.861   .184   .023  -.089  -.003  -.003   .977   .350 -1.474  1.543
2.946   .179   .022  -.090  -.003  -.003   .950   .350 -1.502  1.544
3.030   .174   .021  -.090  -.003  -.003   .926   .350 -1.529  1.544
3.114   .170   .021  -.091  -.003  -.003   .903   .350 -1.554  1.545
3.198   .165   .020  -.091  -.003  -.003   .881   .350 -1.577  1.545
3.282   .161   .020  -.091  -.003  -.003   .860   .350 -1.599  1.546
3.366   .157   .019  -.092  -.003  -.003   .841   .350 -1.620  1.546
3.451   .153   .019  -.092  -.003  -.003   .822   .350 -1.640  1.547
3.535   .149   .018  -.092  -.003  -.003   .805   .350 -1.658  1.547
3.619   .146   .018  -.092  -.003  -.003   .788   .350 -1.676  1.547
```

Figure 8.1: Theoretical pressure head results obtained for 6.2 lt/s (continued).

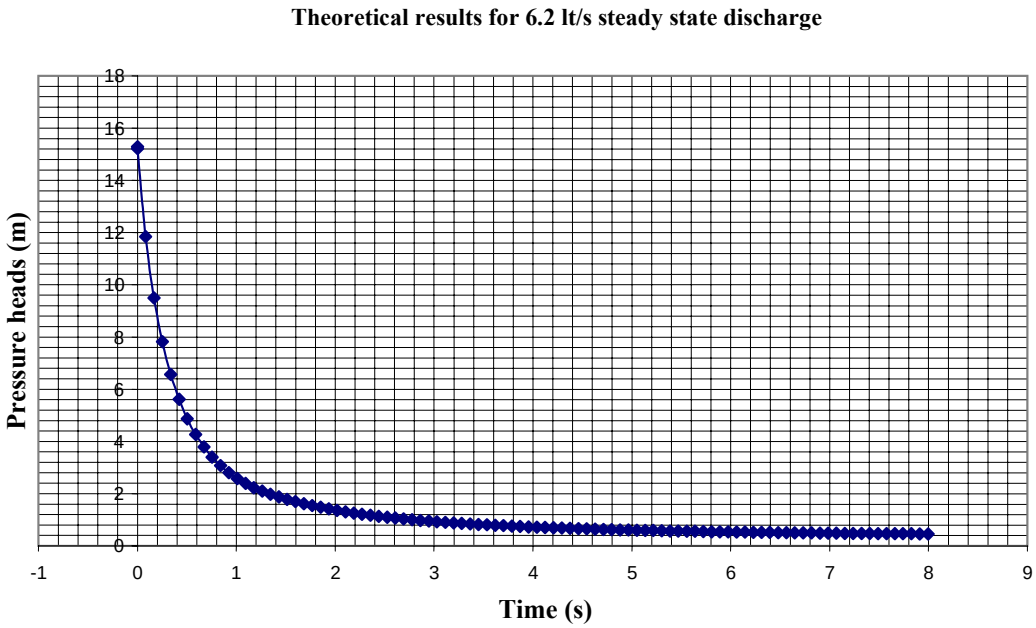

Figure 8.2: Theoretical pressure head results obtained for 6.2 lt/s.

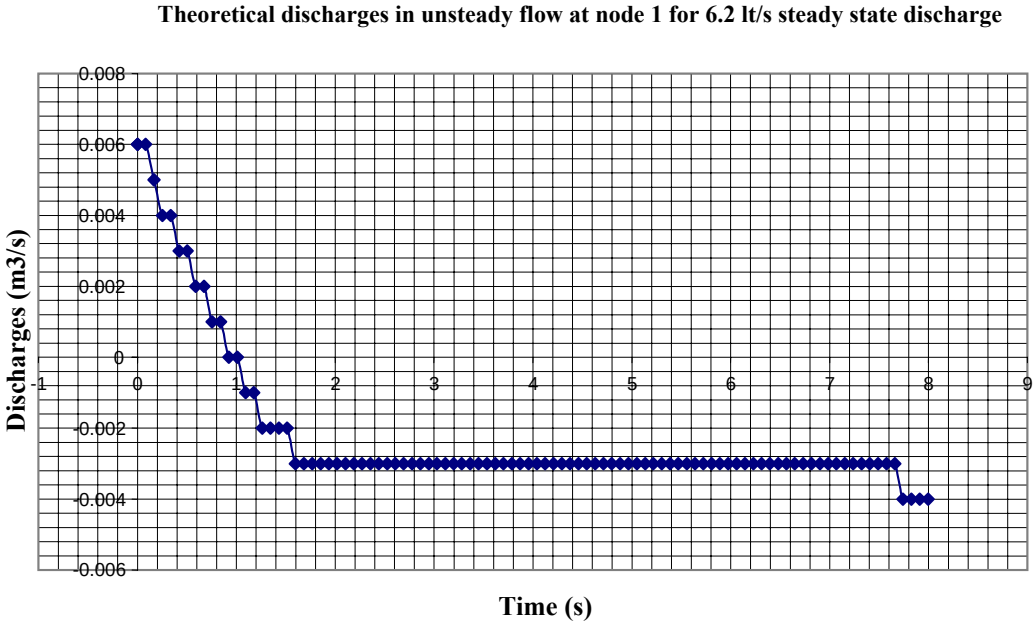

Figure 8.3: Theoretical transient discharges obtained for 6.2 lt/s.

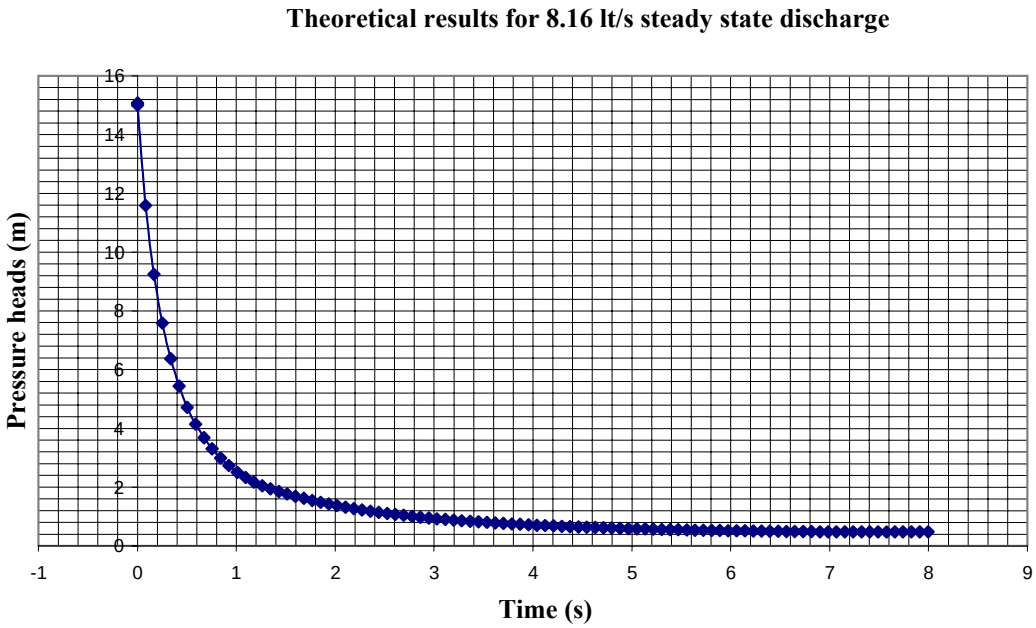

Figure 8.4: Theoretical pressure head results obtained for 8.16 lt/s.

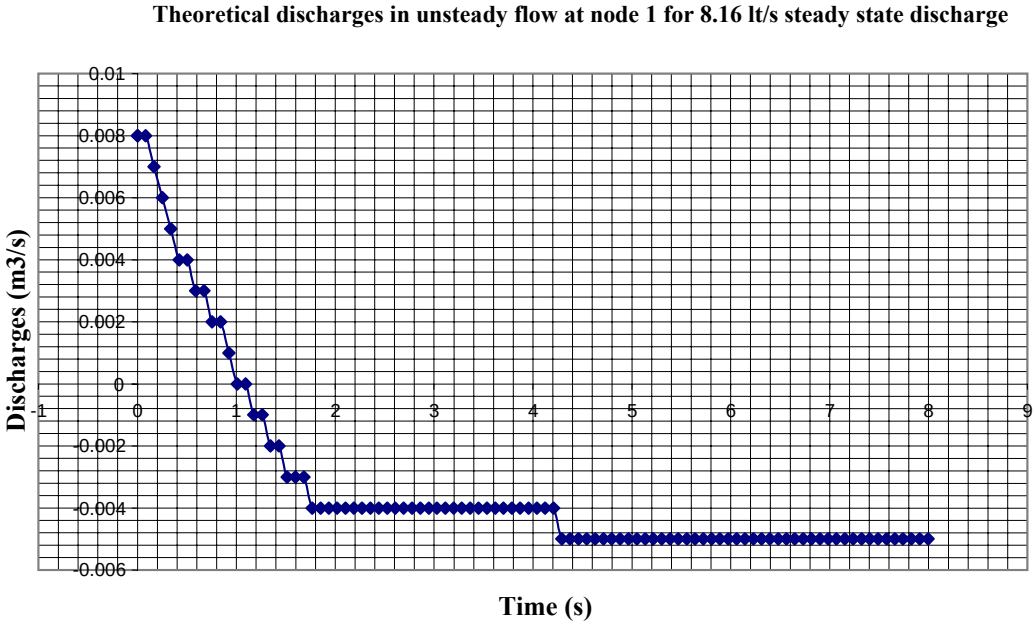

Figure 8.5: Theoretical transient discharges obtained for 8.16 lt/s.

8.1.2 Results of computation performed for moderate steady state discharge

In these computations, moderate steady state discharges are taken as 12.31 lt/s (1 m/s), 18.32 lt/s (1.5 m/s), 22.64 lt/s (1.85 m/s). The output and results are shown below.

The numerical solution result is given in Figure 8.6. The graph of pressure heads and discharge values at measurement points drawn according to the results of numerical solution are given in Figures 8.7, 8.8, 8.9, 8.10, 8.11 and 8.12 respectively.

```
                          ******************
                          * INITIAL VALUES *
                          ******************


EL (M)=    3.7200        A (M3/SEC)= 1331.0000       XL (M)=   28.0000
F=      .0226            D (M)=     .1250           G (M/S2)=    9.8060
TM (S)=    8.0000        RN (RPM)= 1450.0000        TR (NT.M)=   32.1800
HR (M)=   11.0000        QR (M3/S)=     .0360       WRR (NT.M2)=     .8300
TOL=     .0002           V=     .3419               N= 28
DX (RAD)=     .0714      CK=  201.0000              PI=    3.1416
AL=    1.0000            AL0=    1.0000             AL00=    1.0000
AKS(M)=     .0002        DT (S)=     .0008          VN (M2/S)=   .000001
HMIN=     .0000          T=     .0000               JPR= 56
K=  0                    QQA (M3/S)=     .0123      KIT=  5
NSS= 23


                          *****************
                          * RESULT VALUES *
                          *****************


HP1=PIEZOMETRIC HEAD IN METERS BEFORE VALVE
HP2=PIEZOMETRIC HEAD IN METERS AFTER VALVE
HP=HEADLOSS IN METERS AT VALVE (NODE NSS)

HP1 HP2 HP   13.9314    3.7718   10.1596

NUMBER OF NODES AND PIEZOMETRIC HEADS AT NODES AS METERS :

 1:    14.13    2:    14.12    3:    14.11    4:    14.10    5:    14.10
 6:    14.09    7:    14.08    8:    14.07    9:    14.06   10:    14.05
11:    14.04   12:    14.03   13:    14.02   14:    14.01   15:    14.00
16:    14.00   17:    13.99   18:    13.98   19:    13.97   20:    13.96
21:    13.95   22:    13.94   23:     3.77   24:     3.76   25:     3.75
26:     3.74   27:     3.74   28:     3.73   29:     3.72

ZH(I) VALUES AS METERS :

 1:     -.34    2:      .16    3:      .41    4:      .46    5:      .46
 6:      .51    7:      .56    8:      .61    9:      .61   10:      .64
11:      .66   12:      .71   13:      .73   14:      .76   15:      .78
```

Figure 8.6: Theoretical pressure head results obtained for 12.31 lt/s.

16:	.81	17:	.86	18:	.87	19:	.91	20:	.95
21:	1.61	22:	2.16	23:	2.16	24:	2.16	25:	2.16
26:	2.16	27:	2.16	28:	2.16	29:	3.36		

TIME	ALPHA	BETA	V	Q(1)	Q(NS)	HPH(1)	HPH(NS)	HP11	HPH(NSS)
.000	1.000	.710	.339	.012	.012	14.472	.357	11.771	1.612
.002	.997	.707	.339	.012	.012	14.394	.357	11.771	1.612
.084	.868	.548	.323	.012	.012	10.881	.357	10.269	1.038
.168	.766	.430	.293	.011	.011	8.532	.357	8.454	.891
.252	.685	.343	.259	.009	.009	6.897	.357	6.833	.887
.337	.620	.279	.228	.008	.008	5.723	.357	5.510	.929
.421	.567	.230	.199	.007	.007	4.862	.357	4.464	.980
.505	.522	.193	.172	.006	.006	4.211	.357	3.642	1.027
.589	.485	.163	.148	.005	.005	3.708	.357	2.994	1.067
.673	.453	.140	.125	.005	.005	3.309	.357	2.483	1.099
.757	.426	.122	.104	.004	.004	2.989	.357	2.078	1.122
.842	.402	.107	.084	.003	.003	2.727	.357	1.760	1.138
.926	.380	.095	.064	.002	.002	2.501	.357	1.510	1.144
1.010	.361	.085	.045	.002	.002	2.310	.357	1.323	1.143
1.094	.345	.076	.026	.001	.001	2.148	.357	1.192	1.135
1.178	.329	.068	.005	.000	.000	2.008	.357	1.119	1.116
1.262	.316	.060	-.016	-.001	-.001	1.890	.357	1.075	1.097
1.347	.304	.054	-.037	-.001	-.001	1.796	.357	.976	1.099
1.431	.293	.049	-.058	-.002	-.002	1.722	.357	.821	1.121
1.515	.283	.047	-.078	-.003	-.003	1.663	.357	.624	1.159
1.599	.273	.045	-.095	-.003	-.003	1.611	.357	.404	1.205
1.683	.264	.044	-.110	-.004	-.004	1.567	.357	.178	1.254
1.767	.255	.044	-.123	-.004	-.004	1.526	.357	-.037	1.301
1.852	.246	.044	-.134	-.005	-.005	1.482	.357	-.235	1.344
1.936	.236	.044	-.142	-.005	-.005	1.441	.357	-.411	1.380
2.020	.227	.045	-.150	-.005	-.005	1.399	.357	-.563	1.410
2.104	.217	.045	-.155	-.006	-.006	1.358	.357	-.693	1.435
2.188	.208	.045	-.160	-.006	-.006	1.315	.357	-.806	1.454
2.272	.198	.045	-.164	-.006	-.006	1.272	.357	-.903	1.468
2.356	.189	.046	-.167	-.006	-.006	1.231	.357	-.986	1.480
2.441	.179	.046	-.170	-.006	-.006	1.193	.357	-1.059	1.489
2.525	.169	.047	-.172	-.006	-.006	1.156	.357	-1.122	1.497
2.609	.159	.047	-.174	-.006	-.006	1.118	.357	-1.179	1.502
2.693	.149	.047	-.176	-.006	-.006	1.081	.357	-1.231	1.506
2.777	.140	.047	-.178	-.006	-.006	1.047	.357	-1.278	1.509
2.861	.130	.047	-.179	-.006	-.006	1.015	.357	-1.321	1.512
2.946	.120	.047	-.181	-.006	-.006	.984	.357	-1.360	1.515
3.030	.110	.047	-.182	-.007	-.007	.956	.357	-1.397	1.517
3.114	.100	.047	-.183	-.007	-.007	.931	.357	-1.429	1.519
3.198	.090	.046	-.184	-.007	-.007	.906	.357	-1.460	1.520
3.282	.080	.046	-.185	-.007	-.007	.882	.357	-1.489	1.521
3.366	.071	.045	-.186	-.007	-.007	.857	.357	-1.517	1.522
3.451	.061	.045	-.186	-.007	-.007	.835	.357	-1.543	1.523
3.535	.052	.044	-.187	-.007	-.007	.815	.357	-1.567	1.524
3.619	.043	.044	-.188	-.007	-.007	.795	.357	-1.589	1.525
3.703	.033	.043	-.189	-.007	-.007	.775	.357	-1.612	1.525
3.787	.025	.042	-.189	-.007	-.007	.756	.357	-1.632	1.526
3.871	.016	.041	-.190	-.007	-.007	.740	.357	-1.652	1.527
3.956	.007	.040	-.190	-.007	-.007	.727	.357	-1.669	1.528
4.040	-.001	.039	-.191	-.007	-.007	.716	.357	-1.684	1.529
4.124	-.009	.038	-.191	-.007	-.007	.703	.357	-1.699	1.530
4.208	-.017	.037	-.192	-.007	-.007	.690	.357	-1.713	1.530
4.292	-.024	.036	-.192	-.007	-.007	.677	.357	-1.728	1.530
4.376	-.032	.035	-.193	-.007	-.007	.665	.357	-1.741	1.531
4.460	-.039	.034	-.193	-.007	-.007	.655	.357	-1.752	1.531
4.545	-.046	.034	-.193	-.007	-.007	.647	.357	-1.763	1.532

Figure 8.6: Theoretical pressure head results obtained for 12.31 lt/s (Continued).

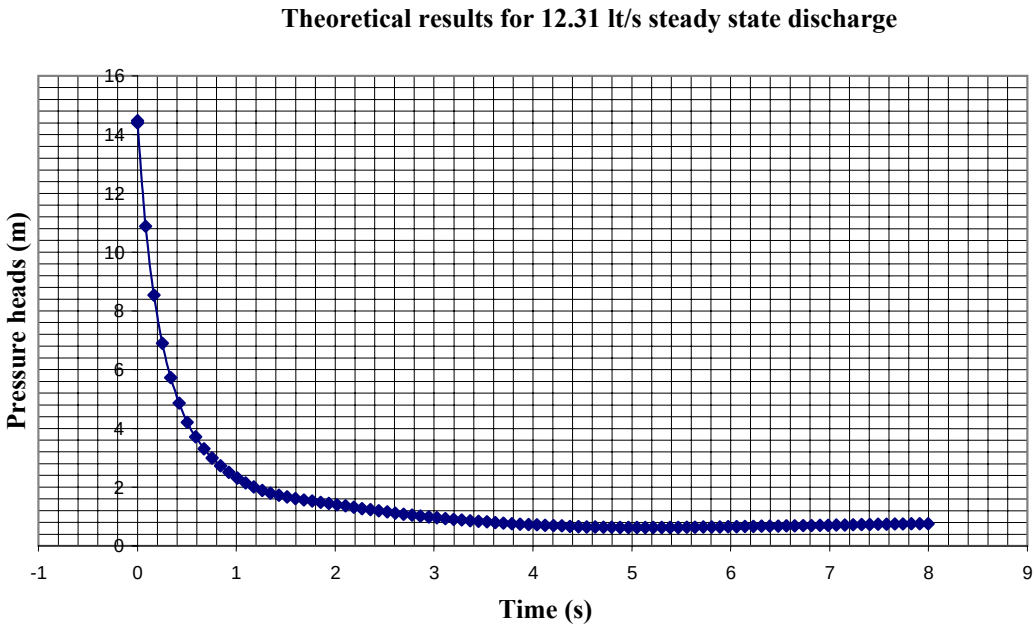

Figure 8.7: Theoretical pressure head results obtained for 12.31 lt/s.

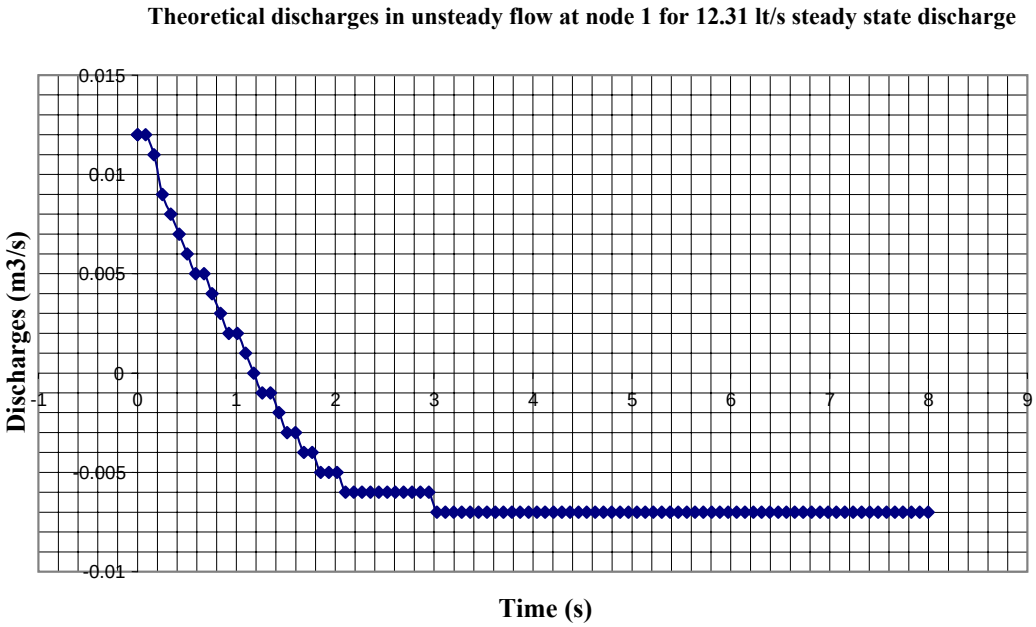

Figure 8.8: Theoretical transient discharges obtained for 12.31 lt/s.

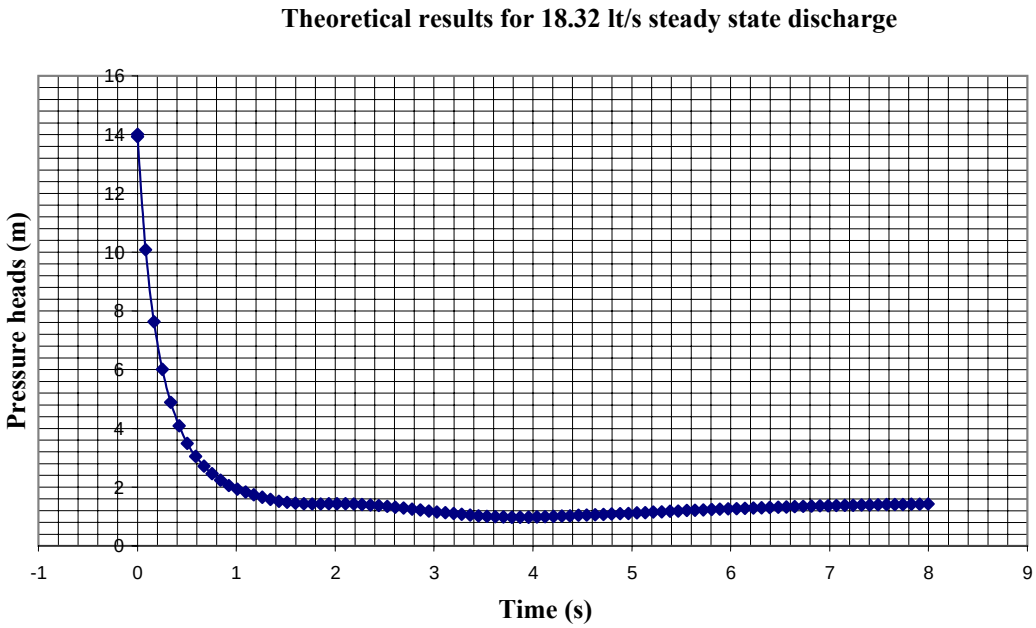

Figure 8.9: Theoretical pressure head results obtained for 18.32 lt/s.

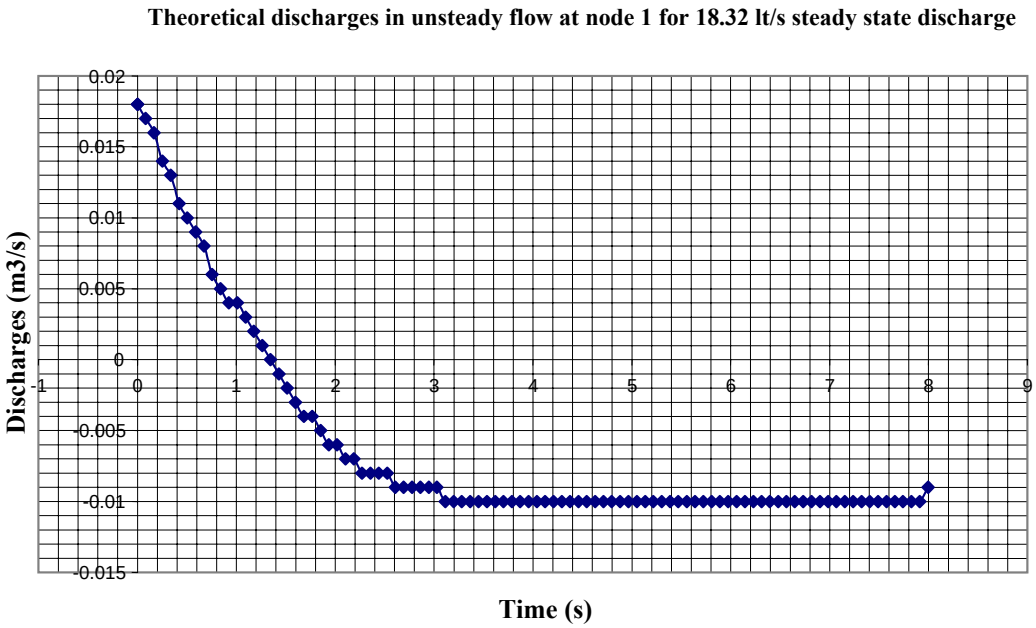

Figure 8.10: Theoretical transient discharges obtained for 18.32 lt/s.

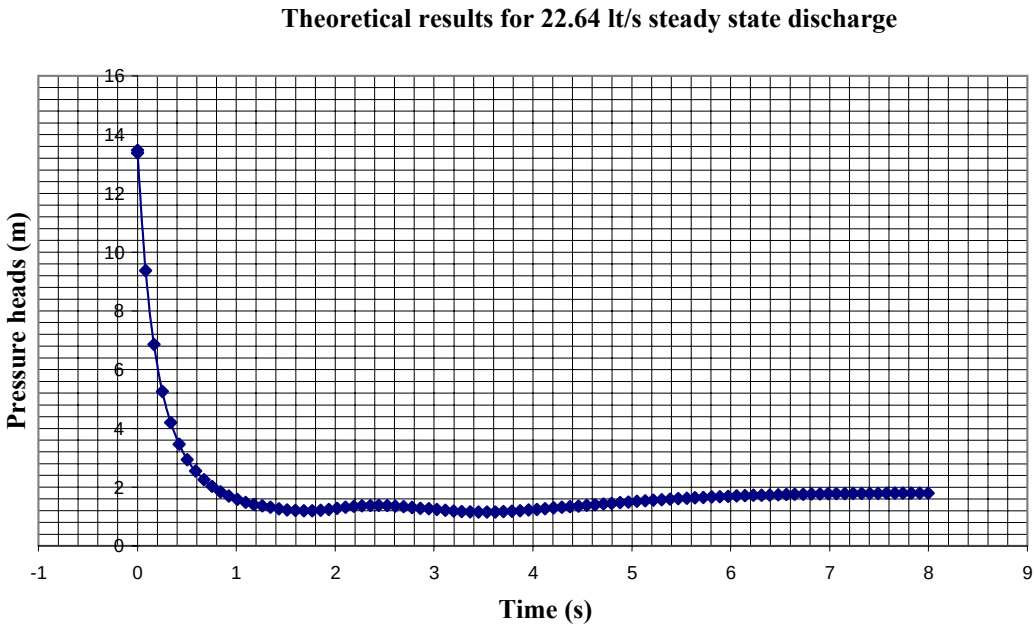

Figure 8.11: Theoretical pressure head results obtained for 22.64 lt/s.

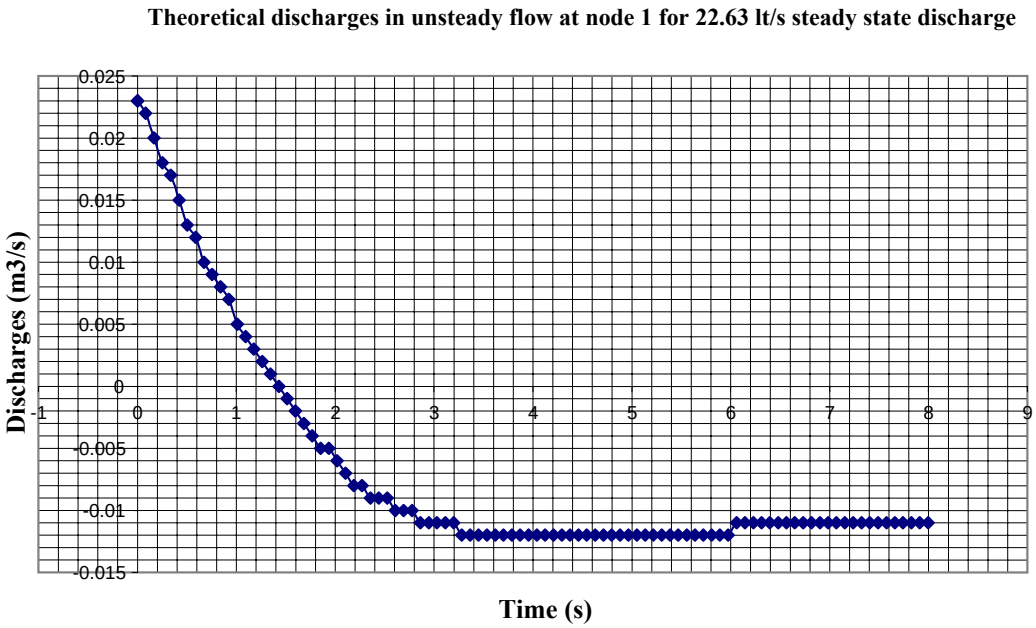

Figure 8.12: Theoretical transient discharges obtained for 22.64 lt/s.

8.1.3 *Results of computation performed for upper steady state discharge*

In this computation, upper steady state discharge was taken as 39.00 lt/s (3.20 m/s).

The numerical solution result is given in Figure 8.13. The graph of pressure head and discharge values at measurement points drawn according to the results of numerical solution are given in Figures 8.14 and 8.15 respectively.

```
                          ******************
                          * INITIAL VALUES *
                          ******************


EL (M)=    3.7500        A (M3/SEC)= 1331.0000       XL (M)=   28.0000
F=      .0213            D (M)=     .1250            G (M/S2)=    9.8060
TM (S)=    8.0000        RN (RPM)= 1450.0000         TR (NT.M)=   32.1800
HR (M)=   11.0000        QR (M3/S)=     .0360        WRR (NT.M2)=     .8300
TOL=     .0002           V=    1.0833               N= 28
DX (RAD)=     .0714      CK=    7.9000               PI=    3.1416
AL=    1.0000            AL0=    1.0000              AL00=    1.0000
AKS(M)=     .0002        DT (S)=     .0008           VN (M2/S)=   .000001
HMIN=     .0000          T=     .0000                JPR= 56
K=  0                    QQA (M3/S)=     .0390       KIT=  5
NSS= 23


                          *****************
                          * RESULT VALUES *
                          *****************


HP1=PIEZOMETRIC HEAD IN METERS BEFORE VALVE
HP2=PIEZOMETRIC HEAD IN METERS AFTER VALVE
HP=HEADLOSS IN METERS AT VALVE (NODE NSS)

HP1 HP2 HP    8.3156    4.2723    4.0433

NUMBER OF NODES AND PIEZOMETRIC HEADS AT NODES AS METERS :

 1:    10.23    2:    10.15    3:    10.06    4:     9.97    5:     9.89
 6:     9.80    7:     9.71    8:     9.62    9:     9.54   10:     9.45
11:     9.36   12:     9.28   13:     9.19   14:     9.10   15:     9.01
16:     8.93   17:     8.84   18:     8.75   19:     8.66   20:     8.58
21:     8.49   22:     8.40   23:     4.27   24:     4.19   25:     4.10
26:     4.01   27:     3.92   28:     3.84   29:     3.75

ZH(I) VALUES AS METERS :

 1:     -.31    2:      .19    3:      .44    4:      .49    5:      .49
 6:      .54    7:      .59    8:      .64    9:      .64   10:      .67
11:      .69   12:      .74   13:      .76   14:      .79   15:      .81
```

Figure 8.13: Theoretical pressure head results obtained for 39 lt/s.

16:	.84	17:	.89	18:	.90	19:	.94	20:	.98
21:	1.64	22:	2.19	23:	2.19	24:	2.19	25:	2.19
26:	2.19	27:	2.19	28:	2.19	29:	3.39		

TIME	ALPHA	BETA	V	Q(1)	Q(NS)	HPH(1)	HPH(NS)	HP11	HPH(NSS)
.000	1.000	.999	1.080	.039	.039	10.545	.359	6.126	2.082
.002	.996	.991	1.080	.039	.039	10.431	.359	6.125	2.083
.084	.827	.668	1.055	.038	.038	5.743	.359	4.955	1.108
.168	.709	.475	1.000	.036	.036	3.369	.359	4.135	.675
.252	.622	.356	.934	.034	.034	2.155	.359	3.527	.509
.337	.556	.279	.866	.031	.031	1.506	.359	3.052	.460
.421	.503	.225	.800	.029	.029	1.158	.359	2.680	.466
.505	.459	.187	.737	.027	.026	.974	.359	2.378	.499
.589	.423	.159	.677	.024	.024	.881	.359	2.130	.540
.673	.392	.137	.621	.022	.022	.838	.359	1.919	.585
.757	.365	.120	.569	.020	.020	.823	.359	1.749	.628
.842	.341	.106	.520	.019	.019	.823	.359	1.607	.673
.926	.320	.095	.474	.017	.017	.830	.359	1.487	.708
1.010	.301	.085	.430	.015	.015	.839	.359	1.377	.734
1.094	.284	.077	.388	.014	.014	.848	.359	1.290	.766
1.178	.268	.070	.349	.013	.013	.859	.359	1.217	.793
1.262	.254	.064	.310	.011	.011	.870	.359	1.148	.810
1.347	.241	.058	.274	.010	.010	.875	.359	1.087	.833
1.431	.230	.053	.238	.009	.009	.873	.359	1.039	.843
1.515	.219	.047	.203	.007	.007	.865	.359	.996	.849
1.599	.210	.041	.169	.006	.006	.852	.359	.958	.854
1.683	.202	.036	.136	.005	.005	.838	.359	.924	.863
1.767	.195	.031	.102	.004	.004	.822	.359	.897	.867
1.852	.189	.026	.069	.002	.002	.809	.359	.884	.870
1.936	.184	.022	.037	.001	.001	.811	.359	.880	.876
2.020	.179	.020	.004	.000	.000	.804	.359	.870	.873
2.104	.175	.018	-.029	-.001	-.001	.800	.359	.871	.873
2.188	.172	.018	-.061	-.002	-.002	.813	.359	.861	.874
2.272	.168	.021	-.094	-.003	-.003	.847	.359	.859	.890
2.356	.163	.028	-.125	-.004	-.004	.906	.359	.851	.908
2.441	.156	.038	-.155	-.006	-.006	.986	.359	.842	.933
2.525	.146	.050	-.184	-.007	-.007	1.075	.359	.842	.958
2.609	.134	.064	-.211	-.008	-.008	1.167	.359	.833	.985
2.693	.119	.078	-.237	-.009	-.009	1.263	.359	.819	1.019
2.777	.102	.090	-.261	-.009	-.009	1.342	.359	.809	1.048
2.861	.081	.102	-.284	-.010	-.010	1.413	.359	.787	1.074
2.946	.059	.113	-.305	-.011	-.011	1.468	.359	.763	1.087
3.030	.034	.122	-.325	-.012	-.012	1.511	.359	.736	1.105
3.114	.008	.129	-.345	-.012	-.012	1.562	.359	.711	1.126
3.198	-.020	.134	-.362	-.013	-.013	1.600	.359	.682	1.138
3.282	-.049	.138	-.379	-.014	-.014	1.619	.359	.648	1.151
3.366	-.079	.143	-.395	-.014	-.014	1.638	.359	.616	1.162
3.451	-.109	.150	-.410	-.015	-.015	1.669	.359	.586	1.174
3.535	-.141	.153	-.424	-.015	-.015	1.709	.359	.559	1.187
3.619	-.174	.152	-.437	-.016	-.016	1.758	.359	.533	1.204
3.703	-.206	.151	-.449	-.016	-.016	1.817	.359	.514	1.212
3.787	-.237	.150	-.460	-.017	-.017	1.896	.359	.512	1.242
3.871	-.269	.148	-.469	-.017	-.017	1.983	.359	.502	1.270
3.956	-.300	.145	-.477	-.017	-.017	2.079	.359	.506	1.301
4.040	-.330	.141	-.483	-.017	-.017	2.180	.359	.508	1.322
4.124	-.359	.136	-.489	-.018	-.018	2.281	.359	.517	1.341
4.208	-.387	.130	-.492	-.018	-.018	2.373	.359	.524	1.363
4.292	-.413	.122	-.495	-.018	-.018	2.459	.359	.536	1.385
4.376	-.438	.114	-.497	-.018	-.018	2.544	.359	.555	1.416
4.460	-.462	.107	-.498	-.018	-.018	2.634	.359	.565	1.429
4.545	-.483	.099	-.498	-.018	-.018	2.718	.359	.590	1.447

Figure 8.13: Theoretical pressure head results obtained for 39 lt/s (continued).

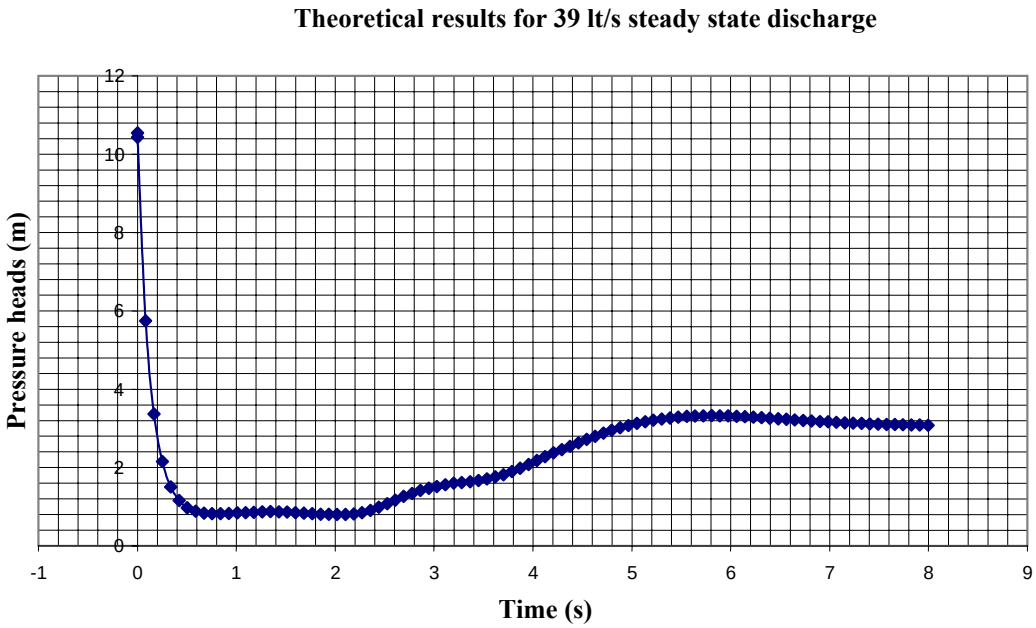

Figure 8.14: Theoretical pressure head results obtained for 39 lt/s.

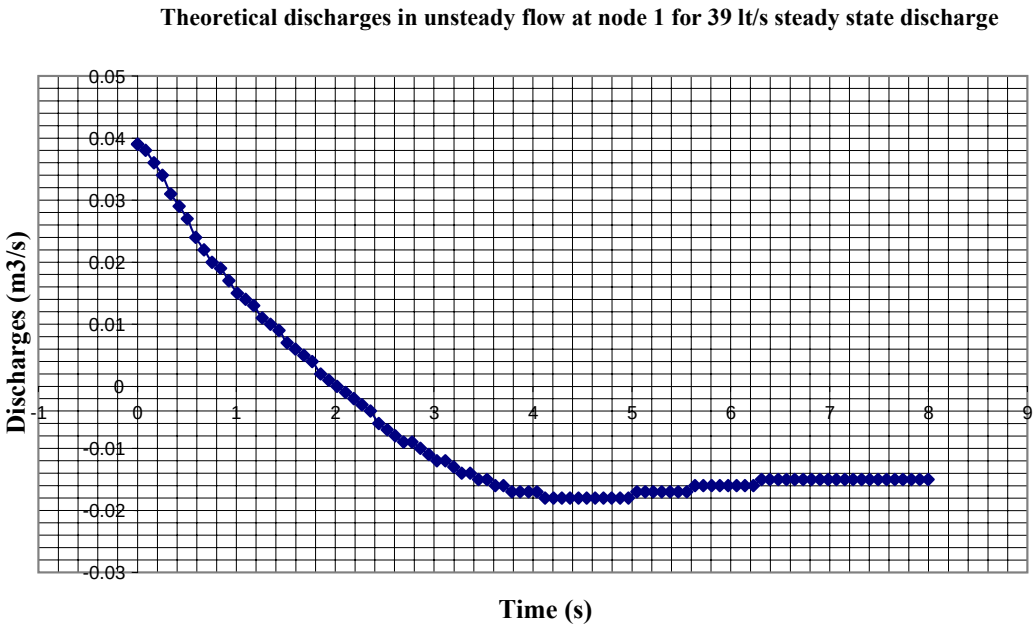

Figure 8.15: Theoretical transient discharges obtained for 39 lt/s.

8.2 Results of computations performed for the second system

Similarly numerical solutions are performed using lower, moderate and upper steady state discharges in the second system. In these computations, experimental steady state discharge values are used in the computer programs. The results are given for two measurement points, namely the upstream point and the interior point.

8.2.1 Results of computation performed for lower steady state discharges

In these computations, lower steady state discharges are taken as 6.6 lt/s (0.54 m/s), 9.01 lt/s (0.74 m/s). The output and results are shown below.

The numerical solution result is given in Figure 8.16. The graph of pressure heads and discharge values at measurement points drawn according to the results of numerical solution are given from Figure 8.17 to Figure 8.20, respectively.

```
                    ******************
                     * INITIAL VALUES *
                     ******************

EL (M)=    4.6000       A (M3/S)= 1331.0000       XL (M)=  108.0000
F=     .0239            D (M)=     .1250          G (M/S2)=    9.8100
TM (S)=   12.0000       RN (RPM)= 1450.0000       TR (NT.M)=   32.1800
HR (M)=   11.0000       QR (M3/S)=     .0360      WRR (NT.M2)=     .8300
TOL=     .0002          VI=     .1830             N= 42
DX (RAD)=     .0714     CK =   10.8700            PI=    3.1416
AKV1 =   17.2900        AKV2=  585.9800           DTAU (S)=     .1000
TAU(1)=    1.0000       TAU(2)=     .9474         TAU(3)=     .8947
TAU(4)=     .8421       TAU(5)=     .7895         TAU(6)=     .7368
TAU(7)=     .6842       TAU(8)=     .6316         TAU(9)=     .5789
TAU(10)=     .5263      TAU(11)=     .4737        TAU(12)=     .4211
TAU(13)=     .3684      TAU(14)=     .3158        TAU(15)=     .2632
TAU(16)=     .2105      TAU(17)=     .1579        TAU(18)=     .1053
TAU(19)=     .0526      TAU(20)=     .0000        M2=27
AL=    1.0000           AL0=    1.0000           AL00=    1.0000
HMIN=     .0000         T=     .0000             JPR= 21
K=  0                   NSV = 42                 KIT=  5
CCT (S)=    1.9000      NTAU = 20                QQA (M3/S)=     .0066
DT (S)=     .0019       AKS (M)=     .0002       VN (M2/S)=   .000001

                    ******************
                    * RESULT VALUES *
                    ******************
```

Figure 8.16: Theoretical pressure head results obtained for 6.6 lt/s.

```
HP1=PIEZOMETRIC HEAD IN METERS BEFORE VALVE
HP2=PIEZOMETRIC HEAD IN METERS AFTER VALVE
HP=HEADLOSS IN METERS AT VALVE (NODE NSV)

HP1 HP2 HP   13.3869    4.6074    8.7795

NUMBER OF NODES AND PIEZOMETRIC HEADS AT NODES AS METERS :

 1:    13.69    2:    13.68    3:    13.67    4:    13.67    5:    13.66
 6:    13.65    7:    13.64    8:    13.64    9:    13.63   10:    13.62
11:    13.62   12:    13.61   13:    13.60   14:    13.59   15:    13.59
16:    13.58   17:    13.57   18:    13.56   19:    13.56   20:    13.55
21:    13.54   22:    13.53   23:    13.53   24:    13.52   25:    13.51
26:    13.50   27:    13.50   28:    13.49   29:    13.48   30:    13.48
31:    13.47   32:    13.46   33:    13.45   34:    13.45   35:    13.44
36:    13.43   37:    13.42   38:    13.42   39:    13.41   40:    13.40
41:    13.39   42:     4.61   43:     4.60

ZH(I) VALUES AS METERS :

 1:     -.30    2:      .05    3:      .12    4:      .21    5:      .04
 6:      .10    7:      .15    8:      .30    9:     1.39   10:     1.42
11:     1.39   12:     1.34   13:     1.35   14:     1.36   15:     1.36
16:     1.35   17:     1.35   18:     1.33   19:     1.32   20:     1.32
21:     1.34   22:     1.34   23:     1.30   24:     1.28   25:     1.30
26:     1.41   27:     1.70   28:     1.60   29:     1.60   30:     1.60
31:     1.60   32:     1.60   33:     1.60   34:     1.60   35:     1.58
36:     1.61   37:     1.61   38:     1.60   39:     1.60   40:     1.60
41:     1.61   42:     1.61   43:     4.10
```

TIME	TAU	ALPHA	BETA	V	Q(1)	Q(M2)	Q(NS)	HPH(1)	HPH(M2)	HP11	HPH(NSV)	HPH(NS)
.0000	1.000	1.000	.556	.185	.007	.007	.007	13.989	11.797	11.777	2.997	.500
.0812	.957	.898	.455	.178	.006	.007	.007	11.243	10.654	11.777	2.997	.500
.1623	.915	.813	.380	.173	.006	.006	.006	9.189	9.316	10.675	2.905	.500
.2435	.872	.742	.318	.161	.006	.006	.006	7.661	8.238	9.978	2.940	.500
.3246	.829	.683	.271	.151	.005	.005	.005	6.466	7.153	8.838	2.883	.500
.4058	.786	.632	.231	.138	.005	.005	.005	5.554	6.300	8.092	2.926	.500
.4869	.744	.588	.200	.128	.005	.005	.005	4.817	5.491	7.162	2.885	.500
.5681	.701	.550	.174	.116	.004	.004	.004	4.236	4.855	6.543	2.926	.500
.6492	.658	.517	.153	.106	.004	.004	.004	3.753	4.264	5.832	2.891	.500
.7304	.616	.488	.134	.095	.003	.003	.003	3.367	3.799	5.359	2.929	.500
.8115	.573	.463	.119	.086	.003	.003	.003	3.039	3.371	4.829	2.899	.500
.8927	.530	.440	.106	.076	.003	.003	.003	2.774	3.034	4.480	2.933	.500
.9739	.487	.419	.095	.068	.002	.002	.002	2.545	2.725	4.090	2.905	.500
1.0550	.445	.401	.085	.058	.002	.002	.002	2.361	2.486	3.843	2.936	.500
1.1362	.402	.384	.077	.050	.002	.002	.002	2.197	2.266	3.562	2.910	.500
1.2173	.359	.369	.070	.041	.001	.002	.002	2.066	2.099	3.398	2.938	.500
1.2985	.317	.356	.064	.034	.001	.001	.001	1.953	1.952	3.205	2.912	.500
1.3796	.274	.344	.058	.025	.001	.001	.001	1.868	1.848	3.110	2.938	.500
1.4608	.231	.332	.053	.017	.001	.001	.001	1.793	1.760	2.993	2.914	.500
1.5419	.188	.322	.048	.009	.000	.000	.000	1.739	1.710	2.962	2.938	.500
1.6231	.146	.313	.044	.001	.000	.000	.000	1.684	1.673	2.914	2.913	.500
1.7042	.103	.304	.040	-.007	.000	.000	.000	1.665	1.647	2.925	2.936	.500
1.7854	.060	.296	.037	-.013	.000	-.001	-.001	2.155	1.727	2.864	2.919	.500
1.8665	.018	.289	.036	-.011	.000	-.001	-.001	6.354	2.660	2.882	2.986	.500
1.9477	.000	.286	.037	.000	.000	.000	.000	12.778	9.394	3.369	3.351	.500
2.0289	.000	.286	.037	.000	.000	.001	.001	7.874	3.129	3.092	2.994	.500
2.1100	.000	.286	.037	.000	.000	.000	.000	-2.778	-3.458	2.648	2.630	.500

Figure 8.16: Theoretical pressure head results obtained for 6.6 lt/s (continued).

2.1912	.000	.286	.037	.000	.000	-.001	-.001	1.956	2.852	3.084	2.986	.500
2.2723	.000	.286	.037	.000	.000	.000	.000	12.772	9.389	3.368	3.351	.500
2.3535	.000	.286	.037	.000	.000	.001	.001	7.872	3.129	3.092	2.994	.500
2.4346	.000	.286	.037	.000	.000	.000	.000	-2.773	-3.453	2.648	2.630	.500
2.5158	.000	.286	.037	.000	.000	-.001	-.001	1.957	2.852	3.084	2.986	.500
2.5969	.000	.286	.037	.000	.000	.000	.000	12.766	9.384	3.368	3.350	.500
2.6781	.000	.286	.037	.000	.000	.001	.001	7.870	3.128	3.092	2.994	.500
2.7592	.000	.286	.037	.000	.000	.000	.000	-2.767	-3.448	2.648	2.630	.500
2.8404	.000	.286	.037	.000	.000	-.001	-.001	1.959	2.852	3.084	2.986	.500
2.9216	.000	.286	.037	.000	.000	.000	.000	12.760	9.379	3.368	3.350	.500
3.0027	.000	.286	.037	.000	.000	.001	.001	7.868	3.128	3.091	2.994	.500
3.0839	.000	.286	.037	.000	.000	.000	.000	-2.761	-3.443	2.648	2.631	.500
3.1650	.000	.286	.037	.000	.000	-.001	-.001	1.961	2.852	3.084	2.986	.500
3.2462	.000	.286	.037	.000	.000	.000	.000	12.754	9.374	3.368	3.350	.500
3.3273	.000	.286	.037	.000	.000	.001	.001	7.866	3.128	3.091	2.994	.500
3.4085	.000	.286	.037	.000	.000	.000	.000	-2.756	-3.439	2.648	2.631	.500
3.4896	.000	.286	.037	.000	.000	-.001	-.001	1.963	2.852	3.084	2.986	.500
3.5708	.000	.286	.037	.000	.000	.000	.000	12.748	9.369	3.367	3.350	.500
3.6519	.000	.286	.037	.000	.000	.001	.001	7.864	3.128	3.091	2.994	.500
3.7331	.000	.286	.037	.000	.000	.000	.000	-2.750	-3.434	2.649	2.631	.500
3.8142	.000	.286	.037	.000	.000	-.001	-.001	1.965	2.852	3.084	2.986	.500
3.8954	.000	.286	.037	.000	.000	.000	.000	12.742	9.364	3.367	3.349	.500
3.9766	.000	.286	.037	.000	.000	.001	.001	7.862	3.128	3.091	2.994	.500
4.0577	.000	.286	.037	.000	.000	.000	.000	-2.744	-3.429	2.649	2.631	.500
4.1389	.000	.286	.037	.000	.000	-.001	-.001	1.967	2.852	3.083	2.986	.500
4.2200	.000	.286	.037	.000	.000	.000	.000	12.736	9.359	3.367	3.349	.500
4.3012	.000	.286	.037	.000	.000	.001	.001	7.860	3.127	3.091	2.994	.500
4.3823	.000	.286	.037	.000	.000	.000	.000	-2.738	-3.424	2.649	2.631	.500
4.4635	.000	.286	.037	.000	.000	-.001	-.001	1.969	2.852	3.083	2.986	.500
4.5446	.000	.286	.037	.000	.000	.000	.000	12.730	9.354	3.367	3.349	.500
4.6258	.000	.286	.037	.000	.000	.001	.001	7.858	3.127	3.091	2.994	.500
4.7069	.000	.286	.037	.000	.000	.000	.000	-2.733	-3.419	2.649	2.632	.500
4.7881	.000	.286	.037	.000	.000	-.001	-.001	1.971	2.852	3.083	2.986	.500
4.8693	.000	.286	.037	.000	.000	.000	.000	12.724	9.349	3.366	3.349	.500
4.9504	.000	.286	.037	.000	.000	.001	.001	7.856	3.127	3.091	2.994	.500
5.0316	.000	.286	.037	.000	.000	.000	.000	-2.727	-3.415	2.650	2.632	.500
5.1127	.000	.286	.037	.000	.000	-.001	-.001	1.973	2.852	3.083	2.986	.500
5.1939	.000	.286	.037	.000	.000	.000	.000	12.718	9.344	3.366	3.348	.500
5.2750	.000	.286	.037	.000	.000	.001	.001	7.854	3.127	3.090	2.994	.500
5.3562	.000	.286	.037	.000	.000	.000	.000	-2.722	-3.410	2.650	2.632	.500
5.4373	.000	.286	.037	.000	.000	-.001	-.001	1.975	2.851	3.083	2.986	.500
5.5185	.000	.286	.037	.000	.000	.000	.000	12.712	9.339	3.366	3.348	.500
5.5996	.000	.286	.037	.000	.000	.001	.001	7.852	3.127	3.090	2.994	.500
5.6808	.000	.286	.037	.000	.000	.000	.000	-2.716	-3.405	2.650	2.632	.500
5.7619	.000	.286	.037	.000	.000	-.001	-.001	1.977	2.851	3.083	2.986	.500
5.8431	.000	.286	.037	.000	.000	.000	.000	12.707	9.334	3.366	3.348	.500
5.9243	.000	.286	.037	.000	.000	.001	.001	7.850	3.126	3.090	2.994	.500
6.0054	.000	.286	.037	.000	.000	.000	.000	-2.710	-3.401	2.650	2.633	.500
6.0866	.000	.286	.037	.000	.000	-.001	-.001	1.979	2.851	3.082	2.986	.500
6.1677	.000	.286	.037	.000	.000	.000	.000	12.701	9.329	3.365	3.348	.500
6.2489	.000	.286	.037	.000	.000	.001	.001	7.848	3.126	3.090	2.994	.500
6.3300	.000	.286	.037	.000	.000	.000	.000	-2.705	-3.396	2.650	2.633	.500
6.4112	.000	.286	.037	.000	.000	-.001	-.001	1.981	2.851	3.082	2.986	.500
6.4923	.000	.286	.037	.000	.000	.000	.000	12.695	9.324	3.365	3.347	.500

Figure 8.16: Theoretical pressure head results obtained for 6.6 lt/s (continued).

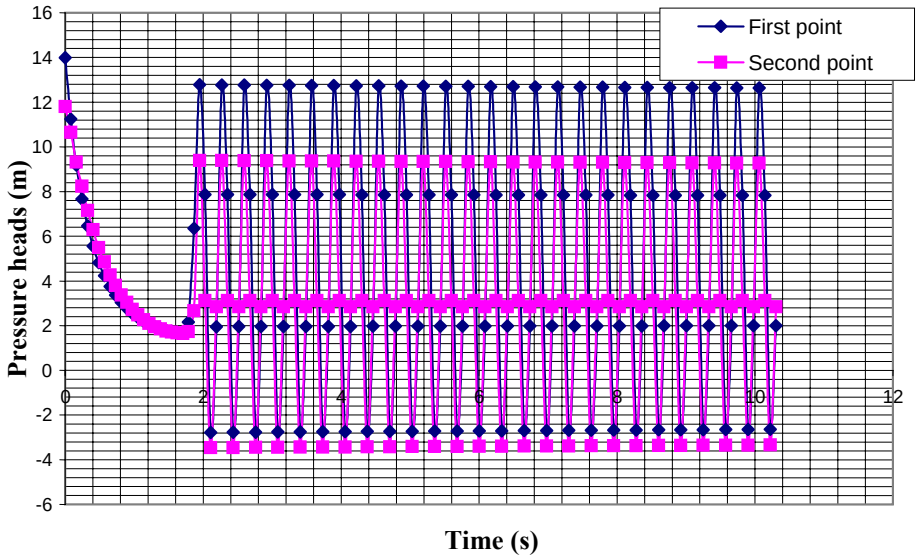

Figure 8.17: Theoretical pressure head results obtained for 6.6 lt/s.

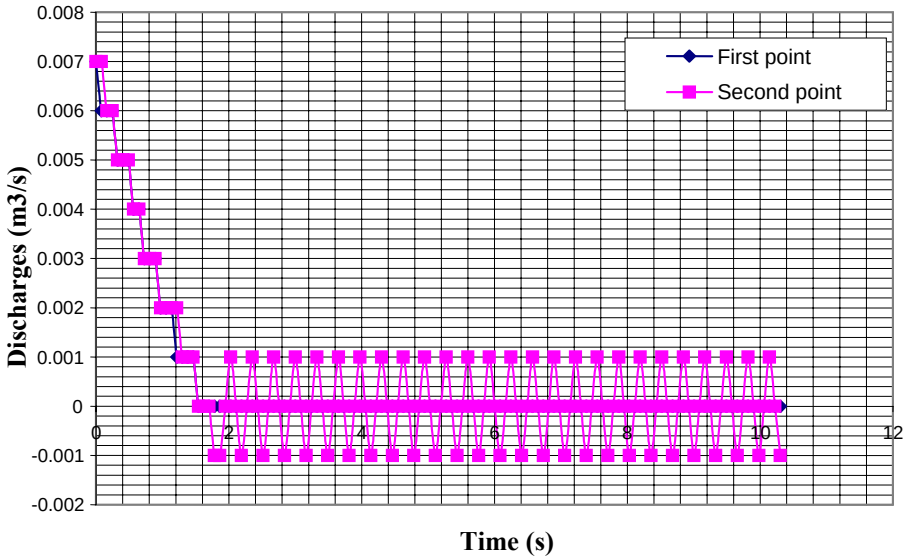

Figure 8.18: Theoretical transient discharges obtained for 6.6 lt/s.

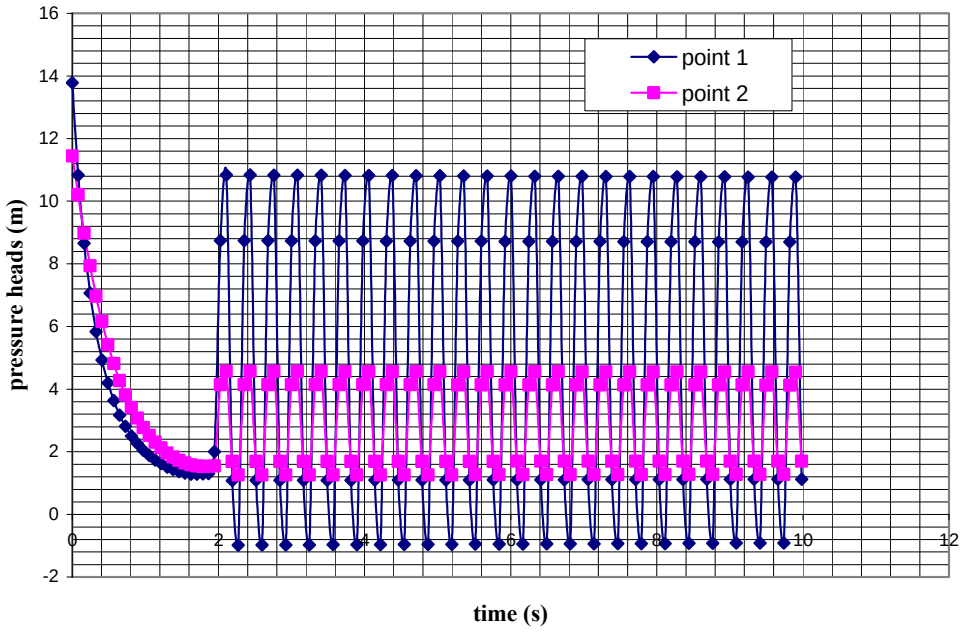

Figure 8.19: Theoretical pressure head results obtained for 9.01 lt/s.

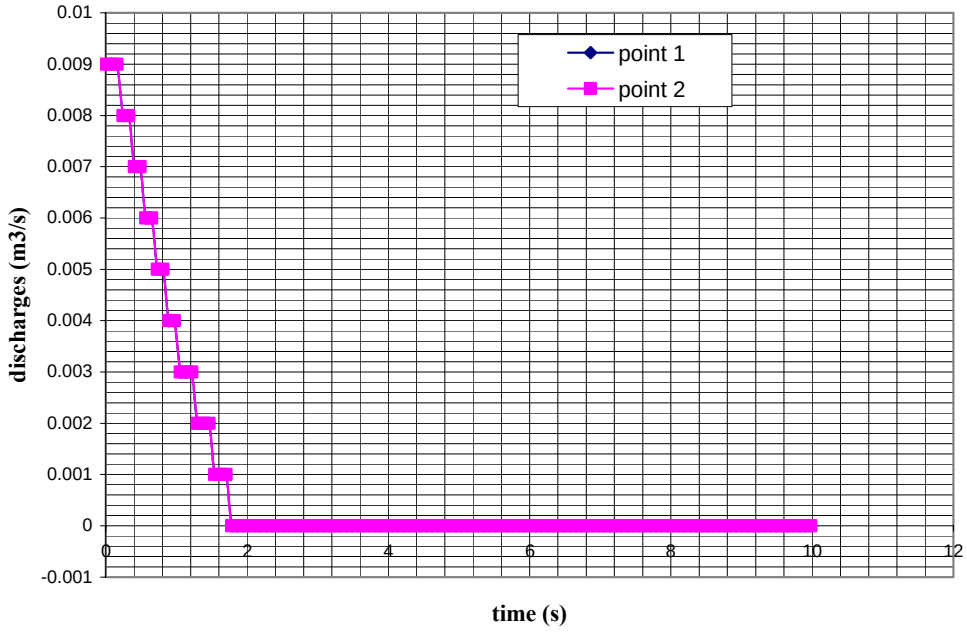

Figure 8.20: Theoretical transient discharges obtained for 9.01 lt/s.

8.2.2 Results of computation performed for moderate steady state discharges

In these computations, moderate steady state discharges are taken as 16.49 lt/s (1.35 m/s), 19.14 lt/s (1.57 m/s) and 20.55 lt/s (1.68 m/s). The output and results are shown below.

The numerical solution result is given in Figure 8.21. The graph of pressure heads and discharge values at measurement points drawn according to the results of numerical solution are given from Figure 8.22 to Figure 8.27, respectively.

```
                    ******************
                    * INITIAL VALUES *
                    ******************


EL (M)=    4.6000        A (M3/S)= 1330.8000        XL (M)=  108.0000
F=      .0221            D (M)=     .1250          G (M/S2)=    9.8100
TM (S)=   10.0000        RN (RPM)= 1450.0000       TR (NT.M)=   32.1800
HR (M)=   11.0000        QR (M3/S)=     .0360      WRR (NT.M2)=     .8300
TOL=     .0002           VI=      .4600            N= 42
DX (RAD)=     .0714      CK =    6.6200           PI=    3.1416
AKV1 =    4.9800         AKV2=   74.0000          DTAU (S)=     .1316
TAU(1)=    1.0000        TAU(2)=     .9474        TAU(3)=     .8947
TAU(4)=     .8421        TAU(5)=     .7895        TAU(6)=     .7368
TAU(7)=     .6842        TAU(8)=     .6316        TAU(9)=     .5789
TAU(10)=     .5263       TAU(11)=     .4737       TAU(12)=     .4211
TAU(13)=     .3684       TAU(14)=     .3158       TAU(15)=     .2632
TAU(16)=     .2105       TAU(17)=     .1579       TAU(18)=     .1053
TAU(19)=     .0526       TAU(20)=     .0000       M2=27
AL=    1.0000            AL0=    1.0000           AL00=    1.0000
HMIN=     .0000          T=     .0000             JPR= 21
K=  0                    NSV = 42                 KIT=  5
CCT (S)=    2.5000       NTAU = 20                QQA (M3/S)=     .0166
DT (S)=     .0019        AKS (M)=     .0002       VN (M2/S)=   .000001


                    *****************
                    * RESULT VALUES *
                    *****************


HP1=PIEZOMETRIC HEAD IN METERS BEFORE VALVE
HP2=PIEZOMETRIC HEAD IN METERS AFTER VALVE
HP=HEADLOSS IN METERS AT VALVE (NODE 23)

HP1 HP2 HP   11.0854    4.6397    6.4457

PIEZOMETRIC HEADS AT NODES AS METERS :

 1:    12.71    2:    12.67    3:    12.63    4:    12.59    5:    12.55
 6:    12.51    7:    12.47    8:    12.43    9:    12.39   10:    12.35
11:    12.32   12:    12.28   13:    12.24   14:    12.20   15:    12.16
16:    12.12   17:    12.08   18:    12.04   19:    12.00   20:    11.96
21:    11.92   22:    11.88   23:    11.84   24:    11.80   25:    11.76
26:    11.72   27:    11.68   28:    11.64   29:    11.60   30:    11.56
31:    11.52   32:    11.48   33:    11.44   34:    11.40   35:    11.36
```

```
36:    11.32   37:    11.28   38:    11.24   39:    11.20   40:    11.16
41:    11.13   42:     4.64   43:     4.60

ZH(I) VALUES AS METERS :

 1:     -.30    2:      .05    3:      .12    4:      .21    5:      .04
 6:      .10    7:      .15    8:      .30    9:     1.39   10:     1.42
11:     1.39   12:     1.34   13:     1.35   14:     1.36   15:     1.36
16:     1.35   17:     1.35   18:     1.33   19:     1.32   20:     1.32
21:     1.34   22:     1.34   23:     1.30   24:     1.28   25:     1.30
26:     1.41   27:     1.70   28:     1.60   29:     1.60   30:     1.60
31:     1.60   32:     1.60   33:     1.60   34:     1.60   35:     1.58
36:     1.61   37:     1.61   38:     1.60   39:     1.60   40:     1.60
41:     1.61   42:     1.61   43:     4.10
```

TIME	TAU	ALPHA	BETA	V	Q(1)	Q(M2)	Q(NS)	H(1)	H(27)	H(NSV1)	H(NSV2)	H(NS)
.0000	1.000	1.000	.736	.446	.016	.016	.016	13.012	9.980	9.475	3.030	.500
.0812	.968	.867	.581	.437	.016	.016	.016	9.457	8.482	9.475	3.030	.500
.1623	.935	.761	.470	.431	.016	.015	.015	6.958	7.416	8.885	2.897	.500
.2435	.903	.675	.381	.411	.015	.015	.015	5.256	6.429	8.609	2.938	.500
.3246	.870	.604	.315	.398	.014	.014	.014	3.988	5.742	7.947	2.848	.500
.4058	.838	.546	.261	.376	.014	.014	.014	3.113	5.039	7.609	2.902	.500
.4869	.805	.497	.221	.360	.013	.013	.013	2.423	4.564	6.997	2.833	.500
.5681	.773	.456	.188	.337	.012	.012	.012	1.951	4.047	6.678	2.890	.500
.6492	.740	.420	.161	.321	.012	.011	.011	1.549	3.706	6.151	2.832	.500
.7304	.708	.390	.139	.300	.011	.011	.011	1.280	3.311	5.877	2.888	.500
.8115	.675	.363	.122	.284	.010	.010	.010	1.035	3.061	5.435	2.837	.500
.8927	.643	.340	.106	.264	.010	.010	.010	.878	2.754	5.209	2.890	.500
.9739	.610	.320	.094	.249	.009	.009	.009	.721	2.568	4.843	2.843	.500
1.0550	.578	.302	.083	.231	.008	.008	.008	.627	2.326	4.662	2.893	.500
1.1362	.546	.286	.075	.217	.008	.008	.008	.521	2.187	4.360	2.850	.500
1.2173	.513	.272	.066	.199	.007	.007	.007	.464	1.993	4.217	2.896	.500
1.2985	.481	.259	.060	.186	.007	.007	.007	.390	1.889	3.968	2.856	.500
1.3796	.448	.247	.054	.170	.006	.006	.006	.356	1.733	3.858	2.899	.500
1.4608	.416	.237	.049	.157	.006	.006	.006	.302	1.656	3.654	2.861	.500
1.5419	.383	.228	.044	.142	.005	.005	.005	.284	1.532	3.571	2.901	.500
1.6231	.351	.219	.040	.130	.005	.005	.005	.242	1.475	3.405	2.866	.500
1.7042	.318	.211	.036	.115	.004	.004	.004	.236	1.376	3.345	2.903	.500
1.7854	.286	.205	.032	.103	.004	.004	.004	.202	1.336	3.212	2.870	.500
1.8665	.253	.198	.029	.089	.003	.003	.003	.205	1.259	3.172	2.903	.500
1.9477	.221	.193	.026	.078	.003	.003	.003	.178	1.235	3.067	2.873	.500
2.0289	.188	.188	.023	.065	.002	.002	.002	.191	1.177	3.044	2.903	.500
2.1100	.156	.183	.021	.053	.002	.002	.002	.174	1.169	2.966	2.876	.500
2.1912	.124	.179	.019	.040	.001	.001	.001	.207	1.131	2.958	2.902	.500
2.2723	.091	.175	.017	.029	.001	.001	.001	.206	1.143	2.905	2.878	.500
2.3535	.059	.172	.015	.017	.001	.001	.001	.296	1.135	2.911	2.901	.500
2.4346	.026	.169	.013	.006	.000	.000	.000	.417	1.198	2.884	2.883	.500
2.5158	.000	.167	.013	.000	.000	.000	.000	2.780	1.380	2.907	2.906	.500
2.5969	.000	.167	.013	.000	.000	.000	.000	6.905	4.874	3.098	3.097	.500
2.6781	.000	.167	.013	.000	.000	.000	.000	7.022	4.423	3.075	3.074	.500
2.7592	.000	.167	.013	.000	.000	.000	.000	2.897	.930	2.884	2.883	.500
2.8404	.000	.167	.013	.000	.000	.000	.000	2.780	1.380	2.907	2.906	.500

Figure 8.21: Theoretical pressure head results obtained for 16.5 lt/s (continued).

2.9216	.000	.167	.013	.000	.000	.000	.000	6.904	4.873	3.098	3.097	.500
3.0027	.000	.167	.013	.000	.000	.000	.000	7.021	4.423	3.075	3.074	.500
3.0839	.000	.167	.013	.000	.000	.000	.000	2.898	.931	2.884	2.883	.500
3.1650	.000	.167	.013	.000	.000	.000	.000	2.782	1.380	2.907	2.906	.500
3.2462	.000	.167	.013	.000	.000	.000	.000	6.904	4.872	3.098	3.098	.500
3.3273	.000	.167	.013	.000	.000	.000	.000	7.019	4.423	3.075	3.074	.500
3.4085	.000	.167	.013	.000	.000	.000	.000	2.899	.932	2.883	2.882	.500
3.4896	.000	.167	.013	.000	.000	.000	.000	2.783	1.380	2.907	2.906	.500
3.5708	.000	.167	.013	.000	.000	.000	.000	6.903	4.871	3.099	3.098	.500
3.6519	.000	.167	.013	.000	.000	.000	.000	7.019	4.422	3.075	3.074	.500
3.7331	.000	.167	.013	.000	.000	.000	.000	2.900	.933	2.883	2.882	.500
3.8142	.000	.167	.013	.000	.000	.000	.000	2.783	1.380	2.907	2.906	.500
3.8954	.000	.167	.013	.000	.000	.000	.000	6.901	4.871	3.099	3.098	.500
3.9766	.000	.167	.013	.000	.000	.000	.000	7.018	4.422	3.075	3.074	.500
4.0577	.000	.167	.013	.000	.000	.000	.000	2.901	.933	2.883	2.883	.500
4.1389	.000	.167	.013	.000	.000	.000	.000	2.783	1.381	2.907	2.906	.500
4.2200	.000	.167	.013	.000	.000	.000	.000	6.901	4.870	3.098	3.097	.500
4.3012	.000	.167	.013	.000	.000	.000	.000	7.018	4.421	3.075	3.073	.500
4.3823	.000	.167	.013	.000	.000	.000	.000	2.902	.934	2.884	2.883	.500
4.4635	.000	.167	.013	.000	.000	.000	.000	2.784	1.382	2.907	2.907	.500
4.5446	.000	.167	.013	.000	.000	.000	.000	6.899	4.870	3.098	3.097	.500
4.6258	.000	.167	.013	.000	.000	.000	.000	7.018	4.421	3.074	3.073	.500
4.7069	.000	.167	.013	.000	.000	.000	.000	2.903	.934	2.884	2.883	.500
4.7881	.000	.167	.013	.000	.000	.000	.000	2.783	1.382	2.907	2.907	.500
4.8693	.000	.167	.013	.000	.000	.000	.000	6.899	4.869	3.098	3.097	.500
4.9504	.000	.167	.013	.000	.000	.000	.000	7.019	4.421	3.074	3.073	.500
5.0316	.000	.167	.013	.000	.000	.000	.000	2.903	.935	2.885	2.884	.500
5.1127	.000	.167	.013	.000	.000	.000	.000	2.784	1.382	2.907	2.906	.500
5.1939	.000	.167	.013	.000	.000	.000	.000	6.899	4.868	3.098	3.097	.500
5.2750	.000	.167	.013	.000	.000	.000	.000	7.018	4.420	3.074	3.074	.500
5.3562	.000	.167	.013	.000	.000	.000	.000	2.903	.936	2.885	2.884	.500
5.4373	.000	.167	.013	.000	.000	.000	.000	2.784	1.383	2.907	2.906	.500
5.5185	.000	.167	.013	.000	.000	.000	.000	6.899	4.868	3.098	3.096	.500
5.5996	.000	.167	.013	.000	.000	.000	.000	7.018	4.420	3.074	3.074	.500
5.6808	.000	.167	.013	.000	.000	.000	.000	2.903	.936	2.885	2.884	.500
5.7619	.000	.167	.013	.000	.000	.000	.000	2.784	1.383	2.907	2.906	.500
5.8431	.000	.167	.013	.000	.000	.000	.000	6.899	4.867	3.098	3.096	.500
5.9243	.000	.167	.013	.000	.000	.000	.000	7.017	4.419	3.074	3.074	.500
6.0054	.000	.167	.013	.000	.000	.000	.000	2.903	.937	2.884	2.883	.500
6.0866	.000	.167	.013	.000	.000	.000	.000	2.785	1.384	2.907	2.906	.500
6.1677	.000	.167	.013	.000	.000	.000	.000	6.898	4.867	3.098	3.097	.500
6.2489	.000	.167	.013	.000	.000	.000	.000	7.017	4.419	3.075	3.074	.500
6.3300	.000	.167	.013	.000	.000	.000	.000	2.904	.938	2.884	2.883	.500
6.4112	.000	.167	.013	.000	.000	.000	.000	2.786	1.384	2.907	2.906	.500
6.4923	.000	.167	.013	.000	.000	.000	.000	6.898	4.866	3.098	3.097	.500
6.5735	.000	.167	.013	.000	.000	.000	.000	7.016	4.419	3.075	3.074	.500
6.6546	.000	.167	.013	.000	.000	.000	.000	2.904	.939	2.884	2.883	.500
6.7358	.000	.167	.013	.000	.000	.000	.000	2.786	1.384	2.907	2.906	.500
6.8170	.000	.167	.013	.000	.000	.000	.000	6.897	4.865	3.098	3.097	.500
6.8981	.000	.167	.013	.000	.000	.000	.000	7.015	4.418	3.075	3.074	.500
6.9793	.000	.167	.013	.000	.000	.000	.000	2.904	.939	2.884	2.883	.500
7.0604	.000	.167	.013	.000	.000	.000	.000	2.787	1.385	2.906	2.906	.500
7.1416	.000	.167	.013	.000	.000	.000	.000	6.897	4.864	3.098	3.097	.500
7.2227	.000	.167	.013	.000	.000	.000	.000	7.015	4.418	3.075	3.074	.500

Figure 8.21: Theoretical pressure head results obtained for 16.5 lt/s (continued).

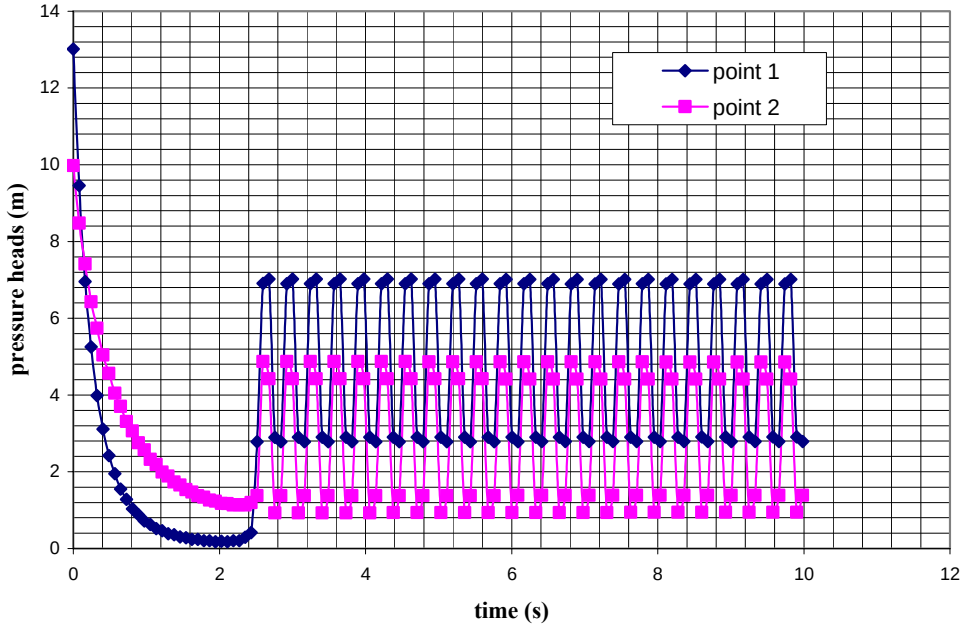

Figure 8.22: Theoretical pressure head results obtained for 16.5 lt/s.

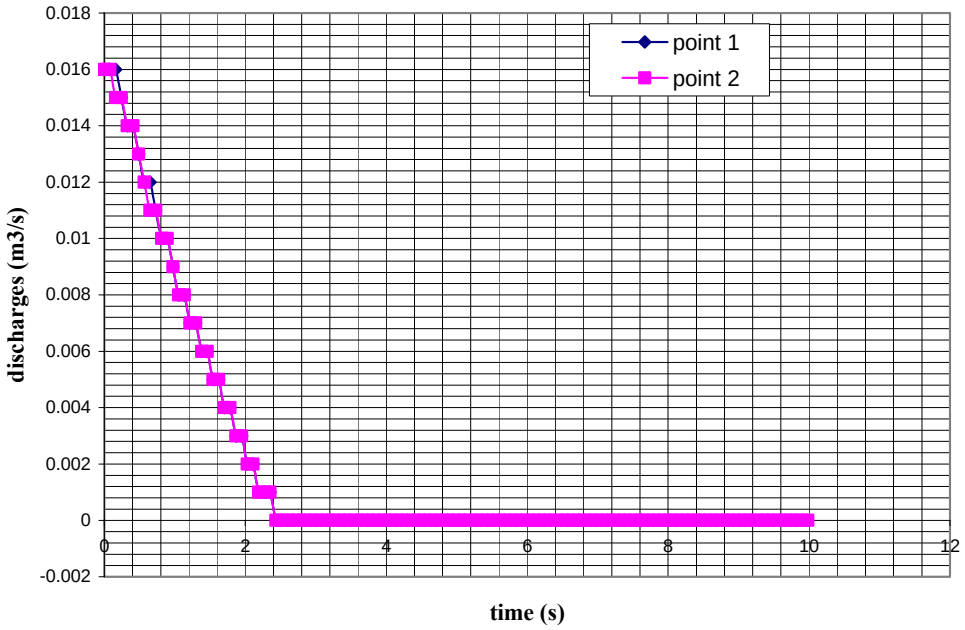

Figure 8.23: Theoretical transient discharges obtained for 16.5 lt/s.

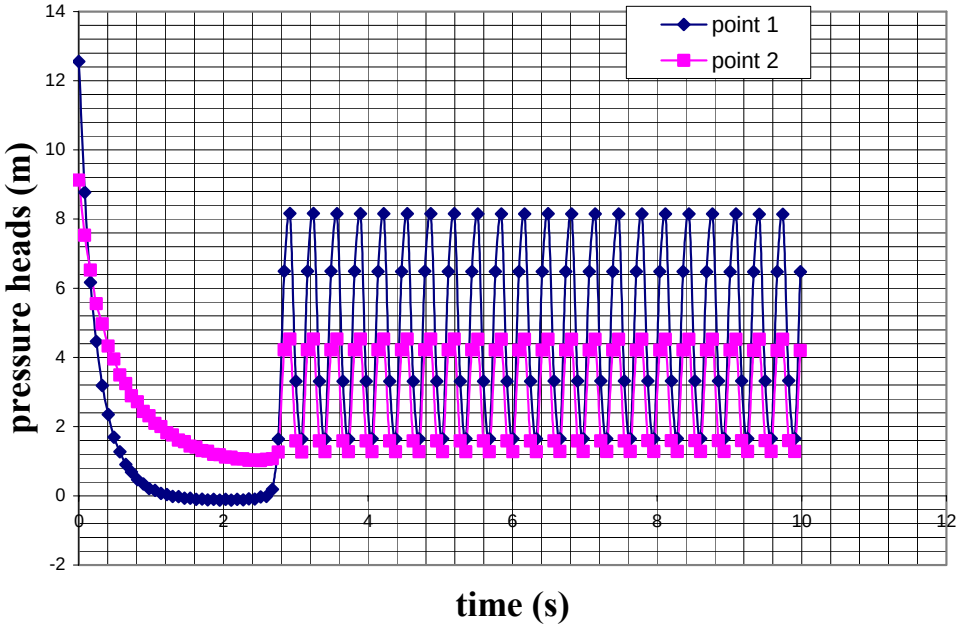

Figure 8.24: Theoretical pressure head results obtained for 19.14 lt/s.

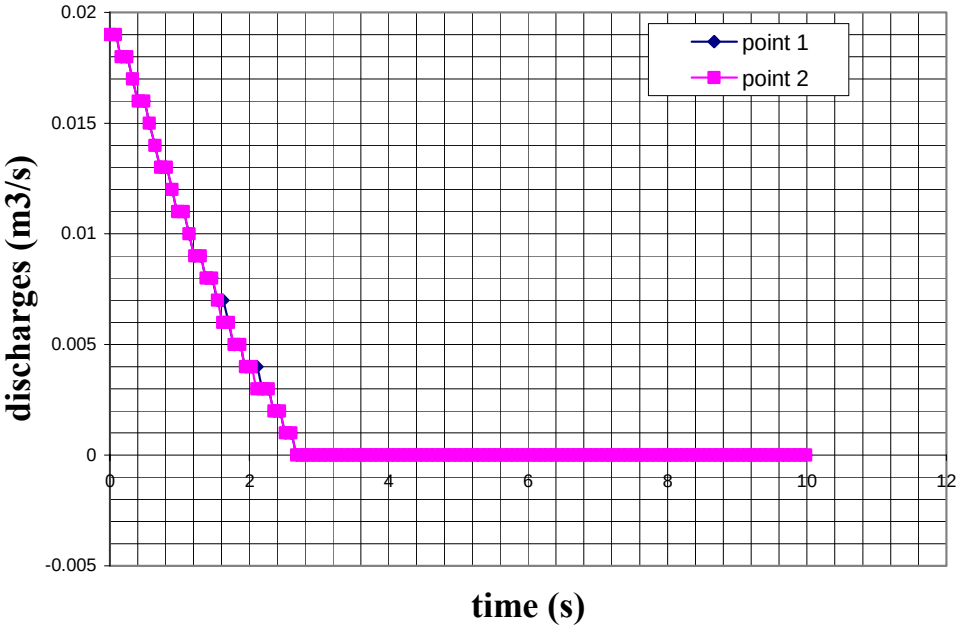

Figure 8.25: Theoretical transient discharges obtained for 19.14 lt/s.

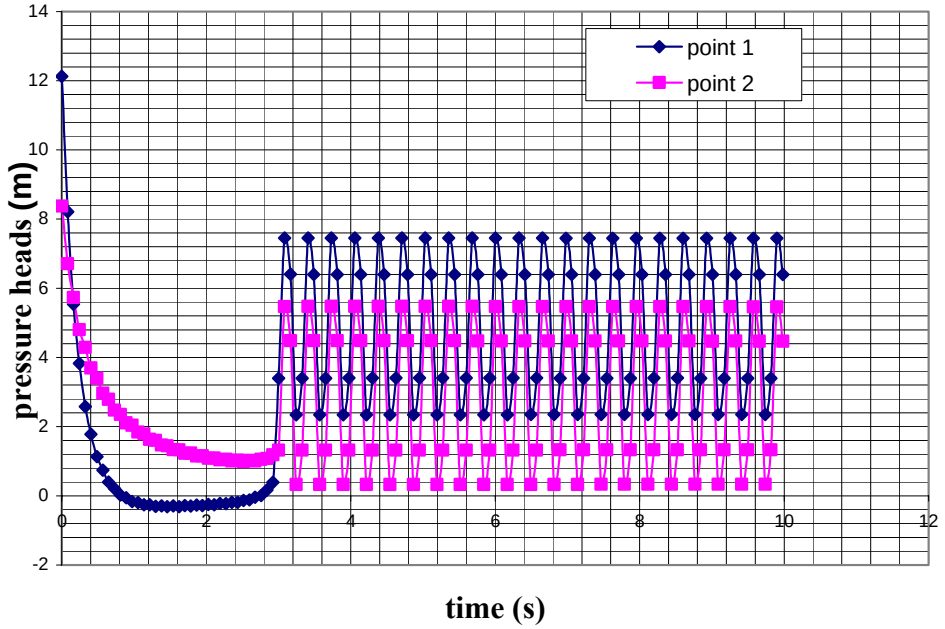

Figure 8.26: Theoretical pressure head results obtained for 20.55 lt/s.

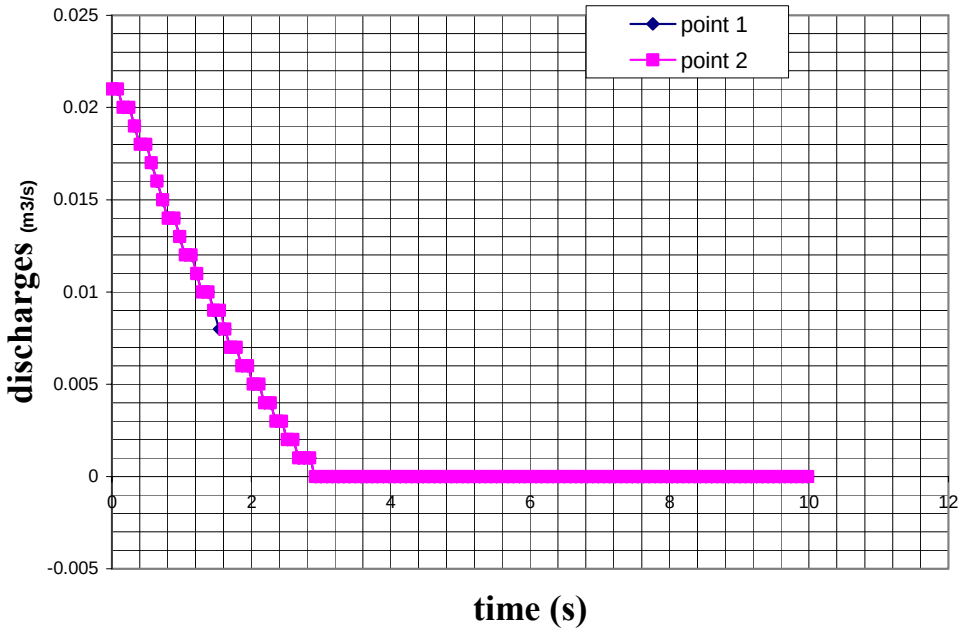

Figure 8.27: Theoretical transient discharges obtained for 20.55 lt/s.

8.2.3 Results of computation performed for upper steady state discharges

In these computations, moderate steady state discharges are taken as 24.51 lt/s (2.00 m/s), 25.16 lt/s (2.06 m/s). The output and results are shown below.

The numerical solution result is given in Figure 8.28. The graph of pressure heads and discharge values at measurement points drawn according to the results of numerical solution are given from Figure 8.29 to 8.32, respectively.

```
                    ******************
                    * INITIAL VALUES *
                    ******************

EL (M)=    4.6000       A (M3/S)= 1331.0000       XL (M)=  108.0000
F=     .0217            D (M)=     .1250          G (M/S2)=    9.8100
TM (S)=   12.0000       RN (RPM)= 1450.0000       TR (NT.M)=   32.1800
HR (M)=   11.0000       QR (M3/S)=     .0360      WRR (NT.M2)=     .8300
TOL=     .0002          VI=     .7000             N= 42
DX (RAD)=     .0714     CK =    2.0000            PI=    3.1416
AKV1 =    2.9000        AKV2=   15.6200           DTAU (S)=     .3158
TAU(1)=    1.0000       TAU(2)=     .9474         TAU(3)=     .8947
TAU(4)=     .8421       TAU(5)=     .7895         TAU(6)=     .7368
TAU(7)=     .6842       TAU(8)=     .6316         TAU(9)=     .5789
TAU(10)=     .5263      TAU(11)=     .4737        TAU(12)=     .4211
TAU(13)=     .3684      TAU(14)=     .3158        TAU(15)=     .2632
TAU(16)=     .2105      TAU(17)=     .1579        TAU(18)=     .1053
TAU(19)=     .0526      TAU(20)=     .0000        M2=27
AL=    1.0000           AL0=    1.0000            AL00=    1.0000
HMIN=     .0000         T=     .0000              JPR= 21
K=  0                   NSV = 42                  KIT=  5
CCT (S)=    6.0000      NTAU = 20                 QQA (M3/S)=     .0252
DT (S)=     .0019       AKS (M)=     .0002        VN (M2/S)=   .000001

                    ******************
                    * RESULT VALUES *
                    ******************

HP1=PIEZOMETRIC HEAD IN METERS BEFORE VALVE
HP2=PIEZOMETRIC HEAD IN METERS AFTER VALVE
HP=HEADLOSS IN METERS AT VALVE (NODE NSV)

HP1 HP2 HP    7.9775    4.6937    3.2838

NUMBER OF NODES AND PIEZOMETRIC HEADS AT NODES AS METERS :

 1:    11.82    2:    11.72    3:    11.63    4:    11.54    5:    11.44
 6:    11.35    7:    11.26    8:    11.16    9:    11.07   10:    10.97
11:    10.88   12:    10.79   13:    10.69   14:    10.60   15:    10.51
16:    10.41   17:    10.32   18:    10.23   19:    10.13   20:    10.04
```

Figure 8.28: Theoretical pressure head results obtained for 24.51 lt/s.

```
21:     9.94   22:     9.85   23:     9.76   24:     9.66   25:     9.57
26:     9.48   27:     9.38   28:     9.29   29:     9.20   30:     9.10
31:     9.01   32:     8.91   33:     8.82   34:     8.73   35:     8.63
36:     8.54   37:     8.45   38:     8.35   39:     8.26   40:     8.16
41:     8.07   42:     4.69   43:     4.60

ZH(I) VALUES AS METERS :

 1:     -.30    2:      .05    3:      .12    4:      .21    5:      .04
 6:      .10    7:      .15    8:      .30    9:     1.39   10:     1.42
11:     1.39   12:     1.34   13:     1.35   14:     1.36   15:     1.36
16:     1.35   17:     1.35   18:     1.33   19:     1.32   20:     1.32
21:     1.34   22:     1.34   23:     1.30   24:     1.28   25:     1.30
26:     1.41   27:     1.70   28:     1.60   29:     1.60   30:     1.60
31:     1.60   32:     1.60   33:     1.60   34:     1.60   35:     1.58
36:     1.61   37:     1.61   38:     1.60   39:     1.60   40:     1.60
41:     1.61   42:     1.61   43:     4.10
```

TIME	TAU	ALPHA	BETA	V	Q(1)	Q(M2)	Q(NS)	HPH(1)	HPH(M2)	HP11	HPH(NSV)	HPH(NS)
.0000	1.000	1.000	.879	.692	.025	.025	.025	12.118	7.682	6.367	3.084	.500
.0812	.986	.844	.664	.682	.025	.025	.025	7.997	5.919	6.367	3.084	.500
.1623	.973	.725	.514	.675	.024	.024	.024	5.300	5.024	6.031	2.928	.500
.2435	.959	.633	.401	.652	.023	.024	.024	3.596	4.125	5.965	2.980	.500
.3246	.946	.561	.316	.637	.023	.023	.023	2.348	3.679	5.621	2.866	.500
.4058	.932	.503	.254	.610	.022	.022	.022	1.603	3.158	5.541	2.938	.500
.4869	.919	.456	.209	.593	.021	.021	.021	1.028	2.944	5.223	2.844	.500
.5681	.905	.417	.174	.565	.020	.020	.021	.705	2.598	5.146	2.919	.500
.6492	.892	.385	.148	.547	.020	.020	.020	.435	2.504	4.867	2.840	.500
.7304	.878	.357	.127	.521	.019	.019	.019	.300	2.246	4.804	2.909	.500
.8115	.865	.333	.110	.503	.018	.018	.018	.158	2.200	4.552	2.839	.500
.8927	.851	.312	.096	.478	.017	.017	.017	.109	1.994	4.501	2.906	.500
.9739	.838	.294	.085	.461	.017	.017	.016	.036	1.980	4.281	2.839	.500
1.0550	.824	.277	.076	.438	.016	.016	.016	.030	1.812	4.245	2.904	.500
1.1362	.811	.263	.068	.422	.015	.015	.015	-.005	1.815	4.054	2.845	.500
1.2173	.797	.250	.061	.400	.014	.014	.015	.012	1.676	4.023	2.906	.500
1.2985	.784	.238	.055	.385	.014	.014	.014	-.002	1.686	3.853	2.850	.500
1.3796	.770	.227	.050	.365	.013	.013	.013	.026	1.568	3.835	2.906	.500
1.4608	.757	.217	.046	.350	.013	.013	.013	.025	1.584	3.685	2.856	.500
1.5419	.743	.208	.043	.331	.012	.012	.012	.058	1.483	3.674	2.911	.500
1.6231	.729	.200	.039	.318	.011	.011	.011	.064	1.507	3.540	2.862	.500
1.7042	.716	.192	.036	.299	.011	.011	.011	.098	1.418	3.538	2.913	.500
1.7854	.702	.185	.034	.287	.010	.010	.010	.108	1.441	3.418	2.864	.500
1.8665	.689	.179	.032	.269	.010	.010	.010	.142	1.367	3.421	2.914	.500
1.9477	.675	.172	.029	.257	.009	.009	.009	.154	1.389	3.313	2.869	.500
2.0289	.662	.167	.028	.240	.009	.009	.009	.186	1.323	3.321	2.917	.500
2.1100	.648	.161	.026	.229	.008	.008	.008	.199	1.348	3.226	2.871	.500
2.1912	.635	.156	.024	.213	.008	.008	.008	.229	1.289	3.235	2.917	.500
2.2723	.621	.151	.023	.202	.007	.007	.007	.242	1.312	3.149	2.877	.500
2.3535	.608	.147	.022	.187	.007	.007	.007	.272	1.261	3.161	2.917	.500
2.4346	.594	.142	.020	.176	.006	.006	.006	.286	1.285	3.084	2.878	.500
2.5158	.581	.138	.019	.161	.006	.006	.006	.313	1.237	3.100	2.916	.500
2.5969	.567	.135	.018	.151	.005	.005	.005	.326	1.266	3.033	2.879	.500
2.6781	.554	.131	.017	.137	.005	.005	.005	.351	1.223	3.048	2.914	.500
2.7592	.540	.128	.016	.126	.005	.004	.004	.363	1.252	2.989	2.880	.500
2.8404	.527	.124	.015	.113	.004	.004	.004	.382	1.211	3.008	2.916	.500
2.9216	.513	.121	.014	.103	.004	.004	.004	.391	1.237	2.952	2.882	.500

Figure 8.28: Theoretical pressure head results obtained for 24.51 lt/s (continued).

3.0027	.500	.119	.013	.089	.003	.003	.003	.409	1.198	2.975	2.917	.500
3.0839	.486	.116	.012	.079	.003	.003	.003	.417	1.228	2.925	2.884	.500
3.1650	.472	.114	.011	.066	.002	.002	.002	.431	1.195	2.949	2.917	.500
3.2462	.459	.112	.010	.057	.002	.002	.002	.437	1.220	2.904	2.886	.500
3.3273	.445	.110	.008	.044	.002	.002	.002	.447	1.190	2.933	2.919	.500
3.4085	.432	.108	.008	.034	.001	.001	.001	.451	1.217	2.893	2.885	.500
3.4896	.418	.107	.006	.021	.001	.001	.001	.456	1.189	2.921	2.918	.500
3.5708	.405	.106	.006	.012	.000	.000	.000	.456	1.215	2.887	2.883	.500
3.6519	.391	.105	.005	-.001	.000	.000	.000	.455	1.190	2.918	2.918	.500
3.7331	.378	.104	.004	-.011	.000	.000	.000	.455	1.213	2.883	2.885	.500
3.8142	.364	.103	.004	-.024	-.001	-.001	-.001	.463	1.189	2.915	2.918	.500
3.8954	.351	.102	.004	-.033	-.001	-.001	-.001	.474	1.215	2.877	2.882	.500
3.9766	.337	.101	.004	-.046	-.002	-.002	-.002	.498	1.196	2.906	2.918	.500
4.0577	.324	.101	.005	-.055	-.002	-.002	-.002	.524	1.229	2.864	2.887	.500
4.1389	.310	.100	.006	-.067	-.002	-.002	-.002	.573	1.217	2.891	2.917	.500
4.2200	.297	.098	.006	-.076	-.003	-.003	-.003	.621	1.256	2.850	2.892	.500
4.3012	.283	.097	.008	-.088	-.003	-.003	-.003	.701	1.252	2.868	2.922	.500
4.3823	.270	.095	.010	-.097	-.003	-.004	-.004	.778	1.301	2.831	2.896	.500
4.4635	.256	.093	.012	-.108	-.004	-.004	-.004	.898	1.311	2.849	2.924	.500
4.5446	.243	.090	.014	-.116	-.004	-.004	-.004	1.015	1.373	2.810	2.904	.500
4.6258	.229	.087	.016	-.127	-.005	-.005	-.005	1.194	1.406	2.823	2.928	.500
4.7069	.216	.084	.018	-.134	-.005	-.005	-.005	1.372	1.492	2.790	2.913	.500
4.7881	.202	.080	.020	-.143	-.005	-.005	-.005	1.632	1.554	2.801	2.935	.500
4.8693	.188	.076	.022	-.148	-.005	-.005	-.005	1.899	1.676	2.771	2.926	.500
4.9504	.175	.071	.024	-.156	-.006	-.006	-.006	2.281	1.785	2.788	2.950	.500
5.0316	.161	.066	.025	-.160	-.006	-.006	-.006	2.683	1.959	2.768	2.946	.500
5.1127	.148	.061	.026	-.165	-.006	-.006	-.006	3.243	2.137	2.789	2.971	.500
5.1939	.134	.056	.026	-.166	-.006	-.006	-.006	3.854	2.395	2.779	2.972	.500
5.2750	.121	.050	.026	-.167	-.006	-.006	-.006	4.685	2.676	2.810	3.002	.500
5.3562	.107	.045	.025	-.165	-.006	-.006	-.006	5.615	3.067	2.823	3.012	.500
5.4373	.094	.040	.024	-.161	-.006	-.006	-.006	6.851	3.506	2.868	3.050	.500
5.5185	.080	.036	.021	-.152	-.005	-.006	-.006	8.263	4.082	2.909	3.076	.500
5.5996	.067	.031	.018	-.141	-.005	-.005	-.005	10.076	4.756	2.978	3.120	.500
5.6808	.053	.028	.014	-.124	-.004	-.005	-.005	12.152	5.589	3.052	3.164	.500
5.7619	.040	.026	.010	-.102	-.004	-.004	-.004	14.668	6.550	3.146	3.224	.500
5.8431	.026	.024	.005	-.074	-.003	-.003	-.003	17.417	7.643	3.244	3.287	.500
5.9243	.013	.024	.001	-.039	-.001	-.001	-.002	20.312	8.780	3.346	3.355	.500
6.0054	.000	.023	.000	.000	.000	.000	.000	21.649	9.788	3.419	3.418	.500
6.0866	.000	.023	.000	.000	.000	.001	.002	4.808	2.390	2.634	2.623	.500
6.1677	.000	.023	.000	.000	.000	.000	.000	-11.818	-3.981	2.561	2.564	.500
6.2489	.000	.023	.000	.000	.000	-.001	-.002	4.992	3.420	3.372	3.355	.500
6.3300	.000	.023	.000	.000	.000	.000	.000	21.634	9.780	3.418	3.418	.500
6.4112	.000	.023	.000	.000	.000	.001	.002	4.810	2.392	2.636	2.623	.500
6.4923	.000	.023	.000	.000	.000	.000	.000	-11.798	-3.973	2.564	2.564	.500
6.5735	.000	.023	.000	.000	.000	-.001	-.002	4.991	3.418	3.367	3.358	.500
6.6546	.000	.023	.000	.000	.000	.000	.000	21.609	9.776	3.415	3.415	.500
6.7358	.000	.023	.000	.000	.000	.001	.002	4.808	2.395	2.637	2.623	.500
6.8170	.000	.023	.000	.000	.000	.000	.000	-11.774	-3.970	2.565	2.566	.500
6.8981	.000	.023	.000	.000	.000	-.001	-.002	4.992	3.415	3.368	3.355	.500
6.9793	.000	.023	.000	.000	.000	.000	.000	21.587	9.770	3.416	3.415	.500
7.0604	.000	.023	.000	.000	.000	.001	.002	4.809	2.394	2.636	2.623	.500
7.1416	.000	.023	.000	.000	.000	.000	.000	-11.756	-3.966	2.566	2.566	.500
7.2227	.000	.023	.000	.000	.000	-.001	-.002	4.988	3.417	3.367	3.353	.500
7.3039	.000	.023	.000	.000	.000	.000	.000	21.570	9.769	3.415	3.412	.500

Figure 8.28: Theoretical pressure head results obtained for 24.51 lt/s (continued).

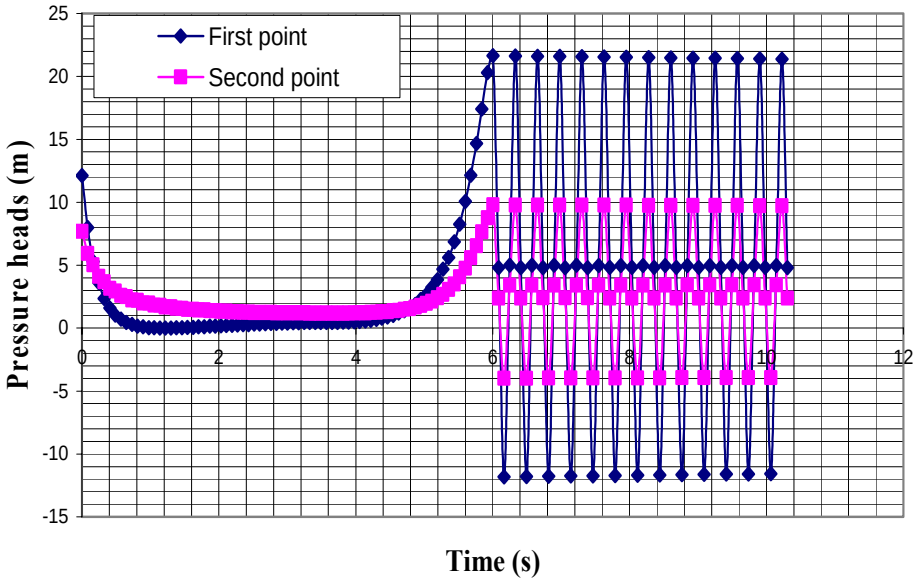

Figure 8.29: Theoretical pressure head results obtained for 24.51 lt/s.

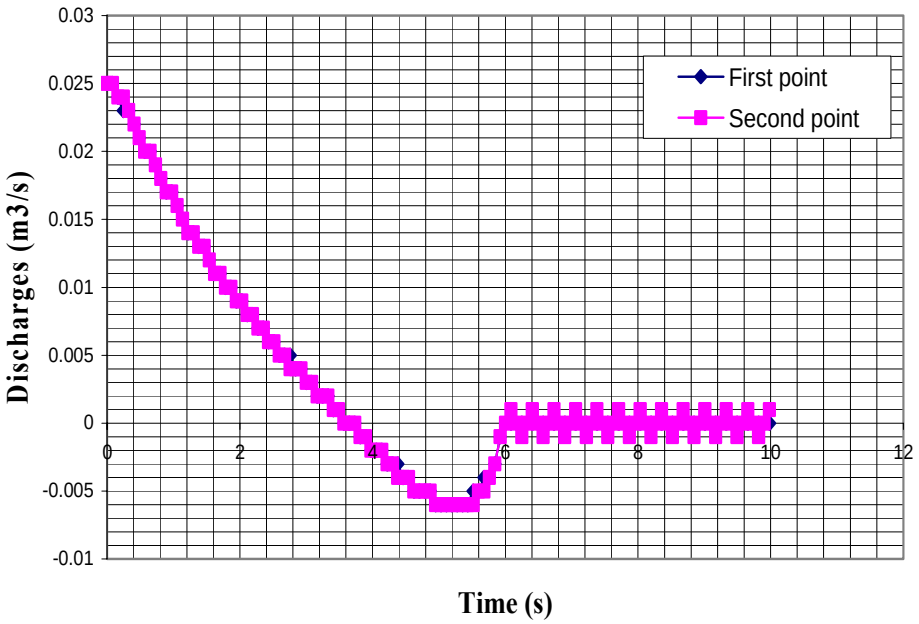

Figure 8.30: Theoretical transient discharges obtained for 24.51 lt/s.

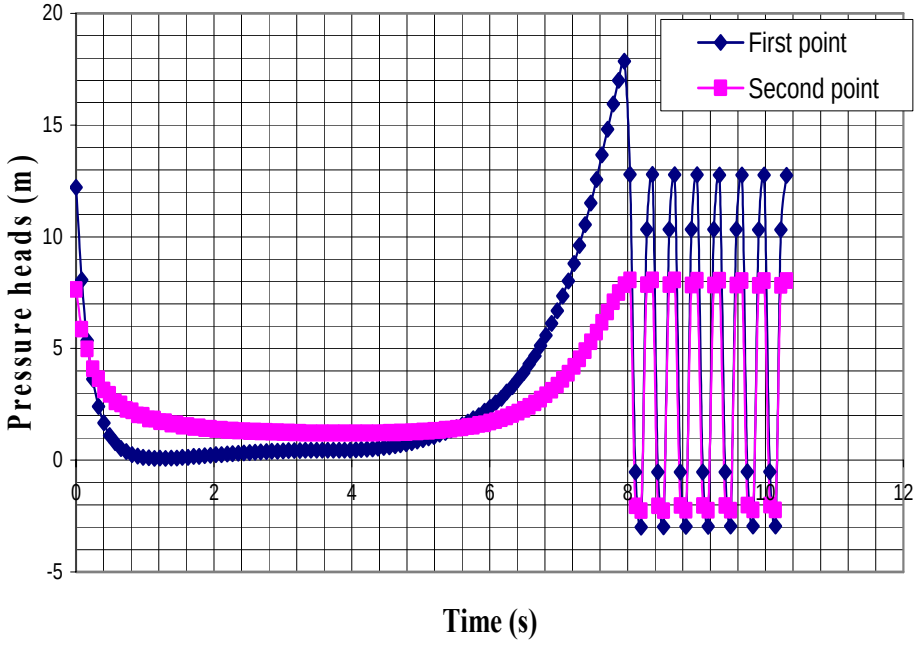

Figure 8.31: Theoretical pressure head results obtained for 25.16 lt/s.

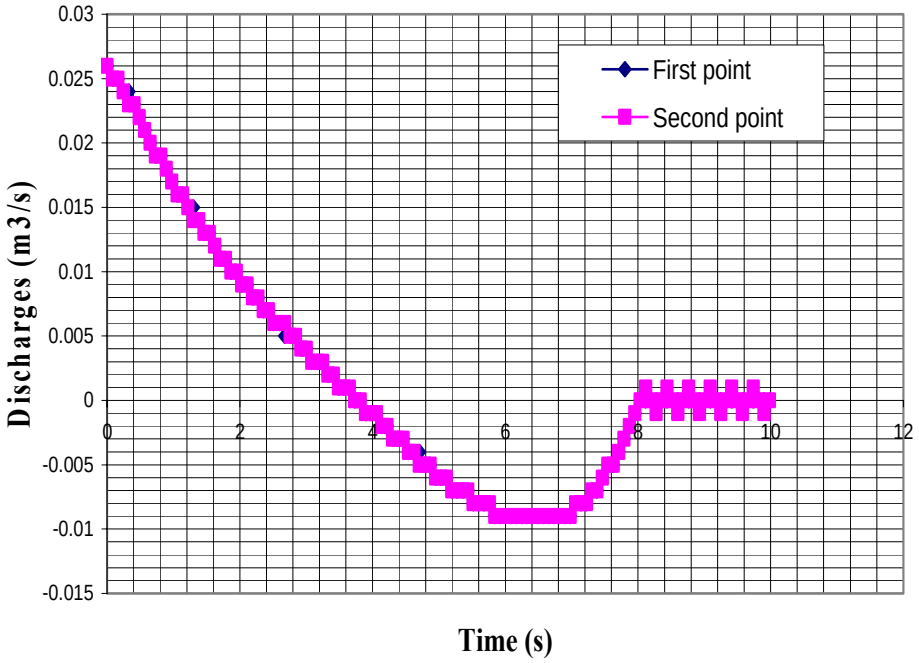

Figure 8.32: Theoretical transient discharges obtained for 25.16 lt/s.

CHAPTER NINE
COMPARISON OF EXPERIMENTAL AND THEORETICAL RESULTS

Experimental results and theoretical ones had been presented in chapter seven and chapter eight respectively. In this chapter, experimental results and theoretical results will be presented in the same figure for comparing.

9.1 Comparison of experimental results with those obtained from computations performed for the first system.

9.1.1 Comparison of experimental results with theoretical results performed for lower steady state discharges

In the case of discharges of 6.2 lt/s (0.5 m/s) and 8.16 lt/s (0.67 m/s), the graphs corresponding to experimental and numerical results are presented in Figures 9.1 and 9.2 respectively.

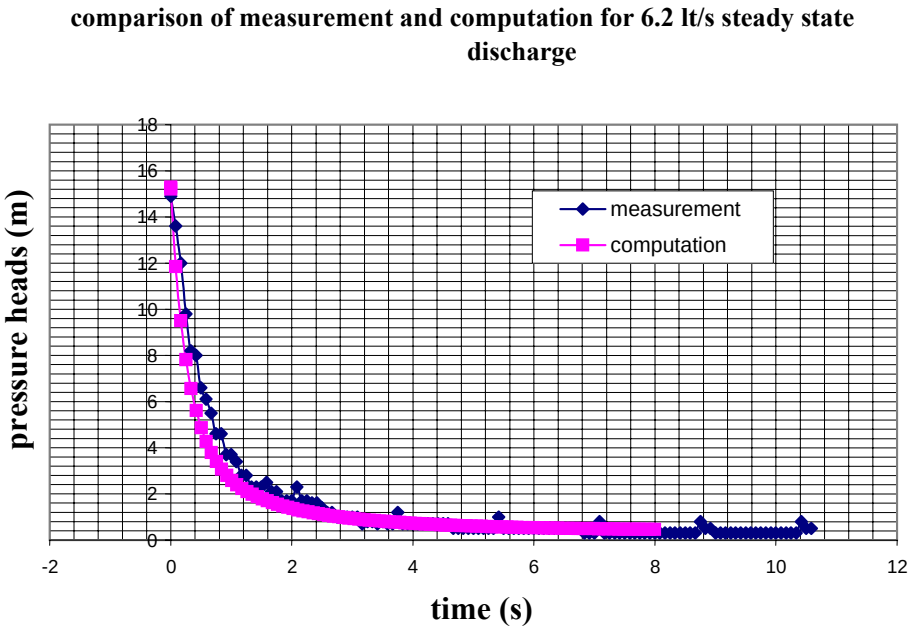

Figure 9.1: Pressure heads correspond to 6.2 lt/s steady state discharge.

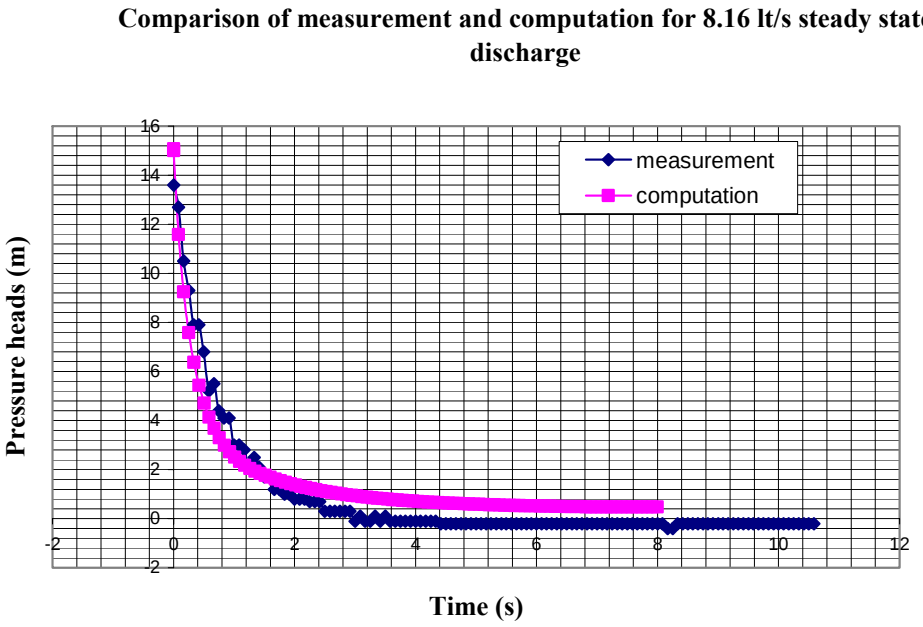

Figure 9.2: Pressure heads correspond to 8.16 lt/s steady state discharge.

9.1.2 Comparison of experimental results with theoretical results performed for moderate steady state discharges

In these comparisons, moderate steady state discharges are taken as 12.31 lt/s (1 m/s), 18.32 lt/s (1.5 m/s) and 22.63 lt/s (1.85 m/s). The graphs corresponding to experimental and numerical results are presented from Figures 9.3 to 9.5 respectively.

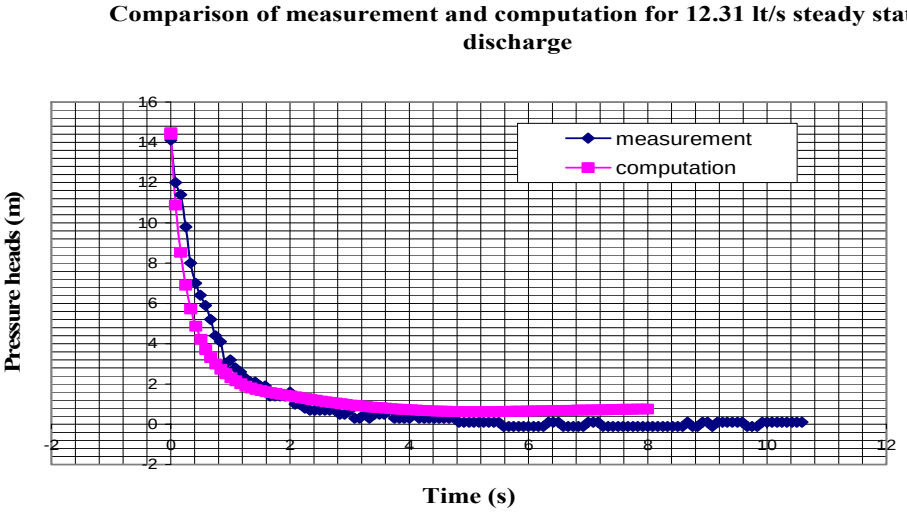

Figure 9.3: Pressure heads correspond to 12.31 lt/s steady state discharge.

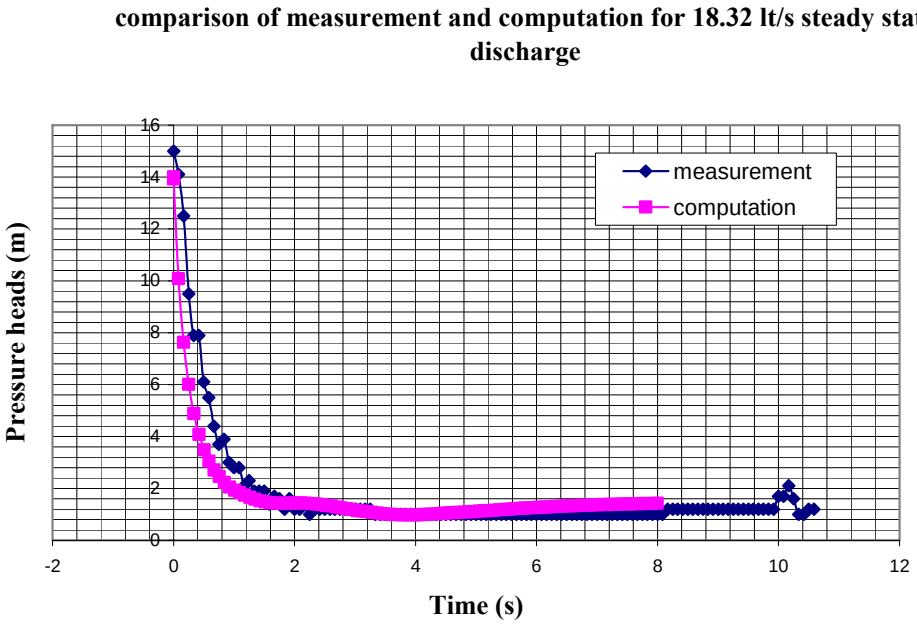

Figure 9.4: Pressure heads correspond to 18.32 lt/s steady state discharge.

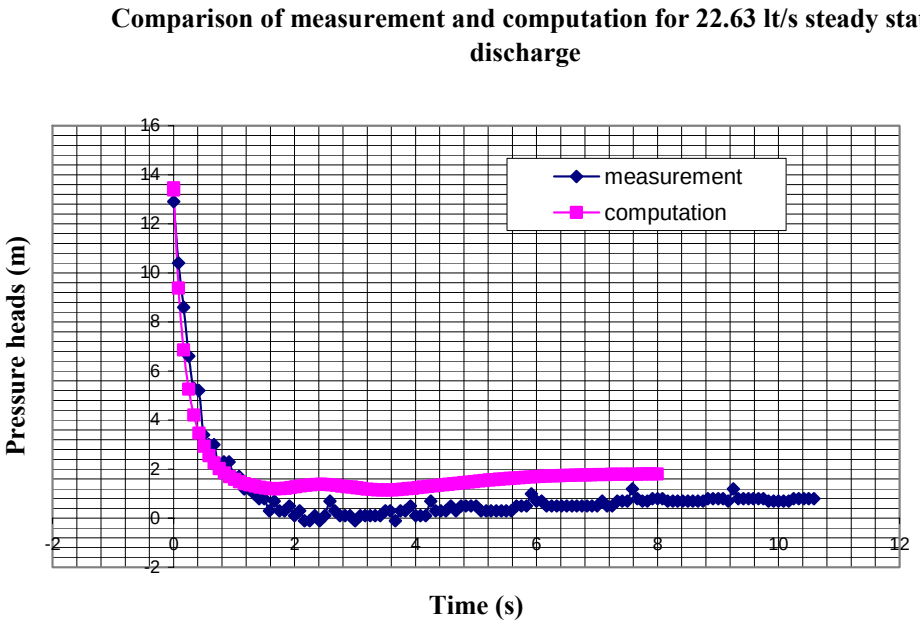

Figure 9.5: Pressure heads correspond to 22.63 lt/s steady state discharge.

9.1.3 Comparison of experimental results with theoretical results performed for upper steady state discharge

In this comparison, upper steady state discharge was taken as 39.00 lt/s (3.2 m/s). The graph corresponding to experimental and numerical results is presented in Figure 9.6.

Similarly, red line corresponds to computation results and blue line corresponds to measurement results.

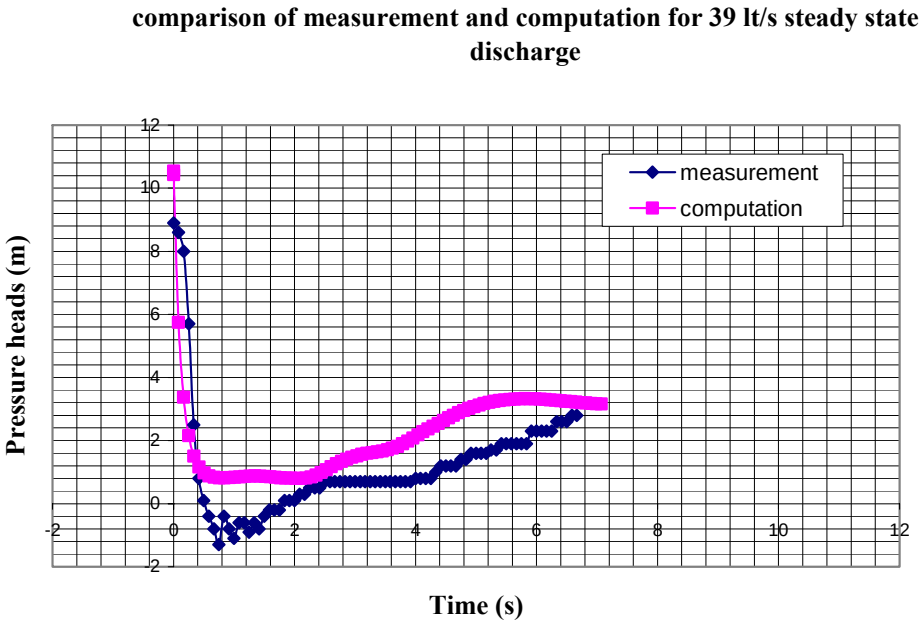

Figure 9.6: Pressure heads correspond to 39 lt/s steady state discharge.

9.2 Comparison of experimental results with those obtained from computations performed for the second system

In this section, experimental results and theoretical results will be compared to each other and exhibited on the same graph for system two. We have computations for lower, normal and upper steady state discharges for system two. However we have two measuring point in system two, therefore we drawn the graphics separately for first point and second point.

We realised comparisons for lower steady state discharges as 6.6 and 9.01 lt/s, normal steady state discharges as 16.50, 19.14 and 20.55 lt/s, upper steady state discharges as 24.51 and 25.16 lt/s according to system 2.

9.2.1 Comparison of experimental results with theoretical results performed for lower steady state discharge

The comparisons are made for two measurements points. As mentioned, the first point is placed just after the pump while the second one corresponds to the interior point which is 66.7 m far from the upstream end.

In this comparison, lower steady state discharges are taken as 6.6 lt/s (0.54 m/s) and 9.02 lt/s (0.74 m/s). The graphs corresponding to experimental and numerical results are presented in Figures 9.7, 9.8, 9.9 and 9.10 respectively.

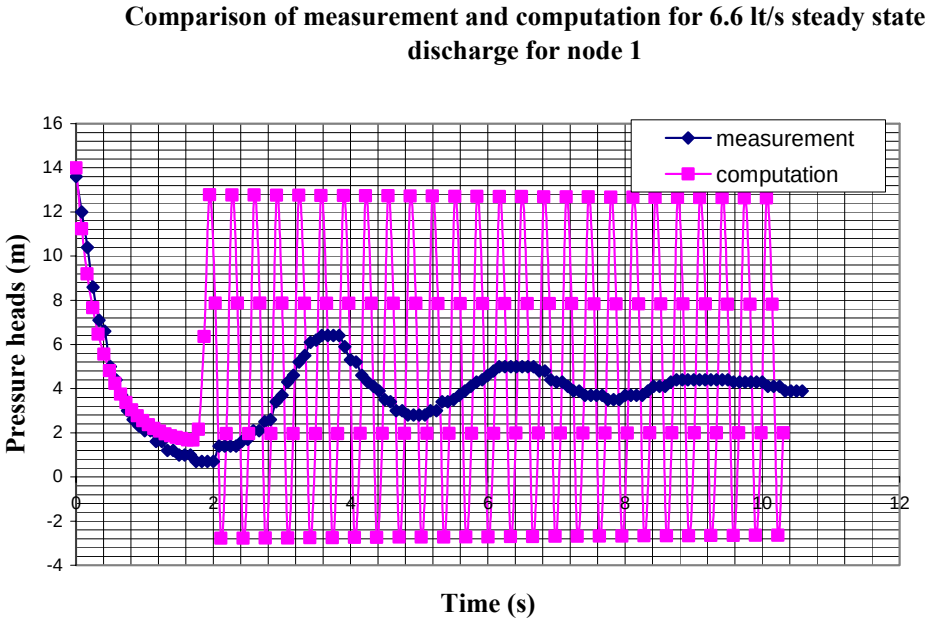

Figure 9.7: Pressure heads correspond to 6.6 lt/s steady state discharge for measuring point 1 (check valve closing time, CCT=1.9 s).

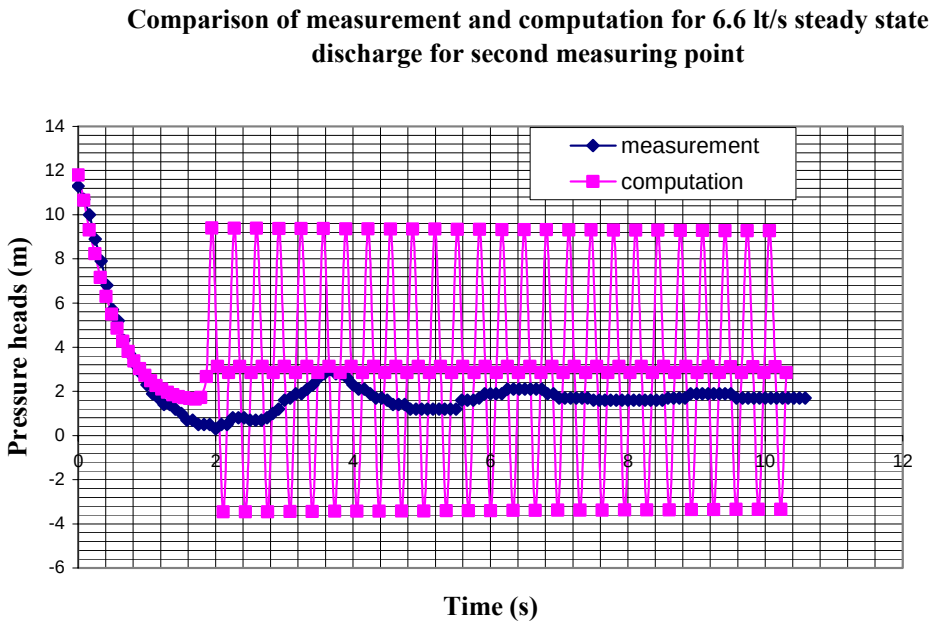

Figure 9.8: Pressure heads correspond to 6.6 lt/s steady state discharge for measuring point 2 (check valve closing time, CCT=1.9 s).

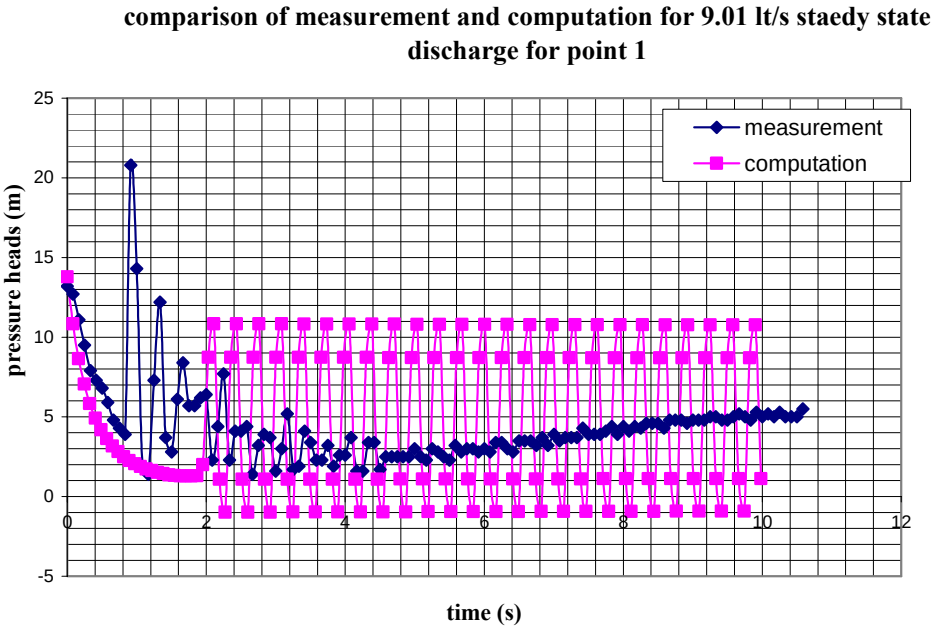

Figure 9.9: Pressure heads correspond to 9.01 lt/s steady state discharge for measuring point 1 (check valve closing time, CCT=2 s).

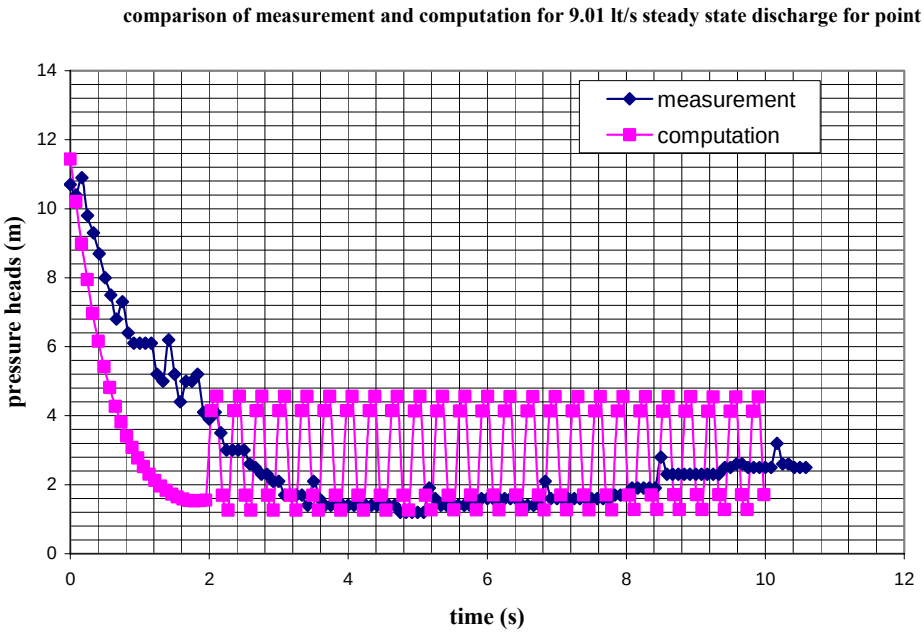

Figure 9.10: Pressure heads correspond to 9.01 lt/s steady state discharge for measuring point 2. 1 (check valve closing time, CCT=2 s).

9.2.2 Comparison of experimental results with theoretical results performed for moderate steady state discharges

The comparisons are made for two measurements points. As mentioned in Section 9.2.1., the first point is placed just after the pump while the second one corresponds to the interior point which is 66.7 m far from the upstream end.

In these comparisons, moderate steady state discharges are taken as 16.5 lt/s (1.35 m/s), 19.14 lt/s (1.57 m/s) and 20.55 lt/s (1.68 m/s).

The graphs corresponding to experimental and numerical results are presented in Figure 9.11, 9.12, 9.13, 9.14, 9.15 and 9.16 respectively.

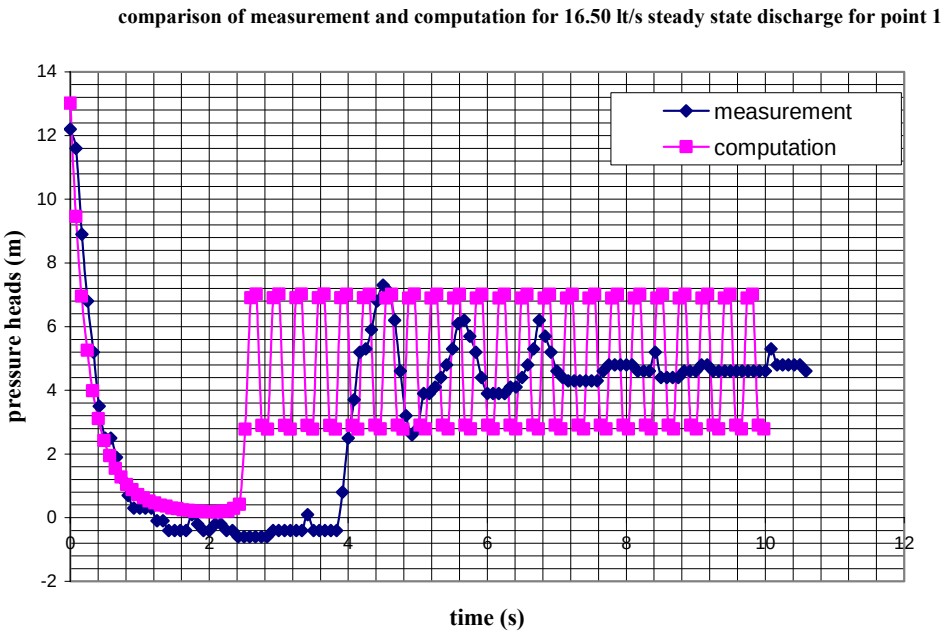

Figure 9.11: Pressure heads correspond to 16.5 lt/s steady state discharge for measuring point 1 (check valve closing time, CCT=2.5 s).

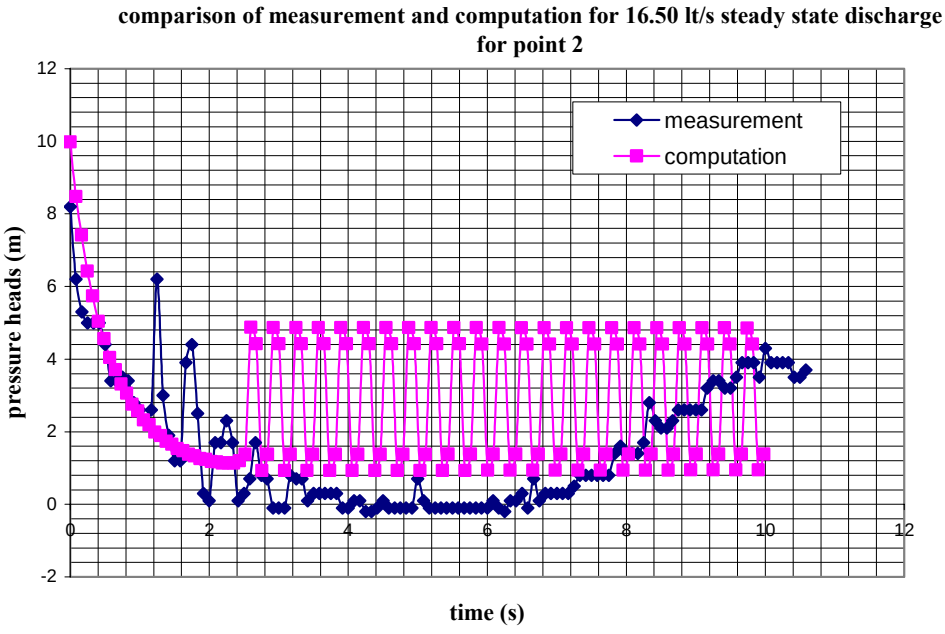

Figure 9.12: Pressure heads correspond to 16.5 lt/s steady state discharge for measuring point 2 (check valve closing time, CCT=2.5 s).

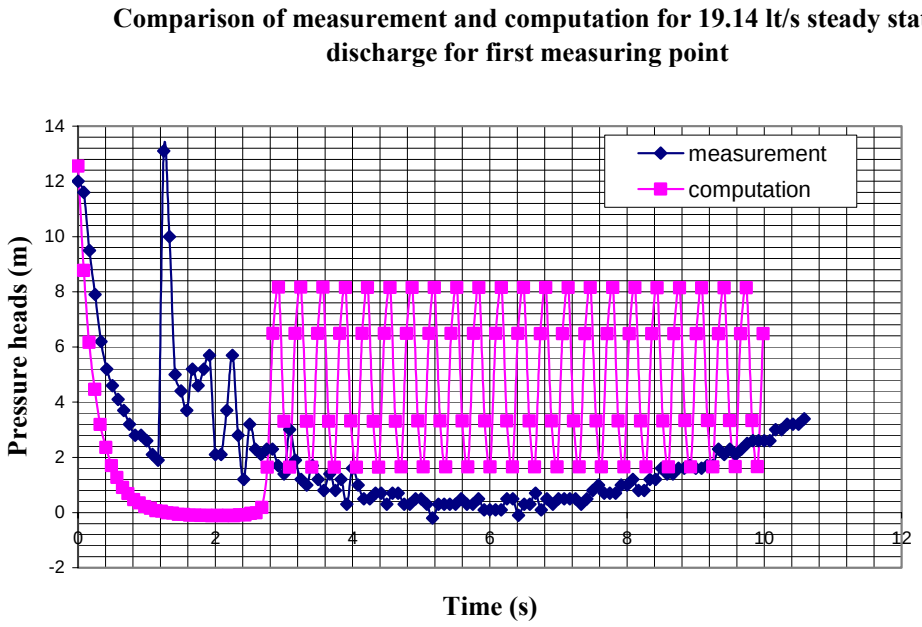

Figure 9.13: Pressure heads correspond to 19.14 lt/s steady state discharge for measuring point 1 (check valve closing time, CCT=2.75 s).

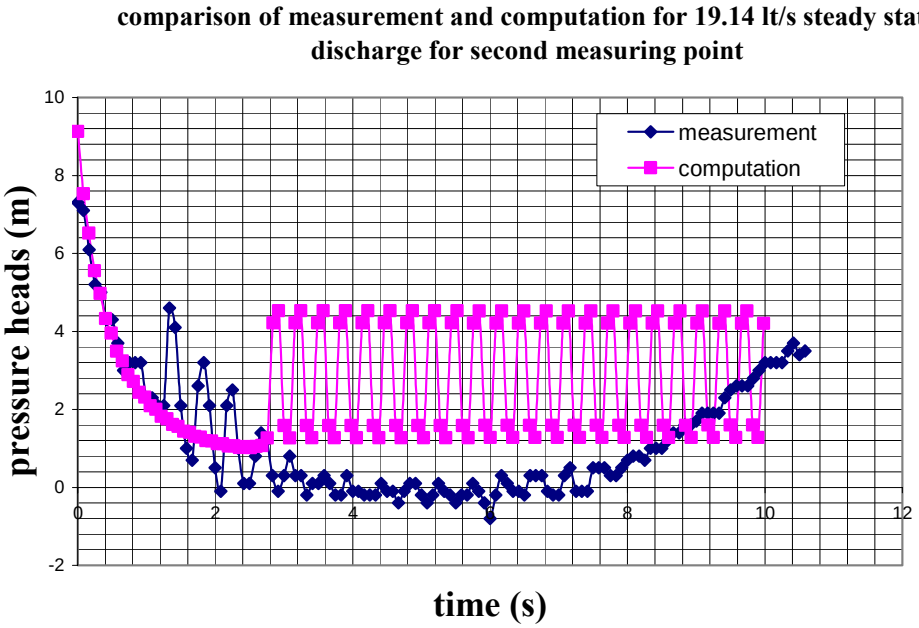

Figure 9.14: Pressure heads correspond to 19.14 lt/s steady state discharge for measuring point 2 (check valve closing time, CCT=2.75 s).

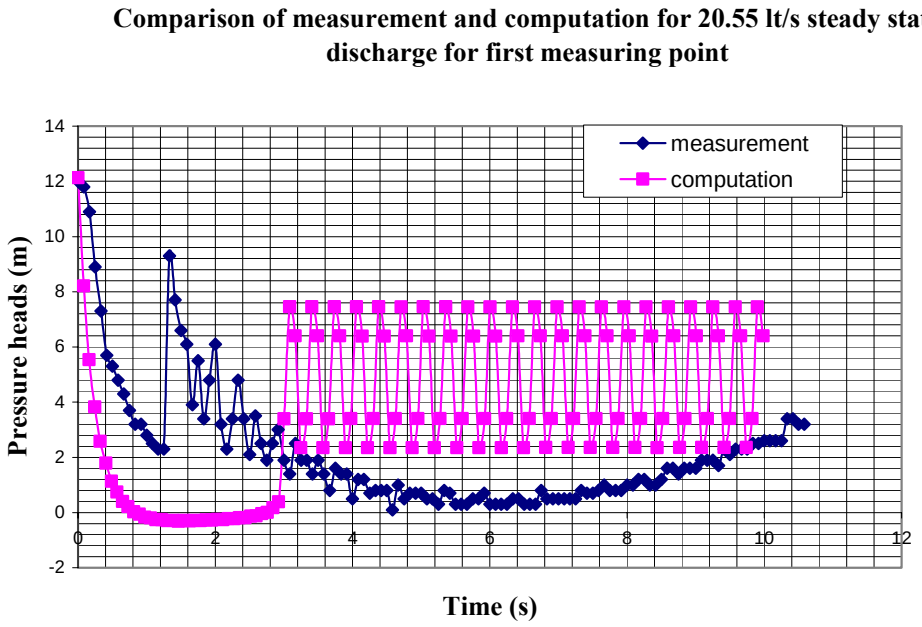

Figure 9.15: Pressure heads correspond to 20.55 lt/s steady state discharge for measuring point 1 (check valve closing time, CCT=3 s).

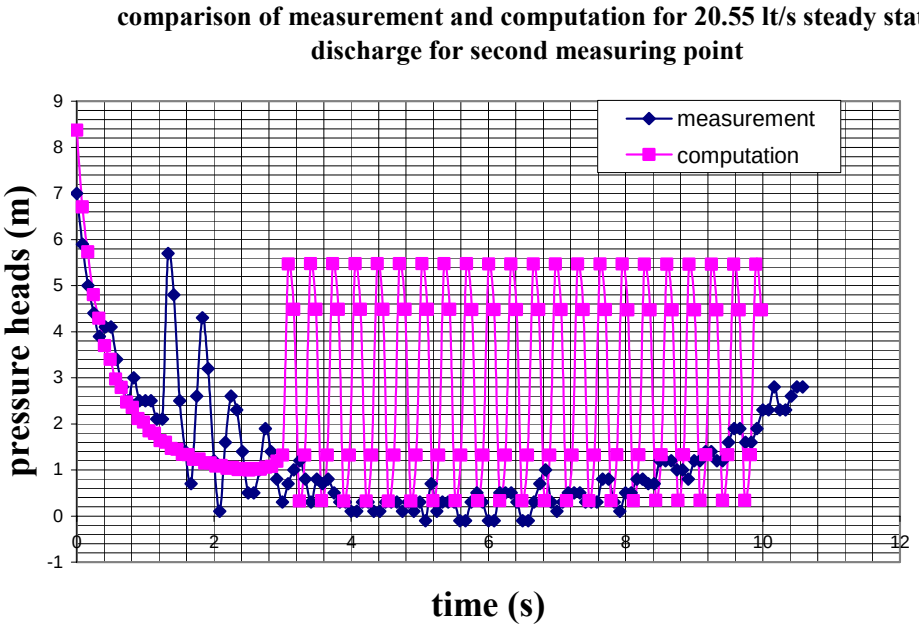

Figure 9.16: Pressure heads correspond to 20.55 lt/s steady state discharge for measuring point 2 (check valve closing time, CCT=3 s).

9.2.3 Comparison of experimental results with theoretical results performed for upper steady state discharges

In these comparisons, upper steady state discharges are taken as 24.51 lt/s (2 m/s) and 25.16 lt/s (2.06 m/s). The graphs corresponding to experimental and numerical results are presented in Figure 9.17, 9.18, 9.19 and 9.20 respectively.

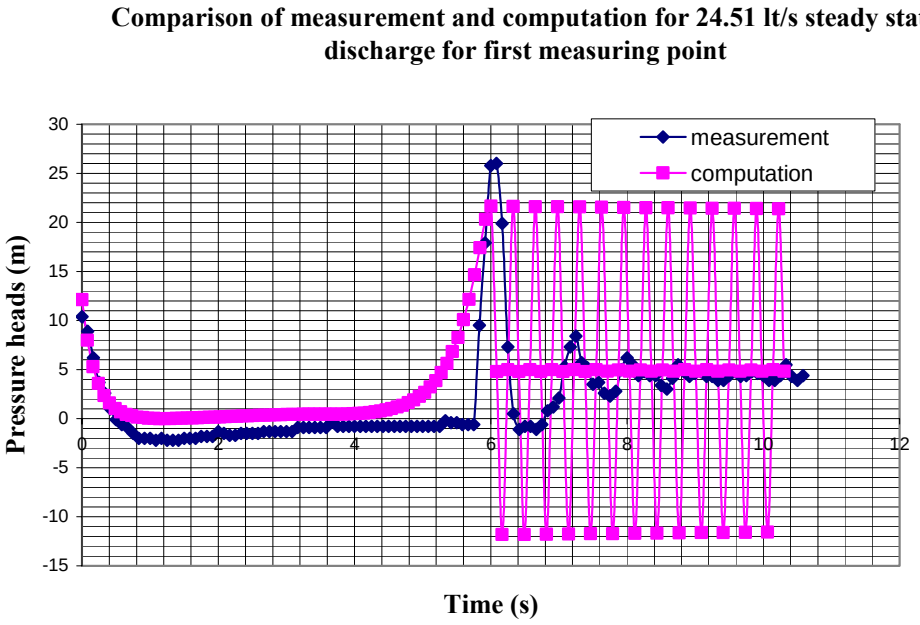

Figure 9.17: Pressure heads correspond to 24.51 lt/s discharge for point 1 (CCT=6 s).

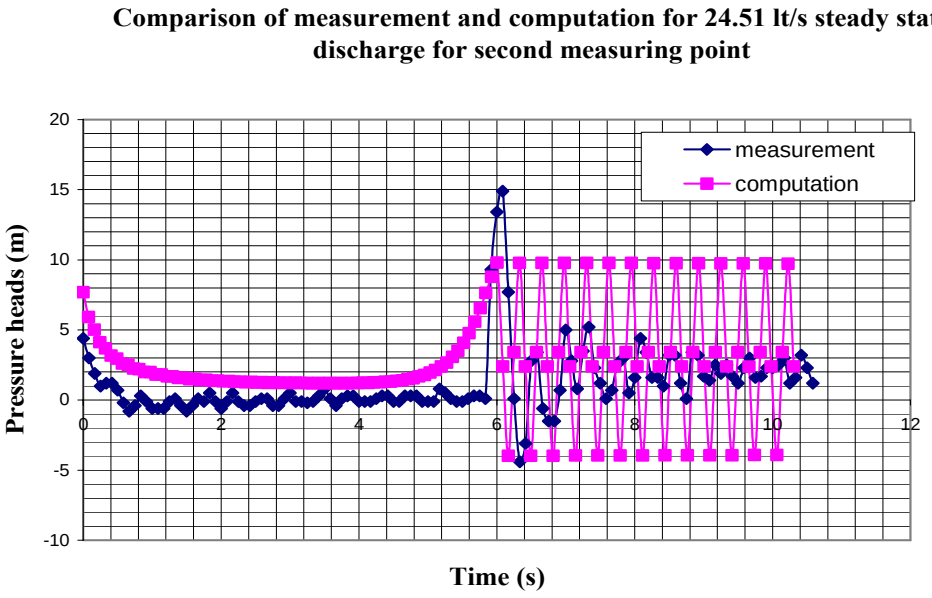

Figure 9.18: Pressure heads correspond to 24.51 lt/s discharge for point 2 (CCT=6 s).

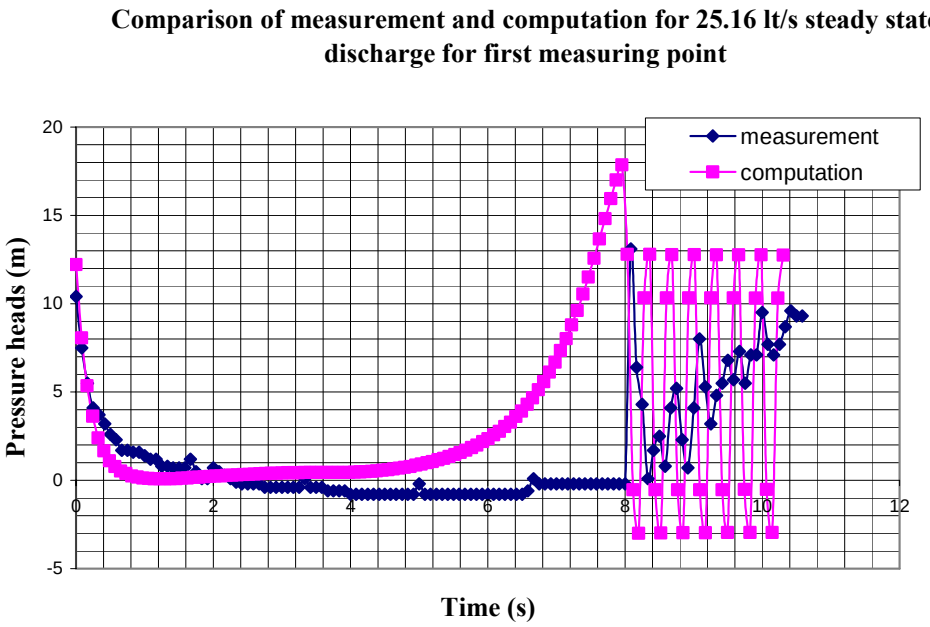

Figure 9.19: Pressure heads correspond to 25.16 lt/s steady state discharge for measuring point 1, CCT=8 s

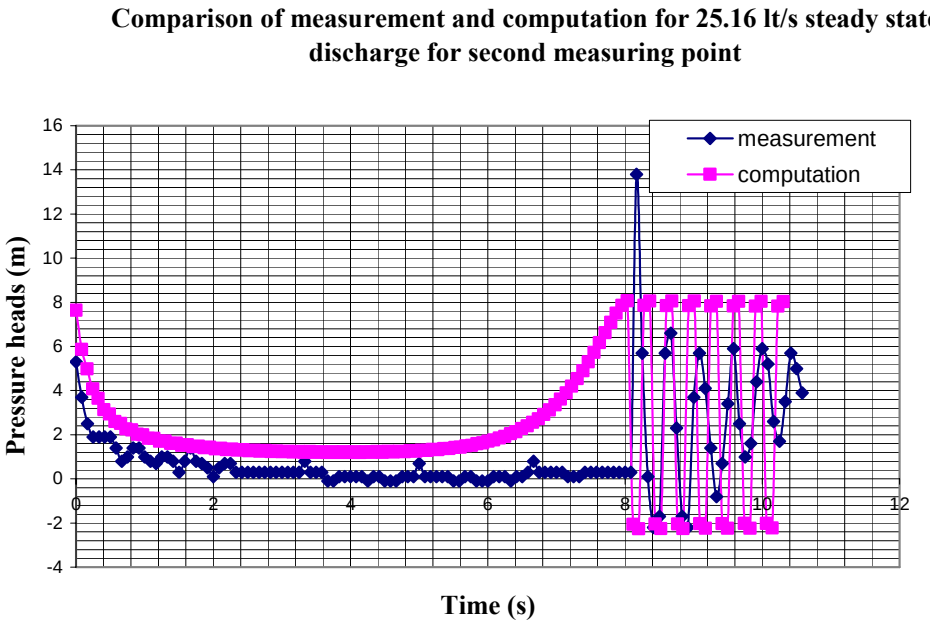

Figure 9.20: Pressure heads correspond to 25.16 lt/s steady state discharge for measuring point 2, CCT=8 s.

CHAPTER TEN
CONCLUSIONS

In practice, it is of vital importance to know the unsteady flow conditions in the hydraulic systems whose designs are generally based on steady flow conditions. That's why, in this study it is aimed to build experimental systems involving a pump in order to study the behaviour of such systems by taking into consideration the boundary conditions described by pump, valve, check valve,…etc.

Two different experimental systems are installed in the Hydraulics Laboratory of Civil Engineering Department, Dokuz Eylül University. These two systems are built to study the unsteady flow due to pump failure. The discharge pipe of the second experimental set up is longer and there exist a check valve after the pump.

The minor losses due to valve, check valve and elbows are determined experimentally by using U tube and gauge manometers. The discharges are measured by means of triangular weir manufactured in the Laboratory. The pressure heads are measured by pressure transient data logger. The pump is shut down manually.

In Wylie & Streeter (1993), there exist 89 pump dimensionless parameters, WH and WB, in terms of various specific speeds, N_s. The 89 pump dimensionless parameters of WH and WB which are used in our study, are obtained by interpolation based on our pump's specific speed, N_s (45.5 SI). These founded pump dimensionless parameters are used in Fortran computations as input values. The interpolation is realised between pump dimensionless parameters of N_s=25 SI and N_s=147 SI.

The computer program given in Wylie & Streeter, 1993 is used after the modifications required in order to adapt to our experimental systems. This program is based on the common Method of Characteristics which solves the ordinary differential equations by using the finite differences technique. The explicit approach is used with the Courant's criterion. After the calculation of piezometric heads in the

computer programs, elevations according to datum are subtracted from piezometric heads, therefore the results are transformed to pressure heads (P/γ), in order to compare directly with experimental results.

Some water hammer pressure waves are observed in the measurements in the second system where there exists a check valve.

It is observed that the theoretical and experimental results are in an acceptable accord in the first system. This accordance is better for lower and moderate discharges.

It is observed that the check valve is closing late for upper steady state discharges and early for lower steady state discharges in the second system.

In the second system, some discrepancies exist between theoretical and experimental results. They are due to the difficulty for reflecting the behaviour of the check valve. That's why, additional investigations, mainly about the time and shape of its closure need to be performed.

The oscillations of large amplitude observed at first point are likely to occur because of water hammer due to the closure of the check valve.

Some provisions need to be taken in order to decrease the fluctuations in the measurements, mainly at the point close to the pump and check valve.

The accord between theoretical and experimental results may be improved by translating the behaviour of the check valve more realistically. The computer program handled for the second system should be revised in order to translate the transient behaviour after the closure of the check valve.

It will be interesting to investigate the effect of the variable head loss coefficients involved during unsteady state flow determination in the Fortran programs.

REFERENCES

A GFP Company. (n.d.). Retrieved June 01, 2007, from web address http://www.mechanicalroomsuplies.com

Advanced Valves. (n.d.). Retrieved June 01, 2007, from web address http://www.advancevalves.com

Alves, E. G. (2004). Hydraulic analysis of sudden flow changes in a complex piping circuit. *Conference paper*. Delaware, USA.

Bergant, A., Simpson, A.R. & Tijsseling, A.S. (2005). Water hammer with column separation: A historical review.

Bryan Karney, W., & McInnis, D., (1990). Transient analysis of water distribution system. *Journal of American water works association (AWWA)*, 82, 7, 62-70.

Burmann, W. (1975). Water hammer in coaxial pipe systems. *Journal of hydraulic division of ASCE*, 101, 6, 699-715.

Champion Valves. (n.d.). Retrieved June 01, 2007, from web address http://www.wafercheck.com/Championvalves

Charles Darwin University, School of Engineering, Fluid Mechanics laboratory experiment, Eng 243, . (n.d.). Retrieved June 01, 2007, from web address http://www.cs.ntu.edu.au/homepages/jmitroy/eng243/FlowComplexPipeSystem

Chaudhry, M.H. (1987). *Applied hydraulic transients*. Van Nostrand Reinhold Company.

Clark, G. A., Smajstrla, A.G. & Haman, D.Z. (2003). Water hammer in irrigation systems. *Institute of Food and Agricultural Sciences, University of Florida, Gainesville*.

Control Valve Monovar, hydraulic characteristics. (n.d.). Retrieved June 01, 2007, from web address http://www.4engr.com/product/catalog/1157/index.html

Diesselhorst, T., Neumann, U. (2005). Optimization of loads in piping systems by the realistic calculation method: Applying fluid-structure interaction (FSI) and dynamic friction. *Journal of pressure vessel technology of ASME,* 127, 1, 1-6.

Donsky, B. (1961). Complete pump characteristic and the effects of specific speeds on hydraulic transients. *Journal of basic engineering, ASME*, 685-699.

Duyar Valve (2006), *Valve cataloque*. Duyar valve mechanical industry Gaziosmanpaşa, İstanbul

Ezzeddine, H.T. & Lili, T. (1998). Transient flow of homogeneous gas-liquid mixtures in pipelines. *International Journal of numerical methods for heat and fluid flow,* 8, 3, 350-368.

Fleming, K.K., Dugandzic, J.P., LeChevallier, M.W. & Gullick, R.W. (2006). Susceptibility of potable water distribution systems to negative pressure transients. *Research project summary*. Division of science, research and technology, Trenton, NJ, USA.

Flowserve Flow Control (UK) Ltd. (n.d.). Retrieved June 01, 2007, from web address http://www.worcestercontrols.co.uk

Hayward Industrial Products, Inc. (n.d.). Retrieved June 01, 2007, from web address http://www.haywardindustrial.com

Kaliatka, A., Uspuras, E. & Vaisnoras, M. (2005). RELAP5 code analysis of water hammer wave behaviour. *Conference paper*. Laboratory of Nuclear Installation Safety, Lithuanian Energy Institute, Kaunas, Lithuania.

Kameswara, R. C. V. & Eswaran, K. (1999). Pressure transients in incompressible fluid pipeline networks. *Journal of nuclear engineering and design,* 188, 1, 1-11.

Kirkland, C. (1998). Controlling and understanding the effects of air in pipelines. *Conference paper,* Amiad Australia Pty. Ltd.

Koç, A.C. (2001). Computation of unsteady flows in hydraulic systems with hydraulic machinery. *A thesis submitted to the graduate school of natural and applied sciences of Dokuz Eylül University, İzmir*.

Kono, Y., Watanabe, M. & Ito, T. (1998). Phase change analysis in water hammer by upstream finite difference method. *Conference paper*. Japan.

Larock, B.E., Jeppson, R.W., & Watters, G.Z. (2000). *Hydraulics of pipeline systems*. CRC press.

Leishear, R.A. (2007). Dynamic pipe stresses during water hammer: A finite element approach. *Journal of pressure vessel technology, ASME*, 129, 2, 226-233.

LMNO Engineering. (n.d.). Retrieved June 01, 2007, from web address http://www.lmnoengineering.com

Mays, L.W. (1999). *Hydraulic design handbook*. McGraw-Hill.

Popescu, M., Arsenie, D., Vlase, P. (2003). *Applied hydraulic transients*. A.A. Balkema Publishers.

Rahmeyer, W. (1996). Dynamic flow testing of check valves. *Journal of nuclear industry check valve group, winter meeting, St. Petersburg, Florida, USA.*

Reduced Bore Valves, Engineering Toolbox. (n.d.). Retrieved June 01, 2007, from web address http://www.engineeringtoolbox.com/ball-valves-flow-coefficients-d_223.html

Streeter, V.L., & Wylie, E.B. (1975). Transient analysis of offshore loading systems. *Journal of manufacturing science and engineering*, 97, (1), 259-265.

Sunrise Systems Ltd. (1999). Pipeline transient module. Computer program.

Thorley, A. R. D. (1989). Check valve behaviour under transient flow conditions: A state-of-the-art review. *Journal of fluids engineering*, (111), 178-183.

Thorley, A. R. D. (1991). *Fluid transients in pipeline systems*. D&L George ltd.

Tullis, J. P. (1989). *Hydraulics of pipelines*. John Wiley & Sons Inc.

Ward, D. (2004). Automatic and remotely controlled shutoff for direct flow liquid manure application systems.

Watters, G. Z. (1979). *Modern analysis and control of unsteady flow in pipelines*. Michigan: Ann Arbor Science.

White, F. (2003). *Fluid Mechanics*. 5th edition, McGraw-Hill.

Wylie, E. B., & Streeter, V. L. (1978). *Fluid transients*. Prentice hall.

Wylie, E. B., & Streeter, V. L. (1993). *Fluid transients in systems*. Prentice hall.

Yanmaz, M. (2001). *Applied water resources engineering.* METU Press.

APPENDICES

APPENDIX A: The geometric characteristics of Reduced Bore Ball valve and those of the disc type check valve, Head loss coefficients for minor losses.

APPENDIX B : The list of computer program adopted for the first system, Typical data file

APPENDIX C : The list of computer program adopted for the second system, Typical data file

APPENDIX A

A.1. The geometric characteristics of Reduced Bore Ball valve and those of the disc type check valve

In the experimental systems, PN6 DN125-100 reduced bore ball valve is used. It has an interior diameter of 100 mm and an exterior diameter of 125 mm (Figure A.1.1). The used disc type check valve is named as NEK NW 100 ND 16, 100 PN 10-16. The general view and the section of this valve is given in Figure A.1.2.

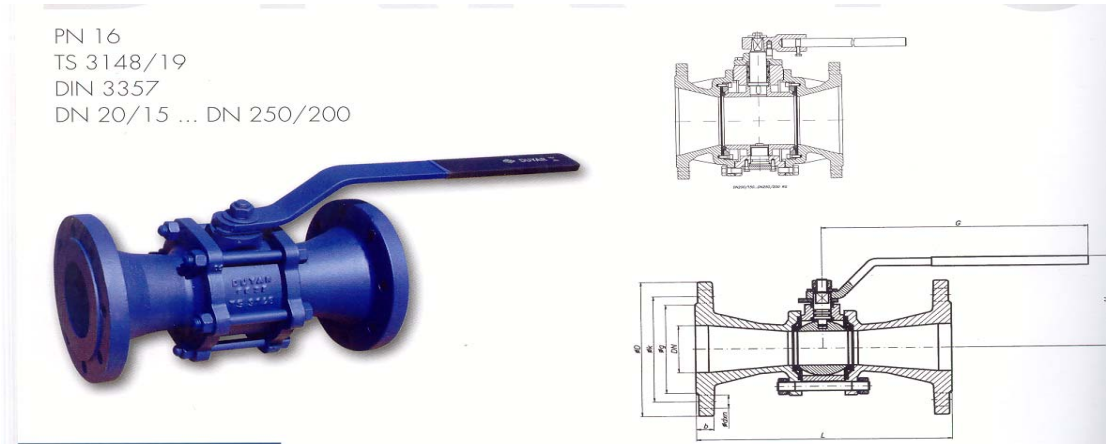

Figure A.1.1: The view of Reduced Bore Ball Valve (trademark: Asvan) .

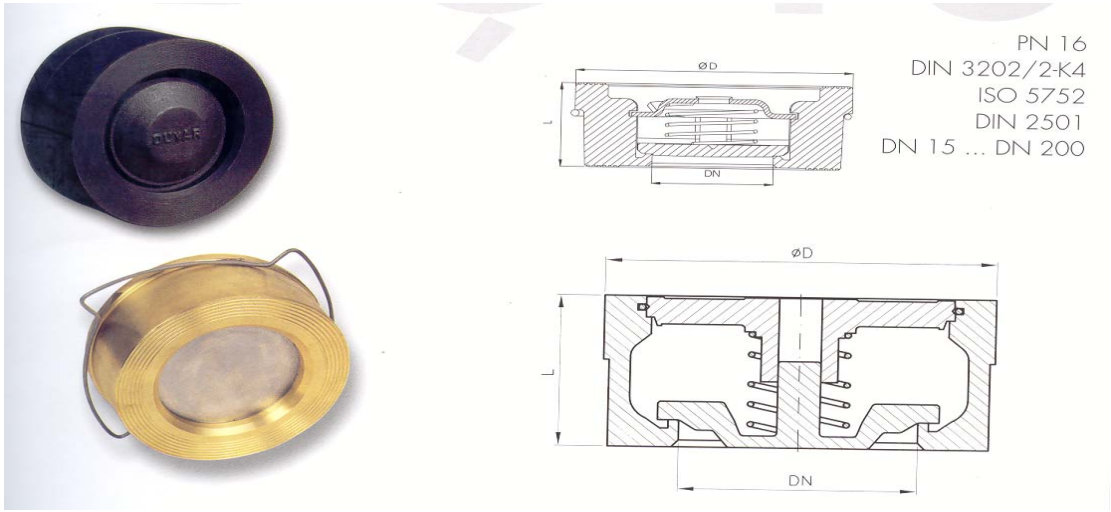

Figure A.1.2: The Disc Type Check Valve.

A.2. Head loss coefficients for minor losses.

Various loss coefficients for the Disc type check valve were investigated from the literature. The loss coefficients against to various steady state discharges are presented as tables and graphics in this section.

Table A.2.1: Check valve loss coefficients against to discharges obtained from 'Duyar valve' company. The valve diameter is equal to 125 mm.

Steady state discharges, Q (m^3/s)	Check valve loss coefficient, K
0.0075	10.50
0.010	9.45
0.015	9.19
0.020	8.86
0.030	8.21
0.040	7.39

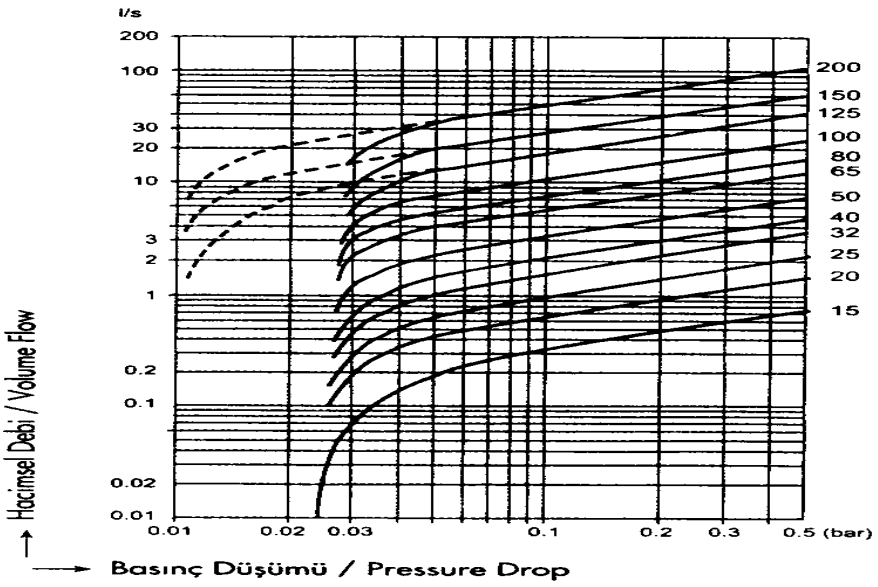

Figure A.2.1: Pressure drop against to discharges for check valve corresponding to Table A.2.1 obtained from 'Duyar Valve Company'. x axis is pressure drop by bar and y axis is discharge in lt/s.

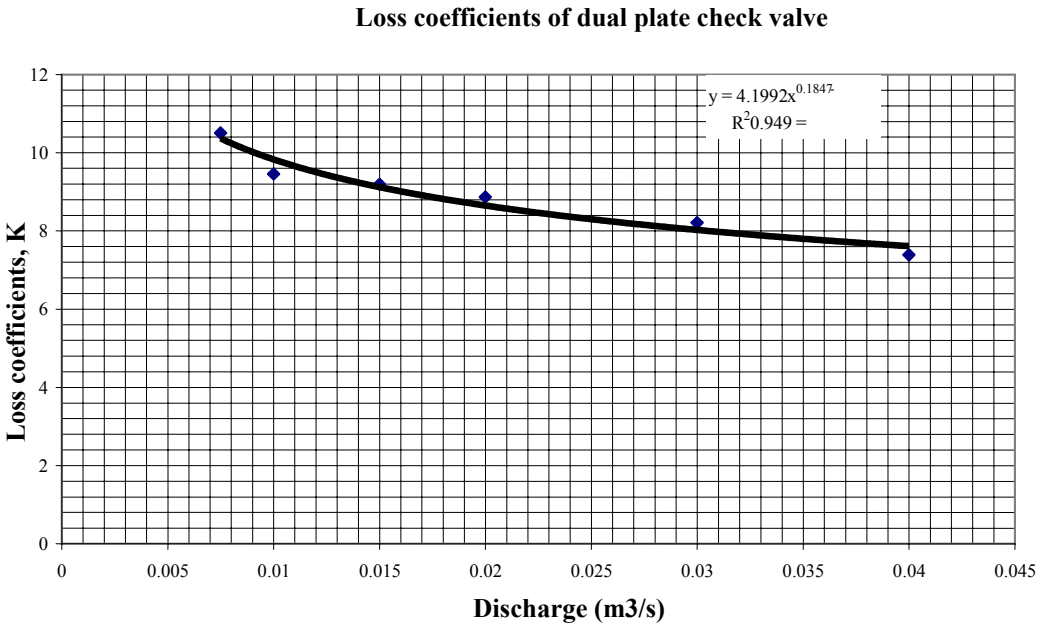

Figure A.2.2: Loss coefficients, K of check valve against to steady state discharges corresponding to Table A.2.1 obtained from 'Duyar Valve' company. Diameter = 125 mm.

The equation obtained from curve fitting will be $K=4,1992.Q^{-0,1847}$.

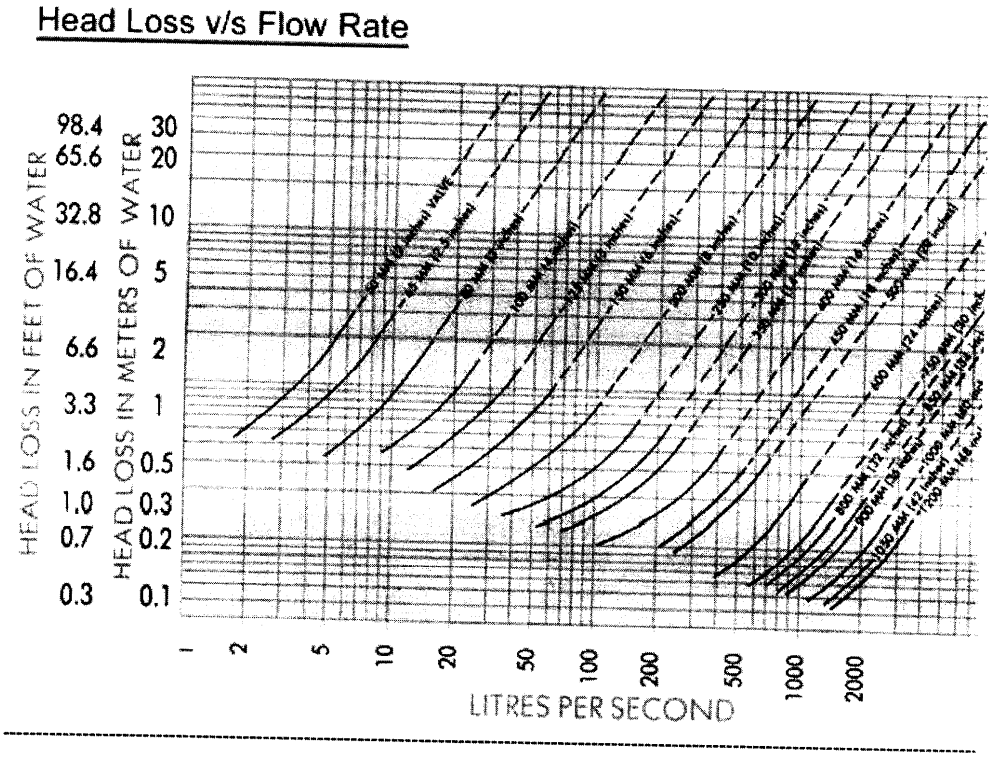

Figure A.2.3: Head Losses vs Flow rate is drawn for check valve obtained from 'Advanced Valves' company.

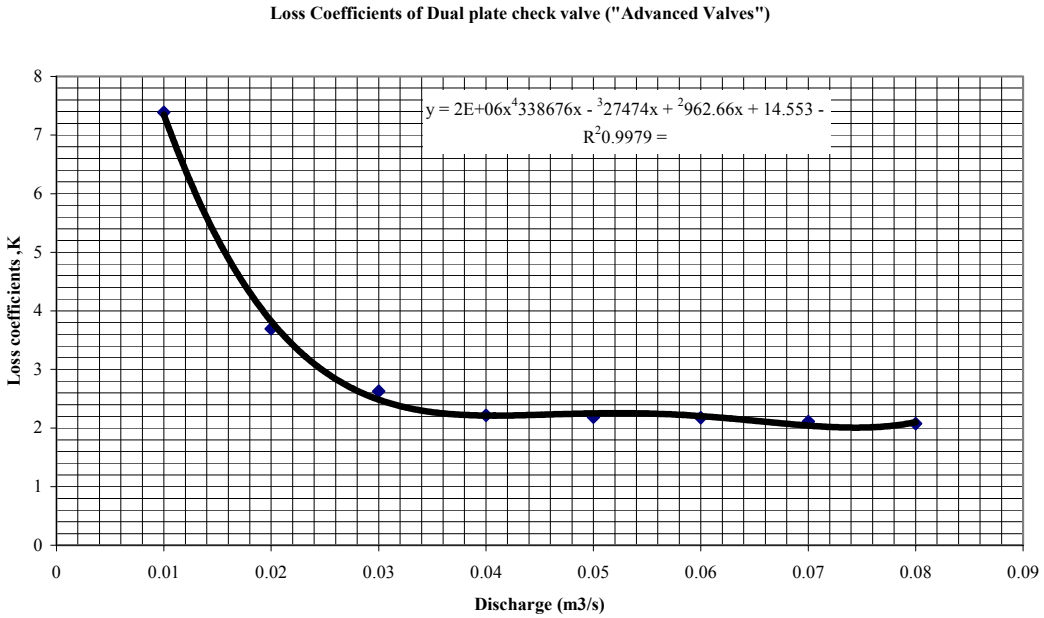

Figure A.2.4: Against steady state discharges, Q to loss coefficients, K for check valve obtained from 'Advanced Valves' company, corresponding to Figure A.2.3. D = 125 mm.

The equation found after curve fitting will be $K=(2.10^6.Q^4)-(338676.Q^3)+(27474.Q^2)-(962,66.Q)+14,553$.

Table A.2.2: Check valve loss coefficients against to discharges obtained from 'Advanced valves' company, corresponding to Figure A.2.3. D=125 mm.

Steady state discharge, Q (m^3/s)	Loss coefficient; K (for check valve)
0.01	7.39
0.02	3.69
0.03	2.63
0.04	2.22
0.05	2.19
0.06	2.17
0.07	2.11
0.08	2.08

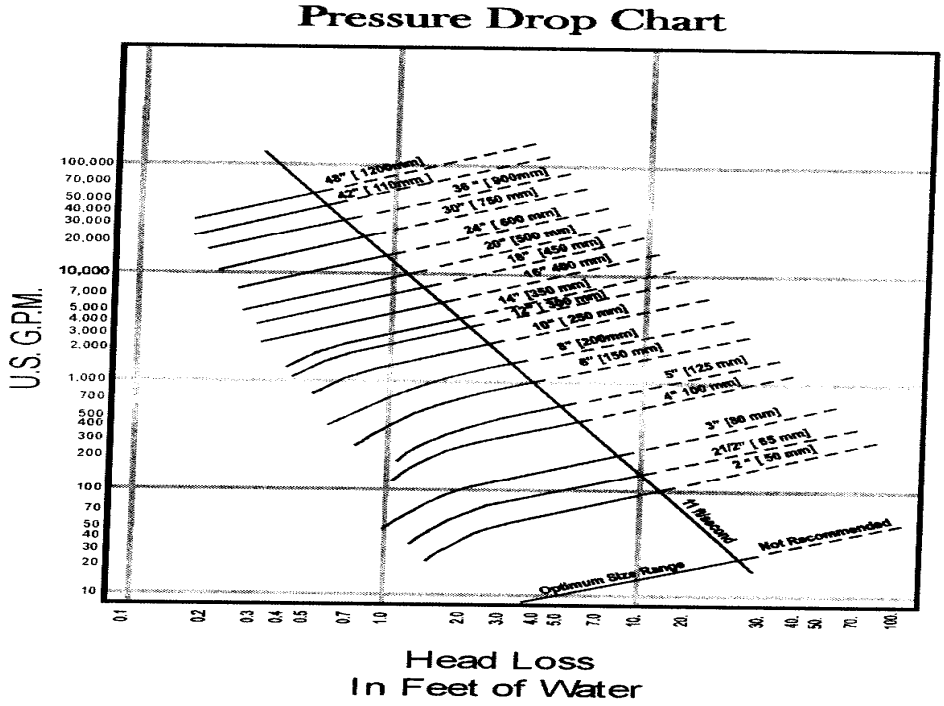

Figure A.2.5: Head losses vs steady state discharges for check valve obtained from 'Champion valves' company.

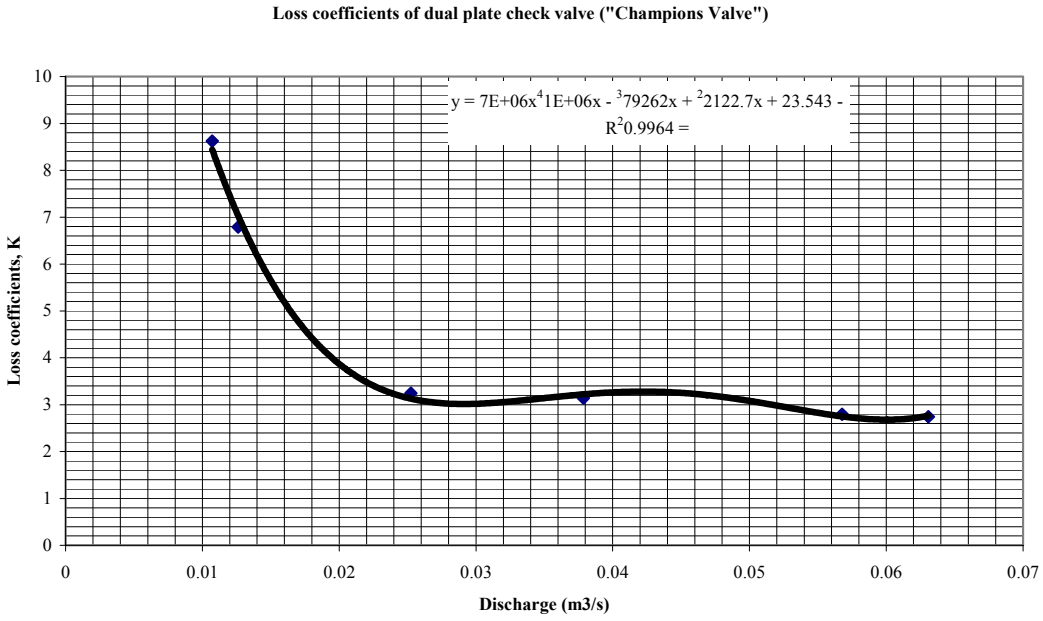

Figure A.2.6: Steady state discharges, Q against to loss coefficients, K for check valve obtained from 'Champion Valves' company, corresponding to Figure A.2.5. D=125 mm.

The equation obtained from curve fitting is $K=(7.10^6.Q^4)-(10^6.Q^3)+(79262.Q^2)-(2122,7.Q)+23,543$.

Table A.2.3: Check valve loss coefficients against to discharges obtained from 'Champion valves' company, corresponding to Figure A.2.5. D=125 mm.

Steady state discharges, Q (m^3/s)	Loss coefficient, K
0.010	8.62
0.012	6.79
0.025	3.25
0.037	3.14
0.056	2.79
0.063	2.75

Table A.2.4: Loss coefficients of different trademarks about disc type check valve against to steady state discharges (lt/s). Column 1 refers to steady state discharges (lt/s). Column 2, 3 and 4 refer to loss coefficients correspond to steady state discharges presented in Figures A.2.1, A.2.3 and A.2.5 respectively. In the last column at the right side refers to mean values of the summations of column 2, 3 and 4. D=125 mm.

Steady state discharge (lt/s)	From Figure A.2.1 , Loss coeff., K	From Figure A.2.3 , Loss coeff., K	From Figure A.2.5 , Loss coeff., K	Mean loss coeff., with column 2, 3 and 4
6.60	10.61	9.30	12.71	10.87
9.01	10.02	7.87	10.16	9.35
16.49	8.96	4.78	6.12	6.62
19.14	8.72	4.08	5.88	6.23
20.55	8.60	3.79	5.96	6.12
24.51	8.33	3.20		
25.16	8.29	3.13		

Table A.2.5: Flow coefficients Cv according to Valve sizes (Note that Cv=The number of US gpm of water that will flow thru the valve with a 1 psi pressure drop across the valve) obtained from 'A GFP Company' for Dual Disc Non Slam Check valve.

Valve Size, inches	Valve sizes, mm	Flow Coefficient, Cv
2.0	51	80
2.5	63	90
3.0	76	150
4.0	102	300
5.0	127	500
6.0	152	900
8.0	203	1700
10.0	254	3000
12.0	305	4000
14.0	356	5350
16.0	406	7400

Table A.2.6: Flow coefficients Cv according to Valve sizes (Note that Cv=The number of US gpm of water that will flow thru the valve with a 1 psi pressure drop across the valve) obtained from 'Hayward Industrial Products, Inc' for Swing Type Check valve ($\Delta P=(Q/Cv)^2$ in which ΔP=pressure drop in psi, Q=Flow rate in gpm, Cv=flow coefficient).

Valve Size, inches	Valve sizes, mm	Flow Coefficient, Cv
3	76	328
4	101	514
6	152	1278
8	203	2549

A.3. Head loss coefficients for reduced bore ball valves in the literature

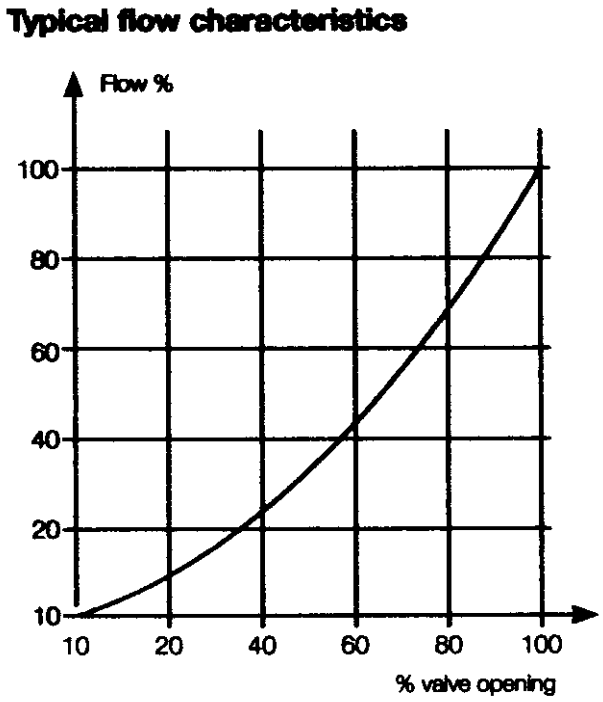

Figure A.3.1: % Flow vs % valve opening (from Monovar control valve)

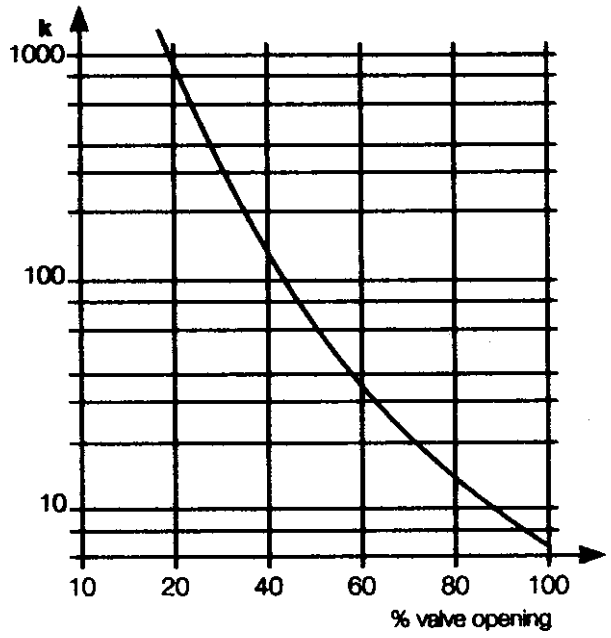

Figure A.3.2: Headloss coefficient K vs % valve opening (from Monovar control valve).

Table A.3.1: Loss coefficients, K in valves (obtained from Charles Darwin University)

% Opening of valve	K for Gate valve	K for Globe valve
100	0.2	10.0
75	0.9	11.0
50	5.0	12.5
25	24.0	50.0

Table A.3.2: Loss coefficient ratio of globe valve, K/K_{open} corresponding to % opening of valve (obtained from White, 2003)

% Opening of valve	K/K_{open}
100	1.00
80	1.03
70	1.13
60	1.38
50	1.50
40	1.75
30	2.63
25	3.75

Table A.3.3: Typical flow coefficients, Cv (for US Customary Units) for reduced bore valves (obtained from 'Ball valves and typical flow coefficients' web page).

Diameter of pipe in mm	Diameter of pipe in inches	Flow coefficient, Cv
75	3	420
100	4	770
150	6	1800
200	8	2500
250	10	4500
300	12	8000
350	14	12000

Table A.3.3 : (Continued)

400	16	14000
450	18	18000
500	20	22000

Table A.3.4: Ball valve head loss coefficient, K vs % opening of valve (obtained from 'LMNO Engineering' home web page).

% Opening of valve	Head loss coefficient, K
Angle, 100	5.00
Ball, 100	0.05
Ball, 67	5.50
Ball, 33	210.00

Table A.3.5: Flow coefficients, Cv (for US Customary Units, i.e. Cv is flow in US gpm, pressure is psi) and Kv (for SI Units, i.e. flow in m^3/h and pressure is bar) versus valve sizes (obtained from 'Flowserve Flow Control (UK) Ltd' web page).

Valve size in mm	Valve size in inches	Flow coefficient, Cv	Flow coefficient, Kv
15	0.50	6.00	7
20	0.75	8.70	10
25	1.00	26.00	30
40	1.50	77.00	89
50	2.00	112.50	130
65	2.50	230.00	267
80	3.00	303.00	350
100	4.00	623.00	720
150	6.00	882.00	1020
200	8.00	1557.00	1800
250	10.00	2560.00	2970

Table A.3.6 : Flow coefficients, Cv (for US Customary Units, i.e. Cv is flow in US gpm, pressure is psi) versus valve sizes (obtained from Larock et al, 2000) for Ball valves.

Valve size in inches	Valve size in mm	Flow coefficient, Cv
6	152	5250
8	203	9330
10	254	14600
12	305	21000
14	356	28600
16	406	37300
18	457	47300
20	508	58300
24	610	84000
30	762	131300
36	914	189000
42	1067	257300
48	1219	336000
54	1372	425300
60	1524	525100

Table A.3.7 : Flow coefficients, Cv (for US Customary Units, i.e. Cv is flow in US gpm, pressure is psi) corresponding to degrees open (obtained from Larock et al, 2000) for Ball valves.

Degrees Opening	Percentage of fully open Cv
5	0.16
10	0.88
15	1.4
20	1.8
25	2.4
30	3.1
35	3.7
40	4.7

Table A.3.7 : (Continued)

45	5.9
50	7.2
55	9.0
60	11.2
65	14.1
70	18.0
75	24.5
80	41.5
85	73
90	100

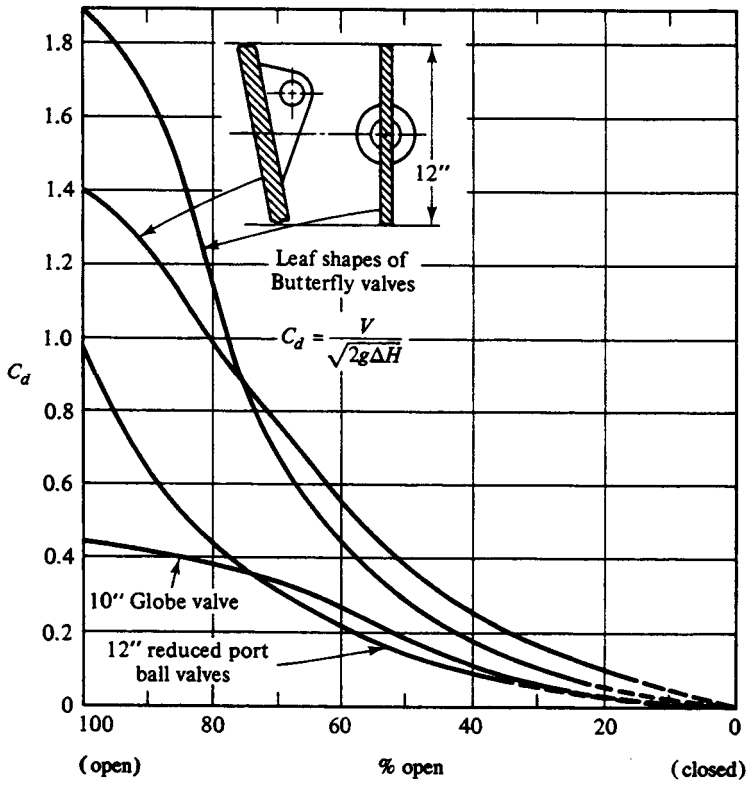

Figure A.3.3 : Discharge coefficients for valves. V is the mean velocity and ΔH is the head loss. We concern with 12" reduced ball valves. ($K = 1 / (Cd)^2$ where K is the local head loss coefficient).

Table A.3.8 : Discharge coefficient, Cd corresponding to % opening (obtained from Wylie & Streeter, 1993) for Figure A.3.3 ($K = 1 / (Cd)^2$ where K is the local head loss coefficient).

% Opening	Discharge Coefficient, Cd	Head loss coefficient, K
0	0.000	0
20	0.030	1111.11
30	0.050	400.00
40	0.095	110.80
50	0.125	64.00
60	0.215	21.63
70	0.300	11.11
80	0.450	4.94
90	0.610	2.69
100	0.990	1.02

APPENDIX B

B.1. The list of computer program adopted for the first system

```
C FOR THE FIRST PIPELINE SYSTEM
C SINGLE PUMP,VALVE IS PERMANANTLY OPEN
C NO CHECK VALVE IN A LINE
C DISCHARGE VALVE IS NEARLY CLOSE TO DOWNSTREAM END POINT
       DIMENSION Q(150),H(150),WH(89),WB(89)
       DIMENSION HPH(150),ZH(150),HD(150)
       OPEN (5,FILE='WH316E1.DAT',STATUS='OLD')
       OPEN (6,FILE='WH316E1.OUT',STATUS='NEW')
C EL=ELEVATION DIFFERENCE BETWEEN DOWNSTREAM RES SURF & DATUM (M)
C WATER SURFACE ELEVATION OF THE RESERVOIR A IS DATUM
C A=WAVE CELERITY (M/S), XL=PIPE LENGTH (M)
C F=DARCY-WEISBACH FRICTION COEFFICIENT
C D=PIPE DIAMETER (M), G=ACCELARATION DUE TO GRAVITY (9.806 M/S2)
C CK=REDUCED BORE BALL VALVE HEADLOSS COEFFICIENT
C TM=MAXIMUM CALCULATION TIME PERIOD (S)
C RN=RATED ROTATIONAL SPEED (RPM)
C TR=RATED TORQUE (NT.M)
C HR=RATED HEAD (M)
C QR=RATED DISCHARGE (M3/S)
C WRR=ROTATIONAL MOMENT OF INERTIA (NT.M2)
C REAL WRR VALUE=0.83 NT.M2
C TOL=TOLERANCE INTO THE NEWTON-RAPHSON METHOD
C V=THE RATIO OF VELOCITY OF WATER IN STEADY STATE TO VELOCITY OF WATER
C    IN RATED CONDITION OR DISCHARGE RATES
C N=NUMBER OF REACHES IN THE PIPELINE
C JPR=INTEGER NUMBER OF TIME STEP ITERATIONS BETWEEN EACH PRINT
C KIT=MAXIMUM ITERATION NUMBER IN NEWTON-RAPHSON NUMERICAL PROCEDURE
C DX=DIMENSIONLESS PUMP DATA SPACE (RADIAN)=PI/44=0.0714
C PI=PI NUMBER=3.1416
C AL,AL0,AL00=DIMENSIONLESS PUMP VELOCITY
C T=TIME INCREMENT IN THE SUCCESSIVE TIME STEP
C K=COUNTER DESIGNATES MAXIMUM CALCULATION TIME PERIOD
C WH(I),WB(I)=DIMENSIONLESS PUMP DATA
C ZH=ELEVATIONS OF MEASURING NODES ACCORDING TO DATUM (UPSTR RES LEVEL)
C AKS=ROUGHNESS HEIGHT IN STEEL PIPE (M)
C QQA=STEADY STATE DISCHARGE (M3/S)
C H=PIEZOMETRIC HEAD IN METERS
C HPH=PRESSURE HEAD IN METERS
C NSS=NUMBER OF NODE IN WHICH THERE IS A DISCHARGE ADJUSTMENT VALVE
C VN=KINEMATIC VISCOSITY OF WATER (M2/S)
       READ (5,*) EL,A,XL,D,G,CK,TM,RN,TR,HR,QR,WRR
       READ (5,*) TOL,N,JPR,KIT,VN
       READ (5,*) DX,PI,AKS,QQA,NSS
       READ (5,*) AL,AL0,AL00,T,K,HMIN
       READ (5,*) (ZH(I),I=1,N+1)
       READ (5,*) (WH(I),I=1,89)
       READ (5,*) (WB(I),I=1,89)
       UU=QQA/(PI*D*D/4)
       RE=UU*D/VN
       F=(1./(1.14-(2.*ALOG10((AKS/D)+(21.25/(RE**0.9))))))**2.
       V=QQA/QR
       DT=XL/(A*N)
       WRITE (6,1)
       WRITE (6,2)
       WRITE (6,3) EL,A,XL
       WRITE (6,4) F,D,G
       WRITE (6,500) TM,RN,TR
```

```
      WRITE (6,501) HR,QR,WRR
      WRITE (6,502) TOL,V,N
      WRITE (6,503) DX,CK,PI
      WRITE (6,504) AL,AL0,AL00
      WRITE (6,509) AKS,DT,VN
      WRITE (6,505) HMIN,T,JPR
      WRITE (6,506) K,QQA,KIT
      WRITE (6,510) NSS
      WRITE (6,507)
      WRITE (6,508)
      IF (MOD(N,2).NE.0) N=N+1
      NS=N+1
      NG=(NS+1)/2
      KMAX=INT((0.5*TM+0.001)/DT)+1
      AR=0.7854*D*D
      R=F*A*DT/(2.*G*D*AR*AR)
      B=A/(G*AR)
      CTORQ=WRR*PI*RN/(G*30.*TR*DT)
C  STEADY STATE FLOW DETERMINATION
      DH=CK*((QR/AR)**2.)/(2.*G)
      C=((N*R)*QR*QR)+(DH)
      X=PI+ATAN2(V,AL)
      I=X/DX+1
      KK=0
C  BEGINNING OF LOOP TO FIND STEADY STATE FLOW AND PUMP OPERATING POINT
   10 A1=(WH(I+1)-WH(I))/DX
      A0=WH(I+1)-A1*I*DX
      DO 15 KI=1,KIT
      F1=-EL-C*V*V+HR*(1.+V*V)*(A0+A1*X)
      F1V=-2.*C*V+HR*(2.*V*(A0+A1*X)+A1)
      V=V-F1/F1V
      X=PI+ATAN2(V,AL)
   15 CONTINUE
      II=X/DX+1
      IF (II.NE.I) THEN
      KK=KK+1
      IF (KK.GT.3) THEN
      WRITE (6,701)
  701 FORMAT ('      TROUBLE WITH STEADY STATE')
      STOP
      ENDIF
      I=II
      GO TO 10
      ENDIF
C  FIND STEADY STATE TORQUE AND STORE INITIAL VARIABLES
      Q0=V*QR
      B1=(WB(I+1)-WB(I))/DX
      B0=WB(I+1)-B1*I*DX
      BETA=(AL*AL+V*V)*(B0+B1*(PI+ATAN2(V,AL)))
      BET0=BETA
C  DETERMINATION OF Q AND H
      WRITE (6,400)
  400 FORMAT ('HP1=PIEZOMETRIC HEAD IN METERS BEFORE VALVE')
      WRITE (6,401)
  401 FORMAT ('HP2=PIEZOMETRIC HEAD IN METERS AFTER VALVE')
      WRITE (6,402)
  402 FORMAT ('HP=HEADLOSS IN METERS AT VALVE (NODE NSS)',/)
      H3=CK*(Q0**2)/(2.*G*AR*AR)
      DO 20 I=1,NS
      IF (I.GT.NSS) THEN
      H(I)=EL+(R*(NS-I)*Q0*ABS(Q0))
      ELSE IF (I.LE.NSS) THEN
      H(I)=EL+(R*(NS-I)*Q0*ABS(Q0))+H3
      ENDIF
      Q(I)=Q0
```

```
      IF (I.EQ.NSS) GO TO 699
      GO TO 20
  699 HP1=H(I)
      HP2=H(I)-H3
      H(I)=HP2
      HP=HP1-HP2
      WRITE (6,698) HP1,HP2,HP
  698 FORMAT ('HP1 HP2 HP',3F10.4,/)
   20 CONTINUE
      WRITE (6,403)
  403 FORMAT ('NUMBER OF NODES AND PIEZOMETRIC HEADS AT NODES AS METERS
      $:',/)
      WRITE (6,702) (I,H(I),I=1,NS)
  702 FORMAT (5(I2,':',1X,F8.2,3X))
      WRITE (6,404)
  404 FORMAT (/,'ZH(I) VALUES AS METERS :',/)
      WRITE (6,702) (I,ZH(I),I=1,NS)
C
      HMAX=EL
      V0=V
      V00=V
      HP11=HP1-ZH(NSS)
      DO 21 I=1,NS
   21 HPH(I)=H(I)-ZH(I)
C
      WRITE (6,405)
  405 FORMAT (/)
      WRITE (6,703)
  703 FORMAT (' TIME  ALPHA   BETA     V    Q(1)   Q(NS)  H(1)  H(NS) H
     1(NSS1) H(NSS2)')
      WRITE (6,704) T,AL,BETA,V,Q(1),Q(NS),HPH(1),HPH(NS),HP11,HPH(NSS)
  704 FORMAT (F5.3,9F7.3)
C  BEGINNING OF TRANSIENT LOOP
      DO 80 K=1,KMAX-1
      T=2.*DT*K
C  COMPUTATION OF INTERIOR POINTS
      DO 30 I1=2,3
      DO 25 I=I1,N,2
      BP=R*ABS(Q(I-1))+B
      IF (I.EQ.(NSS-1)) GO TO 667
      IF (I.EQ.NSS) GO TO 668
      IF (I.EQ.(NSS+1)) GO TO 666
      GO TO 26
  667 Q(I)=(H(I-1)-HP1+B*(Q(I-1)+Q(I+1)))/(BP+B+R*ABS(Q(I+1)))
      H(I)=H(I-1)+B*Q(I-1)-BP*Q(I)
      GO TO 25
  666 IF ((NSS+1).EQ.(N+1)) GO TO 25
      Q(I)=(HP2-H(I+1)+B*(Q(I-1)+Q(I+1)))/(BP+B+R*ABS(Q(I+1)))
      H(I)=HP2+B*Q(I-1)-BP*Q(I)
      GO TO 25
  668 CM=H(I+1)-(B*Q(I+1))+(R*Q(I+1)*ABS(Q(I+1)))
      CP=H(I-1)+(B*Q(I-1))-(R*Q(I-1)*ABS(Q(I-1)))
      IF (V.LT.0.0) GO TO 996
      C3=CK/(2.*G*AR*AR)
      C4=(2*B)/C3
      C5=(CM-CP)/C3
      Q(I)=0.5*(-C4+(SQRT((C4*C4)-(4.*C5))))
      HP1=CP-(B*Q(I))
      HP2=CM+(B*Q(I))
      H(I)=HP2
      GO TO 25
  996 C3=CK/(2.*G*AR*AR)
      C4=(2.*B)/C3
      C5=(CM-CP)/C3
      Q(I)=0.5*(C4-(SQRT(((-C4)**2.)+(4.*C5))))
```

```
      HP1=CP-(B*Q(I))
      HP2=CM+(B*Q(I))
      H(I)=HP2
      GO TO 25
   26 Q(I)=(H(I-1)-H(I+1)+B*(Q(I-1)+Q(I+1)))/(BP+B+R*ABS(Q(I+1)))
      H(I)=H(I-1)+B*Q(I-1)-BP*Q(I)
   25 CONTINUE
      IF (N.LE.2) GO TO 35
   30 CONTINUE
C
C  PUMP BOUNDARY CONDITION
C
C
   35 CM=H(2)-Q(2)*B
      BM=B+R*ABS(Q(2))
C  BALANCE HEAD AND TORQUE EQUATIONS
      AL=2.*AL0-AL00
      V=2.*V0-V00
      X=PI+ATAN2(V,AL)
      I=X/DX+1
C  BEGINNING OF LOOP TO FIND PUMP FLOW AND SPEED
   40 A1=(WH(I+1)-WH(I))/DX
      A0=WH(I+1)-A1*I*DX
      B1=(WB(I+1)-WB(I))/DX
      B0=WB(I+1)-B1*I*DX
C  NEWTON RAPHSON
      DO 50 KI=1,KIT
      F1=(HR*(AL**2+V*V)*(A0+A1*X)-(CM+BM*QR*V))
      F2=(AL**2+V*V)*(B0+B1*X)+BET0+CTORQ*(AL-AL0)
      F1A=HR*(2.*AL*(A0+A1*X)-V*A1)
      F1V=(HR*(2.*V*(A0+A1*X)+AL*A1)-BM*QR)
      F2A=2.*AL*(B0+B1*X)-V*B1+CTORQ
      F2V=2.*V*(B0+B1*X)+AL*B1
      DAL=(F2/F2V-F1/F1V)/(F1A/F1V-F2A/F2V)
      DV=-F1/F1V-DAL*F1A/F1V
      AL=AL+DAL
      V=V+DV
      X=PI+ATAN2(V,AL)
      IF (ABS(DAL)+ABS(DV).LT.TOL) GO TO 55
   50 CONTINUE
C  CHECK TO SEE IF SOLUTION HAS MOVED TO ANOTHER PART OF PUMP CURVE
   55 II=X/DX+1
      IF (II.NE.I) THEN
      I=II
      GO TO 40
      ENDIF
C  SOLUTION HAS BEEN GENERATED
      V00=V0
      V0=V
      AL00=AL0
      AL0=AL
      BETA=(AL**2+V*V)*(B0+B1*X)
      Q(1)=V*QR
      H(1)=CM+BM*Q(1)
C  DOWNSTREAM BOUNDARY CONDITION
C
C
      Q(NS)=(H(N)-H(NS)+B*Q(N))/(R*ABS(Q(N))+B)
      BET0=BETA
      DO 70 I=1,NS,2
      IF (H(I).GT.HMAX) HMAX=HD(I)
      IF (H(I).LT.HMIN) HMIN=HD(I)
      IF (H(I).GT.HMAX) HMAX=H(I)
      IF (H(I).LT.HMIN) HMIN=H(I)
   70 CONTINUE
```

```
      IF (K.EQ.1) GO TO 5
      IF (MOD(K,JPR).EQ.0) GO TO 5
      GO TO 80
    5 HPH(1)=H(1)-ZH(1)
      HPH(NS)=H(NS)-ZH(NS)
      HP11=HP1-ZH(NSS)
      HPH(NSS)=H(NSS)-ZH(NSS)
      WRITE (6,704) T,AL,BETA,V,Q(1),Q(NS),HPH(1),HPH(NS),HP11,HPH(NSS)
   80 CONTINUE
C  END OF TRANSIENT LOOP
      HMAX1=HMAX
      HMIN1=HMIN
      WRITE (6,705) HMAX1,HMIN1
  705 FORMAT ('HMAX HMIN ',2F8.3)
    1 FORMAT (26X,18('*'),26X,/,26X,'* INITIAL VALUES *',26X)
    2 FORMAT (26X,18('*'),26X,/,/)
    3 FORMAT ('EL (M)=',F10.4,8X,'A (M3/SEC)=',F10.4,7X,'XL (M)=',F10.4
     $)
    4 FORMAT ('F=',F10.4,13X,'D (M)=',F10.4,12X,'G (M/S2)=',F10.4)
  500 FORMAT ('TM (S)=',F10.4,8X,'RN (RPM)=',F10.4,9X,'TR (NT.M)=',F10.
     $4)
  501 FORMAT ('HR (M)=',F10.4,8X,'QR (M3/S)=',F10.4,8X,'WRR (NT.M2)=',F
     $10.4)
  502 FORMAT ('TOL=',F10.4,11X,'V=',F10.4,16X,'N=',I3)
  503 FORMAT ('DX (RAD)=',F10.4,6X,'CK=',F10.4,15X,'PI=',F10.4)
  504 FORMAT ('AL=',F10.4,12X,'AL0=',F10.4,14X,'AL00=',F10.4)
  509 FORMAT ('AKS(M)=',F10.4,8X,'DT (S)=',F10.4,11X,'VN (M2/S)=',F10.6
     $)
  505 FORMAT ('HMIN=',F10.4,10X,'T=',F10.4,16X,'JPR=',I3)
  506 FORMAT ('K=',I3,20X,'QQA (M3/S)=',F10.4,7X,'KIT=',I3)
  510 FORMAT ('NSS=',I3)
  507 FORMAT (/,/,26X,17('*'),26X,/,26X,'* RESULT VALUES *',26X)
  508 FORMAT (26X,17('*'),26X,/,/)
      STOP
      END
```

B.2. Typical data file

```
3.73 1331.0 28 0.125 9.806 84 8 1450 32.18 11 0.036 0.83
0.0002 28 56 5 0.000001
0.0714 3.1416 0.00015 0.0183 23
1 1 1 0 0 0
-0.39 0.17 0.42 0.47 0.47 0.52 0.57 0.62 0.62 0.65 0.67 0.72 0.74
0.77 0.79 0.82 0.87 0.88 0.92 0.96 1.62 2.17 2.17 2.17 2.17
2.17 2.17 2.17 3.38
0.411 0.4338 0.451 0.4618 0.4719 0.4793 0.4816 0.4763 0.4644 0.4557
0.451 0.4519 0.4637 0.4852 0.5034 0.5272 0.5617 0.6077 0.6634 0.725
0.7983 0.8754 0.9426 0.9935 1.0503 1.1094 1.1541 1.1884 1.2223
1.2388 1.2447 1.2573 1.2642 1.2729 1.2746 1.2926 1.3069 1.3281
1.3541 1.3733 1.3936 1.4066 1.4121 1.412 1.4029 1.3785 1.34 1.2833
1.2032 1.1154 1.0436 0.9395 0.8427 0.7349 0.6209 0.5 0.369 0.2317
0.1041 -0.0229 -0.1495 -0.2382 -0.3444 -0.4481 -0.5513 -0.6419   -
0.715 -0.8423 -0.9085 -0.9429 -0.953 -0.9446 -0.9203 -0.9027 -0.8577
-0.8193 -0.7642 -0.71 -0.6624 -0.5907 -0.4982 -0.3722 -0.2236 -
0.0519 0.0887 0.1976 0.2889 0.3606 0.411
-0.808 -0.6785 -0.5482 -0.4207 -0.302 -0.2013 -0.1406 -0.0972 -
0.0291 0.0416 0.1028 0.1888 0.2693 0.3604 0.4437 0.5308 0.6201
```

```
0.7153 0.8096 0.8652 0.9321 1.0058 1.0696 1.1217 1.1545 1.1723
1.1731 1.1494 1.1259 1.0831 1.0149 0.9463
0.8702 0.7878 0.7056 0.6467 0.5994 0.5621 0.5407 0.5318 0.5374
0.5502 0.5659 0.5933 0.6252 0.6376 0.6384 0.6355 0.6346 0.6385
0.6413 0.6367 0.6181 0.5891 0.55 0.5 0.4278 0.3462 0.2641 0.1818
0.0728 -0.0331 -0.1426 -0.2649 -0.376 -0.4762 -0.5721 -0.831 -1.0331
-1.1865 -1.2981 -1.403 -1.511 -1.6041 -1.6955 -1.7668 -1.8082
-1.8163 -1.866 -1.7494 -1.6793 -1.6008 -1.5076 -1.4177 -1.3428 -
1.2263 -1.1097 -0.9564 -0.808
```

APPENDIX C

C.1. The list of computer program adopted for the second system

```
C WH25.FOR=UNSTEADY FLOW CALCULATIONS FOR SECOND SYSTEM
      DIMENSION Q(50),H(50),WH(89),WB(89),TAU(50)
      DIMENSION HPH(50),ZH(50)
      OPEN (5,FILE='WH25B.DAT',STATUS='OLD')
      OPEN (6,FILE='WH25B.OUT',STATUS='NEW')
C DATUM=UPSTREAM RESERVOIR WATER SURFACE ELEVATION
C EL=ELEVATION DIFFERENCE BETWEEN UPSTREAM & DOWNSTREAM RESERVOIRS (M)
C A=WAVE CELERITY (M/S), XL=PIPE LENGTH (M)
C F=DARCY-WEISBACH FRICTION COEFFICIENT
C D=PIPE DIAMETER (M), G=ACCELARATION DUE TO GRAVITY (9.806 M/S2)
C CK=DISC TYPE CHECK VALVE HEADLOSS COEFFICIENT
C AKV1=HEADLOSS COEFFICIENT OF REDUCED BORE BALL VALVE IMMEDIATELY
C      AFTER PUMP
C AKV2=HEADLOSS COEFFICIENT OF REDUCED BORE BALL VALVE AT THE END
C      OF THE PIPE
C TM=MAXIMUM CALCULATION TIME PERIOD (S)
C RN=RATED ROTATIONAL SPEED (RPM)
C TR=RATED TORQUE (NT.M)
C HR=RATED HEAD (M)
C QR=RATED DISCHARGE (M3/S)
C WRR=ROTATIONAL MOMENT OF INERTIA (NT.M2)
C DTAU=TIME INCREMENT BETWEEN TAU VALUES (S)
C TOL=TOLERANCE INTO THE NEWTON-RAPHSON METHOD
C VI=THE RATIO OF VELOCITY OF WATER IN STEADY STATE TO VELOCITY OF WATER
C    IN RATED CONDITION
C N=NUMBER OF REACHES IN THE PIPELINE
C JPR=INTEGER NUMBER OF TIME STEP ITERATIONS BETWEEN EACH PRINT
C KIT=MAXIMUM ITERATION NUMBER IN NEWTON-RAPHSON NUMERICAL METHOD
C TAU=CHECK VALVE OPENING
C DX=DIMENSIONLESS PUMP DATA SPACE (RADIAN)=PI/44=0.0713
C PI=PI NUMBER=3.1416
C AL,AL0,AL00=DIMENSIONLESS ROTATIONAL SPEED RATIO
C T=TIME INCREMENT IN THE SUCCESSIVE TIME STEP
C K=COUNTER DESIGNATES MAXIMUM CALCULATION TIME PERIOD
C WH(I),WB(I)=DIMENSIONLESS PUMP DATA
C ZH=ELEVATIONS OF MEASURING NODES ACCORDING TO DATUM (UPSTR WAT SUR)
C NSV=NODE NUMBER OF VALVE AT THE END OF THE PIPE
C NTAU=NUMBER OF TAU VALUES
C CCT=CHECK VALVE CLOSING TIME (S)
C     AT PUMP NODE (i.e.NODE 1)
C M2=NODE NUMBER OF SECOND MEASURING POINT
C AKS=ROUGHNESS HEIGHT OF PIPE WALL (M)
C QQA=STEADY STATE DISCHARGE (M3/S)
C VN=KINEMATIC VISCOSITY OF WATER (M2/S)
      READ (5,*) EL,A,XL,D,G,CK,AKV1,AKV2,TM,RN,TR,HR,QR,WRR
      READ (5,*) CCT,NTAU,TOL,VI,N,JPR,KIT,AKS,VN
      READ (5,*) DX,PI,NSV,M2
      READ (5,*) AL,AL0,AL00,T,K,HMIN
      READ (5,*) (ZH(I),I=1,N+1)
      READ (5,*) (WH(I),I=1,89)
      READ (5,*) (WB(I),I=1,89)
      QQA=VI*QR
      UU=QQA/(PI*D*D/4)
      RE=UU*D/VN
      F=(1./(1.14-(2.*ALOG10((AKS/D)+(21.25/(RE**0.9))))))**2.
      IF (MOD(N,2).NE.0) N=N+1
      NS=N+1
```

```
      DT=XL/(A*N)
      TAU(1)=1.
      DO 6 I=2,NTAU
    6 TAU(I)=1.-((I-1.)*(1./(NTAU-1.)))
      DTAU=CCT/(NTAU-1)
      WRITE (6,1)
      WRITE (6,2)
      WRITE (6,3) EL,A,XL
      WRITE (6,4) F,D,G
      WRITE (6,500) TM,RN,TR
      WRITE (6,501) HR,QR,WRR
      WRITE (6,502) TOL,VI,N
      WRITE (6,503) DX,CK,PI
      WRITE (6,511) AKV1,AKV2,DTAU
      WRITE (6,512) TAU(1),TAU(2),TAU(3)
      WRITE (6,513) TAU(4),TAU(5),TAU(6)
      WRITE (6,514) TAU(7),TAU(8),TAU(9)
      WRITE (6,515) TAU(10),TAU(11),TAU(12)
      WRITE (6,516) TAU(13),TAU(14),TAU(15)
      WRITE (6,517) TAU(16),TAU(17),TAU(18)
      WRITE (6,518) TAU(19),TAU(20),M2
      WRITE (6,504) AL,AL0,AL00
      WRITE (6,505) HMIN,T,JPR
      WRITE (6,506) K,NSV,KIT
      WRITE (6,519) CCT,NTAU,QQA
      WRITE (6,520) DT,AKS,VN
      WRITE (6,507)
      WRITE (6,508)
      KMAX=INT((0.5*TM+0.001)/DT)+1
      AR=0.7854*D*D
      R=F*A*DT/(2.*G*D*AR*AR)
      TA=TAU(1)
      B=A/(G*AR)
      V=VI
      CTORQ=WRR*PI*RN/(G*30.*TR*DT)
C  STEADY STATE FLOW DETERMINATION
      DH=CK*((QR/AR)**2.)/(2.*G)
      DHSV1=(AKV1)*((QR/AR)**2.)/(2.*G)
      DHSV2=(AKV2)*((QR/AR)**2.)/(2.*G)
      C=((N*R)*QR*QR)+(DH/TAU(1)**2.)+DHSV1+DHSV2
      X=PI+ATAN2(V,AL)
      I=X/DX+1
      KK=0
C  BEGINNING OF LOOP TO FIND STEADY STATE FLOW AND PUMP OPERATING POINT
   10 A1=(WH(I+1)-WH(I))/DX
      A0=WH(I+1)-A1*I*DX
      DO 15 KI=1,KIT
      F1=-EL-C*V*V+HR*(1.+V*V)*(A0+A1*X)
      F1V=-2.*C*V+HR*(2.*V*(A0+A1*X)+A1)
      V=V-F1/F1V
      X=PI+ATAN2(V,AL)
   15 CONTINUE
      II=X/DX+1
      IF (II.NE.I) THEN
      KK=KK+1
      IF (KK.GT.3) THEN
      WRITE (6,701)
  701 FORMAT ('      TROUBLE WITH STEADY STATE')
      STOP
      ENDIF
      I=II
      GO TO 10
      ENDIF
C  FIND STEADY STATE TORQUE AND STORE INITIAL VARIABLES
      Q0=V*QR
```

```
      B1=(WB(I+1)-WB(I))/DX
      B0=WB(I+1)-B1*I*DX
      BETA=(AL*AL+V*V)*(B0+B1*(PI+ATAN2(V,AL)))
      BET0=BETA
C  DETERMINATION OF Q AND H
C
      WRITE (6,400)
 400  FORMAT ('HP1=PIEZOMETRIC HEAD IN METERS BEFORE VALVE')
      WRITE (6,401)
 401  FORMAT ('HP2=PIEZOMETRIC HEAD IN METERS AFTER VALVE')
      WRITE (6,402)
 402  FORMAT ('HP=HEADLOSS IN METERS AT VALVE (NODE NSV)',/)
C
      DH1=(AKV2*Q0**2.)/(2.*9.81*AR*AR)
      DO 20 I=1,NS
      IF (I.GT.NSV) THEN
      H(I)=EL+(R*(NS-I)*Q0*ABS(Q0))
      ELSE IF (I.LE.NSV) THEN
      H(I)=EL+(R*(NS-I)*Q0*ABS(Q0))+DH1
      ENDIF
      Q(I)=Q0
      IF (I.EQ.NSV) GO TO 699
      GO TO 20
 699  HP1=H(I)
      HP2=H(I)-DH1
      H(I)=HP2
      HP=HP1-HP2
      WRITE (6,698) HP1,HP2,HP
 698  FORMAT ('HP1 HP2 HP',3F10.4,/)
  20  CONTINUE
C
      WRITE (6,403)
 403  FORMAT ('NUMBER OF NODES AND PIEZOMETRIC HEADS AT NODES AS METERS
     $:',/)
      WRITE (6,702) (I,H(I),I=1,NS)
 702  FORMAT (5(I2,':',1X,F8.2,3X))
      WRITE (6,404)
 404  FORMAT (/,'ZH(I) VALUES AS METERS :',/)
      WRITE (6,702) (I,ZH(I),I=1,NS)
      HMAX=EL
      V0=V
      V00=V
      TA=TAU(1)
      HP11=HP1-ZH(NSV)
      DO 21 I=1,NS
  21  HPH(I)=H(I)-ZH(I)
      HPH(NSV)=HP2-ZH(NSV)
      WRITE (6,405)
 405  FORMAT (/)
      WRITE (6,703)
 703  FORMAT ('    TIME     TAU   ALPHA     BETA     V      Q(1)   Q(M2)
     $   Q(NS)   H(1)   H(27)  H(NSV1)  H(NSV2)  H(NS)')
      WRITE (6,704) T,TA,AL,BETA,V,Q(1),Q(M2),Q(NS),HPH(1),HPH(M2),HP11,
     $HPH(NSV),HPH(NS)
 704  FORMAT (F8.4,12F8.3)
C  BEGINNING OF TRANSIENT LOOP
      DO 80 K=1,KMAX-1
      T=2.*DT*K
C  COMPUTATION OF INTERIOR POINTS
      DO 30 I1=2,3
      DO 25 I=I1,N,2
      BP=R*ABS(Q(I-1))+B
      IF (I.EQ.(NSV-1)) GO TO 667
      IF (I.EQ.NSV) GO TO 668
      IF (I.EQ.(NSV+1)) GO TO 666
```

```
      GO TO 26
 667  Q(I)=(H(I-1)-HP1+B*(Q(I-1)+Q(I+1)))/(BP+B+R*ABS(Q(I+1)))
      H(I)=H(I-1)+B*Q(I-1)-BP*Q(I)
      GO TO 25
 666  IF ((NSV+1).EQ.(N+1)) GO TO 25
      Q(I)=(HP2-H(I+1)+B*(Q(I-1)+Q(I+1)))/(BP+B+R*ABS(Q(I+1)))
      H(I)=HP2+B*Q(I-1)-BP*Q(I)
      GO TO 25
 668  CP=H(I-1)+(B*Q(I-1))-(R*Q(I-1)*ABS(Q(I-1)))
      CM=H(I+1)-(B*Q(I+1))+(R*Q(I+1)*ABS(Q(I+1)))
      IF (V.LT.0.) GO TO 333
      C3=AKV2/(2.*G*AR*AR)
      C4=(2*B)/C3
      C5=(CM-CP)/C3
      Q(I)=0.5*(-C4+(SQRT((C4*C4)-(4.*C5))))
      HP1=CP-(B*Q(I))
      HP2=CM+(B*Q(I))
      GO TO 25
 333  C3=AKV2/(2.*9.81*AR*AR)
      C4=(2*B)/C3
      C5=(CM-CP)/C3
      Q(I)=0.5*(C4-(SQRT(((-C4)**2.)+(4.*C5))))
      HP1=CP-(B*Q(I))
      HP2=CM+(B*Q(I))
      GO TO 25
  26  Q(I)=(H(I-1)-H(I+1)+B*(Q(I-1)+Q(I+1)))/(BP+B+R*ABS(Q(I+1)))
      H(I)=H(I-1)+B*Q(I-1)-BP*Q(I)
  25  CONTINUE
      IF (N.LE.2) GO TO 35
  30  CONTINUE
C  PUMP BOUNDARY CONDITION
  35  CM=H(2)-Q(2)*B
      BM=B+R*ABS(Q(2))
      IF (TA.LT.0.0001) GO TO 60
C  VALVE WAS OPEN; FIND CURRENT VALUE OF TAU
      I=T/DTAU+1
      IF (I.GE.NTAU) THEN
      TA=TAU(NTAU)
      ELSE
      TA=TAU(I)+(TAU(I+1)-TAU(I))*(T-(I-1)*DTAU)/DTAU
      ENDIF
C  VALVE IS CLOSED
      IF (TA.LT.0.0) TA=0.0
      IF (TA.LT.0.0001) THEN
      V=0.
      Q(1)=0.0
      GO TO 60
      ENDIF
C  BALANCE HEAD AND TORQUE EQUATIONS
      AL=2.*AL0-AL00
      V=2.*V0-V00
      X=PI+ATAN2(V,AL)
      I=X/DX+1
C  BEGINNING OF LOOP TO FIND PUMP FLOW AND SPEED
  40  A1=(WH(I+1)-WH(I))/DX
      A0=WH(I+1)-A1*I*DX
      B1=(WB(I+1)-WB(I))/DX
      B0=WB(I+1)-B1*I*DX
C  NEWTON RAPHSON
      DO 50 KI=1,KIT
      F1=TA**2*(HR*(AL**2+V*V)*(A0+A1*X)-(CM+BM*QR*V))-(DH*V*ABS(V))-(DH
     $SV1*V*ABS(V))
      F2=(AL**2+V*V)*(B0+B1*X)+BET0+CTORQ*(AL-AL0)
      F1A=TA**2*HR*(2.*AL*(A0+A1*X)-V*A1)
      F1V=TA**2*(HR*(2.*V*(A0+A1*X)+AL*A1)-BM*QR)-(2.*DH*ABS(V))-(2.*DHS
```

```
     $V1*ABS(V))
      F2A=2.*AL*(B0+B1*X)-V*B1+CTORQ
      F2V=2.*V*(B0+B1*X)+AL*B1
      DAL=(F2/F2V-F1/F1V)/(F1A/F1V-F2A/F2V)
      DV=-F1/F1V-DAL*F1A/F1V
      AL=AL+DAL
      V=V+DV
      X=PI+ATAN2(V,AL)
      IF (ABS(DAL)+ABS(DV).LT.TOL) GO TO 55
  50  CONTINUE
C  CHECK TO SEE IF SOLUTION HAS MOVED TO ANOTHER PART OF PUMP CURVE
  55  II=X/DX+1
      IF (II.NE.I) THEN
      I=II
      GO TO 40
      ENDIF
C  SOLUTION HAS BEEN GENERATED
      V00=V0
      V0=V
      AL00=AL0
      AL0=AL
      BETA=(AL**2+V*V)*(B0+B1*X)
      Q(1)=V*QR
  60  H(1)=CM+BM*Q(1)
C  DOWNSTREAM BOUNDARY CONDITION
      Q(NS)=(HP2-H(NS)+B*Q(N))/(R*ABS(Q(N))+B)
      BET0=BETA
      DO 70 I=1,NS,2
      IF (H(I).GT.HMAX) HMAX=H(I)
      IF (H(I).LT.HMIN) HMIN=H(I)
  70  CONTINUE
      IF (MOD(K,JPR).EQ.0) GO TO 5
      GO TO 80
   5  HPH(1)=H(1)-ZH(1)
      HPH(M2)=H(M2)-ZH(M2)
      HP11=HP1-ZH(NSV)
      HPH(NSV)=HP2-ZH(NSV)
      HPH(NS)=H(NS)-ZH(NS)
      WRITE (6,704) T,TA,AL,BETA,V,Q(1),Q(M2),Q(NS),HPH(1),HPH(M2),HP11,
     $HPH(NSV),HPH(NS)
  80  CONTINUE
C  END OF TRANSIENT LOOP
      HMAX1=HMAX
      HMIN1=HMIN
      WRITE (6,705) HMAX1,HMIN1
 705  FORMAT ('HMAX HMIN ',2F8.3)
   1  FORMAT (26X,18('*'),26X,/,26X,'* INITIAL VALUES *',26X)
   2  FORMAT (26X,18('*'),26X,/,/)
   3  FORMAT ('EL (M)=',F10.4,8X,'A (M3/S)=',F10.4,9X,'XL (M)=',F10.4)
   4  FORMAT ('F=',F10.4,13X,'D (M)=',F10.4,12X,'G (M/S2)=',F10.4)
 500  FORMAT ('TM (S)=',F10.4,8X,'RN (RPM)=',F10.4,9X,'TR (NT.M)=',F10.
     $4)
 501  FORMAT ('HR (M)=',F10.4,8X,'QR (M3/S)=',F10.4,8X,'WRR (NT.M2)=',F
     $10.4)
 502  FORMAT ('TOL=',F10.4,11X,'VI=',F10.4,15X,'N=',I3)
 503  FORMAT ('DX (RAD)=',F10.4,6X,'CK =',F10.4,14X,'PI=',F10.4)
 511  FORMAT ('AKV1 =',F10.4,9X,'AKV2=',F10.4,13X,'DTAU (S)=',F10.4)
 504  FORMAT ('AL=',F10.4,12X,'AL0=',F10.4,14X,'AL00=',F10.4)
 505  FORMAT ('HMIN=',F10.4,10X,'T=',F10.4,16X,'JPR=',I3)
 506  FORMAT ('K=',I3,20X,'NSV =',I3,20X,'KIT=',I3)
 512  FORMAT ('TAU(1)=',F10.4,8X,'TAU(2)=',F10.4,11X,'TAU(3)=',F10.4)
 513  FORMAT ('TAU(4)=',F10.4,8X,'TAU(5)=',F10.4,11X,'TAU(6)=',F10.4)
 514  FORMAT ('TAU(7)=',F10.4,8X,'TAU(8)=',F10.4,11X,'TAU(9)=',F10.4)
 515  FORMAT ('TAU(10)=',F10.4,7X,'TAU(11)=',F10.4,10X,'TAU(12)=',F10.4
     $)
```

```
 516  FORMAT ('TAU(13)=',F10.4,7X,'TAU(14)=',F10.4,10X,'TAU(15)=',F10.4
     $)
 517  FORMAT ('TAU(16)=',F10.4,7X,'TAU(17)=',F10.4,10X,'TAU(18)=',F10.4
     $)
 518  FORMAT ('TAU(19)=',F10.4,7X,'TAU(20)=',F10.4,10X,'M2=',I2)
 519  FORMAT ('CCT (S)=',F10.4,7X,'NTAU =',I3,19X,'QQA (M3/S)=',F10.4)
 520  FORMAT ('DT (S)=',F10.4,8X,'AKS (M)=',F10.4,10X,'VN (M2/S)=',F10.6
     $)
 507  FORMAT (/,/,26X,17('*'),26X,/,26X,'* RESULT VALUES *',26X)
 508  FORMAT (26X,17('*'),26X,/,/)
       STOP
       END
```

C.2. Typical data file

```
4.6 1331.0 108 0.125 9.81 6.62 4.98 74 10 1450 32.18 11 0.036 0.83
2.5 20 0.0002 0.46 42 21 5 0.00015 0.000001
0.0714 3.1416 42 27
1 1 1 0 0 0
-0.3 0.05 0.12 0.21 0.04 0.1 0.15 0.3 1.39 1.42 1.39 1.34 1.35
1.36 1.36 1.35 1.35 1.33 1.32 1.32 1.34 1.34 1.3 1.28 1.3 1.41 1.7
1.6 1.6 1.6 1.6 1.6 1.6 1.6 1.58 1.61 1.61 1.6 1.6 1.6 1.61 1.61 4.1
0.634 0.643 0.646 0.640 0.629 0.613 0.595 0.575 0.552 0.533 0.516
0.505 0.504 0.510 0.512 0.522 0.539 0.559 0.580 0.601 0.630 0.662
0.692 0.722 0.753 0.782 0.808 0.832 0.857 0.879 0.904 0.930 0.959
0.996 1.027 1.06 1.090 1.124 1.165 1.204 1.238 1.258 1.271 1.282
1.288 1.281 1.260 1.225 1.172 1.107 1.031 0.942 0.842 0.733 0.617
0.5 0.368 0.24 0.125 0.011 -0.102 -0.168 -0.255 -0.342 -0.423 -0.494
-0.556 -0.620 -0.655 -0.670 -0.670 -0.66 -0.655 -0.640 -0.6 -0.57 -
0.52 -0.47 -0.43 -0.36 -0.275 -0.16 -0.04 0.130 0.295 0.430 0.55
0.620 0.634
-0.684 -0.547 -0.414 -0.292 -0.167 -0.105 -0.053 -0.012 0.042 0.097
0.156 0.227 0.3 0.371 0.444 0.522 0.596 0.672 0.738 0.763 0.797
0.837 0.865 0.883 0.886 0.877 0.859 0.838 0.804 0.758 0.703 0.645
0.583 0.520 0.454 0.408 0.370 0.343 0.331 0.329
0.338 0.354 0.372 0.405 0.450 0.486 0.520 0.552 0.579
0.603 0.616 0.617 0.606 0.582 0.546 0.5 0.432 0.36 0.288 0.214 0.123
0.037 -0.053 -0.161 -0.248 -0.314 -0.372 -0.58  -0.74 -0.88 -1 -1.12
-1.25 -1.37 -1.49 -1.59 -1.66 -1.69 -1.77 -1.65 -1.59 -1.520 -1.420
-1.320 -1.23 -1.1 -0.980 -0.82 -0.684
```